Title
HOPF BIFURCATION AND PLASMA INSTABILITIES

Author
Crawford, J.D.

Publication Date
1983-11-01

LBL-17015

Lawrence Berkeley Laboratory
UNIVERSITY OF CALIFORNIA

Accelerator & Fusion Research Division

HOPF BIFURCATION AND PLASMA INSTABILITIES

J.D. Crawford
(Ph.D. Thesis)

November 1983

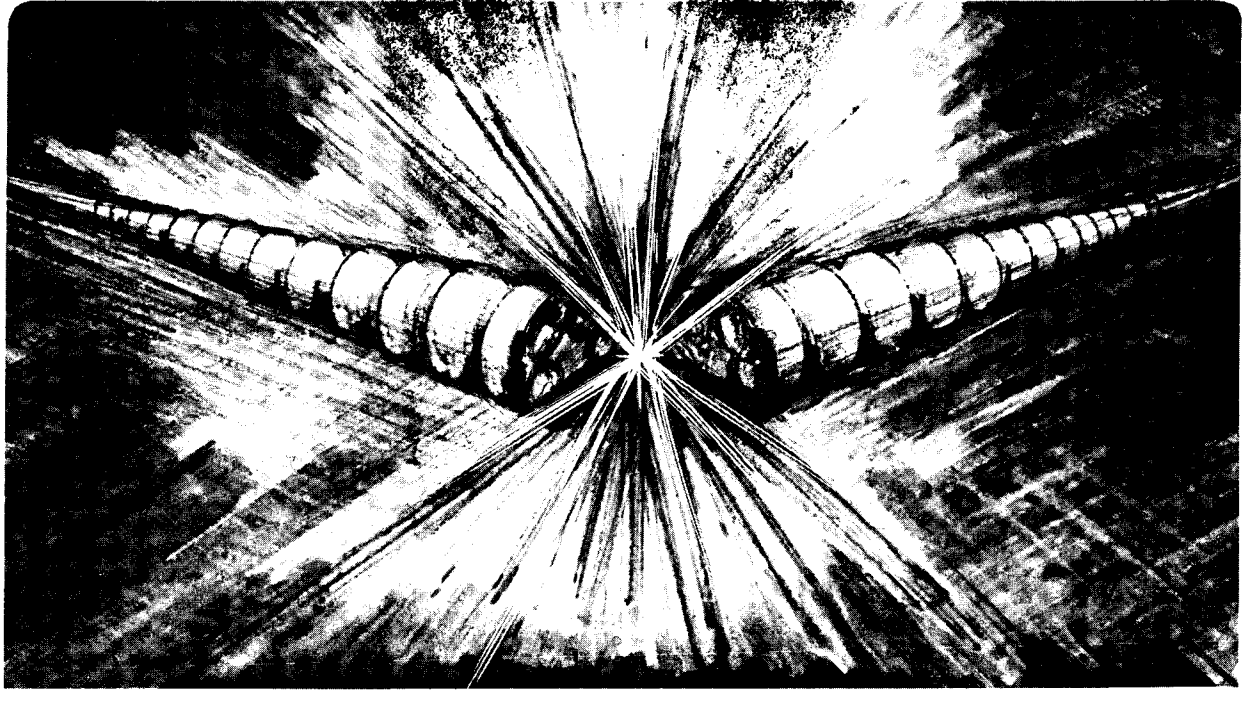

Prepared for the U.S. Department of Energy under Contract DE-AC03-76SF00098

DISCLAIMER

LBL-17015

Hopf Bifurcation and Plasma Instabilities*

John David Crawford

Ph.D. Thesis

Physics Department and Lawrence Berkeley Laboratory
University of California
Berkeley, California 94720

November, 1983

This work was supported by the Office of Basic Energy Sciences of the U.S. Department of Energy under Contract No. DE-AC03-76SF00098.

Hopf Bifurcation and Plasma Instabilities

John David Crawford

Abstract

In physical terms, bifurcation theory is the study of transitions between distinct physical states which occur through the development of instabilities. Such transitions are readily observed in nature, and they are necessarily nonlinear in character. Relatively recent developments in nonlinear analysis make it possible to study bifurcation phenomena of ordinary and partial differential equations in a unified way. Although the theory is by no means fully developed, for transitions from time independent equilibria or for transitions from periodic motions, it is sufficiently complete to be useful in applications.

In this research, center manifold theory and the theory of normal forms are applied to examples of Hopf bifurcation in two models of plasma dynamics. A finite dimensional model of a 3-wave system with quadratic nonlinearities

Abstract

provides a simple example of both supercritical and subcritical Hopf bifurcation. In the second model, the electrostatic instabilities of a collisional plasma correspond to Hopf bifurcations. In this problem, the Vlasov-Poisson equations with a Krook collision term describe the electron dynamics in a weakly ionized gas. The one mode in instability is analyzed in detail; near criticality it always saturates in a small amplitude nonlinear oscillation.

The theory of the center manifold accomplishes two things. First, it establishes that the dynamics of a finite mode instability is always of a finite dimensional character, even when the equations of motion are partial differential equations. Secondly, it provides practical methods for deriving the relevant reduced set of equations which describe the transition. Thus the center manifold methods provide a geometric and rigorous basis for the reduction in dimension which characterizes classical amplitude expansions.

The theory of normal forms applies to the reduced dynamical system derived for the center manifold. Two sorts of results are obtained. First, by considering only the linearized dynamics of the problem, we can specify which nonlinear couplings are essential, and will remain after the normal form coordinate transformations are implemented. Secondly, the coordinate transformations can be explicitly performed, the coefficients of the essential nonlinear terms computed, and the resulting equations analyzed.

Henry D. I. Abarbanel

Edward Ott

To my parents, Stanley and Saradell Crawford,

and my wife, Ann Pacey,

whose love, support, and values

have made my education possible.

Acknowledgements

My research interests have been shaped and enthusiastically encouraged by my thesis advisor, Henry Abarbanel, and my faculty advisor, Allan Kaufman. I am particularly grateful to Henry for posing the challenge which issued into this research: "While I'm on vacation in Amsterdam, why don't you try to compute the limit cycle solution for the 3-wave system?" Allan has generously afforded me opportunities to study nonlinear dynamics as a teaching assistant in his graduate courses.

My conversations with Jerry Marsden, Jürgen Scheurle, and Steve Wan have significantly enriched my understanding of bifurcation theory. Discussions with Peter Hislop, Edgar Knobloch, and Steve Omohundro have been important to my thinking about dynamics.

Contents

Introduction 1

Figures for the Introduction 12

Chapter 1. Invariant Manifolds and Normal Forms 13

Linear Stability Theory 14

Nonlinear Effects: Invariant Manifolds 17

Invariant Manifolds for Hopf Bifurcation 19

Normal Forms for Hopf Bifurcation 26

Final Remarks 38

Figures for Chapter 1 41

Chapter 2. Hopf Bifurcation in a Resonant 3-Wave Interaction 47

The Model 49

Linear Analysis 51

The Dynamics on the Center Manifold 56

Analysis of the Normal Form 63

A Digression: Absence of Secondary Hopf Bifurcations 67

Figures for Chapter 2 71

Chapter 3. Hopf Bifurcation in Plasma Kinetic Theory 89

The Model 91

Linear Spectrum 97

Adjoints and Biorthogonality 102

Linear Instability 106

Computing the Center Manifold 107

The Amplitude Equation 113

Dispersion Relations 115

Low Density Beam 118

Equal Density Beam 123

The $\nu_c \to 0$ Limit 126

Figures for Chapter 3 128

Appendix 186

Calculation of the Transformed Vector Field 188

Determining $\phi^{(2)}(\eta)$ and $\phi^{(3)}(\eta)$ 195

Calculation of $\tilde{\mathcal{V}}_+^{(3,2)}$ and $\tilde{\mathcal{V}}_+^{(5,3)}$ 202

Change of Basis Formulas 208

Final Remarks 213

References 214

Introduction

Whether a plasma is created under laboratory conditions or discovered in some natural setting, its physical state is rarely that of thermal equilibrium. The various mechanisms and instabilities which drive a plasma toward thermal equilibrium are therefore of central importance to the physics of these systems. From one perspective or another most of the scientific literature on plasma is devoted to determining the stability of plasma states, enumerating the possible instabilities which can arise, and calculating the effect of such instabilities on the transport of particles, momentum, and energy through the plasma. Because a plasma exerts forces on itself through self-generated electric and magnetic fields, a self-consistent study of a plasma instability is inevitably a nonlinear analysis. This makes the physics and the mathematics subtle and difficult.

For many plasma problems, existing mathematical theory does not apply,

and physicists proceed by inventing their own methods, and by making approximations on the strength of physical argument. Conversely new developments in mathematics can allow previously intractable physics problems to be treated with greater rigor, with fewer uncontrolled approximations, and often with more insight. This provides a useful check on heuristically developed physical theories, and stimulates the mathematical development through the challenge of concrete applications. Hopefully the relationship between the broad subject of plasma instabilities and the rapidly growing field of bifurcation theory will develop in this way.

To succinctly describe the subject matter of bifucation theory requires the abstract viewpoint of dynamical systems. A dynamical system is an evolution equation (or equation of motion)

$$\frac{dx}{dt} = V(x) \qquad x \in M \tag{I.1}$$

defined on some state space or phase space, M. For example if $M = \Re^n$, then the evolution equation is simply a system of n first order ordinary differential equations. For partial differential equations, M is a function space. The solutions of (I.1) describe curves through M; these curves collectively define the ***flow*** of (I.1). If the evolution equation depends on a free parameter, denoted by μ, then as μ varies the flow varies. In particular there can be critical values $\mu = \mu_c$ at which the flow changes in a ***qualitative*** way. When this happens, a ***bifurcation*** has occurred. In broadest terms, bifurcation theory studies these qualitative

changes.

A specific and relatively well understood example is ***Hopf bifurcation.*** Here the qualitative change in the flow occurs in the neighborhood of an equilibrium or fixed point. For the μ values of interest, let $x = 0$ be the fixed point, i.e. assume

$$V_\mu(0) = 0,$$

where the dependence of the flow on μ is now explicitly indicated. As discussed in Chapter 1, the stability of $x = 0$ with respect to small perturbations is determined by the eigenvalue spectrum of a matrix $DV_\mu(0)$ (or more generally a linear operator). Here $DV_\mu(x)$ is the usual derivative,

$$(DV_\mu(x))_{ij} = \frac{\partial V_\mu{}^i}{\partial x^j}(x).$$

When all eigenvalues have strictly negative real parts, then $x = 0$ attracts nearby solution curves and the fixed point is asymptotically stable; for a proof see Arnol'd (1973). When there are eigenvalues with positive real parts then solution curves are repelled from $x = 0$, and the equilibrium is unstable. A bifurcation occurs when one or more of the eigenvalues for a stable equilibrium cross the imaginary axis as μ increases through μ_c. If the instability is triggered by the crossing of a single complex conjugate pair of eigenvalues, then it is a Hopf bifurcation.

In its simplest form, Hopf bifurcation marks either the creation or the annihilation of a periodic orbit. In the first case, the fixed point is unstable for

$\mu > \mu_c$ but in the process of becoming unstable it "emits" a stable periodic orbit whose amplitude grows as $\sqrt{\mu - \mu_c}$, see Fig. (I.1 a). The second possibility involves a stable fixed point ($\mu < \mu_c$) with an unstable periodic orbit in its neighborhood. As μ approaches μ_c, the unstable orbit collapses onto the fixed point and for $\mu > \mu_c$ only an unstable fixed point survives, see Fig. (I.1 b). In either case the flow near $x = 0$ changes qualitatively when $(\mu - \mu_c)$ changes sign. The theory of Hopf bifurcation gives computable criteria which distinguish these two possibilities. Both possibilities occur in applications, but the theory is most useful when the bifurcation yields a stable periodic orbit (or limit cycle) since then the new stable state can be predicted and its physically relevant properties calculated.

When an evolution equation, describing the dynamics of a physical system, exhibits a Hopf bifurcation, as in Fig. (I.1 a), the experimentally observable properties of the system change in a marked way. A time independent stable equilibrium yields a stable nonlinear oscillation characterized by a single frequency. Observables of the system oscillate at this frequency. Hopf bifurcation is dynamic, i.e. a time dependent state results, and it serves as a simple example of certain phenomena which are quite generally associated with the dynamics of instabilities. For instance, as is clear from Fig. (I.1 a), at criticality the equilibrium state is weakly stable or unstable due to nonlinear effects, and relaxation rates are very slow. In the theory of phase transitions, this is described as

"critical slowing down" (see Hohenberg and Halperin (1977)).

Marsden and McCracken (1976) give a diverse list of phenomena that can be analyzed as Hopf bifurcations which includes biological models, mechanical systems, and geophysical problems. More recently Holmes and Marsden (1978) described the onset of flutter in an airfoil as a Hopf bifurcation, Knobloch and Proctor (1981) similarly identified one of the instabilities in a model of double diffusive convection, and Rand (1982) has given a lucid description of several Couette flow experiments using bifurcation theory in conjunction with group theory. There are many other examples. These last three are of particular interest because the evolution equations involved are partial differential equations.

In qualitative terms this transition from equilibrium to oscillation is frequently discovered in models of plasma behavior: a stable quiescent plasma becomes unstable as some parameter is varied and the instability is marked by the onset of unstable collective oscillations or waves. Such a transition is clearly a candidate for Hopf bifurcation.

There are prerequisites however if the version of Hopf bifurcation described above is to apply. The plasma model must be ***dissipative***. Physically this means that the model should include some dissipative process such as collisions. Abstractly a dissipative system produces a flow which contracts volumes onto attractors such as fixed points, limit cycles, or more complicated sets. In contrast, Hamiltonian systems have flows which conserve volumes in phase space;

this precludes the existence of attractors. (There are bifurcations in Hamiltonian systems analogous to Hopf bifurcation; they will be briefly mentioned in Chapter 3.) A second prerequisite is the requirement that the equilibrium become unstable due to a simple complex conjugate pair of eigenvalues crossing the imaginary axis. This requirement can be relaxed to allow a ***finite*** number of eigenvalues to cross simultaneously, but the resulting instability will have dynamics considerably more complicated than that shown in Fig. (I.1). Examples of these more complex finite mode instabilities are discussed in Takens (1974), Langford (1979), Guckenheimer (1981), Guckenheimer and Holmes (1983), and Scheurle and Marsden (1982). (For plasma models which take the plasma to have infinite spatial extent, instabilities are frequently characterized by a continuum of unstable eigenvalues. Such problems have been attacked by "envelope" methods which are somewhat distinct from the Hopf bifurcation theory discussed here, see Newell and Whitehead (1969) and Newell (1979).)

In spite of the limitations implied by these prerequisites, there are at least two motivations for modeling plasma instabilities as Hopf bifurcations. The first motivation is practical. When a stable equilibrium is destroyed by the onset of growing linear waves, a variety of questions becomes important: How does the wave growth saturate when nonlinear effects are included? Is the saturated state stable? What frequencies, electromagnetic fields, and transport properties characterize the new nonlinear state? If the instability can be analyzed

as a Hopf bifurcation, the calculations required to answer these questions are straightforward though often lengthy. Even nicer, some of these questions turn out to be the same, e.g. if the Hopf bifurcation produces a supercritical periodic orbit (the saturated state), then that orbit is always stable. Moreover, the calculations required to analyze a Hopf bifurcation can be performed in a formalism general enough to be applied to any such bifurcation, regardless of the details of the particular model.

The second motivation is one of principle, and derives from the realization that deterministic, low dimensional evolution equations may generate flows so complex that the resulting physical state is turbulent. To decide if this deterministic turbulence is actually relevant to observed phenomena in plasma is a question which, on the theoretical side, requires that one locate such complex dynamics in the flows of realistic kinetic or fluid plasma equations. Although this task is not accomplished in this thesis, the methods applied here to analyze Hopf bifurcation offer a promising way to locate exotic phenomena such as strange attractors in plasma dynamics. This opportunity exists because the nonlinear dynamics associated with plasma instabilities involving a finite number of eigenvalues is essentially finite dimensional. By deriving the essential finite dimensional system, and locating there a turbulent state associated with a chaotic attractor, the existence of the attractor is reliably established for the full system. Although such a result would apply only to special regions of parameter space,

e.g. neighborhoods of μ_c, it would demonstrate the relevance of low dimensional strange attractors for infinite dimensional systems in a setting free of the ambiguities which surround numerical calculations based on finite mode truncations. Thus the second motivation is simply this: by locating plasma instabilities which correspond to (degenerate) Hopf bifurcations involving three eigenvalues (one real, one conjugate pair) or four eigenvalues (two conjugate pairs) certain forms of plasma turbulence may be analyzed with finite dimensional models.

In Chapter 1, the mathematical theory of Hopf bifurcation is presented. This consists of two distinct sets of ideas. First, associated with the dynamics of Hopf bifuraction are ***invariant nonlinear manifolds*** which allow the problem to be reduced to two dimensions. Second, the resulting two dimensional evolution equation can always be written in a characteristic polar variable form.

$$\begin{aligned} \frac{dr}{dt} &= \mu r + a_1 r^3 + a_2 r^5 + O(r^7) \\ \frac{d\theta}{dt} &= -\Lambda + b_1 r^2 + b_2 r^4 + O(r^6) \end{aligned} \tag{I.2}$$

Here $\mu \pm i\Lambda$ is the conjugate eigenvalue pair associated with the instability and the coefficients $\{a_i\}$ and $\{b_i\}$ are explicitly computable functions of the parameters in the problem. (Although the bifurcation parameter μ in $V_\mu(x)$ is not necessarily the real part of the eigenvalue $\mu + i\Lambda$, there is no loss of generality in assuming this to be the case.) These equations constitute the ***normal form equations*** for Hopf bifurcation; they describe the essential nonlinear effects associated with the instability.

In Chapters 2 and 3, this theory is applied to two Hopf bifurcations drawn from the plasma physics literature. The first example, discussed in Chapter 2, occurs in a finite dimensional model of three interacting plasma waves due to Wersinger, Finn, and Ott (1980). The stable fixed point arises from a balance between the growth of an unstable wave and the decay of two damped waves. If the decay rate of the damped waves is increased the balance becomes "over stable"; this transition is a Hopf bifurcation. The resulting periodic orbit has been studied numerically by Wersinger, et al. (1980); they observed a cascade of period doubling bifurcations resulting in aperiodic motion.

This model presents the interesting feature that the normal form coefficient a_1 in (I.2) changes sign along the bifurcation surface in parameter space. When $a_1 = 0$ then higher order nonlinear effects are crucial. This degenerate bifurcation is discussed in detail; an analysis which requires the normal form coefficients a_1 and a_2 on a neighborhood of the critical parameter values. The calculation of a_2 for this case slightly generalizes the results of Hassard and Wan (1978).

The second example, discussed in Chapter 3, is a simple kinetic equation which exhibits as Hopf bifurcations some familiar microinstabilities; here the setting is infinite dimensional. The model considers electron dynamics in a weakly ionized gas and describes the electron distribution function using the Vlasov-Poisson equations supplemented by a Krook collision term.

The spectral analysis of Case (1959) for the Vlasov-Poisson system is easily

extended to this model to determine the linear spectrum. For an initial distribution function consisting of a plasma component and a beam component the linear dispersion relation is solved to determine the bifurcation surface as a function of beam velocity, beam temperature, beam density, and wave number. The normal form analysis shows $a_1 < 0$ in all cases, and provides explicit results for the saturated distribution function.

Without collisions, the Vlasov-Poisson equations are Hamiltonian; thus the collisionless limit of the Hopf bifurcation is a Hamiltonian bifurcation. Moreover for this limiting Hamiltonian bifurcation a degenerate conjugate pair of eigenvalues is embedded in a continuous spectrum (the van Kampen continuum) at criticality. This makes the collisionless limit of the Hopf normal form singular, i.e. the normal form coefficients become infinite due to divergences arising from resonance denominators. This singular structure raises the interesting question as to whether the collisionless version of the instability can be captured by a finite dimensional normal form, and what those normal form equations might be.

Another interesting aspect of the collisional model is the existence of parameter values for which two conjugate pairs simultaneously cross the imaginary axis. This would correspond to the onset of unstable plasma oscillations at two distinct wavelengths. As indicated earlier such a degenerate bifurcation may involve chaotic dynamics (Guckenheimer and Holmes (1983)).

Figure Captions

Figure (I.1) The two possibilities for Hopf bifurcation when the normal form coefficient a_1 in (I.2) does not vanish at criticality. For these diagrams Λ in (I.2) is assumed negative. (a) In supercritical ($a_1 < 0$) Hopf bifurcation there is a stable periodic orbit for $\mu > \mu_c$. (b) In subcritical ($a_1 > 0$) Hopf bifurcation there is an unstable periodic orbit for $\mu < \mu_c$. In both cases the stability of the fixed point changes at $\mu = \mu_c$, and at $\mu = \mu_c$ the fixed point is weakly attracting or weakly repelling due to nonlinear effects.

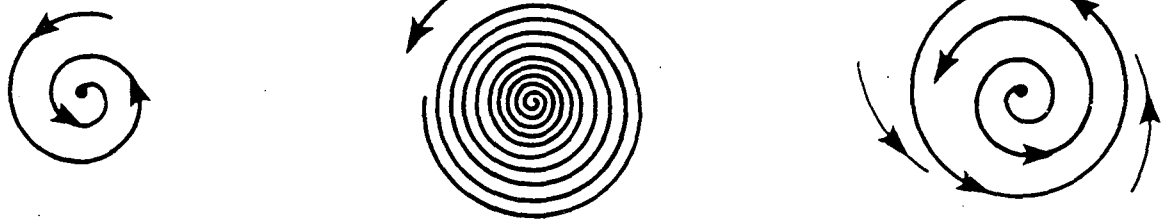

$\mu < \mu_c$ $\mu = \mu_c$ $\mu > \mu_c$

$a_1 < 0$

Figure (I.1a)

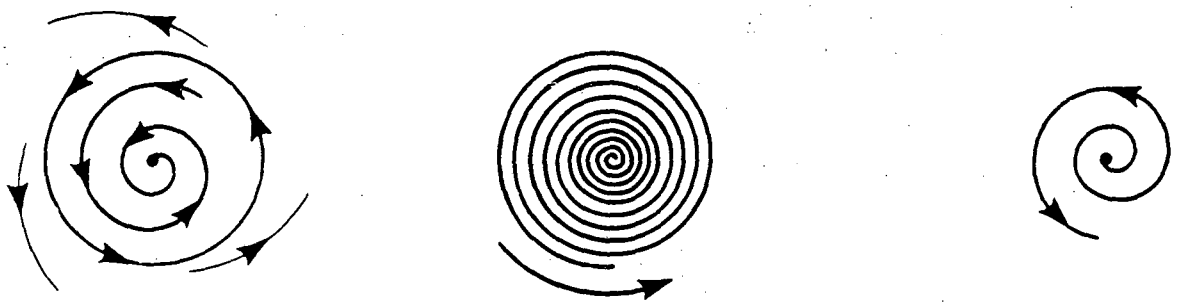

$\mu < \mu_c$ $\mu = \mu_c$ $\mu > \mu_c$

$a_1 > 0$

XBL 837-470

Figure (I.1b)

CHAPTER 1

Invariant Manifolds and Normal Forms

Hopf bifurcation in its simplest form is a ***two dimensional*** phenomenon; this is true regardless of the actual dimension of the dynamical system exhibiting the bifurcation. To understand this fundamental fact one may use the theory of stable, center, and unstable manifolds. This theory can be presented at various levels of abstraction; my discussion will be intuitive, pictorial, and hopefully practical. For more precise mathematical discussions the reader is referred to the growing review literature; see for example Marsden and McCracken (1976), Carr (1981), Holmes (1981), Hassard, Kazarinoff, and Wan (1981), or Guckenheimer and Holmes (1983).

The stable, center, and unstable manifolds which occur in bifurcation theory are nonlinear generalizations of the stable, center, and unstable linear eigenspaces which arise in linear stability theory. For this reason I shall first quickly review

this linear theory, then describe the manifolds. For Hopf bifurcation, often only the stable and center manifolds are present, and the structure they impose on the dynamics allows the bifurcation analysis to be reduced to two dimensions. The calculations required for this reduction will be described, and the virtues and limitations of the resulting equations will be discussed. For all of this, the setting will be finite dimensional, e.g. a flow on $\mathfrak{R}^n$; this is for simplicity–the techniques work for partial differential equations as well. The additional technical issues which arise in infinite dimensional applications are discussed in Marsden and McCracken (1976), Holmes and Marsden (1978), Iooss and Joseph (1980), and Hassard, Kazarinoff, and Wan (1981).

Linear Stability Theory

The starting point for the theory is always the same: an evolution equation for the dependent variable $x(t)$.

$$\frac{dx}{dt} = \mathcal{L}_\mu x + \mathcal{N}_\mu(x) \tag{1.1}$$

Here $\mathcal{L}_\mu$ is a linear operator which depends on a parameter μ. $\mathcal{N}_\mu$ is a smooth nonlinear operator with the property $\mathcal{N}_\mu(0) = 0$, so that $x = 0$ is a stationary solution (fixed point).

To be concrete, assume the evolution equation comes from a smooth vector field, $V_\mu(x)$, on $\mathfrak{R}^n$ such that $V_\mu(0) = 0$. Then the dynamics is governed by

$$\frac{dx}{dt} = V_\mu(x) \qquad x \in \Re^n.$$

This can be written in the form (1.1) by letting $\mathcal{L}_\mu = DV_\mu(0)$, and taking $\mathcal{N}_\mu(x)$ to be the higher order terms in the formal Taylor expansion: $\mathcal{N}_\mu(x) = V_\mu(x) - DV_\mu(0) \cdot x$.

Given that $x = 0$ corresponds to an equilibrium, then its stability against perturbations must be determined. This is first done for the linearized dynamics,

$$\frac{dx}{dt} = \mathcal{L}_\mu x. \tag{1.2}$$

The spectrum of $\mathcal{L}_\mu$, denoted $\sigma(\mathcal{L}_\mu)$, controls the growth or damping of perturbations. On $\Re^n$, $\sigma(\mathcal{L}_\mu)$ consists of n eigenvalues (counting over multiple eigenvalues). Consider such a spectrum shown in Fig. (1.1a); there are eigenvalues in the left half plane $\{\lambda_i^s\}_{i=1}^{n_s}$, on the imaginary axis $\{\lambda_i^c\}_{i=1}^{n_c}$, and in the right half plane $\{\lambda_i^u\}_{i=1}^{n_u}$ such that $n_s + n_c + n_u = n$. Associated with these three sets of eigenvalues are the corresponding eigenvectors: $\{v_i^s\}_{i=1}^{n_s}$, $\{v_i^c\}_{i=1}^{n_c}$, and $\{v_i^u\}_{i=1}^{n_u}$. (In the event that an eigenvalue has an algebraic multiplicity greater than its geometric multiplicity, then these sets of eigenvectors include the generalized eigenvectors also.) Each set of eigenvectors spans a linear subspace of $\Re^n$,

$$\text{span of}\{v_i^s\}_{i=1}^{n_s} = E^s$$

$$\text{span of}\{v_i^c\}_{i=1}^{n_c} = E^c$$

$$\text{span of}\{v_i^u\}_{i=1}^{n_u} = E^u$$

and $\Re^n = E^s \oplus E^c \oplus E^u$.

An arbitrary perturbation, $x(0)$, can be expanded,

$$x(0) = \sum_{i=1}^{n_s} x_i^s(0)v_i^s + \sum_{i=1}^{n_c} x_i^c(0)v_i^c + \sum_{i=1}^{n_u} x_i^u(0)v_i^u$$

and its time evolution under (1.2) simply determined (ignoring the unimportant complications due to generalized eigenvectors).

$$x(t) = \sum_{i=1}^{n_s} x_i^s(0)e^{\lambda_i^s t}v_i^s + \sum_{i=1}^{n_c} x_i^c(0)e^{\lambda_i^c t}v_i^c + \sum_{i=1}^{n_u} x_i^u(0)e^{\lambda_i^u t}v_i^u \qquad (1.3)$$

As t increases the first group of terms decays exponentially, the second group oscillates, and the third group grows exponentially; accordingly E^s is called the ***stable subspace***, E^c the ***center subspace***, and E^u the ***unstable subspace***. The decomposition of $\Re^n$ into these subspaces provides a complete picture of the linearized dynamics, see Fig. (1.1b). Furthermore from (1.3) each subspace is clearly invariant under (1.2). This means that an initial perturbation lying wholly within E^s or E^c or E^u will evolve without leaving that subspace.

If the calculation of $\sigma(\mathcal{L}_\mu)$ reveals that $n_c = n_u = 0$, then all perturbations decay in linear approximation and $x = 0$ is ***linearly*** stable. In finite dimensions, such linear stability implies ***nonlinear*** stability, i.e. sufficiently small perturbations will decay under the full nonlinear dynamics of (1.1). For partial differential equations there are results analogous to this, though their precise statement is more technical (Holmes and Marsden (1978)). In applications these conclusions of nonlinear stability are not always relevant, since the allowed scale of amplitude perturbations may be unphysically small.

Nonlinear Effects: Invariant Manifolds

When the nonlinear effects represented by $N_\mu(x)$ are reintroduced, the dynamics of the linear eigenvectors are coupled by the nonlinear terms and the linear spaces E^s, E^c, and E^u are no longer invariant. There are however nonlinear analogues of the linear eigenspaces. Intuitively, the nonlinear terms distort the solutions of the linear eigenspaces so that the flat linear eigenspaces are "warped" into curved surfaces or manifolds. These manifolds organize the dynamics of the nonlinear problem just as the linear eigenspaces serve to structure the linear dynamics.

Associated with E^s and E^u are unique, local, invariant manifolds: the ***stable manifold*** W^s and the ***unstable manifold*** W^u, respectively. These manifolds and their relation to the underlying linear spaces are indicated in Fig. (1.2a). Each contains the fixed point $x = 0$, and at $x = 0$ is tangent to the appropriate linear eigenspace. In virtue of this fact, each manifold has the same dimension as its associated linear subspace. Furthermore, each local manifold is invariant with respect to the ***full*** nonlinear dynamics: if an initial condition $x(0)$ belongs to W^s or W^u, then, for some time interval $0 \leq t < T$, the solution $x(t)$ to (1.1) lies within the manifold containing $x(0)$. Assuming the flow of (1.1) is well defined for $-\infty < t < \infty$, i.e. globally defined, then the solution curves composing the local manifolds may be globally extended. This extension yields the global stable and unstable manifolds. The relationship between the local

and global manifolds may be subtle; Palis and de Melo (1982) give a simple two dimensional example of a fixed point whose local stable and unstable manifolds are distinct one dimensional sets, but whose global stable and unstable manifolds exactly coincide because they form homoclinic orbits. Furthermore, although the structure of the local manifolds has the simplicity indicated in Fig. (1.2a), the global manifolds can have very complicated shapes.

Similar to E^s and E^u, the center eigenspace has an associated local invariant manifold, the *center manifold* W^c, which is tangent to E^c at $x = 0$. Unlike W^s and W^u, the center manifold may not be unique; Kelley (1967) and Guckenheimer and Holmes (1983) give simple examples of fixed points which have an infinite family of center manifolds. Moreover, less is known about the existence of global center manifolds. Fenichel (1979) and Carr (1981) discuss some singular perturbation problems for which global information about W^c is available, but these results are typically less general and more complicated than the corresponding global theory for W^s and W^u.

For W^c, the difficulty in proving global existence and the possible lack of uniqueness are rooted in the fact that, unlike the stable/unstable manifolds, the flow on a center manifold cannot be characterized in any general way. In particular this prevents the global existence of the center manifold from being established with the same methods used for W^s and W^u. For the applications to bifurcation phenomena considered in this thesis, these issues of global existence

and uniqueness are not essential.

The dynamics of solution curves in W^s or W^u is trivial, at least near $x = 0$. As $t \to \infty$ all solution curves in W^s approach $x = 0$, and as $t \to -\infty$ solution curves in W^u approach $x = 0$; in both cases the asymptotic rate of approach is exponential since the linearized dynamics dominates. As mentioned above, no simple general description is possible for the dynamics in W^c; at $x = 0$ the linear stability is neutral and nonlinear effects remain essential. When the dimension of W^c is greater than two, the center manifold dynamics may encompass all the complex dynamics studied in dynamical systems theory: aperiodic motion, chaotic recurrence, Smale horseshoes, strange attractors, etc. This observation provides strong motivation for attacking bifurcation problems along the lines described in the next section.

Invariant Manifolds for Hopf Bifurcation

In Hopf bifurcation, a stable fixed point at $x = 0$ becomes unstable as a parameter μ is varied. Stability is lost because a complex conjugate pair of eigenvalues in $\sigma(\mathcal{L}_\mu)$ cross the imaginary axis into the right half plane as μ is increased through zero. (The prescription that the fixed point is at $x = 0$ and the critical parameter value is $\mu = 0$ is convenient, and entails no loss of generality.) At criticality, $\mu = 0$ and the eigenvalue pair λ, $\bar{\lambda}$ are pure imaginary, see Fig. (1.2b). (Here the overbar denotes complex conjugation.) Their eigenvectors

satisfy

$$\mathcal{L}_\mu \Psi = \lambda \Psi$$

$$\mathcal{L}_\mu \overline{\Psi} = \overline{\lambda}\,\overline{\Psi}$$

and span the two dimensional linear eigenspace $\mathbf{E}^c$. For this bifurcation there is a two dimensional center manifold and an $(n-2)$ dimensional stable manifold, see Fig. (1.3a).

Near $x = 0$, the solution curves in these manifolds define distinct time scales. For solutions starting near $x = 0$ but not contained within either manifold, the influence of the stable manifold rapidly pushes the solution curves toward the center manifold on a *fast time scale*; on a *slow time scale*, the flow of these solutions is controlled by the dynamics on the center manifold. This is the intuitive basis for the property of W^c known as *local attractivity* which is precisely stated as follows: *there exists a neighborhood U of the fixed point $x = 0$ such that if the solution $x(t)$, corresponding to an initial condition $x(0) \in U$, remains in U for all $t > 0$ then $x(t)$ approaches W^c as $t \to \infty$.*

For $\mu = 0$, $x = 0$ is no longer linearly stable and perturbations may grow; how these perturbations evolve is a nonlinear problem. If we are willing to wait for the local attraction of W^c to pull the perturbed solution close to W^c then the time development of the perturbation involves only the dynamics on W^c. Thus the time asymptotic behavior of the instability requires an analysis of the center manifold dynamics; this however is only a two dimensional problem. This reduction of the time asymptotic problem to two dimensions in fact persists for μ

small and *positive*. Intuitively this is so because for $\mu > 0$ the two dimensional center manifold is replaced by a two dimensional unstable manifold which is locally attracting and controls the time asymptotic behavior. This intuition may be rigorously justified by considering the "suspended system":

$$\begin{aligned} \frac{dx}{dt} &= \mathcal{L}_\mu x + \mathcal{N}_\mu(x) \\ \frac{d\mu}{dt} &= 0, \end{aligned} \tag{1.1s}$$

obtained by "suspending" an equation for the parameter from the original system (1.1) (Ruelle and Takens (1971), Hassard et al. (1981)). Obviously (1.1) and (1.1s) are equivalent; nevertheless we learn something by analyzing the invariant manifolds of the fixed point $(x, \mu) = (0, 0)$ for (1.1s). Now at $\mu = 0$, in addition to the conjugate pair of eigenvalues, there is also a real eigenvalue at zero because of the equation $d\mu/dt = 0$. Thus for (1.1s) there is a three dimensional center manifold and an $(n-2)$-dimensional stable manifold.

The three dimensional center manifold must contain an *interval* of the μ-axis about the point $\mu = 0$; this follows from its local attractivity. An initial condition $(x, \mu) = (0, \mu_0)$, contained in the neighborhood U (as described in the definition of local attractivity above), is a fixed point, and necessarily corresponds to a solution which remains in U for all $t > 0$. Therefore the point $(0, \mu_0)$ in fact belongs to the three dimensional center manifold.

Because $d\mu/dt = 0$ in (1.1s) if we take a "slice" of our three dimensional center manifold by fixing the value of μ, the result is a *two dimensional* invariant

locally attracting manifold. For example, the slice corresponding to $\mu = 0$ is the two dimensional center manifold for (1.1). A slice at $\mu > 0$ gives the two dimensional unstable manifold of $x = 0$. In this way, the three dimensional center manifold of (1.1s) may be regarded as a 1-parameter family of two dimensional invariant manifolds. Let W_μ denote this family; each member of W_μ is tangent at $x = 0$ to the linear space spanned by the eigenvectors Ψ and $\overline{\Psi}$.

This picture leads to the following strategy: "project out" the two dimensional vector field which describes the flow on W_μ, then analyze that flow to understand the asymptotic development of the instability.

Deriving the two dimensional vector field on W_μ requires two steps. First a description of W_μ near $x = 0$ must be calculated, then the restriction of the evolution equation to W_μ is obtained. The analysis of the two dimensional dynamics leads to the theory of normal forms. This is discussed in a subsequent section.

Describing W_μ near $x = 0$ requires constructing local coordinates for W_μ on a neighborhood of $x = 0$. Since W_μ contains $x = 0$ and is tangent there to the $(\Psi, \overline{\Psi})$-plane, local coordinates may be constructed as a mapping from the $(\Psi, \overline{\Psi})$-plane to W_μ, see Fig. (1.3b). Let the coordinates of a point in the $(\Psi, \overline{\Psi})$-plane be $(A, \overline{A})$, then this mapping defines a function $h(A, \overline{A})$

$$h: \mathbb{R}^2 \to \mathbb{R}^{n-2}, \qquad h(0,0) = 0$$

with the property $(A, \overline{A}, h(A, \overline{A})) \in W_\mu$ for $(A, \overline{A})$ sufficiently close to $x = 0$. Away from $x = 0$, W_μ may develop folds which preclude such a simple description, but h is well defined on a neighborhood of $x = 0$.

To determine h requires a rewriting of the evolution equation. Represent the general solution $x(t)$ to (1.1) in the form

$$x(t) = A(t)\Psi + \overline{A}(t)\overline{\Psi} + S(t) \tag{1.4}$$

where $A(t)$ is a complex-valued function of time, and $S(t)$ represents the component of $x(t)$ transverse to the $(\Psi, \overline{\Psi})$-plane. Precisely this means that

$$\langle \tilde{\Psi}, S \rangle = \langle \overline{\tilde{\Psi}}, S \rangle = 0$$

where $\tilde{\Psi}$ and $\overline{\tilde{\Psi}}$ are adjoint eigenvectors to Ψ and $\overline{\Psi}$ respectively, and the bracket $\langle \bullet, \bullet \rangle$ denotes the inner product between adjoints and eigenvectors. The biorthogonality relations between adjoint eigenvectors and eigenvectors are denoted by the pairings,

$$\langle \tilde{\Psi}, \Psi \rangle = \langle \overline{\tilde{\Psi}}, \overline{\Psi} \rangle = 1$$

$$\langle \tilde{\Psi}, \overline{\Psi} \rangle = \langle \overline{\tilde{\Psi}}, \Psi \rangle = 0.$$

The explicit realization of these pairings will vary from one application to the next; here their only role is to allow the component of $x(t)$ in the $(\Psi, \overline{\Psi})$-plane to be split off in an unambiguous way. The definition of A is then

$$A(t) \equiv \langle \tilde{\Psi}, x(t) \rangle.$$

To determine dA/dt and dS/dt, insert (1.4) into (1.1),

$$\frac{dA}{dt}\Psi + \frac{d\overline{A}}{dt}\overline{\Psi} + \frac{dS}{dt} = \mathcal{L}_\mu(A\Psi + \overline{A}\,\overline{\Psi} + S) + \mathcal{N}_\mu(x). \tag{1.5}$$

Projecting with $\tilde{\Psi}$ gives

$$\frac{dA}{dt} = \lambda A + \langle \tilde{\Psi}, \mathcal{N}_\mu(x) \rangle \tag{1.6}$$

where I have used $\langle \tilde{\Psi}, \mathcal{L}_\mu S \rangle = 0$. This is true since $\tilde{\Psi}$ is an eigenvector for the adjoint operator $\mathcal{L}_\mu^\dagger$:

$$\langle \tilde{\Psi}, \mathcal{L}_\mu S \rangle = \langle \mathcal{L}_\mu^\dagger \tilde{\Psi}, S \rangle = \langle \lambda \tilde{\Psi}, S \rangle = 0.$$

Now subtract $(dA/dt)\Psi + (d\overline{A}/dt)\overline{\Psi}$ from (1.5) to obtain the equation for transverse dynamics:

$$\frac{dS}{dt} = \mathcal{L}_\mu S + \mathcal{N}_\mu(x) - \langle \tilde{\Psi}, \mathcal{N}_\mu(x) \rangle - \overline{\langle \tilde{\Psi}, \mathcal{N}_\mu(x) \rangle}. \tag{1.7}$$

Together (1.6) and (1.7) are equivalent to (1.1); all that has been accomplished is a decoupling of the $A(t)$ and $S(t)$ dynamics at linear order. This is the desired rewriting of the dynamics mentioned above. Note that the dA/dt equation is a two dimensional system of ordinary differential equations. However this system is not autonomous since $\langle \tilde{\Psi}, \mathcal{N}_\mu(x) \rangle$ depends on $S(t)$. The equation for dS/dt is an $(n-2)$ dimensional system of equations if the original problem occurs in n dimensions, but when (1.1) is a partial differential equation then so is (1.7).

To see how this decomposition allows the coordinate function, h, to be determined, observe that for a solution $x^c(t)$ lying in W_μ(near $x = 0$) (1.4) becomes

$$x^c(t) = A(t)\Psi + \overline{A}(t)\overline{\Psi} + S^c(t) \tag{1.8}$$

where $S^c(t) = h(A(t), \overline{A}(t))$. This means that there are two ways to calculate the transverse variation, dS^c/dt, for these solutions. First, directly from (1.7),

$$\frac{dS^c}{dt} = \mathcal{L}_\mu S^c + \mathcal{N}_\mu(x^c) - \langle \tilde{\Psi}, \mathcal{N}_\mu(x^c) \rangle - \overline{\langle \tilde{\Psi}, \mathcal{N}_\mu(x^c) \rangle}.$$

Secondly, using $S^c = h$ and (1.6)

$$\begin{aligned} \frac{dS^c}{dt} &= \left[\frac{\partial h}{\partial A}\frac{dA}{dt} + \frac{\partial h}{\partial \overline{A}}\frac{d\overline{A}}{dt} \right]_{x = x^c} \\ &= \frac{\partial h}{\partial A}\Big(\lambda A + \langle \tilde{\Psi}, \mathcal{N}_\mu(x^c) \rangle \Big) + \frac{\partial h}{\partial \overline{A}}\Big(\overline{\lambda A} + \overline{\langle \tilde{\Psi}, \mathcal{N}_\mu(x^c) \rangle} \Big). \end{aligned}$$

Equating these two results for dS^c/dt gives

$$\begin{aligned} \frac{\partial h}{\partial A}(\lambda A + \langle \tilde{\Psi}, \mathcal{N}_\mu(x^c) \rangle) + \frac{\partial h}{\partial \overline{A}}(\overline{\lambda A} + \overline{\langle \tilde{\Psi}, \mathcal{N}_\mu(x^c) \rangle}) \\ = \mathcal{L}_\mu h + \mathcal{N}_\mu(x^c) - \langle \tilde{\Psi}, \mathcal{N}_\mu(x^c) \rangle - \overline{\langle \tilde{\Psi}, \mathcal{N}_\mu(x^c) \rangle} \end{aligned} \tag{1.9}$$

which is a nonlinear partial differential equation for $h = h(A, \overline{A})$ to be solved subject to $h(0,0) = 0$ and $\langle \tilde{\Psi}, h \rangle = \langle \overline{\tilde{\Psi}}, h \rangle = 0$. Geometrically, (1.9) expresses the invariance of W_μ, and will be referred to as the invariance equation.

In practice, (1.9) cannot be solved exactly; fortunately it is sufficient to obtain an asymptotic solution for h which is accurate for small $|A|$. For this purpose, h is computed to some finite order as a power series in $A, \overline{A}$. This is done explicitly in the examples discussed in Chapters 2 and 3. Wan (1977) has shown that the possible nonuniqueness of W^c does not affect this calculation; even if there are several center manifolds, the asymptotic power series of each center manifold is the same.

Given h, the dynamics on W_μ is obtained by substituting (1.8) into (1.6).

$$\frac{dA}{dt} = \lambda A + \langle \tilde{\Psi}, \mathcal{N}_\mu(x^c) \rangle \tag{1.10}$$

This is now a two dimensional, ***autonomous*** system; since x^c is independent of S, even the nonlinear terms are now decoupled. Thus near $x = 0$ the solutions in W_μ have the form of (1.8) where $A(t)$ satisfies (1.10). In terms of real coordinates (x, y), (1.10) becomes,

$$\frac{d}{dt}\begin{pmatrix} x \\ y \end{pmatrix} = \begin{pmatrix} \mu & \Lambda \\ -\Lambda & \mu \end{pmatrix}\begin{pmatrix} x \\ y \end{pmatrix} + \begin{pmatrix} \mathrm{Re}\langle \tilde{\Psi}, \mathcal{N}_\mu(x^c) \rangle \\ \mathrm{Im}\langle \tilde{\Psi}, \mathcal{N}_\mu(x^c) \rangle \end{pmatrix} \tag{1.11}$$

where $A(t) = x(t) + iy(t)$ and $\lambda = \mu - i\Lambda$.

Normal Forms for Hopf Bifurcation

For Hopf bifurcation with a simple complex conjugate pair of eigenvalues, there is a two dimensional vector field, denoted $\mathcal{V}(\varsigma)$, which determines the center manifold dynamics. For a time asymptotic analysis of the bifurcation, only the flow on the center manifold is relevant. Therefore once the center manifold vector field is known any simplification of its structure is welcome. The theory of normal forms allows this vector field to be simplified as much as possible. What this means is that by making nonlinear coordinate changes, certain nonlinear terms in $\mathcal{V}(\varsigma)$ can be eliminated. There are however essential nonlinear terms which cannot be removed and these determine the normal form of $\mathcal{V}(\varsigma)$.

In its philosophy and its results, normal form theory is closely related to the techniques of averaging and Lie transforms. Chow and Mallet-Paret (1977) apply the averaging method to the calculation of normal forms, and in Chow and Hale (1982) Lie series are used to implement averaging. For recent applications of Lie methods to Hamiltonian mechanics and plasma physics see Cary (1981), Cary and Kaufman (1981), and Littlejohn (1979).

In this section the normal form theory appropriate for two dimensional Hopf bifurcation will be presented. My discussion will be heuristic; treatments which are more rigorous may be found in Holmes (1981), Takens (1974), or Guckenheimer and Holmes (1983). The theory is applied to an example in the next chapter.

Writing the two dimensional problem derived in (1.10) as

$$\frac{d\varsigma}{dt} = \mathcal{V}(\varsigma) \qquad \varsigma \in \Re^2 \tag{1.12}$$

where $\mathcal{V}(0) = 0$, and $\mathcal{V}(\varsigma)$ is assumed smooth enough to have a formal Taylor expansion:

$$\mathcal{V}(\varsigma) = \mathcal{V}^{(1)}(\varsigma) + \mathcal{V}^{(2)}(\varsigma) + \mathcal{V}^{(3)}(\varsigma) + \cdots . \tag{1.13}$$

Here $\mathcal{V}^{(j)}(\varsigma)$ is the j^{th} order piece of the expansion, it is a vector field whose components are homogeneous polynomials in $\varsigma = (x, y)$ of degree j. For Hopf bifurcation,

$$\mathcal{V}^{(1)}(\varsigma) = \begin{pmatrix} \mu & \Lambda \\ -\Lambda & \mu \end{pmatrix} \begin{pmatrix} x \\ y \end{pmatrix} \tag{1.14}$$

is the appropriate linear term. The conjugate eigenvalue pair is $\mu \pm i\Lambda$.

The goal is to remove $\mathcal{V}^{(2)}(\varsigma)$, $\mathcal{V}^{(3)}(\varsigma)$, etc. by coordinate changes which are smooth in their dependence on ς and well defined for all μ in a neighborhood of $\mu = 0$. To determine if this can be done, let $\Phi(\varsigma)$ be a diffeomorphism on $\Re^2$ which fixes the origin and defines new coordinates η.

$$\eta = \Phi(\varsigma) \qquad \Phi(0) = 0$$

Now choose the specfic form of $\Phi(\varsigma)$ to eliminate $\mathcal{V}^{(k)}(\varsigma)$ (for fixed $k \geq 2$) as completely as possible. An additional requirement is to leave undisturbed terms in $\mathcal{V}(\varsigma)$ of degree less than k. These goals require a coordinate change of the form,

$$\Phi(\varsigma) = \varsigma + \phi^{(k)}(\varsigma) = \eta \tag{1.15}$$

where $\phi^{(k)}(\varsigma)$ is homogeneous of degree k. Higher order terms in $\Phi(\varsigma)$ are irrelevant to the problem of removing $\mathcal{V}^{(k)}(\varsigma)$ and additional lower order terms in $\Phi(\varsigma)$ would alter the lower order terms in $\mathcal{V}(\varsigma)$. Near the origin $\Phi(\varsigma)$ is invertible with an inverse given by

$$\Phi^{-1}(\eta) = \eta - \phi^{(k)}(\eta) + O(\eta^{k+1}) \tag{1.16}$$

through k^{th} order terms.

In the new coordinates, the vector field becomes

$$\frac{d\eta}{dt} = \tilde{\mathcal{V}}(\eta) \equiv D\Phi(\Phi^{-1}(\eta)) \cdot \mathcal{V}(\Phi^{-1}(\eta)) \tag{1.17}$$

where

$$(D\Phi(\Phi^{-1}(\eta)))_{ij} = \frac{\partial \Phi^i}{\partial x^j}(\Phi^{-1}(\eta)).$$

Using (1.13), (1.15), and (1.16), the right hand side of (1.17) can be expanded through terms of order k. First for $\mathcal{V}(\Phi^{-1}(\eta))$ this gives

$$\begin{aligned}\mathcal{V}(\Phi^{-1}(\eta)) = \mathcal{V}^{(1)}(\eta) + \mathcal{V}^{(1)}(\eta) + \cdots + \mathcal{V}^{(k-1)}(\eta) + \mathcal{V}^{(k)}(\eta) \\ - D\mathcal{V}^{(1)}(\eta) \cdot \phi^{(k)}(\eta) + O(\eta^{k+1})\end{aligned} \tag{1.18}$$

and $D\Phi(\Phi^{-1}(\eta))$ has the expansion

$$\begin{aligned}D\Phi(\Phi^{-1}(\eta)) &= \left(I + D\phi^{(k)}\right)(\Phi^{-1}(\eta)) \\ &= I + D\phi^{(k)}(\Phi^{-1}(\eta)) \\ &= I + D\phi^{(k)}(\eta) + O(\eta^{(k+1)})\end{aligned} \tag{1.19}$$

where I is the identity operator. Multiplying (1.19) and (1.18) to get $\tilde{\mathcal{V}}(\eta)$ gives,

$$\begin{aligned}\tilde{\mathcal{V}}(\eta) = \mathcal{V}^{(1)}(\eta) + \cdots \mathcal{V}^{(k-1)}(\eta) + \mathcal{V}^{(k)}(\eta) - D\mathcal{V}^{(1)}(\eta) \cdot \phi^{(k)}(\eta) \\ + D\phi^{(k)}(\eta) \cdot \mathcal{V}^{(1)}(\eta) + O(\eta^{k+1}).\end{aligned} \tag{1.20}$$

This is the vector field in the new coordinates keeping terms of degree k in η; note that $\Phi(\varsigma)$ has not altered terms of degree less than k. At degree k $\Phi(\varsigma)$ introduces two new terms; appreciating their significance requires some additional terminology.

Denote the set of vector fields on $\mathfrak{R}^2$ whose components are homogeneous polynomials of degree k by $\mathcal{H}^{(k)}(\mathfrak{R}^2)$. This set is a linear vector space of dimension $2k+2$. For example a possible basis for $\mathcal{H}^{(2)}(\mathfrak{R}^2)$ is

$$\begin{pmatrix} x^2 \\ 0 \end{pmatrix}, \begin{pmatrix} xy \\ 0 \end{pmatrix}, \begin{pmatrix} y^2 \\ 0 \end{pmatrix}, \begin{pmatrix} 0 \\ x^2 \end{pmatrix}, \begin{pmatrix} 0 \\ xy \end{pmatrix}, \begin{pmatrix} 0 \\ y^2 \end{pmatrix}$$

so $\mathcal{H}^{(2)}(\Re^2)$ is six dimensional. Now consider a linear operator, $L^{(k)}$, on $\mathcal{H}^{(k)}$ defined by

$$L^{(k)}:\mathcal{H}^{(k)} \to \mathcal{H}^{(k)}$$

$$L^{(k)}(Y) \equiv [\mathcal{V}^{(1)}, Y] = DY \cdot \mathcal{V}^{(1)} - D\mathcal{V}^{(1)} \cdot Y$$

where $Y \in \mathcal{H}^{(k)}$ and $\mathcal{V}^{(1)}$ is the linear term in (1.20). As indicated, $L^{(k)}(Y)$ is the *Lie bracket* of the two vector fields $\mathcal{V}^{(1)}$ and Y. In terms of $L^{(k)}$, $\tilde{\mathcal{V}}(\eta)$ in (1.20) becomes

$$\tilde{\mathcal{V}}(\eta) = \mathcal{V}^{(1)}(\eta) + \cdots + \mathcal{V}^{(k)}(\eta) + \Big(L^{(k)}(\phi^{(k)})\Big)(\eta) + O(\eta^{k+1}).$$

Thus to eliminate $\mathcal{V}^{(k)}(\eta)$ entirely, $\phi^{(k)}(\eta)$ must solve

$$\mathcal{V}^{(k)}(\eta) + \Big(L^{(k)}(\phi^{(k)})\Big)(\eta) = 0. \tag{1.21}$$

This may be done if and only if the range of the linear operator $L^{(k)}$ contains $\mathcal{V}^{(k)}(\eta)$.

If the range of $L^{(k)}$, denoted $\mathcal{R}_L$, is all of $\mathcal{H}^{(k)}$ then $\mathcal{V}^{(k)}(\eta)$ may be removed; when $\mathcal{R}_L$ does not equal $\mathcal{H}^{(k)}$ then there is a direct sum decomposition of $\mathcal{H}^{(k)}$ into $\mathcal{R}_L$ and a complementary subspace, $\mathcal{R}_L^c$,

$$\mathcal{H}^{(k)} = \mathcal{R}_L \oplus \mathcal{R}_L^c$$

and only components of $\mathcal{V}^{(k)}(\eta)$ lying in $\mathcal{R}_L$ may be removed. The components of $\mathcal{V}^{(k)}(\eta)$ in $\mathcal{R}_L^c$ are ***essential*** nonlinear terms which may not be eliminated by changing coordinates. These essential nonlinearities must be retained and analyzed. A vector field containing only essential nonlinear terms is said to be in *normal form.*

Since $\Phi(\varsigma)$ left terms up to degree $k-1$ unchanged, these coordinate transformations to produce the normal form can be performed iteratively: first the inessential quadratic terms are removed, then the cubic terms, etc. In practice the normal form need only be computed to some finite—hopefully low—order. Specifying the minimal number of terms required in the normal forms is the problem of *finite determinacy*. This problem is briefly discussed at the close of this chapter.

To understand the structure of the normal form for Hopf bifurcation, the range of $L^{(k)}$ must be computed. This is most easily accomplished when $L^{(k)}$ is in diagonal form. From the definition of $L^{(k)}$, the operator has two terms,

$$L^{(k)}(Y) = DY \cdot \mathcal{V}^{(1)} - D\mathcal{V}^{(1)} \cdot Y.$$

Diagonalizing the second term, $D\mathcal{V}^{(1)} \cdot Y$, requires coordinates which diagonalize $D\mathcal{V}^{(1)}$; these coordinates will effectively diagonalize the first term as well. For Hopf bifurcation $D\mathcal{V}^{(1)}$ has the form,

$$D\mathcal{V}^{(1)} = \begin{pmatrix} \mu & \Lambda \\ -\Lambda & \mu \end{pmatrix}$$

relative to real coordinates (x, y) on $\Re^2$. To diagonalize $D\mathcal{V}^{(1)}$, starting from this real basis, introduce the complex coordinates given by the linear transformation $\mathcal{T}$.

$$\begin{pmatrix} z \\ \bar{z} \end{pmatrix} = \mathcal{T} \begin{pmatrix} x \\ y \end{pmatrix}$$

where

$$\tau = \begin{pmatrix} 1 & i \\ 1 & -i \end{pmatrix}$$

$$\tau^{-1} = \frac{1}{2}\begin{pmatrix} 1 & 1 \\ -i & i \end{pmatrix}$$

and

$$\tau \begin{pmatrix} \mu & \Lambda \\ -\Lambda & \mu \end{pmatrix} \tau^{-1} = \begin{pmatrix} \mu - i\Lambda & 0 \\ 0 & \mu + i\Lambda \end{pmatrix}.$$

In $(z, \bar{z})$ coordinates an element Y of $\mathcal{H}^{(k)}(\mathbb{R}^2)$ has the form

$$Y = \begin{pmatrix} Y_z(z,\bar{z}) \\ Y_{\bar{z}}(z,\bar{z}) \end{pmatrix} = \tau \begin{pmatrix} Y_x(x(z,\bar{z}), y(z,\bar{z})) \\ Y_y(x(z,\bar{z}), y(z,\bar{z})) \end{pmatrix}$$

where Y_z and $Y_{\bar{z}}$ are homogeneous polynomials of degree k in $z, \bar{z}$. The action of $L^{(k)}$ on Y is therefore

$$\begin{aligned} L^{(k)}(Y) &= DY \cdot \mathcal{V}^{(1)} - D\mathcal{V}^{(1)} \cdot Y \\ &= \begin{pmatrix} \frac{\partial Y_z}{\partial z} & \frac{\partial Y_z}{\partial \bar{z}} \\ \frac{\partial Y_{\bar{z}}}{\partial z} & \frac{\partial Y_{\bar{z}}}{\partial \bar{z}} \end{pmatrix} \begin{pmatrix} (\mu - i\Lambda)z \\ (\mu + i\Lambda)\bar{z} \end{pmatrix} - \begin{pmatrix} \mu - i\Lambda & 0 \\ 0 & \mu + i\Lambda \end{pmatrix} \begin{pmatrix} Y_z \\ Y_{\bar{z}} \end{pmatrix} \\ &= \begin{pmatrix} (\mu - i\Lambda)z\frac{\partial Y_z}{\partial z} + (\mu + i\Lambda)\bar{z}\frac{\partial Y_z}{\partial \bar{z}} - (\mu - i\Lambda)Y_z \\ (\mu - i\Lambda)z\frac{\partial Y_{\bar{z}}}{\partial z} + (\mu + i\Lambda)\bar{z}\frac{\partial Y_{\bar{z}}}{\partial \bar{z}} - (\mu + i\Lambda)Y_{\bar{z}} \end{pmatrix}. \end{aligned}$$

By inspection, the eigenvectors of $L^{(k)}$ consist of vectors with $Y_{\bar{z}} = 0$ and Y_z a simple monomial and vice-versa; denote these eigenvectors by $\xi_+^{(k,l)}$ and $\xi_-^{(k,l)}$ respectively. In $(z, \bar{z})$ coordinates we have,

$$\left.\begin{aligned} \xi_+^{(k,l)}(\eta) &= \begin{pmatrix} z^l(\bar{z})^{k-l} \\ 0 \end{pmatrix} \\ \xi_-^{(k,l)}(\eta) &= \begin{pmatrix} 0 \\ z^l(\bar{z})^{k-l} \end{pmatrix} \end{aligned}\right\} l = 0, 1, \ldots, k. \qquad (1.22)$$

(Note these eigenvectors are themselves *vector fields.*) There are obviously $2k+2$ linearly independent eigenvectors so they span $\mathcal{H}^{(k)}$. A simple calculation gives the corresponding eigenvalues,

$$L^{(k)}\xi_{\pm}^{(k,l)} = \lambda_{\pm}^{(k,l)}\xi_{\pm}^{(k,l)}$$

where $\lambda_{\pm}^{(k,l)} = (k-1)\mu + i(k-2l\pm 1)\Lambda$.

Now the range of $L^{(k)}$ is easy to describe. Since the eigenvectors $\xi_{\pm}^{(k,l)}$ form a basis, $\mathcal{R}_L$ is simply the linear span of the image vectors $\{\lambda_{\pm}^{(k,l)}\xi_{\pm}^{(k,l)}\}$. When all the eigenvalues are non-zero $\mathcal{R}_L = \mathcal{H}^{(k)}$; if N eigenvalues happen to vanish then dim $\mathcal{R}_L$ = dim $\mathcal{H}^{(k)} - N = 2k+2-N$. Since $k \geq 2$, $\operatorname{Re}\lambda_{\pm}^{(k,l)} = 0$ only at criticality $\mu = 0$. Furthermore $\Lambda \neq 0$ implies $\operatorname{Im}\lambda_{\pm}^{(k,l)} = 0$ only if $k - 2l \pm 1 = 0$. Thus when k is even the eigenvalues cannot vanish, but when k is odd the eigenvalues $\lambda_{+}^{(k,(k+1)/2)}$ and $\lambda_{-}^{(k,(k-1)/2)}$ vanish at $\mu = 0$. This means that any change of coordinates $\Phi(\varsigma)$, which removes the components of $\mathcal{V}^{(k)}(\varsigma)$ along $\xi_{+}^{(k,(k+1)/2)}$ or $\xi_{-}^{(k,(k-1)/2)}$, will be singular at $\mu = 0$. Thus these components must be retained to obtain a normal form valid at $\mu = 0$. For k even, there is no such difficulty and nonlinear terms in $\mathcal{V}(\varsigma)$ of even degree can always be removed. These observations lead to a simple prescription for constructing the normal form transformation $\Phi(\varsigma)$, and determine the general form of the normal form equations.

For terms, $\mathcal{V}^{(k)}(\varsigma)$, of even degree (1.21) can be solved exactly. Expanding $\phi^{(k)}(\varsigma)$ and $\mathcal{V}^{(k)}(\varsigma)$ in the eigenbasis,

$$\phi^{(k)}(\varsigma) = \sum_{l=0}^{k} \left\{ \phi_+^{(k,l)} \xi_+^{(k,l)}(\varsigma) + \phi_-^{(k,l)} \xi_-^{(k,l)}(\varsigma) \right\}$$

$$\mathcal{V}^{(k)}(\varsigma) = \sum_{l=0}^{k} \left\{ \mathcal{V}_+^{(k,l)} \xi_+^{(k,l)}(\varsigma) + \mathcal{V}_-^{(k,l)} \xi_-^{(k,l)}(\varsigma) \right\}$$

then plugging into (1.21) yields explicit solutions for the components of $\phi^{(k)}(\varsigma)$.

$$\phi_\pm^{(k,l)} = \frac{-\mathcal{V}_\pm^{(k,l)}}{\lambda_\pm^{(k,l)}} \tag{1.23}$$

For k odd, this also gives the desired components with the already noted exceptions $\phi_+^{(k,(k+1)/2)}$ and $\phi_-^{(k,(k-1)/2)}$ which are not determined, and must be independently specified. This ambiguity in the coefficients of $\Phi(\varsigma)$ means that the normal form equations are not uniquely determined for $\mu \neq 0$. For simplicity I shall adopt the prescription $\phi_+^{(k,(k+1)/2)} = 0$ and $\phi_-^{(k,(k-1)/2)} = 0$; this choice differs from that of Hassard and Wan (1978) and Hassard, Kazarinoff, and Wan (1981).

Although (1.23) for the components of $\Phi(\varsigma)$ is very compact, in practice the indicated calculations are laborious. The primary reason for this is the nonlinearity of $\mathcal{V}(\varsigma)$. Carrying out the normal form transformation at quadratic order,

$$\Phi(\varsigma) = \varsigma + \phi^{(2)}(\varsigma),$$

introduces additional nonlinear terms of degree 3, 4, etc. In order to compute the normal form through terms of degree $k = 3$, the terms of degree 3 contributed by $\phi^{(2)}(\varsigma)$ must be calculated. Computing the normal form through $k = 5$

requires similar bookkeeping on the higher order nonlinear terms introduced by $\phi^{(2)}(\varsigma)$ and $\phi^{(3)}(\varsigma)$. General formulas for extracting the normal form up to terms of fifth degree are derived in the Appendix; these results generalize slightly the previous formulas of Hassard and Wan (1978).

To conclude this discussion of the Hopf bifurcation normal form, consider the general form of the normal form equations. The original vector field $\mathcal{V}(\varsigma)$ may be expanded in the eigenbasis appropriate for each subspace $\mathcal{H}^{(k)}$.

$$\frac{d\varsigma}{dt} = \mathcal{V}(\varsigma) = \mathcal{V}^{(1)}(\varsigma) + \mathcal{V}^{(2)}(\varsigma) + \cdots$$

where

$$\mathcal{V}^{(k)}(\varsigma) = \sum_{l=0}^{k} \left[\mathcal{V}_{+}^{(k,l)} \xi_{+}^{(k,l)}(\varsigma) + \mathcal{V}_{-}^{(k,l)} \xi_{-}^{(k,l)}(\varsigma) \right]$$

for $k \geq 2$. The nonlinear change of coordinates, $\eta = \Phi(\varsigma)$, constructed above transforms $\mathcal{V}(\varsigma)$ into the normal form vector field,

$$\frac{d\eta}{dt} = \tilde{\mathcal{V}}(\eta) = \tilde{\mathcal{V}}^{(1)}(\eta) + \tilde{\mathcal{V}}^{(3)}(\eta) + \tilde{\mathcal{V}}^{(5)}(\eta) + \cdots$$

where $\tilde{\mathcal{V}}^{(1)}(\eta) = \mathcal{V}^{(1)}(\eta)$ and for odd values of $k > 1$,

$$\tilde{\mathcal{V}}^{(k)}(\eta) = \tilde{\mathcal{V}}_{+}^{(k,(k+1)/2)} \xi_{+}^{(k,(k+1)/2)}(\eta) + \tilde{\mathcal{V}}_{-}^{(k,(k-1)/2)} \xi_{-}^{(k,(k-1)/2)}(\eta).$$

Here $\tilde{\mathcal{V}}_{+}^{(k,(k+1)/2)}$ and $\tilde{\mathcal{V}}_{-}^{(k,(k-1)/2)}$ are the components along eigenvectors in the kernel of $L^{(k)}$ at $\mu = 0$. They include the components of $\mathcal{V}(\varsigma)$ plus the contributions arising from $\Phi(\varsigma)$.

To reveal the dynamics of the normal form equations requires re-introducing coordinates explicitly; real polar coordinates are the optimal choice. As an in-

termediate step, first rewrite the normal form equations in real cartesian coordinates. This requires expressing $\xi_+^{(k,(k+1)/2)}$ and $\xi_-^{(k,(k-1)/2)}$ in real coordinates. From (1.22)

$$\xi_+^{(k,(k+1)/2)} = |z|^{k-1}\begin{pmatrix} z \\ 0 \end{pmatrix}$$

in complex coordinates, thus in terms of $x = r\cos\theta$ and $y = r\sin\theta$, $\xi_+^{(k,(k+1)/2)}$ becomes

$$\xi_+^{(k,(k+1)/2)} = |z|^{k-1}\,\mathcal{T}\begin{pmatrix} z \\ 0 \end{pmatrix} = \frac{r^k e^{i\theta}}{2}\begin{pmatrix} 1 \\ -i \end{pmatrix}. \tag{1.24}$$

Similarly $\xi_-^{(k,(k-1)/2)}$ in real coordinates is

$$\xi_-^{(k,(k-1)/2)} = \frac{r^k e^{-i\theta}}{2}\begin{pmatrix} 1 \\ i \end{pmatrix}. \tag{1.25}$$

Overall the normal form vector field becomes

$$\begin{aligned}\frac{d}{dt}\begin{pmatrix} x \\ y \end{pmatrix} &= \begin{pmatrix} \mu & \Lambda \\ -\Lambda & \mu \end{pmatrix}\begin{pmatrix} x \\ y \end{pmatrix} \\ &+ \sum_{k=3,5,\ldots}\left[\tilde{v}_+^{(k,(k+1)/2)}\,\xi_+^{(k,(k+1)/2)} + \tilde{v}_-^{(k,(k-1)/2)}\,\xi_-^{(k,(k-1)/2)}\right]\end{aligned} \tag{1.26}$$

where only odd k values are included in the summation. To express this in polar variables (r,θ) is very simple since $x + iy = re^{i\theta}$. Thus from (1.24), (1.25), and (1.26)

$$\begin{aligned}\frac{dx}{dt} + i\frac{dy}{dt} = (\frac{dr}{dt} + ir\frac{d\theta}{dt})e^{i\theta} &= (\mu x + \Lambda y) + i(-\Lambda x + \mu y) \\ &+ e^{i\theta}\sum_{k=3,5,\ldots}\left[\tilde{v}_+^{(k,(k+1)/2)}\,r^k\right].\end{aligned}$$

Canceling $e^{i\theta}$, and then equating real and imaginary parts yields dr/dt and $d\theta/dt$,

$$\begin{aligned}\frac{dr}{dt} &= \mu r + \sum_{k=3,5,\ldots} \left(\mathrm{Re}\ \tilde{\mathcal{V}}_+^{(k,(k+1)/2)}\right) r^k \\ \frac{d\theta}{dt} &= -\Lambda + \sum_{k=3,5,\ldots} \left(\mathrm{Im}\ \tilde{\mathcal{V}}_+^{(k,(k+1)/2)}\right) r^{k-1}\,.\end{aligned} \tag{1.27}$$

In practice these equations are computed only to some finite order, and one typically analyzes (1.2) which appeared in the Introduction.

$$\begin{aligned}\frac{dr}{dt} &= \mu r + a_1 r^3 + a_2 r^5 + O(r^7) \\ \frac{d\theta}{dt} &= -\Lambda + b_1 r^2 + b_2 r^4 + O(r^6)\end{aligned} \tag{1.28}$$

The final loose end is the explicit relation between the components $\tilde{\mathcal{V}}_+^{(k,(k+1)/2)}$ and the components of the original vector field $\mathcal{V}(\varsigma)$. This relation must be calculated order by order in k; in the Appendix this is done for $k = 3$ and $k = 5$.

Nevertheless by considering the ***possible*** values of the normal form coefficients the "menu" of allowed dynamics may be determined. First of all, since the dr/dt equation is independent of θ, the radial dynamics is one dimensional. Near $r = 0$ for $\mu > 0$ the unstable fixed point pushes the solution curves outward; the subsequent effects of the nonlinear terms can be determined from

$$\frac{dr}{dt} = \mu r + a_1 r^3 + O(r^5). \tag{1.29}$$

For $\mu \geq 0$, the $dr/dt = 0$ equation has two solutions: the unstable fixed point at $r = 0$ and $r_0 = \sqrt{-\mu/a_1}$ which is relevant only if $(\mu/a_1) < 0$. When applicable the solution $r = r_0$ describes a periodic orbit in the neighborhood of

the fixed point. Whether the orbit appears for $\mu < 0$ (subcritical bifurcation) or for $\mu > 0$ (supercritical bifurcation) depends on the algebraic sign of a_1 at $\mu = 0$. (If $a_1 = 0$ at $\mu = 0$ then the r^5 term must be considered. An example of this occurs in the next chapter.) The stability of the periodic orbit is found by linearizing about $r = r_0$. Plugging $r = r_0 + \delta r$ into (1.29) gives

$$\frac{d\delta r}{dt} = -2\mu\delta r + O\big((\delta r)^2\big).$$

Thus, supercritical bifurcation produces a limit cycle, but subcritical bifurcation involves an unstable orbit. The phase portraits for these two cases appear in Fig. (I.1).

Final Remarks

The result obtained in (1.21) did not assume a particular form for the linear term, $\mathcal{V}^{(1)}(\zeta)$. In fact the assumption of a two dimensional vector field could have easily been dropped. However the subsequent analysis, leading to the normal form in (1.27), did depend on the specific form of the linear term in (1.14) for Hopf bifurcation. If (1.14) is generalized to allow a real eigenvalue or a second conjugate pair to cross the imaginary axis simultaneously with the first conjugate pair then the normal form involves a three of four dimensional system respectively. The normal form for bifurcation at a conjugate pair plus a real eigenvalue has been analyzed by Guckenheimer (1981) and Scheurle and Marsden (1982). For the normal form for bifurcation with two conjugate pairs

(which occurs in the model of Chapter 3) see Takens (1974) and Guckenheimer and Holmes (1983).

There are additional special features of this derivation of the normal form for Hopf bifurcation which simplified the calculations. First, the eigenvectors of $L^{(k)}$ form a basis for $\mathcal{H}^{(k)}$; this allows the range of $L^{(k)}$ to be easily determined. Secondly, at $\mu = 0$ the dimension of the kernel of $L^{(k)}$ is either zero or two depending on whether k is even or odd. Moreover, for odd k, the kernel dimension is *always* two; it does not vary with k. In more complicated bifurcations, Spiegel and collaborators (1983) have found that the kernel dimension can increase with k. When this happens it complicates the analysis of the degenerate bifurcations in which the lowest order nonlinear terms vanish.

As mentioned earlier, there is the dilemma of how many nonlinear terms in the normal form must be retained to determine the qualitative features of the phase portrait. For the example of Hopf bifurcation, because the analysis reduces to a one dimensional problem for the radial dynamics there is not much difficulty. For $\mu \neq 0$, there is at most a periodic orbit in the vicinity of the fixed point and both have definite linear stability i.e. they are *hyperbolic*; thus the small perturbation of adding the $a_2 r^5$ term cannot alter the topology of the phase portrait near $r = 0$. For $\mu = 0$, the periodic orbit is absent and the stability of $r = 0$ is determined by $a_1 r^3 + a_1 r^5 + \cdots$. For r sufficiently small stability is clearly controlled by $a_1 r^3$. Thus for a neighborhood of $\mu = 0$, we

can expect the truncated equation

$$\frac{dr}{dt} = \mu r + a_1 r^3 \qquad a_1 \neq 0$$

to topologically determine the flow of $\mathcal{V}(\varsigma)$ near $\varsigma = 0$. How to truncate the normal form equations when the dimension of the system is greater than one is more delicate, but sometimes can be analyzed using Takens' "blowing up" procedure. This technique is discussed in detail by Guckenheimer and Holmes (1983).

The normal form theory presented here is a restricted version of a more general theory developed by Arnold (1972), Takens (1974), Broer (1981), and others. In this more general theory, the deformation of the phase portrait of the original vector field $\mathcal{V}(\varsigma)$ into the phase portrait of the normal form equations is done in a continuous fashion by constructing an "intermediate" vector field whose flow pushes the integral curves of $\mathcal{V}(\varsigma)$ onto the integral curves of the normal form. The change of coordinates $\Phi(\varsigma)$ then corresponds to the time-one map of this intermediate flow. Holmes (1981) provides an introduction to this elegant geometric viewpoint.

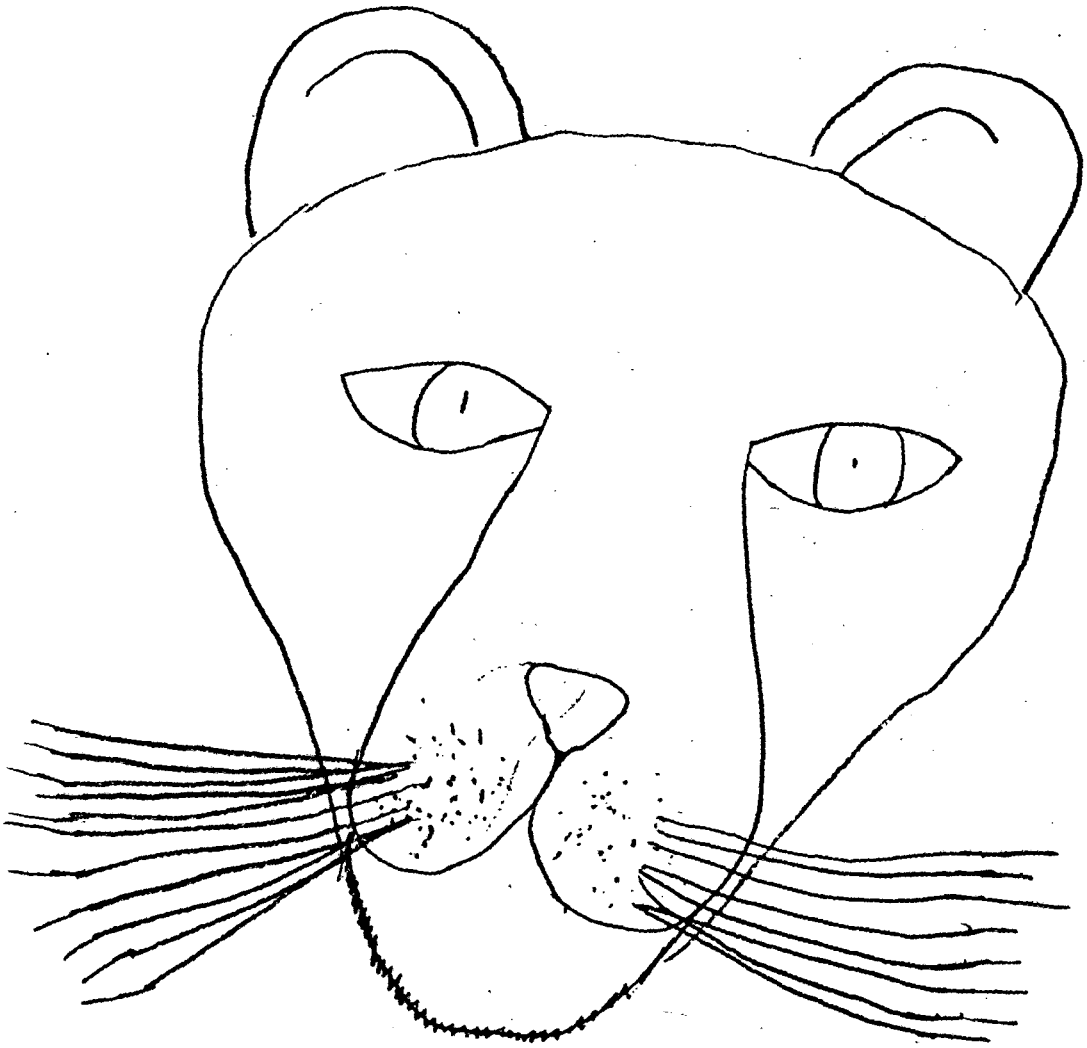

Figure Captions

Figure (1.1) (a) A typical spectrum for $\mathcal{L}_\mu$ consists of real and conjugate pairs of eigenvalues. In infinite dimensional problems, $\mathcal{L}_\mu$ may also have continuous spectrum. (b) The linear invariant subspaces E^s, E^c, and E^u determine the structure of the linearized flow.

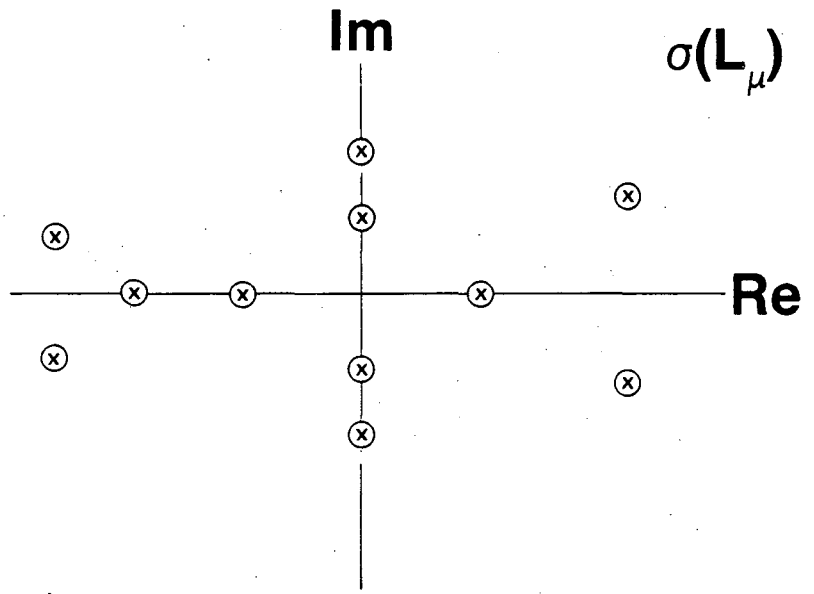

Figure (1.1a)

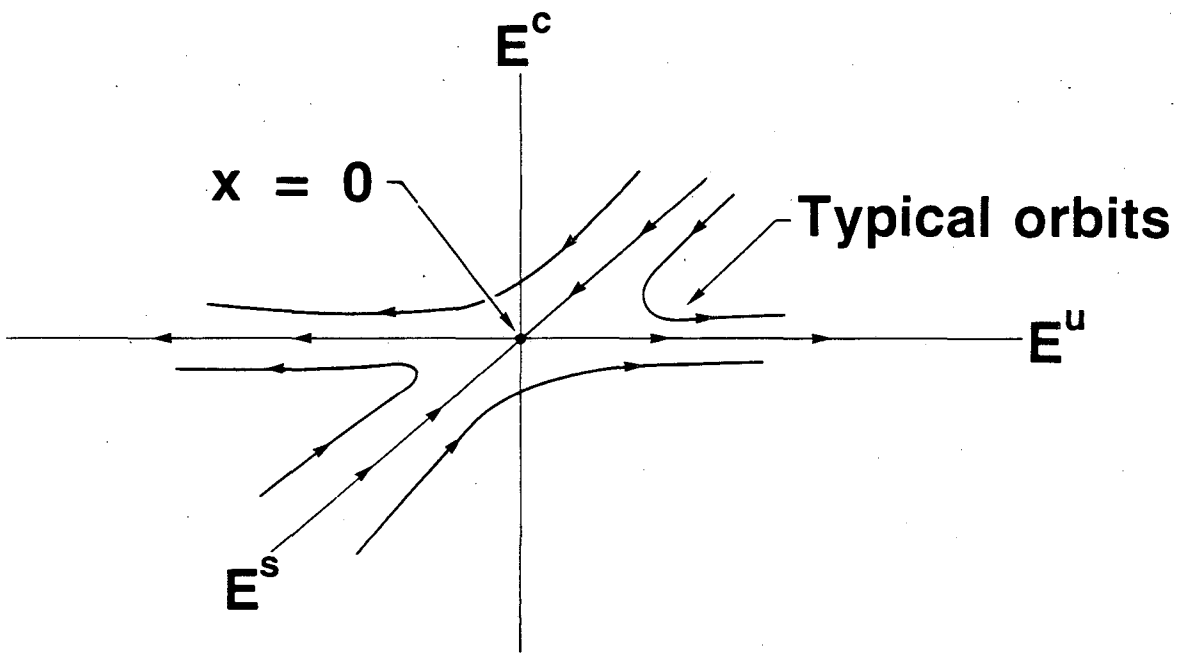

XBL 838-3011

Figure (1.1b)

Figure (1.2) (a) The invariant manifolds W^s, W^c, and W^u are the nonlinear analogues of the linear eigenspaces. Each manifold passes through $x = 0$ and is tangent there to its corresponding eigenspace. (b) At criticality for a nondegenerate Hopf bifurcation the spectrum of $\mathcal{L}_\mu$ has a simple conjugate pair of eigenvalues on the imaginary axis. The rest of the spectrum is in the left half plane a finite distance away from the imaginary axis.

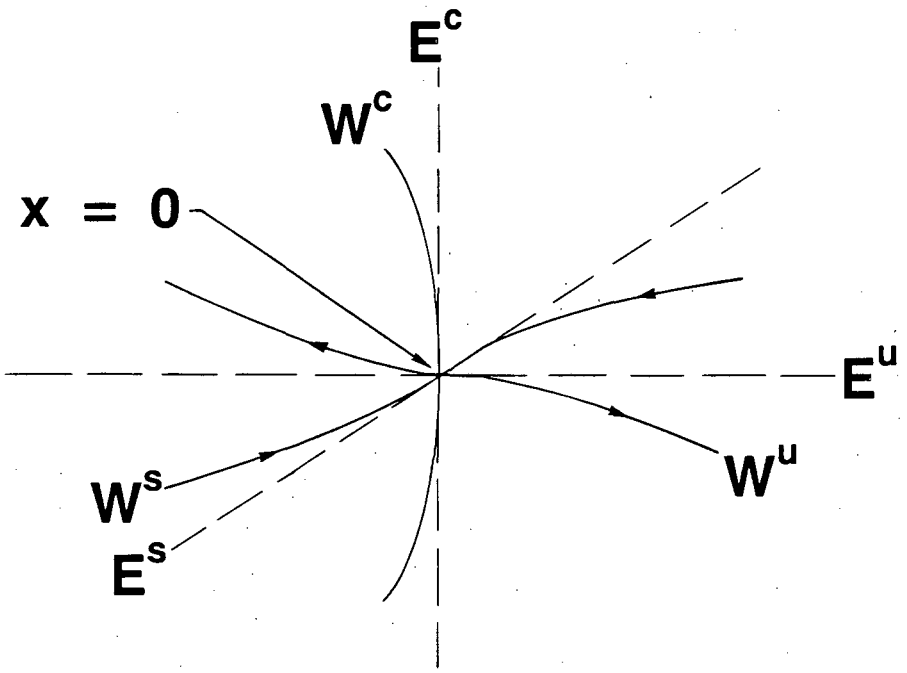

Figure (1.2a)

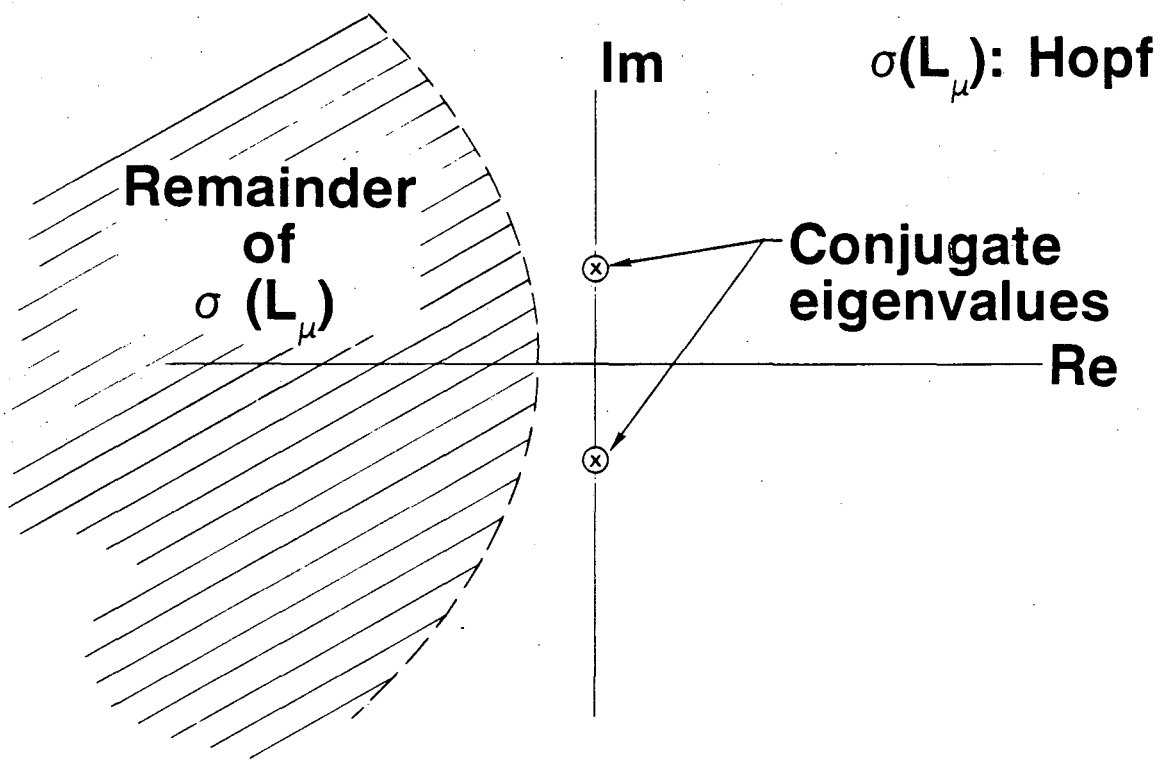

XBL 838-11194

Figure (1.2b)

Figure (1.3) (a) The center manifold W^c for a nondegenerate Hopf bifurcation is two dimensional. There is no unstable manifold, and the dimension of the stable manifold is $n-2$ where n is the dimension of the phase space. (b) Near the fixed point, the invariant manifold W_μ may be described as the graph of a function $h(A, \overline{A})$.

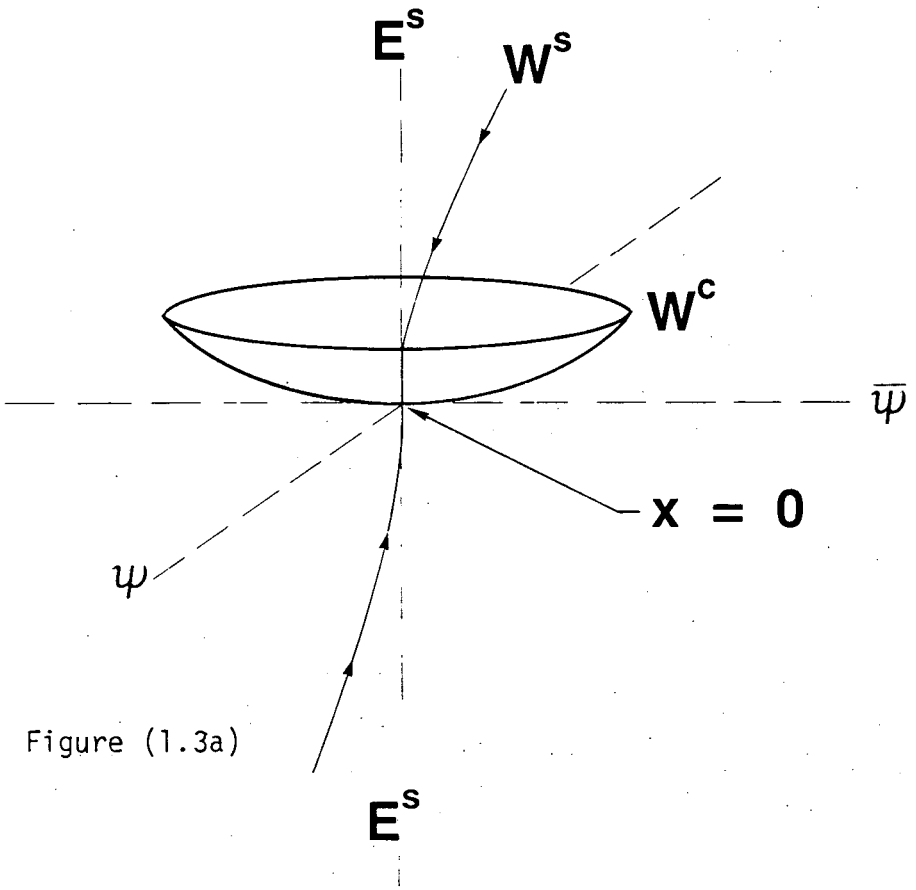

Figure (1.3a)

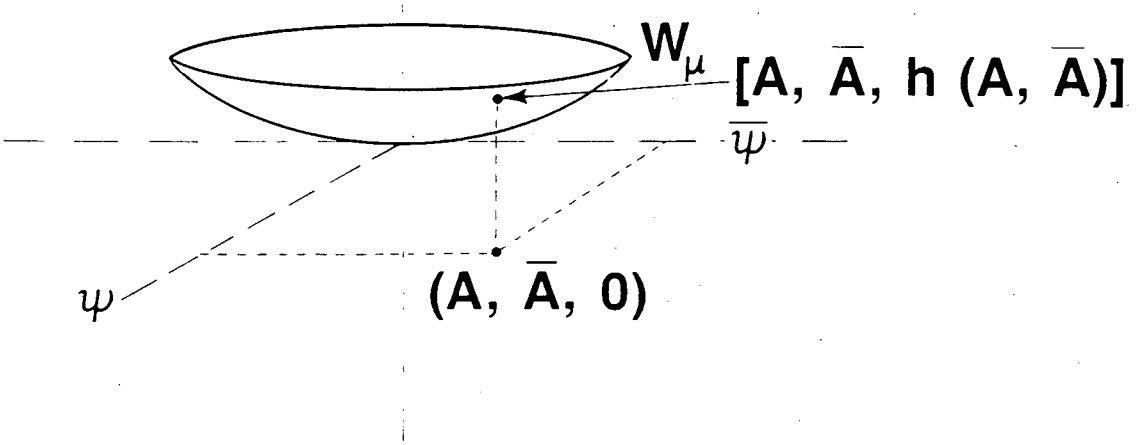

XBL 838-3005A

Figure (1.3b)

CHAPTER 2

Hopf Bifurcation in a Resonant 3-Wave Interaction

Understanding wave dynamics in a plasma requires, in part, an analysis of the interactions between waves (Davidson (1972)). Frequently, the primary interaction to consider occurs between three waves whose frequencies ω_i and wave numbers k_i satisfy the resonance conditions:

$$\omega_1 = \omega_2 + \omega_3 \quad \text{and} \quad k_1 = k_2 + k_3 .$$

When the wave amplitudes are small, this interaction dominates higher order processes involving more waves. If wave-particle interactions (see Chapter 3) are unimportant as well, then the three wave interaction may be the most important nonlinear effect to consider.

Depending on the context, the three wave interaction may serve to produce an instability, such as the "parametric decay" instability (Chen (1974)), or to saturate the growth of an instability. In this chapter, a model for the saturation

of a linearly unstable wave via a three wave interaction is considered. The unstable, high frequency wave couples to two damped, lower frequency waves through nonlinear interactions which are quadratic in the wave amplitudes. Their interaction drains energy at high frequency into lower frequency modes. A well known example of this process is the decay of a Langmuir wave into an ion-acoustic wave plus a second Langmuir wave (Davidson (1972)).

Under suitable conditions an overall balance results between high frequency growth and low frequency decay. This produces a stable equilibrium in the wave dynamics. At this equilibrium or fixed point, the wave amplitudes are time independent. If however the parameters of the interaction are varied to produce less damping or less effective coupling, then this stable balance is destroyed. Some time-dependent state replaces the equilibrium; the fixed point is no longer a stable solution. For the model of this 3-wave interaction considered here, this transition provides an excellent example of a Hopf bifurcation in finite dimension.

On physical grounds, if the damping of the stable modes is decreased, one expects at some point they would no longer be able to arrest the growth of the unstable mode. In the model, this stability boundary marks the shift from supercritical Hopf bifurcation ($a_1 < 0$ in (1.28)) to subcritical Hopf bifurcation ($a_1 > 0$ in (1.28)). The calculation of a_1 allows the location of this transition to be predicted, and the normal form analysis yields a detailed understanding

of the dynamics near this critical region.

The Model

My formulation of the problem follows Wersinger, Finn, and Ott (1980), who studied the model numerically and found a rich bifurcational structure. The model assumes for simplicity a single resonant triad, and neglects the self-consistent evolution of the background plasma. Each wave is represented by a complex amplitude

$$C_j = \alpha_j e^{i\phi_j} \qquad j = 1, 2, 3$$

which evolves on a slow time scale. On a fast time scale the wave frequencies, $\omega_1, \omega_2, \omega_3$, are assumed to be nearly resonant; the frequency mismatch is Ω.

$$\omega_1 = \omega_2 + \omega_3 + \Omega$$

The high frequency wave ω_1 is unstable, and its linear growth rate is normalized to unity. For simplicity, the damped low frequency waves are assigned equal damping and assumed to have the same magnitude: $\alpha_2 = \alpha_3$. This latter assumption is consistent with the assumption of equal damping. In dimensionless variables, the amplitude equations are then

$$\begin{aligned} \frac{dx}{dt} &= x - \Omega y + z - 2y^2 \\ \frac{dy}{dt} &= \Omega x + y + 2xy \qquad \Omega, \Gamma > 0 \\ \frac{dz}{dt} &= -2\Gamma z - 2xz \end{aligned} \tag{2.1}$$

where

$$x = \alpha_1 \cos\phi$$

$$y = \alpha_1 \sin\phi$$

$$z = (\alpha_2)^2$$

$$\phi = \phi_1 - \phi_2 - \phi_3$$

$$\Gamma = \text{linear damping rate for } C_2 \text{ and } C_3.$$

A derivation of these equations from the dynamics of the C_j appears in Wersinger, Finn, and Ott (1980).

This particular set of amplitude equations exhibits very complex dynamics and intricate sequences of bifurcations. Several studies have extended the work of Wersinger et al. (1980). Meunier, Bussac, and Laval (1980) reported extensive numerical calculations of the bifurcation sequences, and Bussac (1982) developed a dynamical theory in terms of one dimensional maps. Some results of this chapter are independently described in those works.

Equation (2.1) defines a two parameter family of vector fields on $\mathfrak{R}^3$, denoted $V_{\Omega,\Gamma}$. The divergence of this family is

$$\text{div}\, V_{\Omega,\Gamma} = 2(1-\Gamma).$$

The wave dynamics can have stable, bounded solutions only for $\Gamma \geq 1$. If $\Gamma > 1$ the flow of $V_{\Omega,\Gamma}$ contracts volumes. Since the amplitude equations are invariant under the shift $\Omega \rightarrow -\Omega$ and $y \rightarrow -y$, the frequency mismatch Ω may be assumed to be positive.

$V_{\Omega,\Gamma}$ has two fixed points. There is a trivial fixed point at $(x, y, z) = (0, 0, 0)$ corresponding to no waves; this solution is unstable since the high frequency wave is unstable. There is a nontrivial fixed point at

$$(x_0, y_0, z_0) = (-\Gamma, \frac{-\Omega\Gamma}{2\Gamma - 1}, \Gamma(1 + \frac{\Omega^2}{(2\Gamma - 1)^2}))$$

whose stability depends on Ω and Γ.

Linear Analysis

The methods of the previous chapter allow a detailed analysis of this nontrivial equilibrium, and the wave dynamics in its neighborhood. The first step is a linear stability analysis. This is an exercise in linear algebra with two goals: determine the spectrum of the linearized dynamics at the fixed point and cast the problem into the form of (1.1) with the linear operator in block diagonal form. The calculations required are simply summarized.

Shift coordinates $x \to x + x_0, y \to y + y_0, z \to z + z_0$ to place the fixed point at the origin, then (2.1) becomes

$$\frac{d}{dt}\begin{pmatrix} x \\ y \\ z \end{pmatrix} = \begin{pmatrix} 1 & (1+\gamma)\rho & 1 \\ -\rho & 1-\gamma & 0 \\ -\gamma(1+\rho^2) & 0 & 0 \end{pmatrix}\begin{pmatrix} x \\ y \\ z \end{pmatrix} + 2\begin{pmatrix} -y^2 \\ xy \\ -xz \end{pmatrix}$$

where $\gamma = 2\Gamma$ and $\rho = \Omega/(\gamma - 1)$. This is an evolution equation for $\varsigma = (x, y, z)$;

$$\frac{d\varsigma}{dt} = \mathcal{L}\varsigma + \mathcal{N}(\varsigma) \tag{2.2}$$

where

$$\mathcal{L} = \begin{pmatrix} 1 & (1+\gamma)\rho & 1 \\ -\rho & 1-\gamma & 0 \\ -\gamma(1+\rho^2) & 0 & 0 \end{pmatrix}$$

and

$$\mathcal{N}(\zeta) = 2\begin{pmatrix} -y^2 \\ xy \\ -xz \end{pmatrix}.$$

The eigenvalues of $\mathcal{L}$, denoted λ_i, are roots of its characteristic polynomial,

$$\lambda_i^3 + (\gamma-2)\lambda_i^2 + [1+(1+2\gamma)\rho^2]\lambda_i + \gamma(\gamma-1)(1+\rho^2) = 0.$$

For $\gamma \geq 2$, all coefficients are nonnegative and the constant term is positive; this implies that any real root must be negative; in particular $\lambda_i = 0$ cannot occur in this region of parameter space. If eigenvalues with $\mathrm{Re}\,\lambda_i = 0$ occur, they must form a conjugate pair $\pm i\Lambda$. Thus in the regions of parameter space where the stability of the fixed point changes, there will be a negative real eigenvalue and a conjugate pair. From the characteristic polynomial, a complex root, $\mu + i\Lambda$, satisfies

$$3\mu^2 - \Lambda^2 + 2(\gamma-2)\mu + 1 + \rho^2(1+2\gamma) = 0, \tag{2.3}$$

$$\mu(\mu^2 - 3\Lambda^2) + (\gamma-2)(\mu^2-\Lambda^2) + [1+\rho^2(1+2\gamma)]\mu + \gamma(\gamma-1)(1+\rho^2) = 0. \tag{2.4}$$

Although Ω and γ are the original physical parameters, μ and γ are more convenient. This is because μ directly measures the distance in parameter space

from criticality ($\mu = 0$). To express the dependence of Ω on (μ, γ) requires ρ as a function of (μ, γ). This is found by solving (2.3) for Λ^2, eliminating Λ^2 from (2.4), and solving for ρ^2.

$$\rho^2 = \frac{(1-2\mu)\gamma^2 - 2[1+4\mu(\mu-1)]\gamma + 2[1-\mu(4\mu^2-8\mu+5)]}{\gamma^2 - 2(1-2\mu)\gamma - 2(1-\mu)}$$

$$\Lambda^2 = 3\mu^2 + 2(\gamma-2)\mu + 1 + \rho^2(1+2\gamma)$$

and $\Omega = \rho(\gamma - 1)$. The parameter space (Ω, γ) for $\Omega \geq 0$, $\gamma \geq 0$ corresponds to $\mu \leq 0.5$ and $\gamma \geq 0$ as shown in Fig. (2.1). The condition $\mu = 0$ determines the curve in parameter space where a conjugate pair of eigenvalues crosses the imaginary axis, and the fixed point loses stability in a Hopf bifurcation.

The eigenvectors of $\mathcal{L}$ satisfy

$$\mathcal{L}v_i = \lambda_i v_i$$

where

$$v_i = \begin{pmatrix} -\rho(1+\gamma)\lambda_i \\ -f(\lambda_i) \\ \rho\gamma(1+\rho^2)(1+\gamma) \end{pmatrix}.$$

with $f(x) \equiv x^2 - x + \gamma(1+\rho^2)$. For the lone real eigenvalue λ_1, denoted henceforth as λ, v_1 has real components. For the conjugate pair, $\lambda_{2,3} = \mu \pm i\Lambda$, the eigenvectors have real and imaginary parts:

$$v_{2,3} = w \pm iu$$

where

$$w = \begin{pmatrix} -\mu\rho(1+\gamma) \\ \Lambda^2 - f(\mu) \\ \rho\gamma(1+\rho^2)(1+\gamma) \end{pmatrix}$$

and

$$u = \Lambda \begin{pmatrix} -\rho(1+\gamma) \\ 1-2\Lambda \\ 0 \end{pmatrix}$$

are real vectors spanning a two dimensional subspace.

The linearly independent set $\{u, w, v_1\}$ determines a linear transformation, S, which puts $\mathcal{L}$ in block diagonal form. Let

$$S \equiv \begin{pmatrix} w & u & v_1 \end{pmatrix} = \begin{pmatrix} -\mu\rho(1+\gamma) & -\rho\Lambda(1+\gamma) & -\rho(1+\gamma)\lambda \\ \Lambda^2 - f(\mu) & \Lambda(1-2\Lambda) & -\lambda f(\lambda) \\ \rho\gamma(1+\rho^2)(1+\gamma) & 0 & \rho\gamma(1+\rho^2)(1+\gamma) \end{pmatrix}$$

then

$$\det S = \alpha\beta^2\Lambda[f(\lambda) - f(\mu) + \Lambda^2 + (\lambda-\mu)(1-2\mu)]$$

and

$$S^{-1} = \left(\frac{\beta}{\det S}\right) \begin{pmatrix} \alpha\Lambda(1-2\mu) & \alpha\beta\Lambda & \Lambda(f(\lambda) + \lambda(1-2\mu)) \\ -\alpha[\Lambda^2 + f(\lambda) - f(\mu)] & \alpha\beta(\lambda-\mu) & \lambda f(\mu) - \mu f(\lambda) - \lambda\Lambda^2 \\ \alpha\Lambda(2\mu-1) & -\alpha\beta\Lambda & \Lambda(\Lambda^2 - f(\mu) - \mu(1-2\mu)) \end{pmatrix}$$

where $\alpha \equiv \gamma(1+\rho^2)$ and $\beta \equiv \rho(1+\gamma)$. With the change of coordinates $\varsigma' = S^{-1}\varsigma \equiv (x', y', z')$, (2.2) becomes

$$\frac{d\varsigma'}{dt} = J\varsigma' + \tilde{N}(\varsigma') \tag{2.5}$$

where

$$J \equiv S^{-1} L S = \begin{pmatrix} \mu & \Lambda & 0 \\ -\Lambda & \mu & 0 \\ 0 & 0 & \lambda \end{pmatrix}$$

and $\tilde{N}(\varsigma') \equiv S^{-1} N(S\varsigma')$.

The parameter dependence of $\tilde{N}(\varsigma')$, though complicated, is easily worked out. From the definition of S,

$$S\varsigma' = \begin{pmatrix} -\beta(\mu x' + \Lambda y' + \lambda z' \\ (\Lambda^2 - f(\mu))x' + \Lambda(1-2\mu)y' - f(\lambda)z' \\ \alpha\beta(x' + z') \end{pmatrix} \equiv \begin{pmatrix} R_1(\varsigma') \\ R_2(\varsigma') \\ R_3(\varsigma') \end{pmatrix}.$$

Applying $N(\varsigma)$ to $S\varsigma'$ yields

$$N(S\varsigma') = 2\begin{pmatrix} -(R_2(\varsigma'))^2 \\ R_1(\varsigma')R_2(\varsigma') \\ -R_1(\varsigma')R_3(\varsigma') \end{pmatrix}.$$

Finally left multiplying by S^{-1} gives $\tilde{N}(\varsigma')$.

This completes the linear analysis and formulation of the evolution equation (2.5). Henceforth the primes on $\varsigma' = (x', y', z')$ will be dropped. As a final remark, the invariance of the trace, $\mathrm{Tr}\, J = \mathrm{Tr}\, L$, gives the dependence of λ on (γ, μ),

$$\lambda = -2\mu - (\gamma - 2).$$

This relationship gives the remaining real eigenvalue when the conjugate pair is on the imaginary axis, e.g. at $\mu = 0$,

$$\lambda = -(\gamma - 2).$$

If $\mu = 0$ and $\gamma = 2$, then all three eigenvalues are simultaneously critical. This situation has been studied by Langford (1979), Guckenheimer (1981), Scheurle and Marsden (1982), and others. It is not quite realized in the present model. Examining the characteristic polynomial and Fig. (2.1) reveals that for small γ, the surface $\mu = 0$ asymptotes to the vertical line $\Gamma \sim 1.3$ or $\gamma \sim 2.6$, and does not reach $\gamma = 2.0$. An interesting extension of the analysis in this chapter would be to seek a modified parameterization of (2.1) which would allow the bifurcation with three eigenvalues to occur.

The Dynamics on the Center Manifold

To compute the normal form for this bifurcation it is sufficient to determine the center manifold, W^c, in the neighborhood of the fixed point. As discussed in Chapter 1, near the fixed point the center manifold has coordinates defined by a mapping from the (x, y)-plane to W^c. Denoting these coordinates by φ,

$$\varphi: \Re^2 \to W^c \subset \Re^3$$

$$\varphi(x, y) = (x, y, h(x, y))$$

where $h(x, y)$ gives the z coordinate of W^c.

The invariance of W^c implies

$$z^c(t) = h(x^c(t), y^c(t)) \tag{2.7}$$

if $\varsigma^c(t) = (x^c(t), y^c(t), z^c(t))$ is a solution to (2.5) with $\varsigma^c(0) \in W^c$. As shown in Chapter 1, differentiating with respect to time leads to the invariance equation

for $h(x,y)$,

$$\begin{aligned}\lambda h(x,y) + N_3(x,y,h(x,y)) &= \frac{\partial h}{\partial x}[\mu x + \Lambda y + N_1(x,y,h(x,y))] \\ &\quad + \frac{\partial h}{\partial y}[-\Lambda x + \mu y + N_2(x,y,h(x,y))]\end{aligned} \tag{2.8}$$

where the N_i are defined by,

$$\tilde{N}(\varsigma) = \begin{pmatrix} N_1(\varsigma) \\ N_2(\varsigma) \\ N_3(\varsigma) \end{pmatrix}.$$

To extract an asymptotic solution for $h(x,y)$, accurate near $(x,y) = (0,0)$, expand $h(x,y)$ in a power series about $(0,0)$ and determine the coefficients from (2.8).

$$h(x,y) = h^{(2)}(x,y) + h^{(3)}(x,y) + h^{(4)}(x,y) + \cdots \tag{2.9}$$

where

$$\begin{aligned} h^{(2)}(x,y) &= B_1 x^2 + B_2 y^2 + B_3 xy \\ h^{(3)}(x,y) &= C_1 x^3 + C_2 x^2 y + C_3 xy^2 + C_4 y^3 \\ h^{(4)}(x,y) &= D_1 x^4 + D_2 x^3 y + D_3 x^2 y^2 + D_4 xy^3 + D_5 y^4. \end{aligned}$$

Since $h(0,0) = 0$, there can be no constant term, and the tangency which W^c has with the (x,y)-plane requires $h^{(1)}(x,y) \equiv 0$. To facilitate the calculation denote the coefficients in $\mathcal{N}(\varsigma)$ by $\{N_{ij}\}$.

$$\mathcal{N}(\varsigma) = \begin{pmatrix} N_{11}x^2 + N_{12}y^2 + N_{13}xy + N_{14}xz + N_{15}yz + N_{16}z^2 \\ N_{21}x^2 + N_{22}y^2 + N_{23}xy + N_{24}xz + N_{25}yz + N_{26}z^2 \\ N_{31}x^2 + N_{32}y^2 + N_{33}xy + N_{34}xz + N_{35}yz + N_{36}z^2 \end{pmatrix} \tag{2.10}$$

Here $\mathcal{N}(\varsigma)$ is homogeneous of degree two; this follows from its definition in (2.5).

Combining (2.9) with (2.8) determines the coefficients in $h(x,y)$ in terms of the $\{N_{ij}\}$. At quadratic order, (2.8) becomes

$$\lambda(B_1x^2 + B_2y^2 + B_3xy) + N_{31}x^2 + N_{32}y^2 + N_{33}xy$$
$$= (2B_1x + B_3y)(\mu x + \Lambda y) + (2B_2y + B_3x)(-\Lambda x + \mu y).$$

Equating the coeffcients of x^2, y^2, and xy determines the B_i.

$$B_3 = \frac{2\Lambda(N_{32} - N_{31}) + (2\mu - \lambda)N_{33}}{(2\Lambda)^2 + (2\mu - \lambda)^2}$$

$$B_1 = \frac{\Lambda B_3 + N_{31}}{2\mu - \lambda}$$

$$B_2 = \frac{-\Lambda B_3 + N_{32}}{2\mu - \lambda}$$

The calculation of the cubic coefficients, C_i, and the quartic coefficients, D_i, is similar but more tedious. The results are simply summarized. At cubic order the balance in (2.8) is

$$\begin{aligned}\lambda h^{(3)}(x,y) + (N_{34}x + N_{35}y)h^{(2)}(x,y) &= (2B_1x + B_3y)(N_{11}x^2 + N_{12}y^2 + N_{13}xy)\\ &+ (2B_2y + B_3x)(N_{21}x^2 + N_{22}y^2 + N_{23}xy)\\ &+ (3C_1x^2 + 2C_2xy + C_3y^2)(\mu x + \Lambda y)\\ &+ (C_2x^2 + 2C_3xy + 3C_4y^2)(-\Lambda x + \mu y)\end{aligned}$$

which implies

$$C_2 = \frac{[3\Lambda^2 + (3\mu - \lambda)^2][(3\mu - \lambda)C_2' - 3\Lambda C_1'] + 2\Lambda(3\mu - \lambda)[(3\mu - \lambda)C_3' + 3\Lambda C_4']}{(3\Lambda^2 + (3\mu - \lambda)^2)^2 + 4\Lambda^2(3\mu - \lambda)^2}$$

$$C_3 = \frac{(3\mu - \lambda)C_3' + 3\Lambda C_4' - 2\Lambda(3\mu - \lambda)C_2}{3\Lambda^2 + (3\mu - \lambda)^2}$$

$$C_1 = \frac{C_1' + \Lambda C_2}{(3\mu - \lambda)}$$

$$C_4 = \frac{C_4' - \Lambda C_3}{(3\mu - \lambda)}$$

where

$$C_1' \equiv B_1(N_{34} - 2N_{11}) - B_3 N_{21}$$
$$C_2' \equiv B_1(N_{35} - 2N_{13}) - 2B_2 N_{21} + B_3(N_{34} - N_{11} - N_{23})$$
$$C_3' \equiv -2B_1 N_{12} + B_2(N_{34} - 2N_{23}) + B_3(N_{35} - N_{13} - N_{22})$$
$$C_4' \equiv B_2(N_{35} - 2N_{22}) - B_3 N_{12}.$$

Thus the C_i' are calculated from the original nonlinear terms N_{ij} and the quadratic coefficients of $h(x, y)$, then C_2, C_3, C_1, and C_4 are computed in that order.

Finally, the results of the quartic balance in (2.8) are

$$D_4 = \frac{6\Lambda^2[2\Lambda(2D_1'' - D_3'') - (4\mu - \lambda)D_2'']}{(10\Lambda^2 + (4\mu - \lambda)^2)^2 - (6\Lambda^2)^2}$$
$$- \frac{(10\Lambda^2 + (4\mu - \lambda)^2)[2\Lambda(2D_5'' - D_3'') + (4\mu - \lambda)D_4'']}{(10\Lambda^2 + (4\mu - \lambda)^2)^2 - (6\Lambda^2)^2}$$
$$D_2 = \frac{2\Lambda(2D_1'' - D_3'') - (4\mu - \lambda)D_2'' + 6\Lambda^2 D_4}{10\Lambda^2 + (4\mu - \lambda)^2}$$
$$D_3 = \frac{3\Lambda(D_4 - D_2) - D_3''}{(4\mu - \lambda)}$$
$$D_1 = \frac{\Lambda D_2 - D_1''}{(4\mu - \lambda)}$$
$$D_5 = \frac{-\Lambda D_4 - D_5''}{(4\mu - \lambda)}$$

where

$$D_1'' \equiv D_1' + B_1 B_1'$$
$$D_2'' \equiv D_2' + B_1 B_2' + B_3 B_1'$$
$$D_3'' \equiv D_3' + B_1 B_3' + B_2 B_1' + B_3 B_2'$$
$$D_4'' \equiv D_4' + B_2 B_2' + B_3 B_3'$$
$$D_5'' \equiv D_5' + B_2 B_3'$$

with

$$D_1' \equiv C_1(3N_{11} - N_{34}) + C_2 N_{21}$$
$$D_2' \equiv C_1(3N_{13} - N_{35}) + C_2(2N_{11} + N_{23} - N_{34}) + 2N_{21}C_3$$
$$D_3' \equiv 3C_1 N_{12} + C_2(2N_{13} + N_{22} - N_{35}) + C_3(2N_{23} + N_{11} - N_{34}) + 3N_{21}C_4$$
$$D_4' \equiv 2C_2 N_{12} + C_3(2N_{22} + N_{13} - N_{35}) + C_4(3N_{23} - N_{34})$$
$$D_5' \equiv C_3 N_{12} + C_4(3N_{22} - N_{35})$$

and

$$B_1' \equiv B_1(2N_{14} - N_{36}) + B_3 N_{24}$$
$$B_2' \equiv 2B_1 N_{15} + B_3(N_{14} - N_{36} + N_{25}) + 2N_{24}B_2$$
$$B_3' \equiv B_2(2N_{25} - N_{36}) + N_{15}B_3.$$

In using these formulas, B_i' and D_i' are first evaluated from the known quadratic and cubic coefficients, then the D_i'' can be computed. D_4 is given in terms of the D_i'', and D_2 involves D_4; knowing D_2 and D_4 fixes D_1, D_3, and D_5.

In this chapter, the Hopf normal form will be evaluated through terms of fifth degree. This means that the center manifold vecter field must be computed through fifth order. To do this, $h(x, y)$ is needed through fourth order (i.e. quartic terms), since the nonlinear terms in $N(\varsigma)$ begin at second order. Thus

the calculation of $h(x,y)$ is complete.

The center manifold dynamics is extracted by restricting (2.5) to the center manifold, i.e. set $z = h(x,y)$. Since h by definition satisfies (2.8), the component equation for dz/dt in (2.5) is automatically satisfied, and only the two dimensional flow on W^c remains. (Note that the (x,y) components of (2.5) correspond to (1.6). In this example the formal projection by adjoint vectors amounts to simply dropping the z component of (2.5).) To resume the notation of Chapter 1, write this flow as

$$\frac{d\varsigma}{dt} = \mathcal{V}(\varsigma) \qquad \varsigma = (x,y) \in \Re^2$$

where

$$\mathcal{V}(\varsigma) = \begin{pmatrix} \mu & \Lambda \\ -\Lambda & \mu \end{pmatrix}\begin{pmatrix} x \\ y \end{pmatrix} + \begin{pmatrix} N_{11}x^2 + N_{12}y^2 + N_{13}xy \\ N_{21}x^2 + N_{22}y^2 + N_{23}xy \end{pmatrix}$$
$$+ \begin{pmatrix} N_{14}xh(x,y) + N_{15}yh(x,y) + N_{16}(h(x,y))^2 \\ N_{24}xh(x,y) + N_{25}yh(x,y) + N_{26}(h(x,y))^2 \end{pmatrix}.$$

Thus, in the notation of (1.13),

$$\mathcal{V}^{(1)}(\zeta) = \begin{pmatrix} \mu x + \Lambda y \\ -\Lambda x + \mu y \end{pmatrix}$$

$$\mathcal{V}^{(2)}(\zeta) = \begin{pmatrix} N_{11}x^2 + N_{12}y^2 + N_{13}xy \\ N_{21}x^2 + N_{22}y^2 + N_{23}xy \end{pmatrix}$$

$$\mathcal{V}^{(3)}(\zeta) = \begin{pmatrix} N_{14}x + N_{15}y \\ N_{24}x + N_{25}y \end{pmatrix} h^{(2)}(x,y)$$

$$\mathcal{V}^{(4)}(\zeta) = \begin{pmatrix} N_{14}x + N_{15}y \\ N_{24}x + N_{25}y \end{pmatrix} h^{(3)}(x,y) + \begin{pmatrix} N_{16} \\ N_{26} \end{pmatrix} (h^{(2)}(x,y))^2$$

$$\mathcal{V}^{(5)}(\zeta) = \begin{pmatrix} N_{14}x + N_{15}y \\ N_{24}x + N_{25}y \end{pmatrix} h^{(4)}(x,y) + 2\begin{pmatrix} N_{16} \\ N_{26} \end{pmatrix} h^{(2)}(x,y)h^{(3)}(x,y).$$

Examining these formulas reveals the essential role played by the curvature of W^c. A satisfactory analysis of the dynamics must take into account $h^{(2)}(x,y) \not\equiv 0$. If this curvature were neglected and $h(x,y) \equiv 0$ assumed, then geometrically the nonlinear manifold, W^c, would be replaced by the linear (x,y)-plane. The effect on $\mathcal{V}(\zeta)$ would be to leave $\mathcal{V}^{(1)}(\zeta)$ and $\mathcal{V}^{(2)}(\zeta)$ unchanged, but enforce $\mathcal{V}^{(j)}(\zeta) = 0$ for $j \geq 3$. However, $\mathcal{V}^{(3)}(\zeta)$ is required to correctly determine the normal form coefficients a_1 and b_1 in (1.28). From (1.27), recall that these coefficients are fixed by the terms of degree 3 lying in the kernel of the operator $L^{(3)}$. Neglecting $\mathcal{V}^{(3)}(\zeta)$ would in general alter these terms; hence the effects of $h^{(2)}(x,y) \not\equiv 0$ must be included.

Analysis of the Normal Form

The normal form theory of Chapter 1 allows the two dimensional flow

$$\frac{d\zeta}{dt} = \mathcal{V}(\zeta)$$

to be rewritten in polar coordinates,

$$\frac{dr}{dt} = \mu r + a_1(\mu,\gamma)r^3 + a_2(\mu,\gamma)r^5 + O(r^7) \tag{2.11a}$$

$$\frac{d\theta}{dt} = -\Lambda + b_1(\mu,\gamma)r^2 + b_2(\mu,\gamma)r^4 + O(r^6). \tag{2.11b}$$

The formulas which express the coefficients a_1, a_2, b_1, and b_2 in terms of the coefficients in $\mathcal{V}^{(2)}(\zeta)$, $\mathcal{V}^{(3)}(\zeta)$, $\mathcal{V}^{(4)}(\zeta)$, and $\mathcal{V}^{(5)}(\zeta)$ are explicitly derived in the Appendix.

The normal form coefficient a_1 is of greatest interest since it controls the appearance or disappearance of the periodic orbit. For small r there are two solutions to $dr/dt = 0$.

$$\frac{dr}{dt} \approx \mu r + a_1 r^3 = 0$$

The $r = 0$ solution is unstable when $\mu > 0$; if $a_1(\mu = 0, \gamma) < 0$ then the new stable solution is $r_0 = \sqrt{(-\mu/a_1)}$ which corresponds to a stable periodic orbit. If $a_1(0,\gamma) > 0$ this second solution is relevant for $\mu < 0$ and then describes an unstable periodic orbit.

The graph of $a_1(0,\gamma)$ appears in Fig. (2.2a). Notice that $a_1(0,\gamma)$ changes sign at $\gamma_c \sim 3.29$. Only for damping rates greater than γ_c will the instability

saturate in a small amplitude oscillation. For $\gamma < \gamma_c$ the normal form implies that there is no stable attractor in the neighborhood of $r = 0$; in fact, numerical studies indicate the wave amplitudes grow without bound.

In the vicinity of $(\gamma = \gamma_c, \mu = 0)$, the stable Hopf orbit must be destroyed in a separate bifurcation. This is clear, since for $\gamma \leq \gamma_c$, $0 < \mu \ll 1.0$ there is no periodic orbit in the neighborhood of the fixed point. Thus the Hopf bifurcation surface at $\mu = 0$ in parameter space must intersect at least one additional bifurcation surface at $(\gamma = \gamma_c, \mu = 0)$.

At $(\gamma = \gamma_c, \mu = 0)$ the instability of $r = 0$ is a ***degenerate*** Hopf bifurcation. It is one of the simplest examples of a ***co-dimension two*** bifurcation. The analysis of this degenerate case in Golubitsky and Langford (1981) shows that there is only one bifurcation surface which intersects the Hopf surface. This second surface marks parameter values at which the stable Hopf orbit collides with an unstable periodic orbit and both disappear. In the return map for the Hopf orbit, this collision is a saddle-node bifurcation which annihilates two fixed points (see Guckenheimer (1984)). For this reason, this second surface may be referred to as the saddle-node surface; it was discovered numerically by Meunier et al. (1980).

To determine how the saddle-node surface approaches the Hopf surface (at $\mu = 0$) requires an analysis which includes both periodic orbits. Since the saddle-node surface intersects the Hopf surface, the saddle-node bifurcation occurs for arbitrarily small positive values of μ; see Fig. (2.6). This means that the two

orbits can collide while the Hopf orbit is still in a very small neighborhood of $r = 0$. Under these circumstances the local attractivity of W^c near $r = 0$ will not permit a periodic orbit which is not in fact contained in W^c. For this reason, both periodic orbits must lie in W^c and their collision is a feature of the center manifold dynamics.

When this saddle-node bifurcation occurs at small μ and small r, (2.11b) implies that the flow is cylindrically symmetric. Therefore (2.11a) for dr/dt suffices to describe the bifurcation.

At the saddle-node bifurcation the linear stability of the Hopf orbit is lost, but the orbit still exists. The bifurcation surface is determined by these two facts. The existence of the Hopf orbit at criticality means that $r = r_0$ is still a solution to $dr/dt = 0$. From (2.11a) this implies

$$\mu + a_1 r_0^2 + a_2 r_0^4 = 0 \tag{2.12}$$

where the r_0^4 term must be kept since $a_1 = 0$ is allowed. Linearizing (2.11a) about the Hopf orbit determines the orbit's linear stability within W^c. For $\rho \equiv r - r_0$,

$$\frac{d\rho}{dt} = (\mu + 3a_1 r_0^2 + 5a_2 r_0^4)\rho + \cdots.$$

Linear stability of $\rho = 0$ changes when

$$\mu + 3a_1 r_0^2 + 5a_2 r_0^4 = 0. \tag{2.13}$$

Equations (2.12) and (2.13) suffice to determine the saddle-node surface at

small μ. To eliminate r_0, subtract (2.12) from (2.13) to get

$$2r_0^2(2a_2r_0^2 + a_1) = 0.$$

Here a solution for $r_0 \neq 0$ exists only if

$$\frac{a_1}{a_2} < 0 \tag{2.14}$$

then

$$r_0^2 = \frac{-a_1}{2a_2} > 0.$$

Inserting this solution into either (2.12) or (2.13) yields

$$4\mu = \frac{(a_1)^2}{a_2}. \tag{2.15}$$

Equations (2.14) and (2.15) describe the saddle-node surface for $0 \leq \mu \ll 1$. There are two cases: the saddle-node surface branches from the point $(a_1 = 0, \mu = 0)$ to the right $(a_1 < 0)$ or to the left $(a_1 > 0)$ depending on the algebraic sign of a_2. These cases are sketched in Fig. (2.3). The graph of $a_2(0, \gamma)$ appears in Fig. (2.2a); at $\gamma = \gamma_c$, a_2 is positive and the situation in Fig. (2.3b) applies.

The normal form coefficients b_1 and b_2 describe amplitude dependent corrections to the linear frequency, Λ. Their dependence on γ at $\mu = 0$ is shown in Fig. (2.2b).

The information obtained from this normal form analysis was checked numerically. Fig. (2.4) shows the Hopf bifurcation to a stable limit cycle for $\gamma > \gamma_c$. As γ decreases (at fixed $\mu = 0.01$), the limit cycle loses stability at $\gamma \sim$

3.55. This transition appears in Fig. (2.5), and represents the "experimental" manifestation of the global saddle-node bifurcation.

A comparison of the theoretical saddle-node surface and the numerically determined surface appears in Table 2.1 and Fig. (2.6).

Table 2.1		
μ	γ_c(Normal Form)	γ_c(Numerical)
0.005	3.57	3.49
0.0075	3.66	3.53
0.01	3.74	3.55
0.02	4.08	3.70
0.03	4.52	3.75
0.04	5.08	3.78
0.05	5.72	3.85
0.10	7.64	4.05

Comparison of numerical results with the saddle-node surface computed from equation (2.15)

The results from (2.15) compare poorly for $\mu > 0.01$; it is not clear why the range of validity is so restricted.

A Digression: Absence of Secondary Hopf Bifurcation

There is a very simple argument which shows that in this model it is not possible to have a secondary Hopf bifurcation to an *attracting* torus. This

argument also applies to a number of other finite dimensional systems which exhibit period doubling cascades; see Feigenbaum (1980) and McLaughlin (1981).

The linear stability of a periodic orbit is determined by the eigenvalues of its linearized return map, or equivalently by the Floquet multipliers of the vector field obtained by linearizing the evolution equation (equation (2.5) for example) about the periodic orbit. If all the multipliers are within the unit circle, the orbit is linearly stable. The bifurcations of a stable orbit occur when multipliers escape from the unit circle as parameters in the evolution equation are varied. For example, the saddle-node bifurcation just discussed corresponds to a real multiplier exiting the unit circle at $+1$. Period doubling corresponds to a multiplier passing through -1, and secondary Hopf bifurcation occurs when a complex conjugate pair of multipliers leave the unit circle at points which are not low order roots of unity (Guckenheimer (1984)).

In $\Re^3$, there is a simple criterion for a bifurcation involving a conjugate pair of multipliers. Let the evolution equation

$$\frac{dx}{dt} = V(x) \qquad x \in \Re^3$$

have a periodic orbit, $x_\tau(t)$, with period τ.

$$x_\tau(t) = x_\tau(t+\tau).$$

The linear stability of $x_\tau(t)$ is determined from the multipliers of the linearized equation:

$$\frac{d\delta x}{dt} = DV(x_\tau(t)) \cdot \delta x.$$

There are three multipliers, but one is always equal to unity since perturbations δx along the orbit $x_\tau(t)$ have strictly neutral stability (Iooss and Joseph (1980)). A simple result from Floquet theory relates the product of the multipliers, $\rho_1\rho_2\rho_3$, to the trace of $DV(x_\tau(t))$ (Jordan and Smith (1977)).

$$\rho_1\rho_2\rho_3 = \exp\left[\int_0^\tau \operatorname{Tr} DV(x_\tau(t))\, dt\right] \tag{2.16}$$

Now in the stability problem for $x_\tau(t)$ when a conjugate pair of multipliers, $\rho_1 = \overline{\rho_2}$, cross the unit circle, (2.16) reduces to

$$1 = \exp\left[\int_0^\tau \operatorname{Tr} DV(x_\tau(t))\, dt\right] \tag{2.17}$$

since $\rho_3 \equiv 1$ as noted above. Equation (2.17) implies a ***necessary and sufficient*** condition for criticality:

$$\int_0^\tau \operatorname{Tr} DV(x_\tau(t))\, dt = 0.$$

Since $\operatorname{Tr} DV(x) = (\operatorname{div} V)(x)$, this is equivalent to

$$\int_0^\tau (\operatorname{div} V)(x_\tau(t))\, dt = 0. \tag{2.18}$$

Equation (2.18) requires that the average divergence of $V(x)$ around $x_\tau(t)$ vanish at criticality for a bifurcation involving a conjugate pair of multipliers. This is a geometrically intuitive requirement. For the 3-wave model the left hand side of (2.18) is trivial to evaluate since $\operatorname{div} V_{\Omega,\Gamma} = 2(1-\Gamma)$. Hence $\Gamma = \gamma/2 = 1$ determines the curve in parameter space along which these bifurcations occur.

However for $\Gamma < 1$, the flow expands volumes, and there cannot exist a stable, zero volume attractor. In particular this shows that a limit cycle for $\Gamma > 1$ cannot bifurcate to a stable torus since the torus would have to exist for $\Gamma < 1$. The only allowed bifurcations are those involving real multipliers at ± 1, and indeed both types are observed in the numerical studies of Wersinger, Finn, and Ott (1980) and Meunier, Bussac, and Laval (1980).

Figure Captions

Figure (2.1) Surfaces of constant μ in the (Ω, Γ) parameter space. The Hopf bifurcation surface is $\mu = 0$. Note that μ is never larger than 0.5 despite the fact that Ω and Γ are each unbounded.

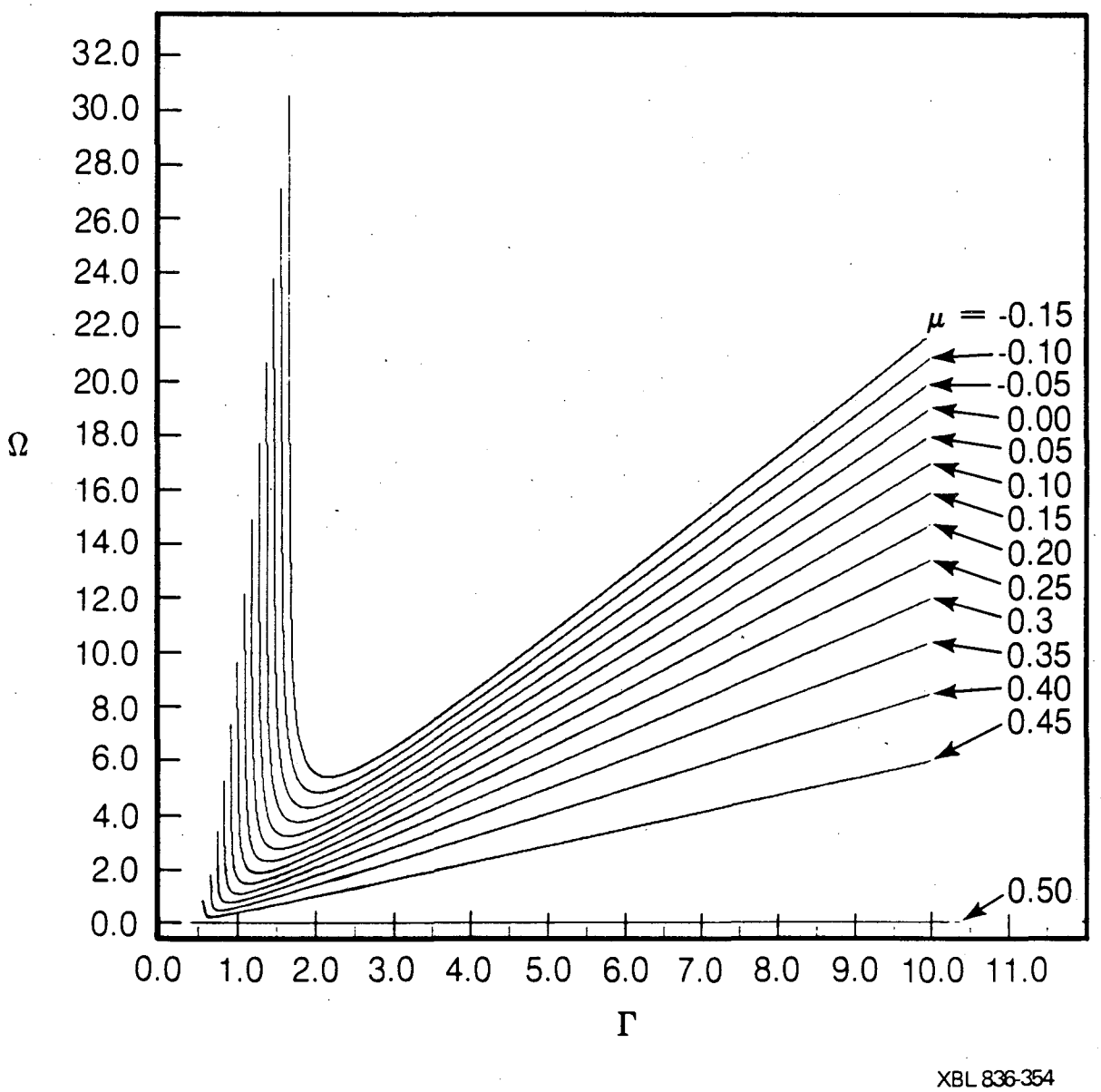
32.0
30.0
28.0
26.0
24.0
22.0
20.0
18.0
16.0
14.0
12.0
10.0
8.0
6.0
4.0
2.0
0.0
Ω
μ = -0.15
-0.10
-0.05
0.00
0.05
0.10
0.15
0.20
0.25
0.3
0.35
0.40
0.45
0.50
0.0 1.0 2.0 3.0 4.0 5.0 6.0 7.0 8.0 9.0 10.0 11.0
Γ
XBL 836-354

Figure (2.1)

Figure (2.2a) At criticality ($\mu = 0$) the normal form coefficients a_1 and a_2 in (2.11a) are plotted against γ ($\gamma = 2\Gamma$). The vertical scale is logarithmic in terms of the function $f(a) \equiv \mathrm{sgn}(a)\log(1.0 + a)$.

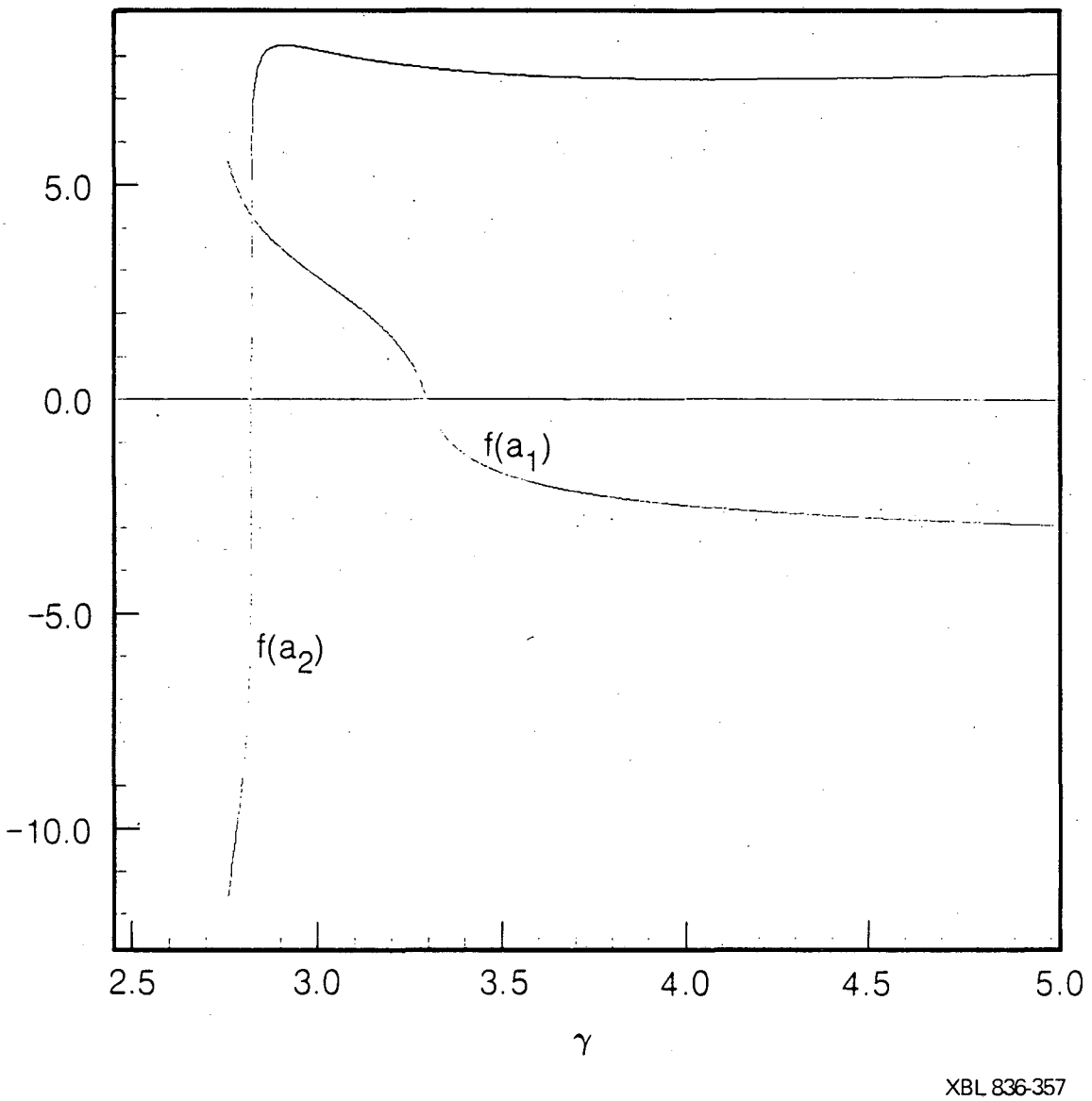

Figure (2.2a)

Figure (2.2b) At criticality the normal form coefficients b_1 and b_2 in (2.11a) are plotted logarithmically against γ. The function f(b) is the same as in Fig. (2.2a).

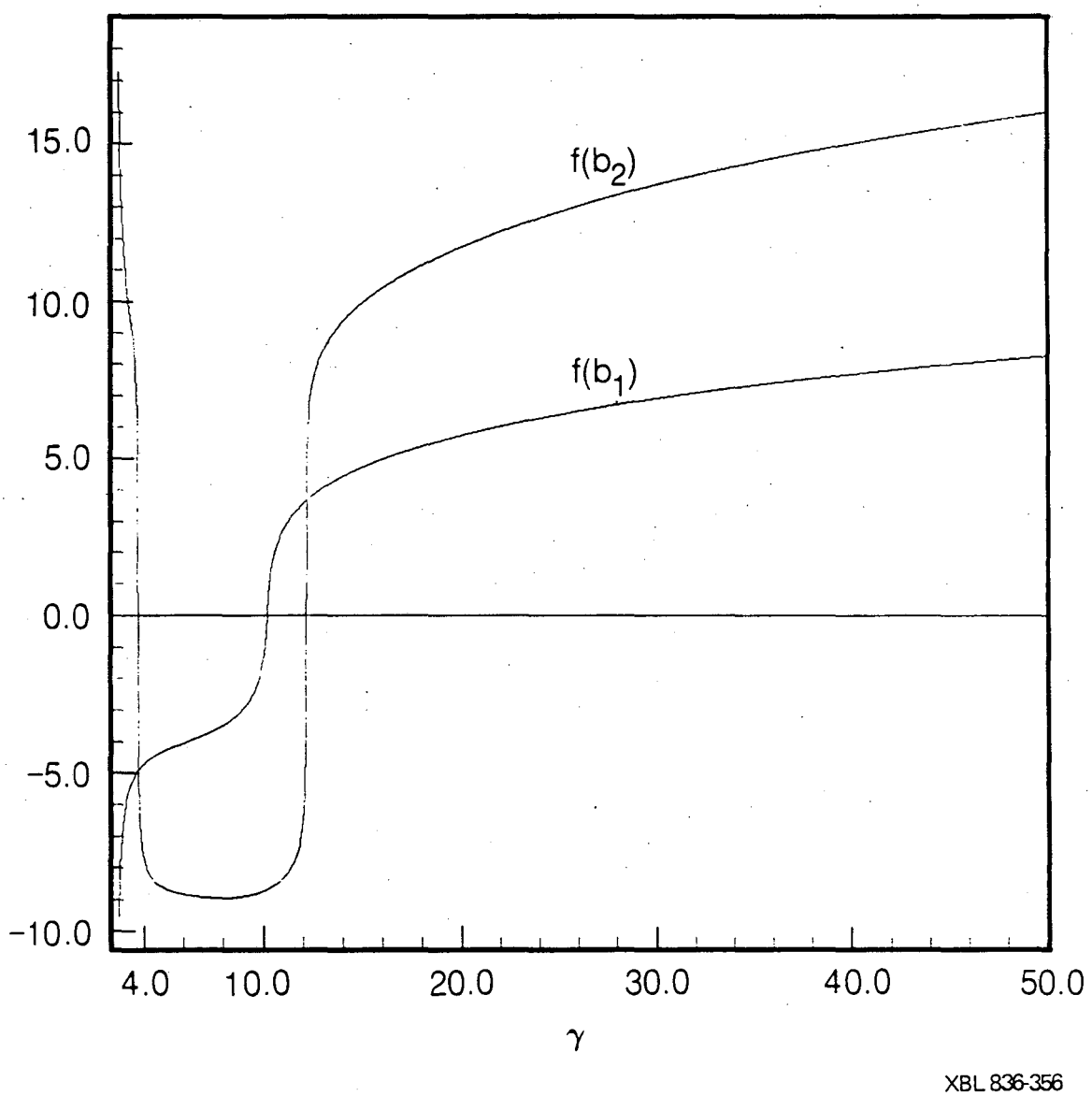

Figure (2.2b)

Figure (2.3) For the degenerate Hopf bifurcation corresponding to $a_1 = 0$ and $a_2 \neq 0$ there are two possibilities depending on the sign of a_2 at criticality. For $a_2 > 0$, the saddle-node surface (SN) branches toward negative values of a_1. For $a_2 < 0$, the SN surface branches toward positive values of a_1. The unstable periodic orbit which collides with the stable Hopf orbit is not shown.

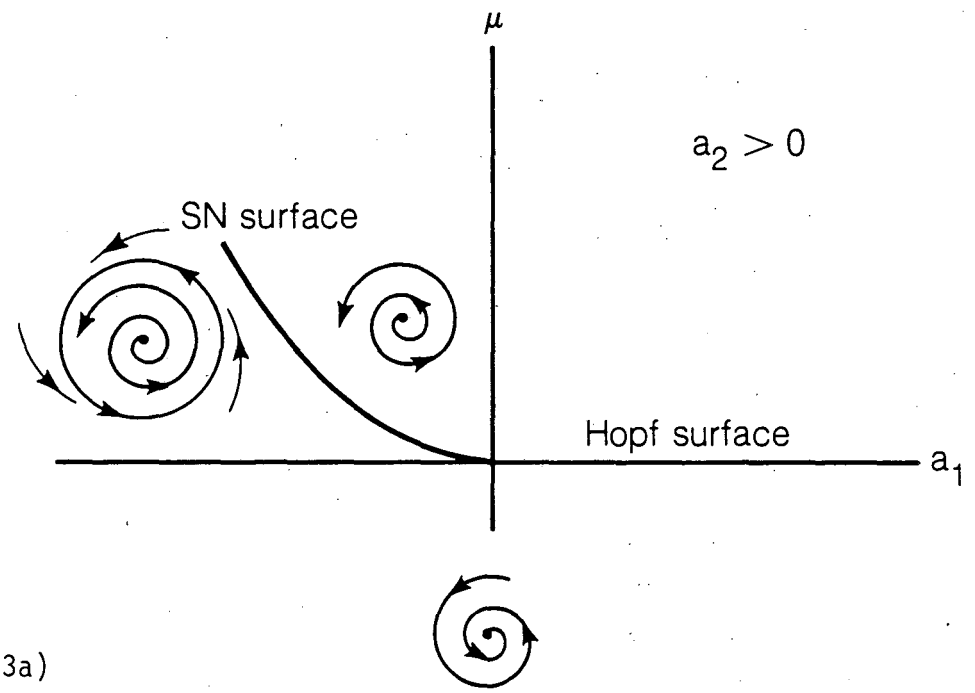

Figure (2.3a)

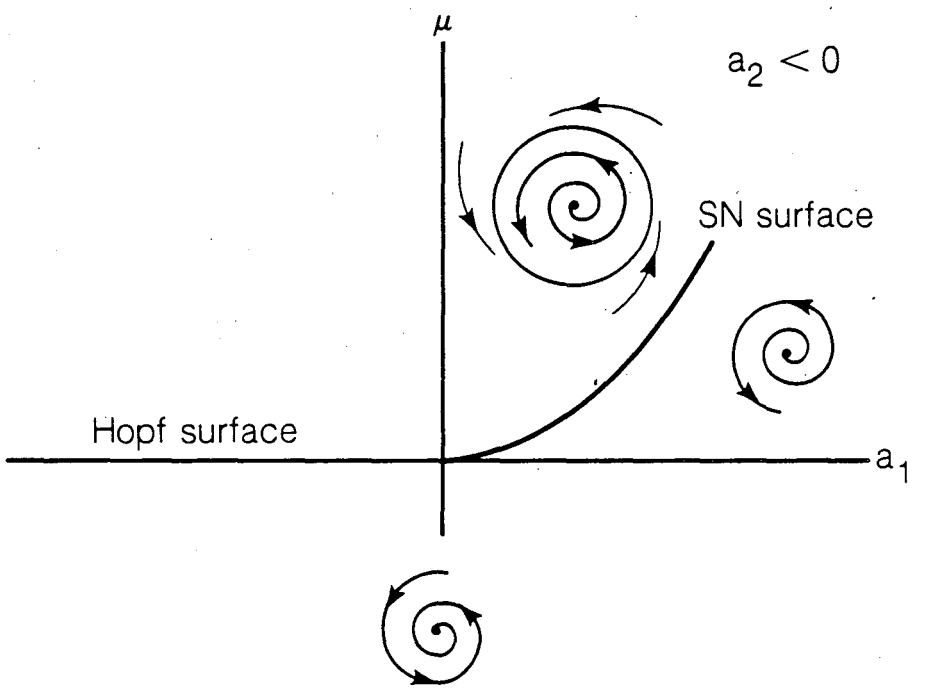

Figure (2.3b)

XBL 836-359

Figure (2.4a) $x(t)$ from (2.1) versus t. The horizontal line shows the x coordinate of the stable fixed point.

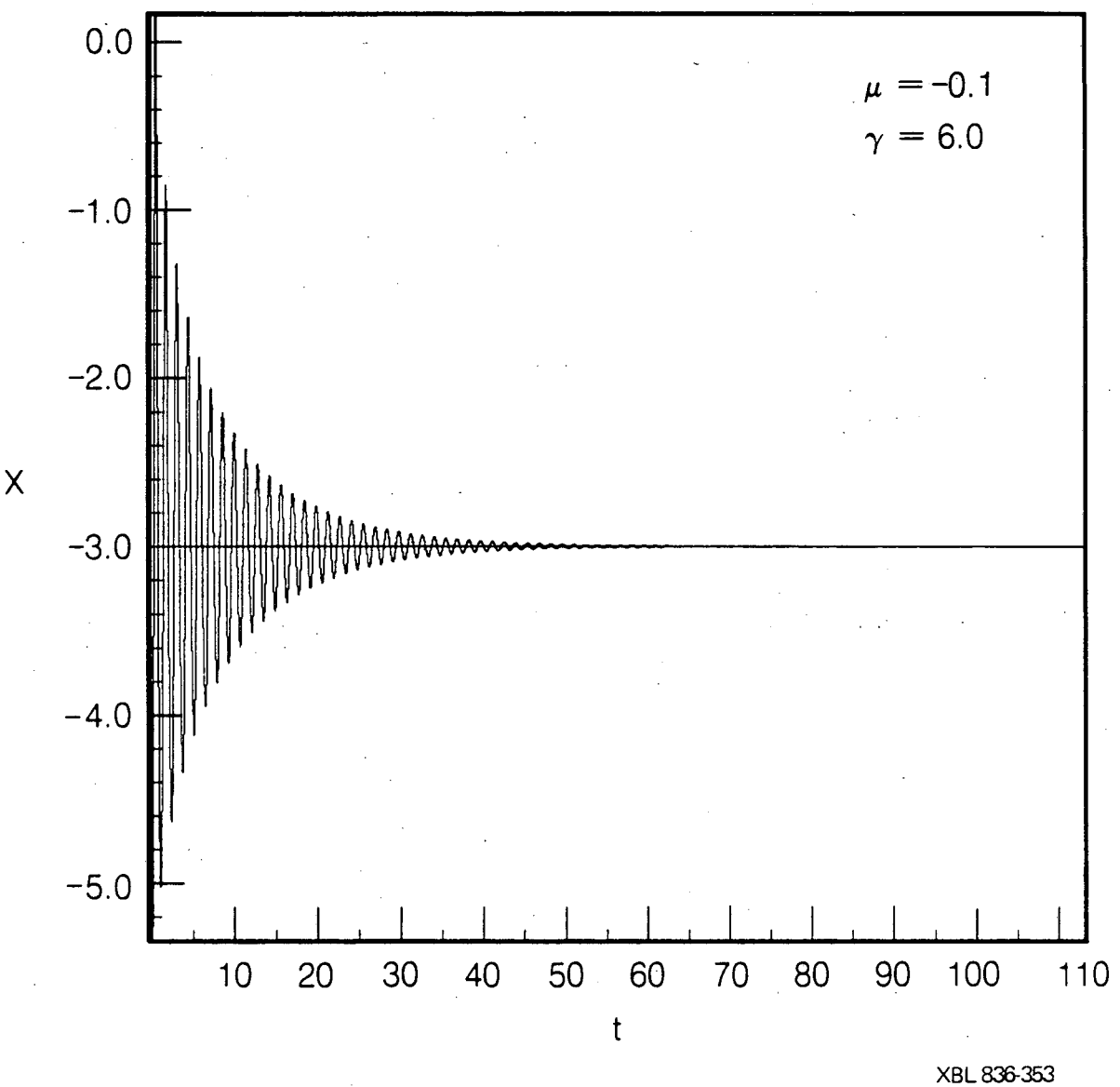
0.0
-1.0
-2.0
-3.0
-4.0
-5.0
X
$\mu = -0.1$
$\gamma = 6.0$
10
20
30
40
50
60
70
80
90
100
110
t
XBL 836-353

Figure (2.4a)

Figure (2.4b) Same as in Fig. (2.4a) except now $\mu = 0.1$. The fixed point is now unstable, and has been replaced by a stable oscillation.

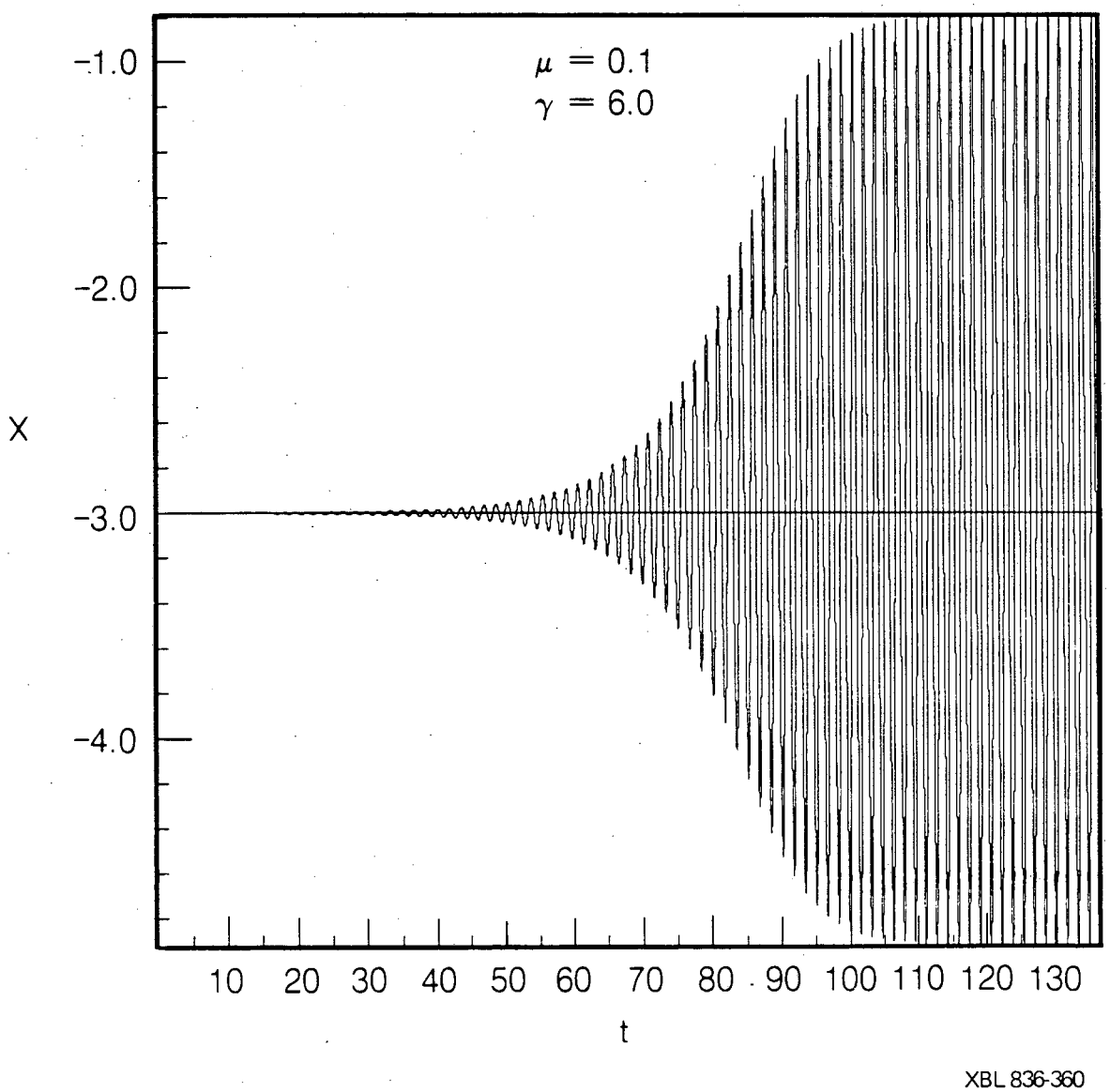
μ = 0.1
γ = 6.0
-1.0
-2.0
-3.0
-4.0
X
10 20 30 40 50 60 70 80 90 100 110 120 130
t
XBL 836-360

Figure (2.4b)

Figure (2.5a) $x(t)$ from (2.1) versus t. The horizontal line shows the x coordinate of the unstable fixed point. The trajectory relaxes onto the stable Hopf orbit.

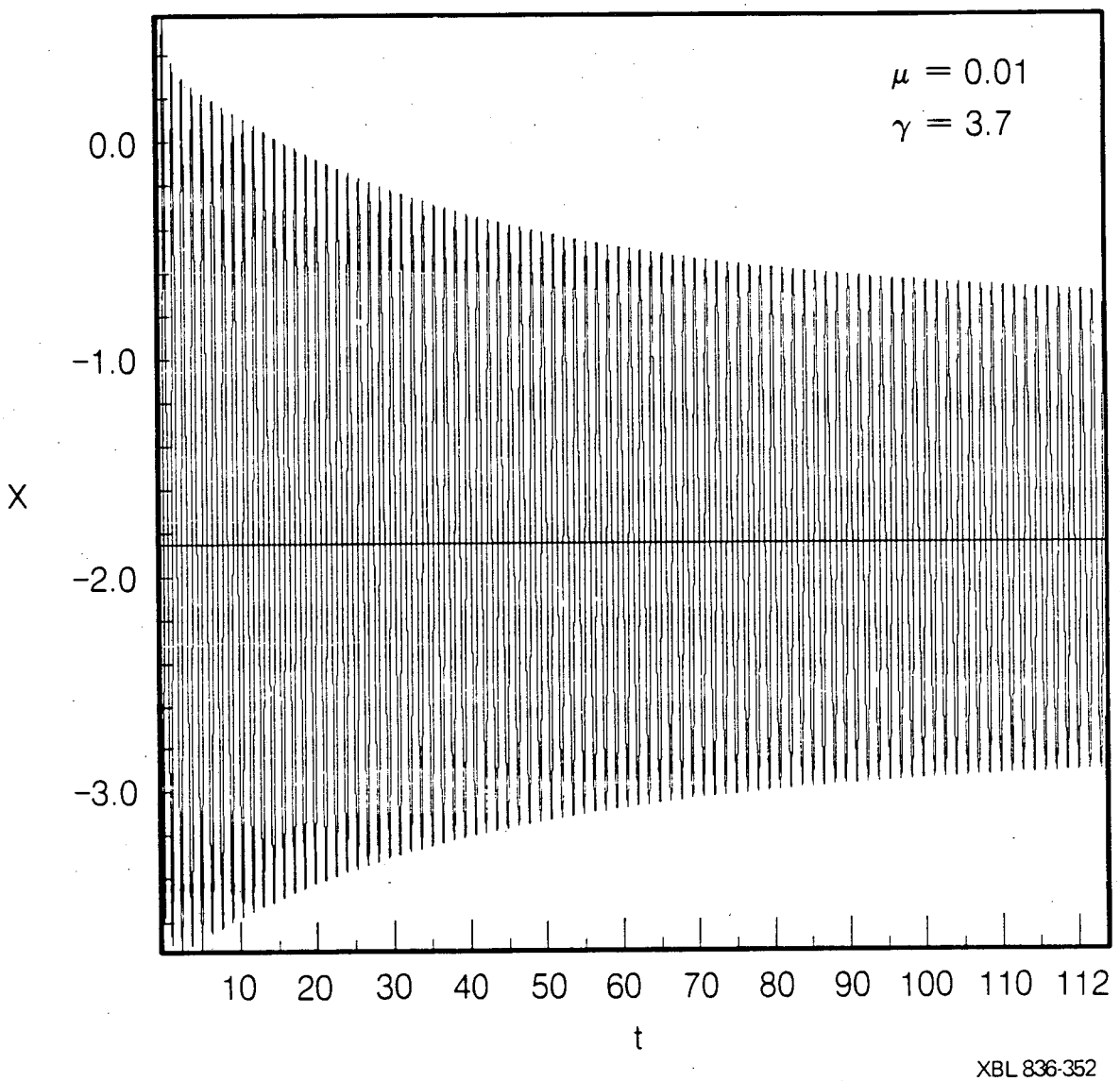
μ = 0.01
γ = 3.7
0.0
-1.0
-2.0
-3.0
X
10
20
30
40
50
60
70
80
90
100
110
112
t
XBL 836-352

Figure (2.5a)

Figure (2.5b) Same as in Fig. (2.5a) except $\gamma = 3.50$ has been decreased across the saddle-node bifurcation surface. No stable orbit remains. Notice the difference in the vertical scale between Fig. (2.5a) and Fig. (2.5b).

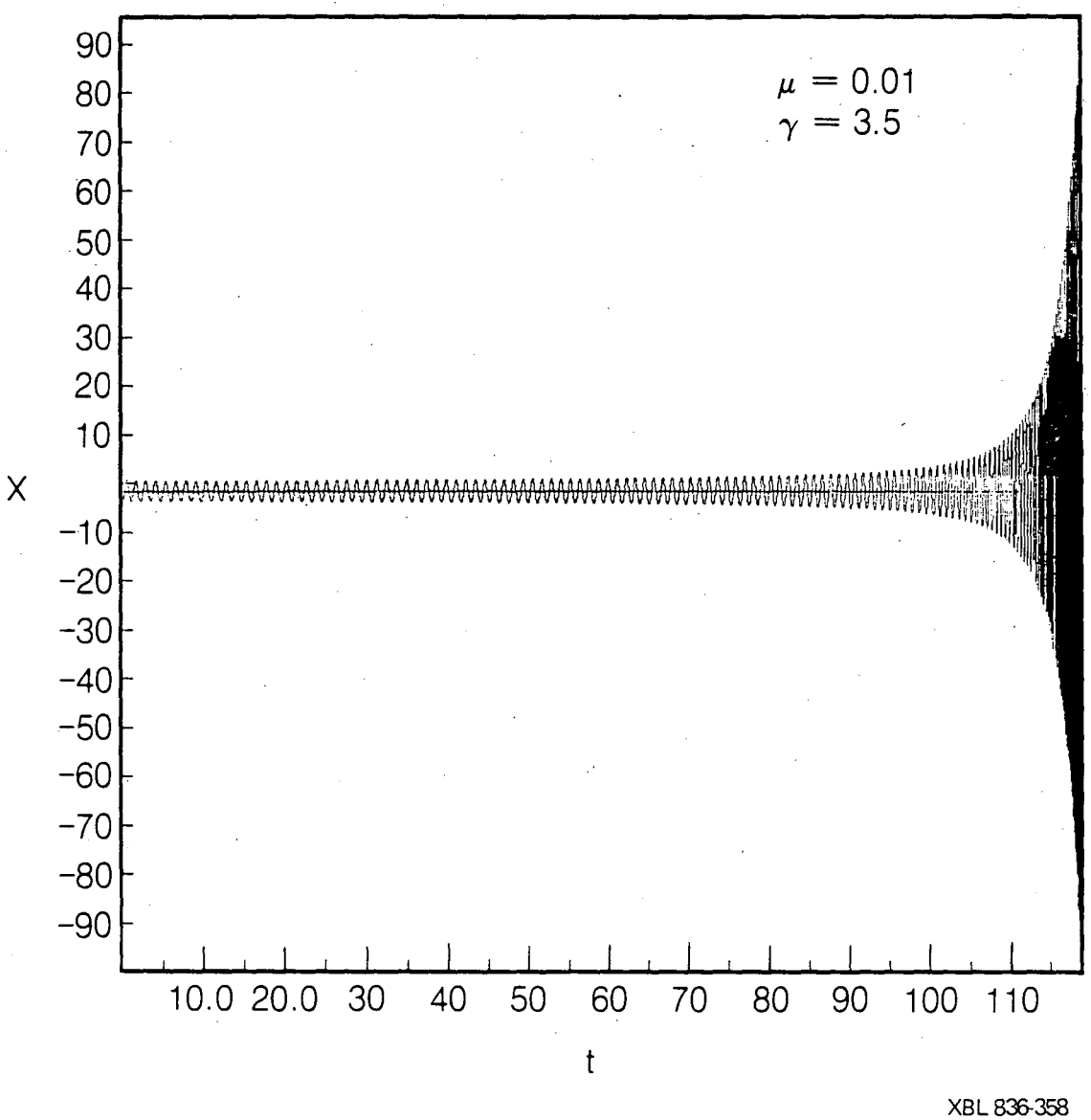
μ = 0.01
γ = 3.5
X
t
90
80
70
60
50
40
30
20
10
-10
-20
-30
-40
-50
-60
-70
-80
-90
10.0
20.0
30
40
50
60
70
80
90
100
110
XBL 836-358

Figure (2.5b)

Figure (2.6) H denotes the Hopf bifurcation surface ($\mu = 0$). SN is the saddle-node surface computed from (2.15). The points (•) are the numerical data where the transition in Figs. (2.5a) and (2.5b) was detected.

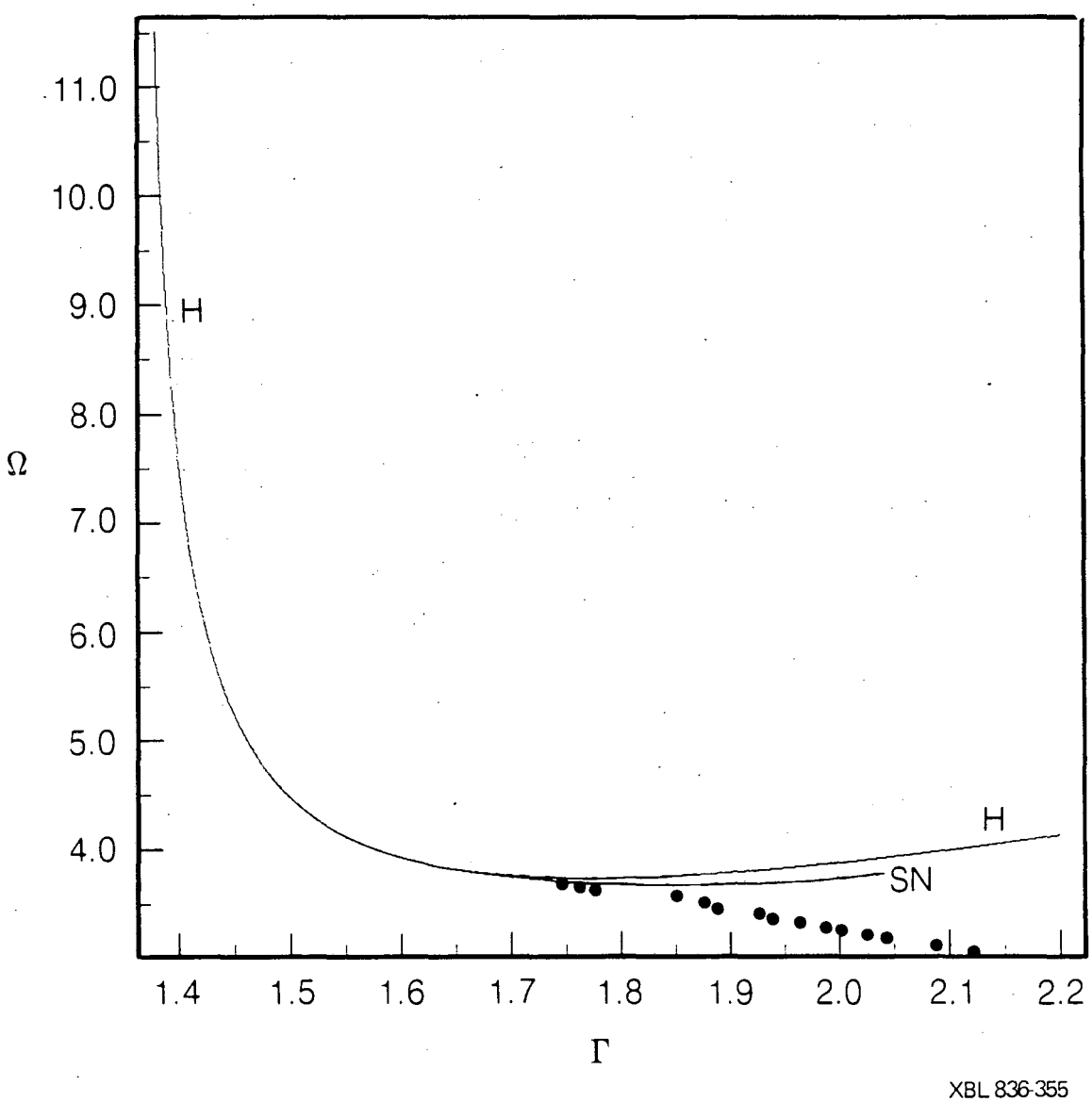
11.0
10.0
9.0
8.0
7.0
6.0
5.0
4.0
Ω
H
H
SN
1.4
1.5
1.6
1.7
1.8
1.9
2.0
2.1
2.2
Γ
XBL 836-355

Figure (2.6)

CHAPTER 3

Hopf Bifurcation in Plasma Kinetic Theory

In nonlinear plasma theory a distinction is frequently made between wave-wave interactions and wave-particle interactions. If the dynamical fields, such as the one particle distribution function, are Fourier decomposed in space and time and the plasma dynamics rewritten in terms of the Fourier amplitudes then roughly speaking nonlinear terms which couple spatially inhomogeneous Fourier modes are wave-wave interactions while nonlinear couplings between homogeneous and inhomogeneous modes are wave-particle interactions. In the last chapter a simple model which derived from a mode truncation keeping only three inhomogeneous modes was considered. The characterization of the model as a 3-wave interaction reflects this choice of modes in the truncation. In this chapter instabilities driven by wave-particle interactions are discussed as Hopf bifurcations. These instabilities serve as sources of waves in an otherwise

quiescent plasma, and therefore provide the raw material for the wave-wave interactions discussed in Chapter 2.

Wave-particle interactions produce unstable wave growth when the distribution of particles provides the wave with a source of energy. One way this can occur is if some particles are in resonance with the wave; this requires that the particle velocity match the wave phase velocity. Resonant particles feel a stationary electric field due to the wave. If the resonant particles are distributed about the phase velocity so that more particles are retarded by this electric field than are accelerated, the net effect of the interaction is a transfer of energy to the wave. The mechanism of such an instability depends crucially on the distribution of particles in velocity; consequently a kinetic theory (rather than a fluid model) is required to study these instabilities.

Collisions between particles is a natural form of dissipation in kinetic theory, and collisions are an important mechanism in the relaxation to thermodynamic equilibrium. Including collisions in a model thus satisfies the dissipative prerequisite for Hopf bifurcation, but at the cost of making thermodynamic equilibrium essentially the unique fixed point for the dynamics. This is physically reasonable, but awkward for the instability analysis since the distribution which exhibits the resonance driven instability is not an equilibrium distribution. Thus the instability occurs on top of the collisional relaxation to equilibrium. Under such circumstances it may not be fruitful to speak of the resonant instability

and the collisional relaxation as distinct phenomena unless the time scales for the two processes are reasonably well separated. In the case for which unstable waves develop, interact, and saturate on a time scale short compared to the time scale required to reach thermodynamic equilibrium, then neglecting the collisional relaxation of the initial distribution and keeping only the effects of collisions on the evolution of the waves is a useful approximation. This is the approximation used in this chapter to extract an autonomous kinetic equation for the dynamics of the perturbations. This leads to an interesting model which exhibits the familiar electrostatic instabilities, but is too idealized to quantitatively describe a laboratory plasma.

The Model

To discuss electrostatic instabilities, consider a one dimensional plasma with the electron dynamics given by the Vlasov-Poisson equations supplemented by a collision term, $C(F)$.

$$\begin{aligned} \frac{\partial F}{\partial t} + v\frac{\partial F}{\partial x} + \frac{e}{m}\frac{\partial \phi}{\partial x}\frac{\partial F}{\partial v} &= C(F) \\ -\frac{\partial^2 \phi}{\partial x^2} &= 4\pi e n_0 \left[1 - \int_{-\infty}^{\infty} dv'\, F\right] \end{aligned} \tag{3.1}$$

Here $F = F(x, v, t)$ is the electron distribution normalized such that

$$\begin{aligned} n_0 \int_{-\infty}^{\infty} dv'\, F(x, v', t) &= n(x, t), \text{ number density of electrons} \\ \int_0^L dx\, n(x, t) &= N, \text{ total number of electrons} \end{aligned} \tag{3.2}$$

and $\phi = \phi(x,t)$ is the self-consistent electrostatic potential. The plasma has finite length $0 \leq x \leq L$ with periodic boundary conditions, an average electron density $n_0 = N/L$, and an electron charge/mass ratio of $-e/m$. The dynamics of ions and neutral atoms is ignored except that a fixed background of ions provides overall charge neutrality in the Poisson equation and electron-ion or electron-neutral collisions could be included in $C(F)$.

Let $F = F_0(v)$ denote a spatially uniform distribution whose stability against electrostatic perturbations is of interest. Let F_1 and F_2 be solutions to (3.1) corresponding to slightly different initial conditions,

$$F_1(x,v,t=0) = F_0(v)$$

$$F_2(x,v,t=0) = F_0(v) + f(x,v,t=0)$$

with $f(x,v,t) \equiv F_2(x,v,t) - F_1(x,v,t)$. Note that

$$\int_0^L \int_{-\infty}^{\infty} dx\, dv\, f(x,v,t) = 0$$

since N is fixed for both initial conditions. The dynamics for $f(x,v,t)$ is obtained by subtracting (3.1) for F_2 from (3.1) for F_1 which yields,

$$\frac{\partial f}{\partial t} + v\frac{\partial f}{\partial x} + \frac{e}{m}\left[\frac{\partial \phi_2}{\partial x}\frac{\partial F_2}{\partial v} - \frac{\partial \phi_1}{\partial x}\frac{\partial F_1}{\partial v}\right] = C(F_2) - C(F_1). \tag{3.3}$$

Using the definition $\phi_f \equiv \phi_2 - \phi_1$ and the Poisson equation for ϕ_2 and ϕ_1, the nonlinear terms in (3.3) become

$$\frac{\partial \phi_2}{\partial x}\frac{\partial F_2}{\partial v} - \frac{\partial \phi_1}{\partial x}\frac{\partial F_1}{\partial v} = \frac{\partial \phi_1}{\partial x}\frac{\partial f}{\partial v} + \frac{\partial \phi_f}{\partial x}\frac{\partial (F_1 + f)}{\partial v}$$

with ϕ_f given in terms of f by,

$$\frac{\partial^2 \phi_f}{\partial x^2} = 4\pi e n_0 \int_{-\infty}^{\infty} dv'\, f(x,v',t). \tag{3.4}$$

So (3.3) becomes

$$\frac{\partial f}{\partial t} + v\frac{\partial f}{\partial x} + \frac{e}{m}\left[\frac{\partial \phi_1}{\partial x}\frac{\partial f}{\partial v} + \frac{\partial \phi_f}{\partial x}\frac{\partial (F_1 + f)}{\partial v}\right] = C(F_1 + f) - C(F_1). \qquad (3.5a)$$

Since the initial condition for F_1 is spatially homogeneous, in the absence of applied electric fields the initial electric field will be zero; i.e.

$$\frac{\partial \phi_1}{\partial x}(x, t = 0) = 0.$$

For collision models, $C(F)$, considered here the spatial Fourier expansion

$$C(F) = \sum_k e^{ikx} C_k(F)$$

has the property that when $F(x, v)$ is spatially homogeneous then $C_k(F) = 0$ for $k \neq 0$. This property of $C(F)$ insures that as F_1 evolves spatial inhomogeneities do not develop and therefore $\partial_x \phi_1 = 0$ for $t > 0$. Hence the term $\partial_x \phi_1 \partial_v f$ in (3.5a) vanishes. If moreover $C(F)$ is ***linear*** then

$$C(F_1 + f) - C(F_1) = C(f)$$

and (3.5a) simplifies to

$$\frac{\partial f}{\partial t} + v\frac{\partial f}{\partial x} + \frac{e}{m}\frac{\partial \phi_f}{\partial x}\frac{\partial (F_1 + f)}{\partial v} = C(f). \qquad (3.5b)$$

Equations (3.5b) and (3.4) for the dynamics of f are not autonomous since F_1 depends on time. The time dependence of F_1 arises because in general $C(F_0) \neq 0$ for interesting choices of F_0 and realistic choices for $C(F)$. This is simply the collisional relaxation of F_1 mentioned earlier. When F_0 is unstable to electrostatic waves, then $f(x, v, t)$ describes the dynamics of these waves. If

the relaxation of F_1 is slower than the growth of the waves, an autonomous approximate description of the waves is obtained by neglecting the variation of F_1 from its initial state, i.e. replace $\partial_v(F_1 + f)$ by $\partial_v(F_0 + f)$. Then the evolution of f is described by,

$$\begin{aligned} \frac{\partial f}{\partial t} + v\frac{\partial f}{\partial x} + \frac{e}{m}\frac{\partial \phi_f}{\partial x}\frac{\partial (F_0 + f)}{\partial v} &= C(f) \\ \frac{\partial^2 \phi_f}{\partial x^2} &= 4\pi e n_0 \int_{-\infty}^{\infty} dv'\, f(x, v', t). \end{aligned} \tag{3.6}$$

The approximation $\partial_v(F_1 + f) \rightarrow \partial_v(F_0 + f)$ does have an unrealistic qualitative effect on the physics which should be borne in mind. In the plasma configurations considered below, the stationary solution $f = 0$ for (3.6) will be (initially) stable. If we consider the original problem (3.5b), then $f = 0$ corresponds to a non-stationary solution. The approximation $\partial_v(F_1 + f) \rightarrow \partial_v(F_0 + f)$ serves to stabilize this non-equilibrium distribution, giving it an exaggerated robustness against perturbations by retaining only those dissipative effects which act to restore $f = 0$. For example when $f = 0$ corresponds to a beam-plasma distribution (see Fig. (3.3a)), the replacement $\partial_v(F_1 + f) \rightarrow \partial_v(F_0 + f)$ serves to stabilize the beam. Effectively those collisional effects which "replenish" the beam are preferentially retained. This exaggerates the amount of energy available to a beam-plasma instablility and inflates the saturated amplitudes of the unstable waves.

The choice for $C(F)$ will vary depending on the plasma in which the waves occur. For a fully ionized gas, a Fokker-Planck description yields a linear collision

operator. A simpler case is the Krook collision model for a weakly ionized gas (Krall and Trivelpiece (1973)); this model will be considered here. The Krook form for $C(F)$ is

$$C(F) = \nu_c(F_{eq} - F), \qquad \nu_c > 0$$

where $F_{eq}(x, v, t) = n(x, t)g_{eq}(v)/n_0$ and

$$g_{eq}(v) = \left(\frac{m}{2\pi kT}\right)^{\frac{1}{2}} e^{-\frac{mv^2}{2kT}}$$

$$\frac{n(x,t)}{n_0} = \int_{-\infty}^{\infty} dv'\, F(x, v', t).$$

For a weakly ionized gas, the dominant collisions are with neutral atoms, and these may be qualitatively viewed as simply exerting a frictional drag on the electrons which brings the electron species to rest with a locally Maxwellian distribution, F_{eq}. This collision model conserves local particle density

$$\int_{-\infty}^{\infty} dv'\, C(F) = 0,$$

but not momentum or energy since the momentum and energy transferred to the neutrals is lost if the dynamics of the neutrals is ignored. Now the right hand side of (3.6) becomes

$$C(f) = -\nu_c\left[f(x, v, t) - g_{eq}(v)\int_{-\infty}^{\infty} dv'\, f(x, v', t)\right]. \tag{3.7}$$

Combining (3.6) and (3.7) produces an evolution equation for f,

$$\frac{\partial f}{\partial t} = Lf + N(f) \tag{3.8}$$

where $\phi_f(x,t)$ has been eliminated using the Fourier expansions for f and ϕ_f

$$f(x,v,t) = \sum_k f_k(v,t)e^{ikx}$$

$$\phi_f(x,t) = \sum_k \phi_k(t)e^{ikx}$$

in Poisson's equation. In these sums the allowed k values are integer multiples of $2\pi/L$. The linear operator in (3.8) is defined by

$$\mathcal{L}f = \mathcal{L}\left(\sum_k f_k e^{ikx}\right) \equiv \sum_k e^{ikx}(L_k f_k)(v) \tag{3.9}$$

where

$$L_0 f_0 = -\nu_c f_0$$

$$L_k f_k = -\left[(ikv + \nu_c)f_k + ik\eta_k \int_{-\infty}^{\infty} dv'\, f_k(v')\right] \qquad k \neq 0$$

with

$$\eta_k(v) \equiv -\left(\frac{\omega_e}{k}\right)^2 \frac{\partial F_0}{\partial v}(v) + \left(\frac{i\nu_c}{k}\right) g_{eq}(v),$$

and the nonlinear operator in (3.8) is

$$\begin{aligned} \mathcal{N}(f) &= \mathcal{N}\Big(\sum_k f_k e^{ikx}\Big) \\ &= \sum_l e^{ilx} \sum_{k\neq 0} \frac{i{\omega_e}^2}{k} \frac{\partial f_{l-k}}{\partial v} \int_{-\infty}^{\infty} dv'\, f_k(v',t). \end{aligned} \tag{3.10}$$

Here ${\omega_e}^2 = 4\pi e^2 n_0/m$ is the plasma frequency.

In (3.8), the point $f = 0$ is a stationary solution; physically it corresponds to the distribution function $F_0(v)$. The linear stability of $f = 0$ is now considered.

Linear Spectrum

If $\nu_c = 0$ in (3.9), then $\mathcal{L}$ reduces to the linear operator which appears in the evolution equation defined by the Vlasov-Poisson equations. The spectral theory for the Vlasov-Poisson operator is well developed. N. van Kampen (1955) considered the case when F_0 is a Maxwellian and showed that the spectrum of $\mathcal{L}$, $\sigma(\mathcal{L})$, consisted of the imaginary axis with associated eigenfunctions which were distributions; there was no discrete spectrum and there were no nonsingular eigenfunctions. Case (1959) analyzed $\mathcal{L}$ for general F_0 and found, in addition to van Kampen's continuous spectrum, there could be discrete spectrum with nonsingular eigenfunctions when a certain function, the dispersion function, had zeros; for F_0 a Maxwellian, the dispersion function does not vanish so only the van Kampen continuum remains. Case also defined an adjoint operator, $\mathcal{L}^\dagger$, whose spectrum coincided with $\sigma(\mathcal{L})$ and whose eigenfunctions satisfied biorthogonality relations with the eigenfunctions of $\mathcal{L}$. Moreover Case proved a completeness theorem for the eigenfunctions of $\mathcal{L}$.

Subsequent applications uncovered two problems. Case's results applied to problems for which the dispersion function had simple roots, and the extension to degenerate roots was not clear. Also for the particular instance of a simple real root of the dispersion function it was discovered that there were two eigenfunctions for $\mathcal{L}^\dagger$, but only one eigenfunction of $\mathcal{L}$. In response to the latter problem, Siewart (1977) constructed a second solution to

$$\frac{\partial f}{\partial t} = \mathcal{L} f$$

which could be combined with Case's eigenfunction to restore the biorthogonality relations and completeness theorem. Case (1978) reviewed Siewart's construction and extended the entire method to include roots of the dispersion function of arbitrary multiplicity.

In a separate development Arthur, Greenberg, and Zweifel (1977) derived a spectral theorem for $\mathcal{L}$ using resolvent integration techniques which had been developed for a similar operator in neutron transport theory. They enlarged the scope of Case's completeness results and also treated the case of a degenerate root for the dispersion function.

Case's normal mode analysis can be carried over to the $\nu_c > 0$ problem in this chapter. Since completeness results are not necessary, a spectral theorem is not required. Furthermore only complex roots of the dispersion function are relevant for the collisional instability so the complications associated with real roots don't come up. In the discussion below it is assumed that the dispersion function has at most simple roots.

For $\nu_c > 0$, $\sigma(\mathcal{L})$ is determined by solutions to

$$\mathcal{L}\Psi = \lambda\Psi \tag{3.11}$$

subject to

$$\int_0^L \int_{-\infty}^{\infty} dx\, dv\, \Psi(x,v) = 0.$$

The latter requirement is imposed in order to be consistent with the analogous property of f. Using (3.9) and the Fourier expansion of Ψ

$$\Psi(x,v) = \sum_k \Psi_k(v) e^{ikx}$$

then (3.11) becomes

$$\begin{aligned} L_0 \Psi_0 &= -\nu_c \Psi_0 = \lambda \Psi_0 \\ L_k \Psi_k &= -\left[(ikv + \nu_c)\Psi_k + ik\eta_k \int_{-\infty}^{\infty} dv'\, \Psi_k(v') \right] = \lambda \Psi_k, \qquad k \neq 0. \end{aligned} \tag{3.12}$$

From the equation for $k = 0$, it is clear that $\Psi(x,v) = \Psi_0(v)$ is an eigenfunction with eigenvalue $\lambda = -\nu_c$. Thus spatially homogeneous perturbations are uniformly damped; these eigenfunctions clearly cannot produce an instability.

For $k \neq 0$, (3.12) can be rewritten, using the definition of L_k in (3.9), to obtain

$$(v - z)\Psi_k(v) = -\eta_k(v) \int_{-\infty}^{\infty} dv'\, \Psi_k(v') \tag{3.13}$$

where $z = -(\nu_c + \lambda)/ik$. The following argument shows that the case where $\int_{-\infty}^{\infty} dv'\, \Psi_k = 0$ does not yield eigenfunctions. If $\int_{-\infty}^{\infty} dv'\, \Psi_k = 0$ then Ψ_k satisfies

$$(v - z)\Psi_k = 0.$$

For $\operatorname{Im} z \neq 0$ clearly $\Psi_k \equiv 0$; when $\operatorname{Im} z = 0$ then $\Psi_k = C\delta(v - z)$ is the distribution which solves (3.13), but the condition $\int_{-\infty}^{\infty} dv'\, \Psi_k = 0$ implies $C = 0$. Hence if $\int_{-\infty}^{\infty} dv'\, \Psi_k = 0$ then $\Psi_k \equiv 0$ and there are no nontrivial solutions.

Since (3.13) is linear in Ψ_k the normalization

$$\int_{-\infty}^{\infty} dv' \, \Psi_k(v') = 1 \tag{3.14}$$

can be imposed, then (3.13) becomes

$$(v - z)\Psi_k(v) = -\eta_k(v). \tag{3.15}$$

This is precisely the eigenvalue problem analyzed by Case (1959) except that here $\eta_k(v)$ has an additional term, $i\nu_c g_{eq}/k$, because $\nu_c \neq 0$.

For $\mathrm{Im}\, z \neq 0$, (3.15) is easily solved for Ψ_k,

$$\Psi_k(v) = \frac{-\eta_k(v)}{v - z}. \tag{3.16}$$

Furthermore the normalization condition (3.14) implies

$$\Lambda_k(z) \equiv 1 + \int_{-\infty}^{\infty} dv' \, \frac{\eta_k(v')}{v' - z} = 0 \tag{3.17}$$

$\Lambda_k(z)$ is Case's dispersion function, and this is his result that a ***complex*** root of $\Lambda_k(z)$ determines an eigenfunction

$$\Psi(x, v) = e^{ikx}\left(\frac{-\eta_k(v)}{v - z}\right), \tag{3.18}$$

and an eigenvalue $\lambda = -\nu_c - ikz$ of $\mathcal{L}$. Moreover since

$$\eta_k(v) = \overline{\eta_{-k}(v)},$$

it follows from (3.17) that if z_0 is a root of Λ_k, then $\overline{z_0}$ is a root of Λ_{-k}. So there is a complex conjugate pair of eigenvalues (with complex conjugate eigenfunctions)

$$\lambda_1 = -\nu_c - ikz_0$$

$$\lambda_2 = -\nu_c - i(-k)\overline{z_0} = -\nu_c + ik\overline{z_0} = \overline{\lambda_1}$$

corresponding to the root z_0. Because linear instability requires $\mathrm{Re}\,\lambda = 0$, it is these elements of $\sigma(\mathcal{L})$ corresponding to $\mathrm{Im}\,z \neq 0$ which are of greatest interest.

Now consider (3.15) for z real, i.e. $z = r \in \mathfrak{R}$. The general solution is now a distribution because the left hand side of (3.15) vanishes at $v = r$.

$$\Psi_k(v) = \mathrm{Pr}\left(\frac{-\eta_k(v)}{v-r}\right) + \lambda_k(v)\delta(v-r) \tag{3.19}$$

where $\lambda_k(v)$ is determined by the normalization of Ψ_k,

$$\lambda_k(r) = 1 + \mathrm{Pr}\int_{-\infty}^{\infty} dv'\,\frac{\eta_k(v')}{v'-r} \tag{3.20}$$

Here Pr denotes the Cauchy principal value of the integral.

For these solutions to be well behaved functions of v requires $\eta_k(r) = \lambda_k(r) = 0$. This can be restated in terms of the boundary values of the dispersion function on the cut; see Roos (1969).

$$\begin{aligned}\Lambda_k^{\pm}(r) &\equiv \lim_{\epsilon\to 0}\Lambda_k(r \pm i\epsilon) \\ &= 1 + \mathrm{Pr}\int_{-\infty}^{\infty} dv'\,\frac{\eta_k(v')}{v'-r} \pm i\pi\eta_k(r)\end{aligned} \tag{3.21}$$

or

$$\Lambda_k^{\pm}(r) = \lambda_k(r) \pm i\pi\eta_k(r).$$

So in the case of z real, the well behaved eigenfunctions correspond to real roots of $\Lambda_k(z)$ which furthermore satisfy the dual conditions $\lambda_k(r) = 0$ and $\eta_k(r) = 0$. When r is not a root of $\Lambda_k(z)$ then it corresponds to a point in the (van Kampen) continuous spectrum for this operator.

For the collisionless problem ($\nu_c = 0$) considered by Case, $\eta_k(v)$ is a real valued function which vanishes at the critical points of F_0. For $\nu_c > 0$, if $g_{eq}(v)$ is chosen to be some smooth positive function which vanishes only as $|v| \to \infty$, then $\eta_k(v)$ defined in (3.9) will vanish only as $|v| \to \infty$, and there will be no finite real roots of $\Lambda_k(z)$ which generate eigenvalues. In this case the line $\lambda = -\nu_c - ikr$, $-\infty < r < \infty$, corresponds to the continuous spectrum. The general picture for $\sigma(\mathcal{L})$ is shown in Fig. (3.1a).

Adjoints and Biorthogonality

To define an adjoint operator introduce the complex inner product,

$$\langle \phi, \Psi \rangle \equiv \int_0^L \int_{-\infty}^{\infty} dx\, dv\, \overline{\phi}(x,v)\Psi(x,v) \tag{3.22}$$

then $\mathcal{L}^\dagger$ is defined to satisfy

$$\langle \mathcal{L}^\dagger \phi, \Psi \rangle = \langle \phi, \mathcal{L}\Psi \rangle. \tag{3.23}$$

Using (3.9) for $\mathcal{L}$, (3.23) implies

$$\mathcal{L}^\dagger \phi = \mathcal{L}^\dagger \left(\sum_k e^{ikx} \phi_k(v) \right) = \sum_k e^{ikx} \left(L_k^\dagger \phi_k \right)(v) \tag{3.24}$$

where

$$\left(L_0^\dagger \phi_0\right)(v) = -\nu_c \phi_0(v)$$

$$\left(L_k^\dagger \phi_k\right)(v) = (ikv - \nu_c)\phi_k(v) + ik \int_{-\infty}^{\infty} dv'\, \overline{\eta_k(v')}\phi_k(v'), \qquad k \neq 0.$$

The adjoint eigenvalue problem

$$\mathcal{L}^\dagger \phi = \lambda \phi \tag{3.25}$$

is similar to the eigenvalue problem for $\mathcal{L}$. From (3.24) and (3.25) the spatially homogeneous functions $\phi(x,v) = \phi_0(v)$ are eigenfunctions with eigenvalue $\lambda = -\nu_c$.

For $k \neq 0$, after taking into account the definition of $L_k^\dagger$, (3.25) becomes

$$(v - z)\phi_k = -\int_{-\infty}^{\infty} dv' \, \overline{\eta_k(v')}\phi_k(v') \tag{3.26}$$

where now $z = (\nu_c + \lambda)/ik$. For $\operatorname{Im} z \neq 0$, $\int_{-\infty}^{\infty} dv' \, \overline{\eta_k(v')}\phi_k(v') = 0$ implies $\phi_k \equiv 0$ so without loss of generality the normalization

$$\int_{-\infty}^{\infty} dv' \, \overline{\eta_k(v')}\phi_k(v') = 1 \tag{3.27}$$

can be adopted. The solution of (3.26) is then

$$\phi_k(v) = \frac{-1}{v - z},$$

and the normalization requires

$$1 + \int_{-\infty}^{\infty} dv' \, \frac{\overline{\eta_k(v')}}{v' - z} = 0$$

which is equivalent to $\Lambda_{-k}(z) = 0$. Thus a complex root of $\Lambda_{-k}(z)$ determines an adjoint eigenfunction

$$\phi(x,v) = e^{ikx}\left(\frac{-1}{v - z}\right)$$

with eigenvalue $\lambda = -\nu_c + ikz$. These adjoint eigenfunctions are the relevant ones for the center manifold analysis.

When $z = r \in \mathfrak{R}$, the solutions to (3.26) depend on whether $\lambda_{-k}(r) = \eta_{-k}(r) = 0$ or not. Consider first those values of r which do not satisfy these

conditions; specifically assume $\lambda_{-k}(r) \neq 0$. Then there are two possibilities: either $\int_{-\infty}^{\infty} dv' \overline{\eta_k(v')}\phi_k(v')$ vanishes or it can be normalized to unity. In the former case, (3.26) implies

$$\phi_k(v) = C\delta(v-r) \tag{3.28}$$

and consistency requires $\overline{\eta_k(r)} = 0$. When $\int_{-\infty}^{\infty} dv' \overline{\eta_k(v')}\phi_k(v') = 1$, then the solution to (3.26) is

$$\phi_k(v) = -\Pr\left(\frac{1}{v-r}\right) + D_k(v)\delta(v-r) \tag{3.29}$$

with the normalization yielding

$$\lambda_{-k}(r) = \eta_{-k}(r)D_k(r). \tag{3.30}$$

Now consistency with $\lambda_k(r) \neq 0$ requires $\eta_{-k}(r) \neq 0$. The remaining possibility allowed by $\Lambda^{\pm}_{-k}(r) \neq 0$ is $\lambda_{-k}(r) = 0$ but $\eta_{-k}(r) \neq 0$. This amounts to setting $D_k(r) = 0$ in (3.30) and (3.29) with the resulting solution

$$\phi_k(v) = -\Pr\left(\frac{1}{v-r}\right). \tag{3.31}$$

If r does satisfy $\lambda_{-k}(r) = \eta_{-k}(r) = 0$ then there are two possibilities. If the right hand side of (3.26) vanishes then the solution is (3.28). When the right hand side does not vanish the solution is (3.31). Thus for these special values of r there are two linearly independent adjoint solutions. As in the discussion for $\mathcal{L}$, it is worth noting that for typical choices of $g_{eq}(v)$ the dispersion function does not have real roots which satisfy $\lambda_{-k}(r) = \eta_{-k}(r) = 0$ except perhaps at $r = \pm\infty$.

The biorthogonality of eigenfunctions and adjoint eigenfunctions follows from (3.23). Let Ψ_λ be an eigenfunction

$$\mathcal{L}\Psi_\lambda = \lambda\Psi_\lambda$$

and ϕ_σ an adjoint eigenfunction

$$\mathcal{L}^\dagger\phi_\sigma = \sigma\phi_\sigma$$

then

$$\begin{aligned} 0 &= \langle \mathcal{L}^\dagger\phi_\sigma, \Psi_\lambda\rangle - \langle \phi_\sigma, \mathcal{L}\Psi_\lambda\rangle \\ &= (\overline{\sigma} - \lambda)\langle \phi_\sigma, \Psi_\lambda\rangle. \end{aligned} \tag{3.32}$$

This will be applied to eigenfunctions associated with complex roots of $\Lambda_k(z)$.

Let z_0 ($\operatorname{Im} z_0 \neq 0$) satisfy $\Lambda_k(z_0) = 0$, then there are two eigenfunctions Ψ and $\overline{\Psi}$,

$$\begin{aligned} \Psi(x,v) &= e^{ikx}\left(\frac{-\eta_k(v)}{v - z_0}\right) \\ \overline{\Psi}(x,v) &= e^{-ikx}\left(\frac{-\eta_{-k}(v)}{v - \overline{z_0}}\right) \end{aligned} \tag{3.33}$$

with eigenvalues $\lambda = -\nu_c - ikz_0$ and $\overline{\lambda}$ respectively. There are also two adjoint eigenfunctions (reverting to the notation of Chapter 1),

$$\begin{aligned} \tilde{\Psi}(x,v) &= Ne^{ikx}\left(\frac{-1}{v - \overline{z_0}}\right) \\ \overline{\tilde{\Psi}}(x,v) &= \overline{N}e^{-ikx}\left(\frac{-1}{v - z_0}\right) \end{aligned} \tag{3.34}$$

with eigenvalues $\overline{\lambda}$ and λ respectively. From (3.32) it follows that

$$\begin{aligned} (\operatorname{Im}\overline{\lambda})\langle\overline{\tilde{\Psi}}, \Psi\rangle &= 0 \\ (\operatorname{Im}\lambda)\langle\tilde{\Psi}, \overline{\Psi}\rangle &= 0 \end{aligned} \tag{3.35}$$

so for a conjugate pair ($\lambda \neq \overline{\lambda}$) the inner products must vanish. The normalization factor N in (3.34) is chosen to enforce

$$\langle \tilde{\Psi}, \Psi \rangle = \langle \overline{\tilde{\Psi}}, \overline{\Psi} \rangle = 1. \tag{3.36}$$

Note that even in the case of a real eigenvalue corresponding to $\mathrm{Re}\, z_0 = 0$, the inner products in (3.35) will vanish due to the integrations over x.

The extension of Case's completeness results to this problem should be possible, as well as a corresponding extension of existing results for $\nu_c = 0$ on the problem of degenerate eigenvalues. However for an analysis of the simplest instability corresponding to a simple complex conjugate pair, the relations in (3.35) and (3.36) are sufficient.

Linear Instability

When $F_0(v)$ depends on parameters then $\sigma(\mathcal{L})$ inherits this dependence. As these parameters are varied, the shape of $F_0(v)$ varies, and the linear stability of $f = 0$ may change. When this instability occurs due to a conjugate pair of eigenvalues, the Hopf bifurcation theory of Chapter 1 can be applied. For the remainder of the chapter, the problem of bifurcation at a simple conjugate pair of eigenvalues (with eigenfunctions in (3.33)) is considered. Aside from this eigenvalue pair the rest of $\sigma(\mathcal{L})$ remains off the imaginary axis in the left half plane.

Using the spectral results define a complex amplitude

$$A(t) \equiv \langle \tilde{\Psi}, f \rangle \tag{3.37}$$

and decompose the distribution function

$$f(x,v,t) = A(t)\Psi(x,v) + \overline{A}(t)\overline{\Psi}(x,v) + S(x,v,t) \tag{3.38}$$

where

$$\langle \tilde{\Psi}, S \rangle = \langle \overline{\tilde{\Psi}}, S \rangle = 0.$$

Using (3.38) the evolution equation (3.8) becomes

$$\begin{aligned} \frac{dA}{dt} &= \lambda A + \langle \tilde{\Psi}, \mathcal{N}(f) \rangle \\ \frac{\partial S}{\partial t} &= \mathcal{L}S + \mathcal{N}(f) - \langle \tilde{\Psi}, \mathcal{N}(f) \rangle - \overline{\langle \tilde{\Psi}, \mathcal{N}(f) \rangle}. \end{aligned} \tag{3.39}$$

Now the restriction of (3.39) to the center manifold associated with Ψ, $\overline{\Psi}$ is required. As before this necessitates a local description of W^c.

Computing the Center Manifold

As discussed in Chapter 1, for small $|A|$ W^c is the graph of a function $h = h(x,v,A,\overline{A})$ defined such that a distribution function

$$f^c(x,v,t) = A\Psi + \overline{A\Psi} + h(x,v,A,\overline{A}) \tag{3.40}$$

evolves on W^c. Note that for this infinite dimensional problem x and v are simply continuous indices, the dynamical arguments of h are $A(t)$ and $\overline{A}(t)$; see

Fig. (1.3b). The invariance of W^c implies an equation for h,

$$\left[\frac{\partial h}{\partial A}\frac{dA}{dt}+\frac{\partial h}{\partial \overline{A}}\frac{d\overline{A}}{dt}\right]_{f=f^c} = \mathcal{L}h+\mathcal{N}(f^c) - \langle\tilde{\Psi},\mathcal{N}(f^c)\rangle - \overline{\langle\tilde{\Psi},\mathcal{N}(f^c)\rangle}. \tag{3.41}$$

To solve (3.41) to lowest order in A, introduce the Fourier expansion in x

$$h(x,v,A,\overline{A}) = \sum_l e^{ilx}h_l(v,A,\overline{A}) \tag{3.42}$$

and the Taylor series in A

$$h_l(v,A,\overline{A}) = h_l^{(1)}(v)A^2 + h_l^{(2)}(v)|A|^2 + h_{-l}^{(1)}\overline{A}^2 + O(A^3)$$

where the reality condition $h_l(v,A,\overline{A}) = \overline{h_{-l}(v,A,\overline{A})}$ has been assumed. Now the Fourier expansion of f^c is

$$\begin{aligned} f^c(x,v,t) = &\left[A(t)\Psi_{z_0}(v)+h_k(v,A(t),\overline{A}(t))\right]e^{ikx} \\ &+\left[\overline{A}(t)\overline{\Psi_{z_0}}(v)+h_{-k}(v,A(t),\overline{A}(t))\right]e^{-ikx} \\ &+\sum_{l\neq k} e^{ilx}h_l(v,A(t),\overline{A}(t)) \end{aligned} \tag{3.43}$$

where the wavelength of the linear instability is assumed to be $(2\pi/k)$, and the velocity space factor of the eigenfunction is denoted Ψ_{z_0}, i.e.

$$\Psi(x,v) = e^{ikx}\left(\frac{-\eta_k(v)}{v-z_0}\right) \equiv e^{ikx}\Psi_{z_0}(v). \tag{3.44}$$

To extract the lowest order balance in (3.41) requires $\mathcal{N}(f^c)$ and $\langle\tilde{\Psi},\mathcal{N}(f^c)\rangle$. Using (3.43) to expand the definition of $\mathcal{N}(f)$ in (3.10) yields

$$\mathcal{N}(f^c) = \frac{i\omega_e{}^2}{k}\left[A^2\frac{\partial\Psi_{z_0}}{\partial v}e^{i2kx} + |A|^2\left(\frac{\partial\overline{\Psi_{z_0}}}{\partial v} - \frac{\partial\Psi_{z_0}}{\partial v}\right) - \overline{A}^2\frac{\partial\overline{\Psi_{z_0}}}{\partial v}e^{-i2kx}\right]$$
$$+ \frac{i\omega_e{}^2}{k}\sum_l e^{ilx}\left[A\frac{\partial h_{l-k}}{\partial v} - \overline{A}\frac{\partial h_{l+k}}{\partial v}\right]$$
$$+ \sum_{l\neq 0}\frac{i\omega_e{}^2}{l}\left[Ae^{ikx}\frac{\partial\Psi_{z_0}}{\partial v} + \overline{A}e^{-ikx}\frac{\partial\overline{\Psi_{z_0}}}{\partial v}\right]e^{ilx}\int_{-\infty}^{\infty}dv'\,h_l(v')$$
$$+ \sum_m e^{imx}\sum_{l\neq 0}\frac{i\omega_e{}^2}{l}\frac{\partial h_{m-l}}{\partial v}\int_{-\infty}^{\infty}dv'\,h_l(v') \tag{3.45}$$

where terms have been collected according to the number of factors of h_l. Projecting with $\tilde{\Psi}$ picks out the e^{ikx} component

$$\langle\tilde{\Psi}, \mathcal{N}(f^c)\rangle = \frac{i\omega_e{}^2}{k}\langle\tilde{\Psi}, e^{ikx}\left[A\frac{\partial h_0}{\partial v} - \overline{A}\frac{\partial h_{2k}}{\partial v}\right]\rangle$$
$$+ \frac{i\omega_e{}^2}{2k}\overline{A}\langle\tilde{\Psi}, e^{ikx}\frac{\partial\overline{\Psi_{z_0}}}{\partial v}\int_{-\infty}^{\infty}dv'\,h_{2k}(v')\rangle \tag{3.46}$$
$$+ \sum_{l\neq 0}\frac{i\omega_e{}^2}{l}\langle\tilde{\Psi}, e^{ikx}\frac{\partial h_{k-l}}{\partial v}\int_{-\infty}^{\infty}dv'\,h_l(v')\rangle.$$

The leading terms in (3.45) and (3.46) are $O(A^2)$ and $O(A^3)$ respectively.

The lowest order balance in (3.41) occurs at $O(A^2)$; the left hand side of (3.41) contributes

$$\left[\frac{\partial h}{\partial A}\frac{dA}{dt}+\frac{\partial h}{\partial \overline{A}}\frac{d\overline{A}}{dt}\right]_{f=f^c}=\left\{\sum_l e^{ilx}\left[2h_l^{(1)}A+h_l^{(2)}\overline{A}\right]\right\}(\lambda A)$$
$$+\left\{\sum_l e^{ilx}\left[h_l^{(2)}A+2\overline{h_{-l}^{(1)}}\,\overline{A}\right]\right\}(\overline{\lambda A})+O(A^3)$$
$$=\sum_l e^{ilx}\left[2\lambda h_l^{(1)}A^2+(\lambda+\overline{\lambda})h_l^{(2)}|A|^2+2\overline{\lambda}\,\overline{h_{-l}^{(1)}}\,\overline{A}^2\right]$$
$$+O(A^3) \tag{3.47}$$

and the quadratic terms on the right hand side of (3.41) are

$$\mathcal{L}h+\mathcal{N}(f^c)-\langle\tilde{\Psi},\mathcal{N}(f^c)\rangle-\overline{\langle\tilde{\Psi},\mathcal{N}(f^c)\rangle}\;=$$
$$\sum_l e^{ilx}L_l\left[h_l^{(1)}A^2+h_l^{(2)}|A|^2+\overline{h_{-l}^{(1)}}\,\overline{A}^2\right]$$
$$+\frac{i\omega_e{}^2}{k}\left[A^2\frac{\partial\Psi_{z_0}}{\partial v}e^{i2kx}+\left(\frac{\partial\overline{\Psi_{z_0}}}{\partial v}-\frac{\partial\Psi_{z_0}}{\partial v}\right)|A|^2\right. \tag{3.48}$$
$$\left.-\frac{\partial\overline{\Psi_{z_0}}}{\partial v}e^{-i2kx}\,\overline{A}^2\right]+O(A^3).$$

Equating coefficients of A^2 and $|A|^2$ yields

$$(L_l-2\lambda)h_l^{(1)}=\begin{cases}-\dfrac{i\omega_e{}^2}{k}\dfrac{\partial\Psi_{z_0}}{\partial v} & \text{for } l=2k\\ 0 & \text{otherwise}\end{cases} \tag{3.49}$$

$$(L_l-(\lambda+\overline{\lambda}))h_l^{(2)}=\begin{cases}-\dfrac{i\omega_e{}^2}{k}\left[\dfrac{\partial\overline{\Psi_{z_0}}}{\partial v}-\dfrac{\partial\Psi_{z_0}}{\partial v}\right] & \text{for } l=0\\ 0 & \text{otherwise}\end{cases} \tag{3.50}$$

Coefficients of $\overline{A}^2$ simply give the conjugate of (3.49).

To solve (3.49) and (3.50) first note that if 2λ or $(\lambda+\overline{\lambda})$ were eigenvalues of L_l this would imply that at criticality, when λ, $\overline{\lambda}$ cross the imaginary axis,

there would also be other eigenvalues, 2λ or $\lambda + \overline{\lambda}$, crossing the imaginary axis simultaneously. For the simplest case of ***nondegenerate*** Hopf bifurcation this does not happen; thus our spectral assumptions on $\sigma(\mathcal{L})$ imply

$$\big(L_l - 2\lambda\big)h_l^{(1)} \neq 0 \qquad \text{unless} \qquad h_l^{(1)} \equiv 0$$

and,

$$\big(L_l - (\lambda + \overline{\lambda})\big)h_l^{(2)} \neq 0 \qquad \text{unless} \qquad h_l^{(2)} \equiv 0.$$

The only nontrivial solutions are for $l = 0, 2k$. For $l = 2k$ (3.49) becomes

$$\left[(i2kv + \nu_c)h_{2k}^{(1)} + i2k\eta_{2k}\int_{-\infty}^{\infty} dv'\, h_{2k}^{(1)}\right] + 2\lambda h_{2k}^{(1)} = \frac{i{\omega_e}^2}{k}\frac{\partial \Psi_{z_0}}{\partial v}$$

which can be compactly rewritten,

$$h_{2k}^{(1)} + \left(\frac{\eta_{2k}}{v - z_1}\right)\int_{-\infty}^{\infty} dv'\, h_{2k}^{(1)}(v') = \frac{1}{2}\Big(\frac{\omega_e}{k}\Big)^2\left(\frac{\partial_v \Psi_{z_0}}{v - z_1}\right) \tag{3.51}$$

where

$$z_1 \equiv \frac{i(\nu_c + 2\lambda)}{2k} = \frac{-i\nu_c}{2k} + z_0.$$

Integrating (3.51) over velocity gives

$$\Lambda_{2k}(z_1)\int_{-\infty}^{\infty} dv'\, h_{2k}^{(1)}(v') = \frac{1}{2}\Big(\frac{\omega_e}{k}\Big)^2\int_{-\infty}^{\infty} dv\, \frac{\partial_v \Psi_{z_0}}{v - z_1}. \tag{3.52}$$

It follows from the spectral assumptions on $\sigma(\mathcal{L})$ that $\Lambda_{2k}(z_1) \neq 0$, otherwise there would be additional eigenvalues on the imaginary axis at criticality. With

$$H_{2k} \equiv \int_{-\infty}^{\infty} dv'\, h_{2k}^{(1)}(v')$$

determined by (3.52), the solution of (3.51) is

$$h_{2k}^{(1)}(v) = \frac{\left[\frac{1}{2}\left(\frac{\omega_e}{k}\right)^2 \partial_v \Psi_{z_0} - H_{2k}\eta_{2k}\right]}{v - z_1} \tag{3.53}$$

where

$$H_{2k} = \frac{1}{2\Lambda_{2k}(z_1)}\left(\frac{\omega_e}{k}\right)^2 \int_{-\infty}^{\infty} dv' \, \frac{\partial_{v'}\Psi_{z_0}}{v' - z_1}.$$

For $l = 0$, (3.50) gives

$$(\nu_c + \lambda + \overline{\lambda})h_0^{(2)} = \frac{i{\omega_e}^2}{k}\left[\frac{\partial\overline{\Psi_{z_0}}}{\partial v} - \frac{\partial\Psi_{z_0}}{\partial v}\right]$$

so,

$$h_0^{(2)}(v) = \frac{i{\omega_e}^2\left[\partial_v\overline{\Psi_{z_0}} - \partial_v\Psi_{z_0}\right]}{k(\nu_c + \lambda + \overline{\lambda})}. \tag{3.54}$$

From (3.42) the solution for h to this order is

$$\begin{aligned} h(x, v, A, \overline{A}) = {} & e^{i2kx}h_{2k}^{(1)}(v)A^2 + h_0^{(2)}(v)|A|^2 \\ & + e^{-i2kx}\,\overline{h_{2k}^{(1)}(v)}\,\overline{A}^2 + O(A^3) \end{aligned} \tag{3.55}$$

with $h_{2k}^{(1)}$ and $h_0^{(2)}$ given by (3.53) and (3.54) respectively.

This calculation breaks down in the collisionless limit as both $h_{2k}^{(1)}$ and $h_0^{(2)}$ become singular. The details of this will not be considered here except to note that taking into account the behavior of Ψ_{z_0} as $\nu_c \to 0$ (see Case (1978)) leads to the following estimate *at criticality*,

$$h_0^{(2)}(v),\ h_{2k}^{(1)}(v) \sim \begin{cases} O(1/\nu_c^2) & v = \mathrm{Re}\, z_0 \\ \text{finite} & v \neq \mathrm{Re}\, z_0 \end{cases}$$

The Amplitude Equation

The two dimensional autonomous system describing the W^c dynamics near $A = 0$ is

$$\frac{dA}{dt} = \lambda A + \langle \tilde{\Psi}, \mathcal{N}(f^c) \rangle \tag{3.56}$$

from (3.39) and (3.40). Given the asymptotic approximation to $h(x, v, A, \overline{A})$ the right hand side of (3.56) may be evaluated through cubic order in A, $\overline{A}$. Plugging the asymptotic expressions,

$$\begin{aligned} h_{2k}(v, A, \overline{A}) &= A^2 h_{2k}^{(1)}(v) + O(A^3) \\ h_0(v, A, \overline{A}) &= |A|^2 h_0^{(2)}(v) + O(A^3) \\ h_{-2k}(v, A, \overline{A}) &= \overline{h_{2k}(v, A, \overline{A})} \\ h_l(v, A, \overline{A}) &= O(A^3) \qquad \text{for } l \neq 0, \pm 2k \end{aligned}$$

into (3.46) yields

$$\begin{aligned} \langle \tilde{\Psi}, \mathcal{N}(f^c) \rangle = \frac{i\omega_e{}^2}{k} |A|^2 A \langle \tilde{\Psi}, e^{ikx} \left[\partial_v h_0^{(2)} - \partial_v h_{2k}^{(1)} \right] \rangle \\ + \frac{i\omega_e{}^2}{2k} |A|^2 A \langle \tilde{\Psi}, e^{ikx} H_{2k} \partial_v \overline{\Psi_{z_0}} \rangle + O(A^4). \end{aligned} \tag{3.57}$$

Thus (3.56) has asymptotic form

$$\frac{dA}{dt} = \lambda A + \beta |A|^2 A + O(A^4) \tag{3.58}$$

where

$$\beta \equiv \frac{i\omega_e{}^2}{k} \langle \tilde{\Psi}, e^{ikx} \left[\partial_v h_0^{(2)} - \partial_v h_{2k}^{(1)} + \tfrac{1}{2} H_{2k} \partial_v \overline{\Psi_{z_0}} \right] \rangle.$$

β consists of two contributions, $\beta = \beta_p + \beta_w$. The instability at wave number k with amplitude A excites secondary waves at wave numbers $2k$ and 0;

these appear at $O(A^2)$ in (3.55). These secondary waves beat with the primary to produce a tertiary wave at wave number k with amplitude $O(A^3)$. This provides the lowest order nonlinear correction to the linear growth rate. β_p is the piece of this nonlinear correction due to the secondary wave at wave number 0, i.e. the modification of the spatially homogeneous background distribution generates β_p,

$$\beta_p \equiv \frac{i{\omega_e}^2}{k}\langle\tilde{\Psi}, e^{ikx}\partial_v h_0^{(2)}\rangle.$$

β_w arises from the secondary wave at $2k$,

$$\beta_w \equiv \frac{i{\omega_e}^2}{k}\langle\tilde{\Psi}, e^{ikx}\left[-\partial_v h_{2k}^{(1)} + \tfrac{1}{2}H_{2k}\partial_v\overline{\Psi_{z_0}}\right]\rangle.$$

As we shall see, β_p is the dominant contribution.

In polar variables, $A = \rho e^{i\theta}$, the amplitude equation (3.58) reads

$$\begin{aligned}\frac{d\rho}{dt} &= (\mathrm{Re}\,\lambda)\rho + (\mathrm{Re}\,\beta)\rho^3 + O(\rho^4)\\ \frac{d\theta}{dt} &= (\mathrm{Im}\,\lambda) + (\mathrm{Im}\,\beta)\rho^2 + O(\rho^3).\end{aligned} \tag{3.59}$$

Through cubic order this is already in normal form, see (1.28); the reason is that because $\mathcal{N}(f)$ is quadratically nonlinear the first nonlinear effects in the e^{ikx} Fourier subspace must be of cubic order. The corrections to $d\rho/dt$ at $O(\rho^4)$ can of course be removed by a normal form transformation, the first essential correction appearing at $O(\rho^5)$.

Dispersion Relations

To apply the results of (3.58) requires a model for $F_0(v)$and $g_{eq}(v)$. Given these functions, the discrete spectrum of $\mathcal{L}$ is determined by the dispersion function, and the coefficient β in (3.58) may be evaluated.

For purposes of illustration, $F_0(v)$ and $g_{eq}(v)$ will be selected to simplify the search for roots of $\Lambda_k(z)$. Let $F_0(v)$ have two Lorentzian components: a plasma with mean density n_p and a beam with mean density n_b and mean velocity u relative to the plasma.

$$\begin{aligned} n_0 &= n_p + n_b \\ n_0 F_0(v) &= \frac{1}{\pi}\left[\frac{\alpha n_p}{v^2+\alpha^2} + \frac{\delta n_b}{(v-u)^2+\delta^2}\right] \end{aligned} \tag{3.60}$$

Instead of representing the equilibrium distribution, g_{eq}, by a Maxwellian, let

$$g_{eq}(v) = \frac{1}{\pi}\left(\frac{\alpha}{v^2+\alpha^2}\right). \tag{3.61}$$

Now $\eta_k(v)$ in (3.9) is

$$\eta_k(v) = \frac{C}{\pi}\left\{2C\left[\frac{n_p v}{(v^2+1)^2} + \frac{n_b\delta(v-u)}{[(v-u)^2+\delta^2]^2}\right] + \frac{i\epsilon}{v^2+1}\right\} \tag{3.62}$$

where $C = \omega_e/k\alpha$, $\epsilon = \nu_c/\omega_e$, velocities have been scaled to α, and densities expressed in terms of n_0.

The dispersion function (3.17) evaluates to

$$\Lambda_k(z) = 1 - \begin{cases} \dfrac{n_p C^2}{(z+i)^2} + \dfrac{n_b C^2}{(z+i\delta-u)^2} + \dfrac{i\epsilon C}{(z+i)} & \operatorname{Im} z > 0 \\ \dfrac{n_p C^2}{(z-i)^2} + \dfrac{n_b C^2}{(z-i\delta-u)^2} + \dfrac{i\epsilon C}{(z-i)} & \operatorname{Im} z < 0. \end{cases} \tag{3.63}$$

Recalling $\lambda = -\nu_c - ikz$, it is clear that instability ($\mathrm{Re}\,\lambda \geq 0$) for $k > 0$ requires $\mathrm{Im}\,z > 0$ and for $k < 0$ requires $\mathrm{Im}\,z < 0$. Since $\Lambda_k(z) = \overline{\Lambda_{-k}(\overline{z})}$, for the conjugate pairs associated with Hopf bifurcation, it is sufficient to consider $k > 0$, $\mathrm{Im}\,z > 0$ and seek solutions to

$$1 - \left[\frac{n_p C^2}{(z+i)^2} + \frac{n_b C^2}{(z+i\delta-u)^2} + \frac{i\epsilon C}{(z+i)}\right] = 0 \qquad \mathrm{Im}\,z > 0. \tag{3.64}$$

This dispersion relation may be rewritten,

$$\begin{aligned}(z+i)^2(z+i\delta-u)^2 &- n_p C^2(z+i\delta-u)^2 \\ &- n_b C^2(z+i)^2 - i\epsilon C(z+i)(z+i\delta-u)^2 = 0\end{aligned} \tag{3.65}$$

and simplified by substituting $z = y - i(\delta+1+iu)/2$ to get

$$\begin{aligned}(y+w)^2(y-w)^2 &- n_p C^2(y-w)^2 \\ &- n_b C^2(y+w)^2 - i\epsilon C(y+w)(y-w)^2 = 0\end{aligned} \tag{3.66}$$

where $w \equiv i(1-\delta-iu)/2$.

The criterion for instability, $\mathrm{Re}\,\lambda \geq 0$, may be restated in the dimensionless variables of (3.64) using $\lambda = -\nu_c - ikz$. For $k > 0$, $\mathrm{Im}\,z > 0$

$$\mathrm{Re}\,\lambda \geq 0 \leftrightarrow \mathrm{Im}\,z \geq \epsilon C \tag{3.67}$$

where λ and ν_c are scaled to ω_e, and z is scaled to α. There will in general be four solutions to the dispersion relation (3.65), but a solution only corresponds to an eigenvalue if $\mathrm{Im}\,z > 0$. The eigenvalue reaches the imaginary axis when $\mathrm{Im}\,z = \epsilon C$.

As a first application of (3.66) consider the stability of a plasma with no beam: $n_p = 1$, $n_b = 0$. Then (3.66) reads

$$(y-w)^2\left[(y+w)^2 - i\epsilon C(y+w) - C^2\right] \quad = 0$$

Since $z = y + w - i$, the solutions are

$$\begin{aligned} z &= 2w - i = u - i\delta, \qquad \text{double root} \\ z &= -i\left(1 - \frac{\epsilon C}{2}\right) \pm C\sqrt{1 - \frac{\epsilon^2}{4}}\,. \end{aligned} \tag{3.68}$$

The double root is in fact spurious since setting $n_b = 0$ in (3.64) produces a quadratic equation not a quartic; even so the double root does not satisfy $\operatorname{Im} z > 0$. The other two roots, which are referred to as the plasma roots, can satisfy $\operatorname{Im} z > 0$ for appropriate choices of ϵ and C, but it is easy to check that the condition for instability (3.67) is never met. Thus the equilibrium plasma $F_0(v) = g_{eq}(v)$ is in fact stable.

Our model has four parameters: beam density, n_b, beam velocity, u, beam thermal speed, δ, and the collision frequency, ν_c. In the computation of the bifurcation results, u and δ will be varied with ϵ held fixed. For beam density only two cases will be considered: a low density beam (the bump-on-tail instability) characterized by $n_b = 0.05$ and $n_p = 0.95$, and an equal density beam (the two stream instability) where $n_b = n_p = 0.5$.

Within the linear problem, varying ϵ shifts the bifurcation surface; increasing ϵ suppresses the linear instability. This is consistent with the dependence of $\sigma(\mathcal{L})$ on ϵ, recall that increasing ϵ shifts the spectrum into the left half plane (see Fig. (3.1a)). In Fig. (3.2) the intersection of the bifurcation surface ($\operatorname{Re}\lambda = 0$) with the (u,k)-plane is plotted for various values of ϵ, and fixed n_b and δ.

Henceforth I shall fix ϵ arbitrarily at $\epsilon = 0.001$ and consider some of the possibilities for $n_b = 0.05$ and $n_b = 0.5$ in detail.

Low Density Beam

In Figs. (3.3a) and (3.8a) linear stability results for $n_b = 0.05$ are given corresponding to a cool beam, $\delta = 0.5$, and a warm beam, $\delta = 5.0$. Superposed on the bifurcation surface in the (u, k)-plane is the surface obtained by halving the k coordinate. This allows the critical beam velocity for the instability at k and $2k$ to be directly compared. The most interesting result of this exercise is the existence of parameter values, (u_c, k_c), for which these two modes *simultaneously* become unstable. For example in Fig. (3.3a), this double instability occurs for $k_c \sim 0.08$ and $2k_c \sim 0.16$. At these special points on the Hopf bifurcation surface, two complex conjugate pairs simultaneously arrive at the imaginary axis resulting in a codimension two, double Hopf bifurcation. This degenerate Hopf bifurcation is considerably more complicated than the codimension two bifurcation analyzed in the previous chapter. The reason is the increase in the dimension of the center manifold from two to four, allowing the possibility of chaotic dynamics right at the linear stability threshold.

A discussion of this codimension two instability will not be pursued here; an introduction to the appropriate normal form theory is given by Guckenheimer and Holmes (1983). It should be clear that the assumptions on the spectrum of

$\mathcal{L}$ required by the center manifold calculations in this chapter can be satisfied only for wave numbers above the codimension two point.

For $\delta = 0.5$ and $\delta = 5.0$, a typical wave number has been chosen and the four solutions of the dispersion relation (3.65) plotted as a function of u in Figs. (3.3b) and (3.8b). In both cases the unstable waves are carried by the "beam roots", i.e. the two solutions of $\Lambda_k(z) = 0$ introduced by the condition $n_b > 0$, and distinguished by the property $\omega \not\to \omega_c$ as $ku \to 0$. For this model the transfer of the unstable waves to the plasma root branch, described by O'Neil and Malmberg (1968), occurs for $\delta \sim 25$.

Now consider the normal form coefficient, β, and the results for the distribution function derived earlier. From (3.58), β was evaluated along the bifurcation surface, and plotted logarithmically in Figs. (3.4) and (3.9). In computing β, β_p and β_w were evaluated separately and their magnitudes compared for wave numbers above k_c. For $\delta = 0.5$ this showed

$$10^{-3} \geq \left| \frac{\mathrm{Re}\,\beta_w}{\mathrm{Re}\,\beta_p} \right| \geq 10^{-5}, \qquad k > k_c$$

and for $\delta = 5.0$,

$$10^{-4} \geq \left| \frac{\mathrm{Re}\,\beta_w}{\mathrm{Re}\,\beta_p} \right| \geq 10^{-6}, \qquad k > k_c.$$

At both values of δ, β_w was relatively larger for wave numbers near the codimension two singularity. Nevertheless $\mathrm{Re}\,\beta_p$ is clearly the dominant contribution to $\mathrm{Re}\,\beta$ and from Fig. (3.4a) $\mathrm{Re}\,\beta < 0$. This is consistent with the physical pic-

ture that the instability saturates because the unstable wave alters the resonant particle distribution.

Since $\mathrm{Re}\,\beta < 0$, the direction of bifurcation is supercritical, and the saturated distribution function is approximately

$$F_2(x,v,t) \approx F_0(v) + A_s(t)\Psi(x,v) + \overline{A}_s(t)\overline{\Psi}(x,v) + A_s^2(t)h_{2k}^{(1)}(v)e^{i2kx} + |A_s|^2 h_0^{(2)}(v) + \overline{A}^2(t)\overline{h_{2k}^{(1)}(v)}e^{-i2kx} + \cdots \tag{3.69}$$

where

$$A_s(t) = \rho_s e^{i\theta(t)}$$

$$\rho_s \approx \sqrt{\frac{\mathrm{Re}\,\lambda}{-\mathrm{Re}\,\beta}}$$

$$\theta(t) = \left[\mathrm{Im}\,\lambda + (\mathrm{Im}\,\beta)\rho_s^2 + \cdots\right] t + \theta(0)$$

is the saturated wave amplitude. By shifting into the reference frame of the wave, (x', v'), defined by

$$v' = v - v_w$$

$$x' = x - v_w t$$

$$kv_w = -\frac{d\theta}{dt}$$

the saturated distribution function (3.69) becomes

$$F_0(v' + v_w) - \rho_s\left\{\left[\frac{\eta_k(v' + v_w)}{v' + v_w - z_0}\right]e^{ikx'} + \left[\frac{\overline{\eta_k(v' + v_w)}}{v' + v_w - \overline{z_0}}\right]e^{-ikx'}\right\}$$
$$+ \rho_s^2\left\{h_{2k}^{(1)}(v' + v_w)e^{i2kx'} + h_0^{(2)}(v' + v_w) + \overline{h_{2k}^{(1)}(v' + v_w)}e^{-i2kx'}\right\}$$
$$+ \cdots.$$

Of interest is the effect of the instability on the homogeneous (or spatially averaged) piece of the distribution,

$$\frac{1}{L}\int_0^L dx\, F_2(x, v' + v_w\,, t) \approx F_0(v' + v_w\,) + \rho_s^2 h_0^{(2)}(v' + v_w\,) + \cdots. \qquad (3.70)$$

The form of the lowest order correction is fixed by $h_0^{(2)}$; its magnitude is determined by ρ_s^2.

For both $\delta = 0.5$ and $\delta = 5.0$, this correction is plotted at small and large growth rates. (As we move away from the bifurcation surface towards larger growth rates, it is quite possible for secondary bifurcations–such as trapped particle instabilities–to occur. These are beyond the reach of this one mode calculation, but might well be captured by the four dimensional normal form associated with the double Hopf bifurcation.) For $\delta = 0.5$ in Figs. (3.5) and (3.7) the parameter values correspond to points A and B in Fig. (3.3a). At point A, the growth rate is low, $\mathrm{Re}\,\lambda \sim 0.009$, and the plot of $h_0^{(2)}$ indicates negligible effects except in the resonant region near the wave velocity. At the wave velocity, $h_0^{(2)}$ shows the resonant particles just above v_w (or $v' = 0$) being slowed as their kinetic energy is transferred into the electrostatic field of the wave. This transfer occurs until ρ^2 reaches $\rho_s^2 \sim 3x10^{-8}$ when saturation occurs. The resulting distortion of F_0 appears in Fig. (3.6).

At point B, the growth rate is an order of magnitude greater, and $h_0^{(2)}$ shows both plasma and beam being heated, i.e. broadened, by the instability. This broadening of the nonresonant particle distribution is also predicted by a weak turbulence theory of this instability (Davidson (1972)). The saturation

amplitude, $\rho_s^2 \sim 2.7x10^{-4}$, is much larger, and the effect on F_0 is much greater. The qualitative shape of the saturated distribution function in Fig. (3.7b) was also found in the numerical studies of Armstrong and Montgomery (1969). They solved the (collisionless) Vlasov-Poisson equations for a beam-plasma distribution with essentially one unstable mode, and observed a depletion of particles from the center of the beam as well as a broadening of the nonresonant plasma distribution. However, these effects are much more pronounced in this calculation.

In fact the approximate saturated distribution function in Fig. (3.7b) becomes negative near the beam velocity. This lack of positivity must be an artifact of the approximations used since the original dynamics in (3.1) will preserve the positivity of $F(x,v,t)$. There have been two approximations: the collisional relaxation of $F_1(x,v,t)$ in (3.5b) was neglected and $f(x,v,t)$ has been computed only through second order in ρ_s. For the parameter values in question, the ratio of the linear growth rate to ν_c is approximately 100 and the replacement $F_1(x,v,t) \approx F_1(x,v,0)$ seems reasonable. This suggests that the higher order terms in ρ_s may be appreciable near the beam velocity. These higher order corrections should be more important in the resonant region of velocity space than elsewhere because the additional (small) factors of ρ_s could be offset by higher order resonant denominators.

For the low density warm beam, similar plots appear in Figs. (3.10) and

(3.12) corresponding to points A and B in Fig. (3.8a). At point A, $\mathrm{Re}\,\lambda \sim 0.013$, and $h_0^{(2)}$ in Fig. (3.10b) already shows some broadening of the plasma distribution in addition to the slowing of the resonant beam particles, but the size of $h_0^{(2)}$ is much smaller than for the case of the cool beam and small growth rate. As seen in Fig. (3.11) the effects on F_0 are negligible even though the saturation amplitude is larger than in the case of $\delta = 0.5$ and small growth rate. For point B, $\mathrm{Re}\,\lambda \sim 0.07$ and the saturation amplitude has increased to $\rho_e^2 \sim 0.9x10^{-4}$ so that the effects of the instability are visible in the peak of the plasma and near the wave velocity.

Equal Density Beam

The bifurcation surfaces for $\delta = 0.5$, 1.0, and 2.0 appear in Figs. (3.14a), (3.19a), and (3.24a). As the temperature increases, the region of unstable parameter values tends to contract toward lower wave numbers and higher beam velocities. The codimension two point discussed earlier occurs here also. At each beam temperature, for a fixed wave number chosen above the $2k$ stability curve, the roots of the dispersion relation are plotted in Figs. (3.14b), (3.19b), and (3.24b). In all cases the unstable waves are associated with the beam roots; as the beam temperature increases the instability shifts from the lower beam root to the upper beam root.

The real and imaginary parts of β are plotted along the bifurcation surface in Figs. (3.15), (3.20), and (3.25). For wave numbers above the codimension two point the bifurcation is supercritical as before. In the vicinity of the codimension two bifurcation, particularly for β corresponding to $\delta = 1.0$, there is a rapid variation in the normal form coefficient. This structure reflects a coincidence. At the codimension two point, both k and $2k$ simultaneously become unstable. This means that there are two roots, z_0 and z_2, to the dispersion relation such that at criticality they satisfy,

$$\Lambda_k(z_0) = 0 \qquad \text{Im } z_0 = \frac{\nu_c}{k}$$

$$\Lambda_{2k}(z_2) = 0 \qquad \text{Im}(z_2) = \frac{\nu_c}{2k}.$$

Generally there is no fixed relationship between Re z_0 and Re z_2 although both will be close to $u/2$. However for the symmetric ($n_b = n_p$, $\delta = 1.0$), collisionless ($\epsilon = 0$) case, the two phase velocities match, Re z_0 = Re z_2, and the second root z_2 is ***exactly*** equal to z_1 in (3.51). This means that $\Lambda_{2k}(z_1)$ which appears in the denominator in (3.53) satisfies

$$\Lambda_{2k}(z_1) = 0$$

at the degenerate bifurcation. In the plots of β for $\delta = 1$, we have $\epsilon = 0.001$ (not zero) so z_1 is not an exact root but it is sufficiently close to a root of $\Lambda_{2k}(z)$ that $h_{2k}^{(1)}(v)$ and hence β exhibit a rapid variation near the codimension two point.

A comparison of β_w with β_p for $k \geq k_c$ shows for $\delta = 0.5$

$$10^{-3} \geq \left| \frac{\mathrm{Re}\,\beta_w}{\mathrm{Re}\,\beta_p} \right| \geq 10^{-6}$$

and for $\delta = 1.0$

$$1.0 \geq \left| \frac{\mathrm{Re}\,\beta_w}{\mathrm{Re}\,\beta_p} \right| \geq 10^{-5}$$

and for $\delta = 2.0$

$$10^{-2} \geq \left| \frac{\mathrm{Re}\,\beta_w}{\mathrm{Re}\,\beta_p} \right| \geq 10^{-6}\,.$$

In each case, the ratio is largest for $k \sim k_c$, and approaches unity for the symmetric situation ($\delta = 1.0$) when the small magnitude of $\Lambda_{2k}(z_1)$ at criticality dramatically increases $|\beta_w|$. Again, the wave-particle effects, represented by β_p, are typically much more important in bringing about saturation.

The figures of $h_0^{(2)}$ and $F_0 + \rho_s^2 h_0^{(2)}$ show the effect of the instability. For relatively weak growth rates at point A on the stability diagram, the primary structure in $h_0^{(2)}$ occurs at the wave velocity. In Fig. (3.21b) for $\delta = 1.0$ particles are symmetrically pushed towards the wave velocity. In Figs. (3.16b) and (3.26b) the shapes of $h_0^{(2)}$ at $\delta = 0.5$ and $\delta = 2.0$ are essentially related by reflection through a line at $v' = 0$.

For the large growth rates at point B, this reflection symmetry recurs, but the form of $h_0^{(2)}$ now shows significant acceleration of particles near the centers of the two unperturbed components as well as bunching near the wave velocity.

The $\nu_c \to 0$ Limit

In the collisionless limit, the dynamics becomes Hamiltonian (Morrison (1980), Marsden and Weinstein (1982)). As indicated above, the Hopf normal form becomes singular due to the resonance at the wave velocity. In terms of $\sigma(\mathcal{L})$ this resonance occurs between a conjugate pair of eigenvalues, $\pm ikr$, of multiplicity two and the continuous spectrum along the imaginary axis. The presence of the continous spectrum precludes a straightforward application of the invariant manifold ideas of Chapter 1; consequently it is no longer clear that the Hamiltonian bifurcation can be analyzed using a finite dimensional set of normal form equations. Even if one assumes this to be true, it is not obvious what the normal form is when $\nu_c = 0$.

This problem becomes more puzzling in view of existing theories of the saturated state which describe the time asymptotic state as a BGK mode with an amplitude proportional to $(\mathrm{Re}\,\lambda)^2$ (Galeev and Sagdeev (1978)). This represents a dramatic change from the scaling $\rho_s \sim \sqrt{\mathrm{Re}\,\lambda}$ found in Hopf bifurcation, and together with the singular behavior at $\nu_c = 0$ of the Hopf normal form, strongly suggests that the limits $\nu_c \to 0$ and $t \to \infty$ may not be interchanged. In other words, the time asymptotic state of the collisionless instability (first $\nu_c \to 0$ then $t \to \infty$) is *not* equal to the collisionless limit of the time asymptotic state for the collisional instability (first $t \to \infty$ then $\nu_c \to 0$). Using a multiple-time-scales perturbation theory, Simon and Rosenbluth (1976) found a saturated

state for the collisionless instability whose amplitude did scale as $\sqrt{\mathrm{Re}\,\lambda}$, but their calculation is somewhat formal and does not include a careful treatment of the continuous spectrum; in particular their calculation was plagued by the singularities noted above. A satisfactory bifurcation theory for the ***collisionless***, one-mode instability remains to be developed.

In the simpler setting of finite dimensional Hamiltonian systems, the analogous bifurcation has been analyzed for two degrees of freedom. Here there are no "extra" spectral elements on the imaginary axis to set up a resonance, and Meyer and Schmidt (1971) have determined that there two possibilities: the "bubble" bifurcation or the "liberation" bifurcation, corresponding (very roughly) to subcritical and supercritical Hopf bifurcation. Abraham and Marsden (1978) provide an introduction to this theory. Whether it has any relevance to the infinite dimensional problem is unclear.

Figure Captions

Figure (3.1) (a) Typical spectrum of the linear operator in (3.11) for $\nu_c > 0$. The continuum is always present. The roots of the dispersion function determine the discrete eigenvalues. (b) For $\nu_c = 0$, $\sigma(\mathcal{L})$ reflects the Hamiltonian structure of the dynamics. Here the fixed point is linearly unstable; at criticality the quadruplet would collapse to a conjugate pair of eigenvalues (of multiplicity two) embedded in the continuous spectrum.

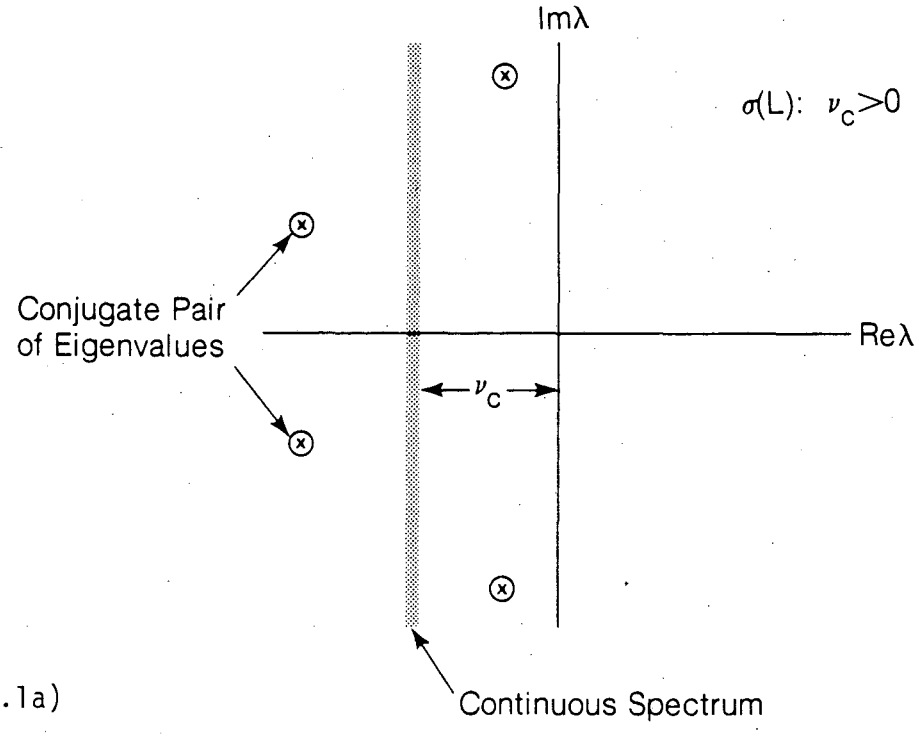

Figure (3.1a)

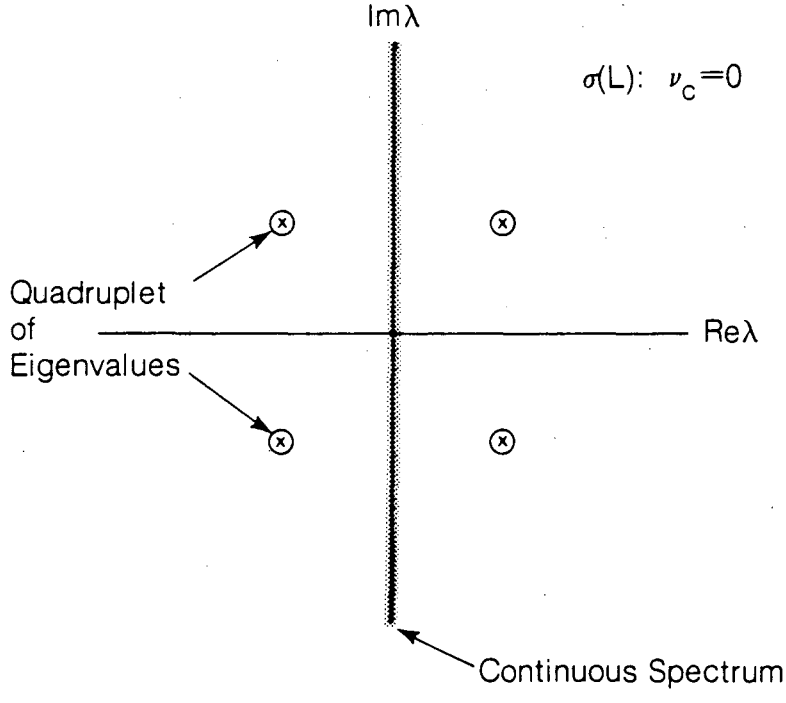

Figure (3.1b)

XBL 837-471

Figure (3.2a) Bifurcation surfaces for $n_b = 0.05$ at various values of the collision frequency, ϵ. The beam velocity is u, and k is the wave number.

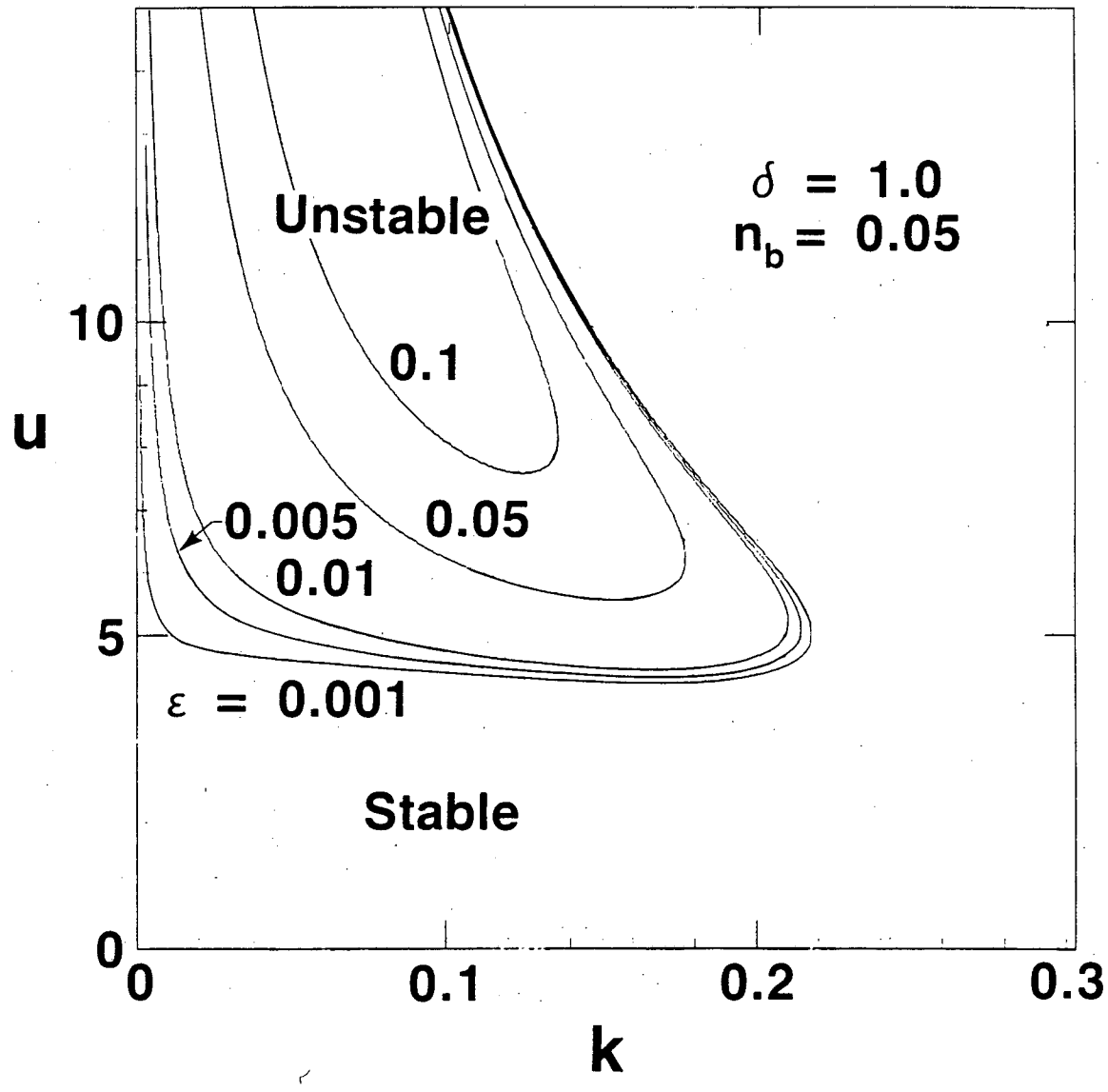

XBL 838-3008

Figure (3.2a)

Figure (3.2b) Bifurcation surfaces for $n_b = 0.5$ at various values of the collision frequency, ϵ. The beam velocity is u, and k is the wave number.

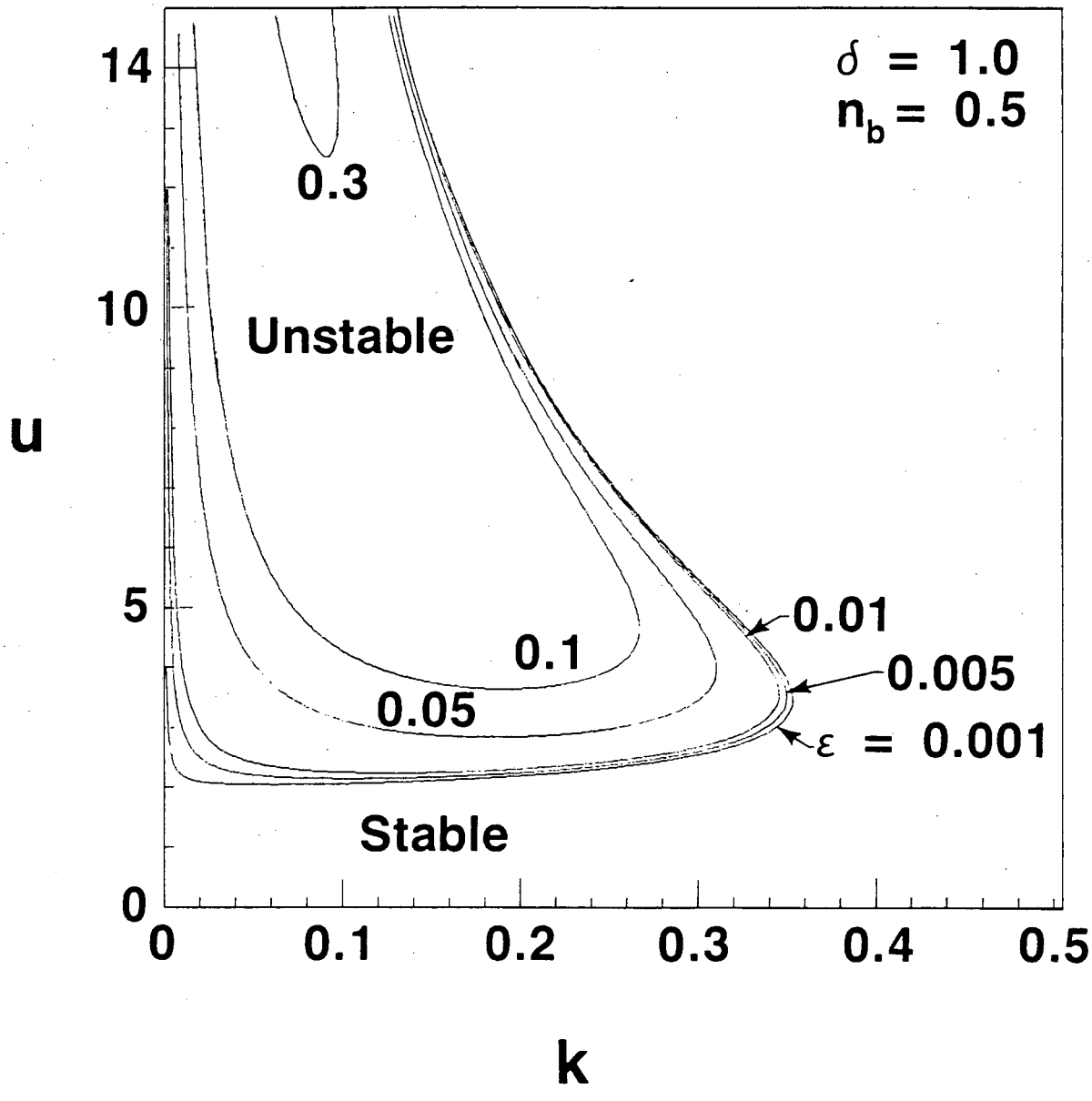

XBL 838-2982

Figure 3.2b

Figure (3.3) (a) Bifurcation surface for a cool, low density beam (solid line). Also shown is the bifurcation surface for $2k$ (dotted line); the intersection of the two surfaces is a double Hopf bifurcation. Points A and B for $k = 0.17$ are the selected points of low and high growth rate. (b) The four solutions to the dispersion relation in (3.65) for $k = 0.17$. The real part of the frequency $\omega = \text{Re}\, kz$ is plotted against the drift frequency ku in units where $\omega_e = 1$. On the branch indicated, the imaginary part of z satisfies condition (3.67) for a linear instability. The remaining three roots correspond to stable solutions.

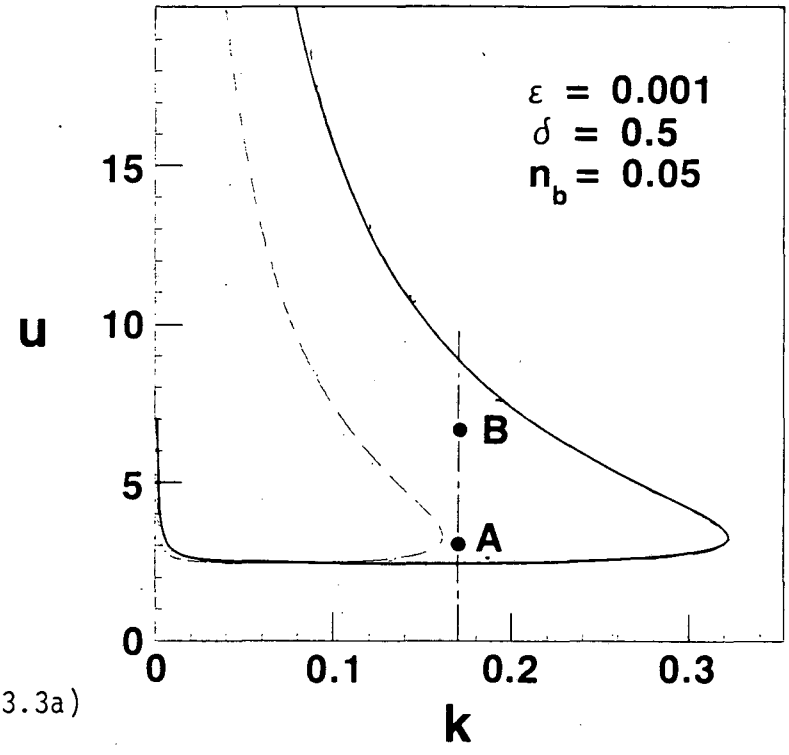

Figure (3.3a)

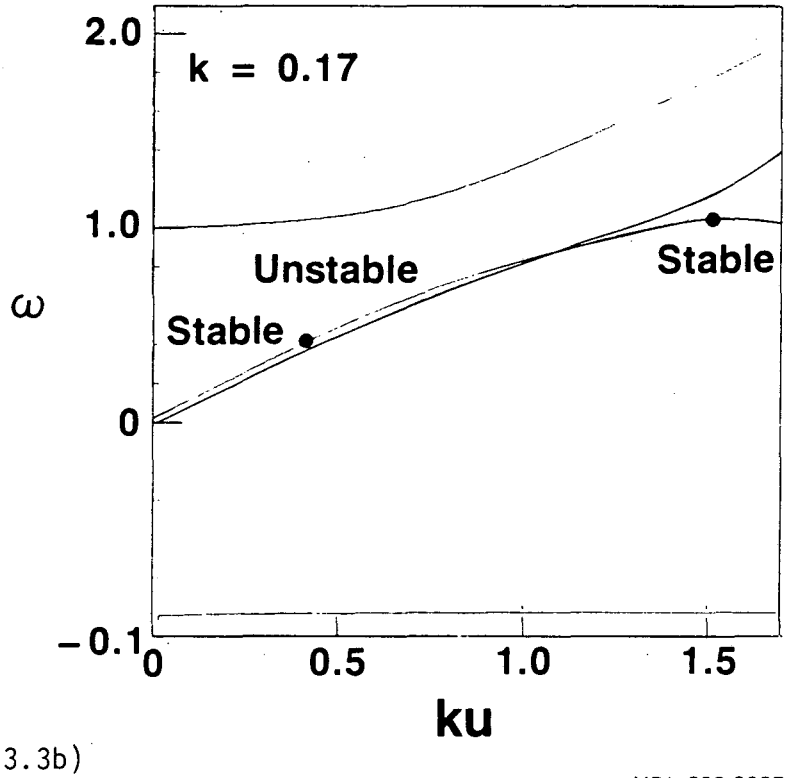

Figure (3.3b)

XBL 838-3007

Figure (3.4) Logarithmic plots of β along the bifurcation surface shown in Fig. (3.3a). The curves presented here may be correlated with Fig. (3.3a) by matching their endpoints at $k \sim 0$ and $k \sim 0.08$ to the corresponding endpoints on the bifurcation surface. As in Fig. (2.2a), $f(\beta) \equiv \mathrm{sgn}(\beta)\log(1.0+\beta)$.

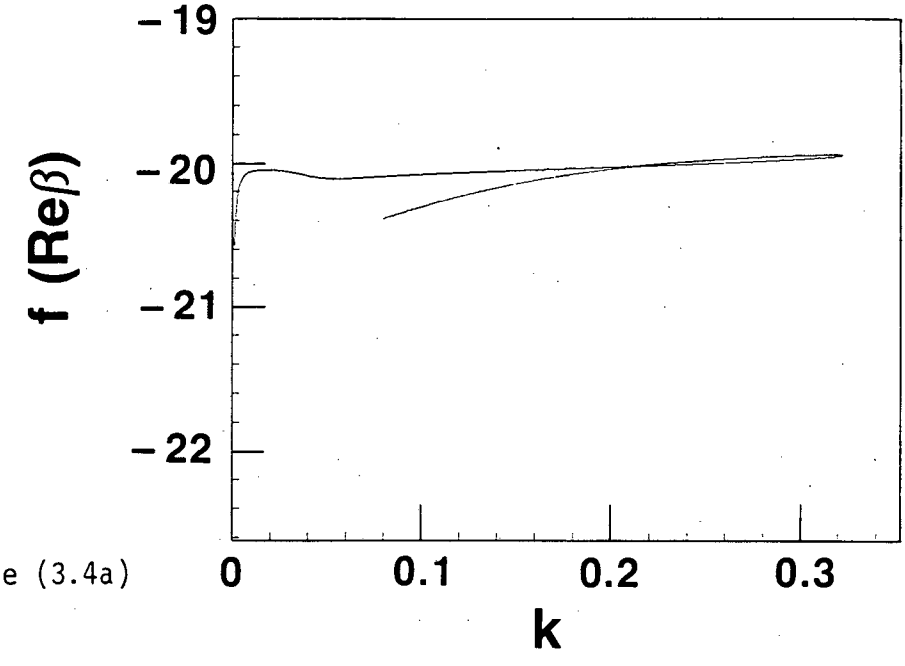

Figure (3.4a)

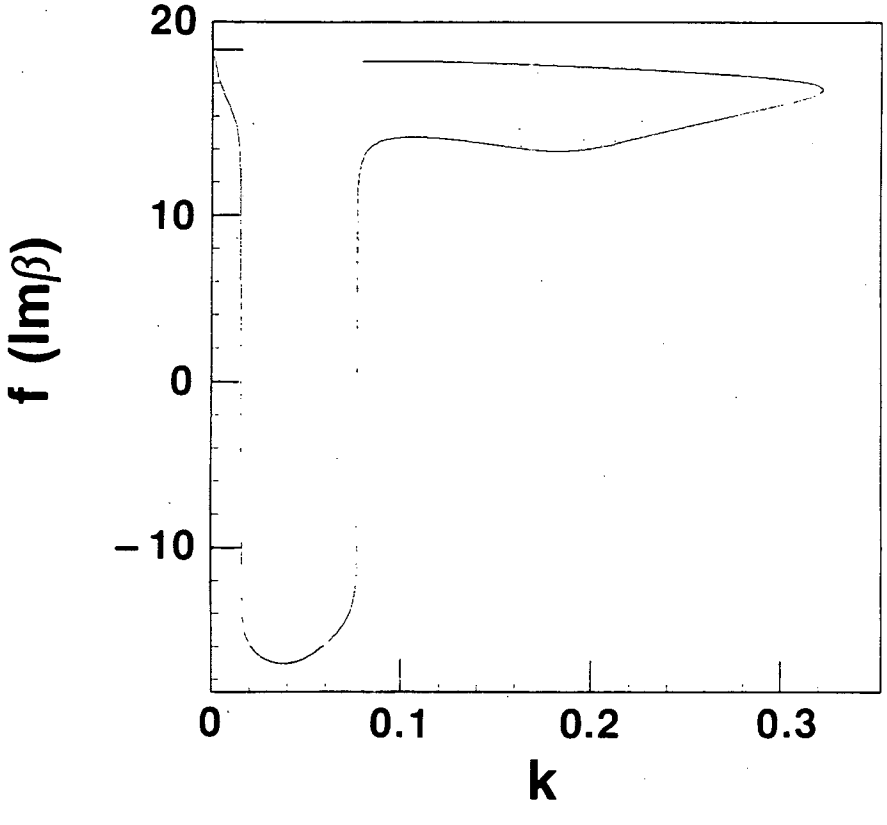

Figure (3.4b)

XBL 838-2975

Figure (3.5) (a) Initial velocity distribution at point A ($\delta = 0.5$, $n_b = 0.05$, $k = 0.17$, and $u \sim 2.5$) in Fig. (3.3a) as seen in the wave frame. (b) The lowest order correction to the spatially homogeneous component of the distribution function. Shown for point A in Fig. (3.3a) in the wave frame.

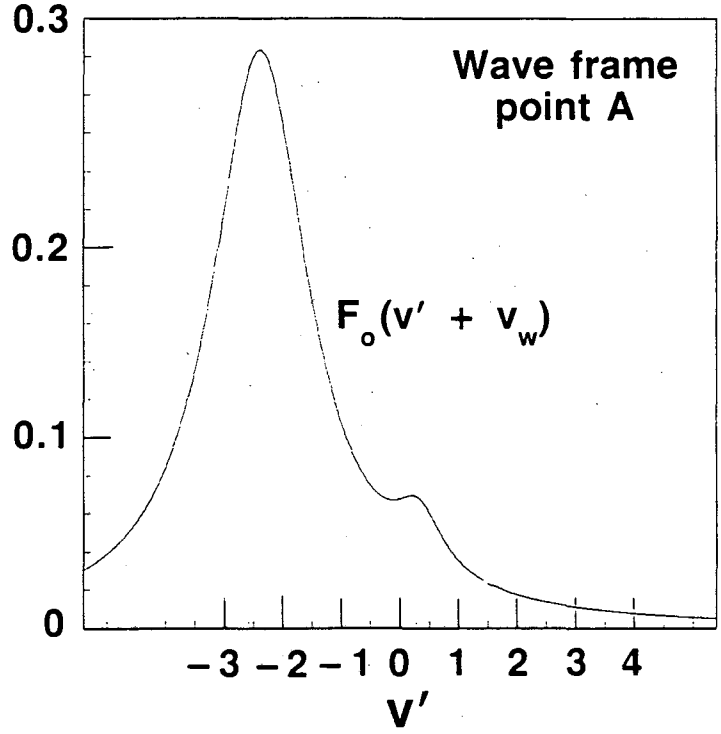

Figure (3.5a)

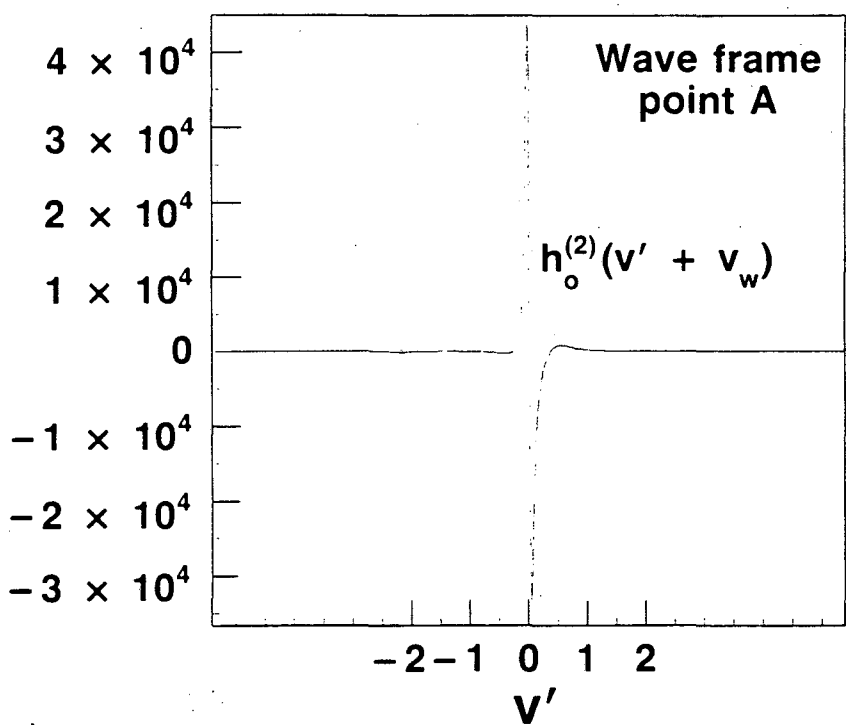

Figure (3.5b)

XBL 838-2977

Figure (3.6) The homogeneous component of the saturated distribution function showing the effect of the lowest order correction: a small rearrangement of the resonant particles near $v' = 0$. Here $\gamma = \mathrm{Re}\,\lambda$ is the linear growth rate. Shown for point A in Fig. (3.3a) in the wave frame.

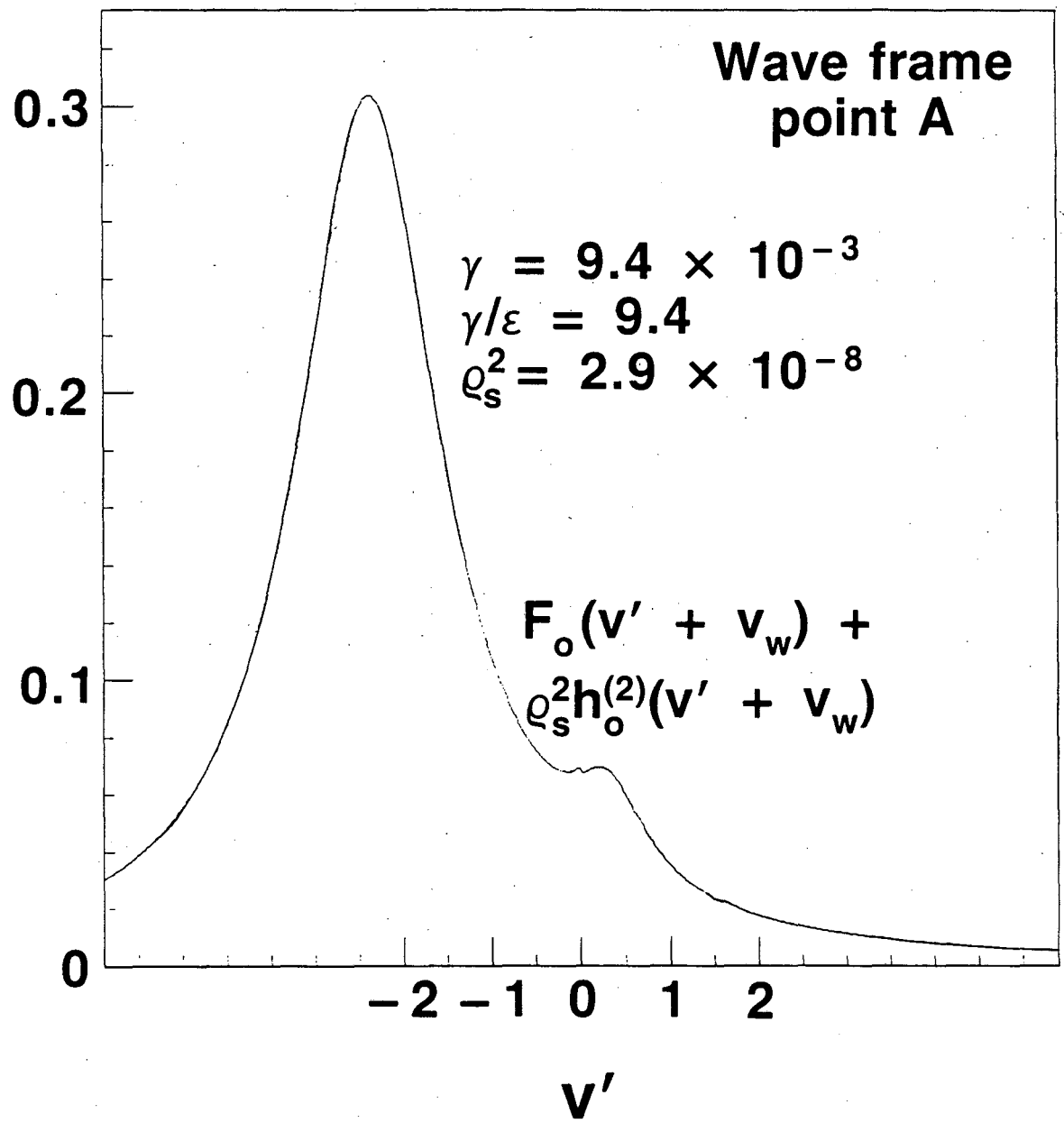

XBL 838-2974

Figure (3.6)

Figure (3.7) (a) The lowest order correction to the spatially homogeneous component of the distribution function. Shown for point B ($\delta = 0.5$, $n_b = 0.05$, $k = 0.17$, and $u \sim 6.0$) in Fig. (3.3a) in the wave frame. (b) The initial velocity distribution (dotted line) and the homogeneous component of the saturated distribution function (solid line) showing the effect of the lowest order correction. γ is defined as in Fig. (3.6). Shown for point B in the wave frame.

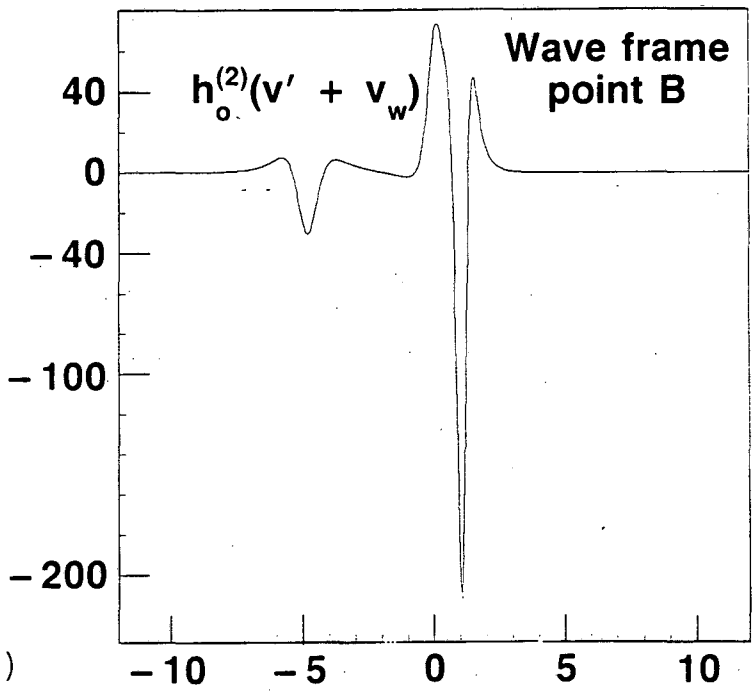

Figure (3.7a)

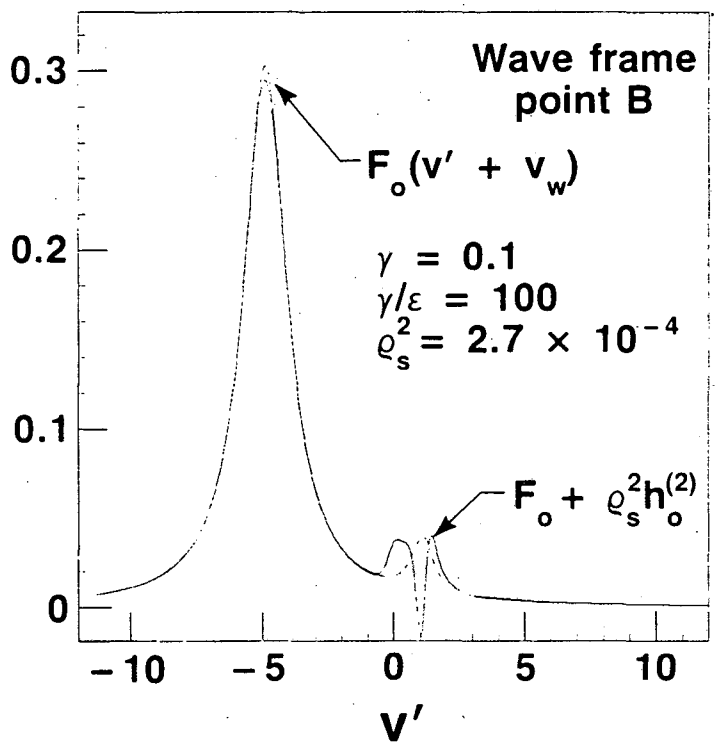

XBL 838-2998

Figure (3.7b)

Figure (3.8) (a) Bifurcation surface for a warm, low density beam (solid line). Also shown is the bifurcation surface for $2k$ (dotted line), the intersection is a double Hopf bifurcation. Points A and B (off scale at $u \sim 23.0$) for $k = 0.05$ are the selected points of low and high growth rate. (b) The four solutions to the dispersion relation in (3.65) for $k = 0.05$. The real part of the frequency $\omega = \mathrm{Re}\, kz$ is plotted against the drift frequency in units where $\omega_e = 1$. On the branch indicated, the imaginary part of z satisfies condition (3.67) for a linear instability. The remaining three roots correspond to stable solutions.

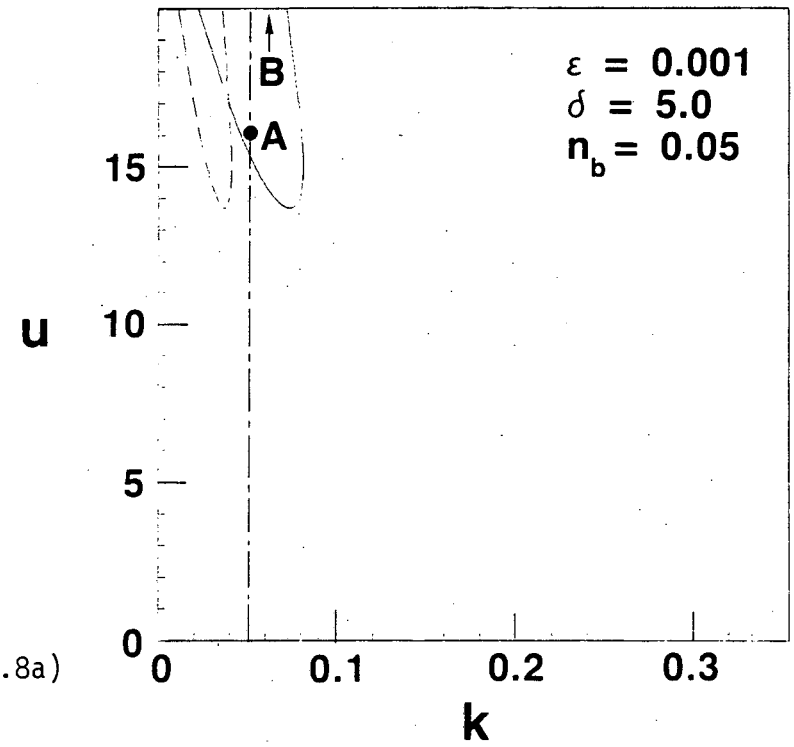

Figure (3.8a)

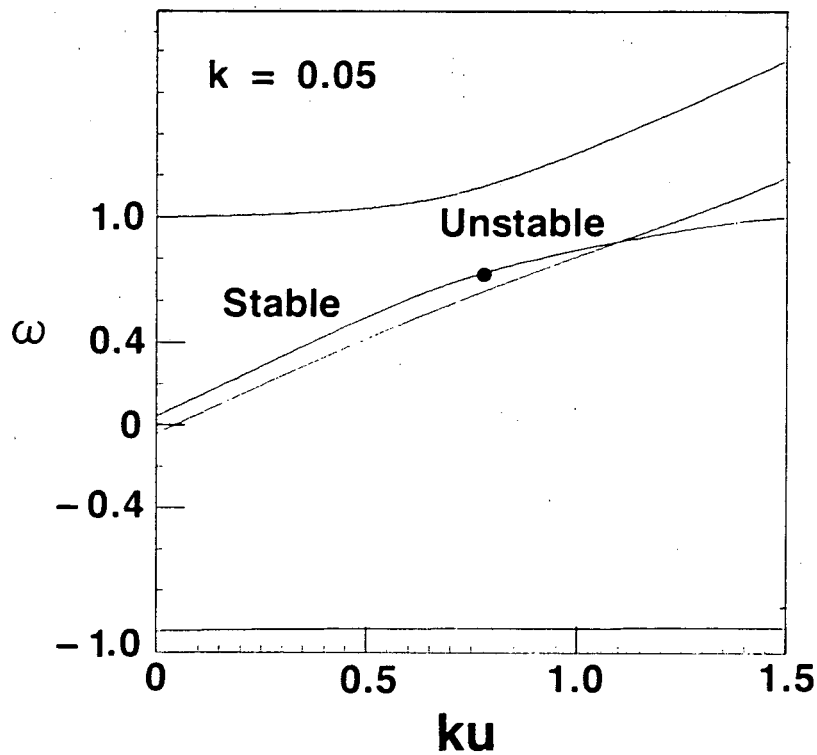

Figure (3.8b)

XBL 838-3006

Figure (3.9) Logarithmic plots of β along the bifurcation surface in Fig. (3.8a). The curves presented should be correlated with Fig. (3.8a) by matching their endpoints at $k \sim 0.02$ and $k \sim 0.07$ to the corresponding endpoints on the bifurcation surface. As in Fig. (2.2a), $\mathrm{f}(\beta) \equiv \mathrm{sgn}(\beta)\log(1.0+\beta)$.

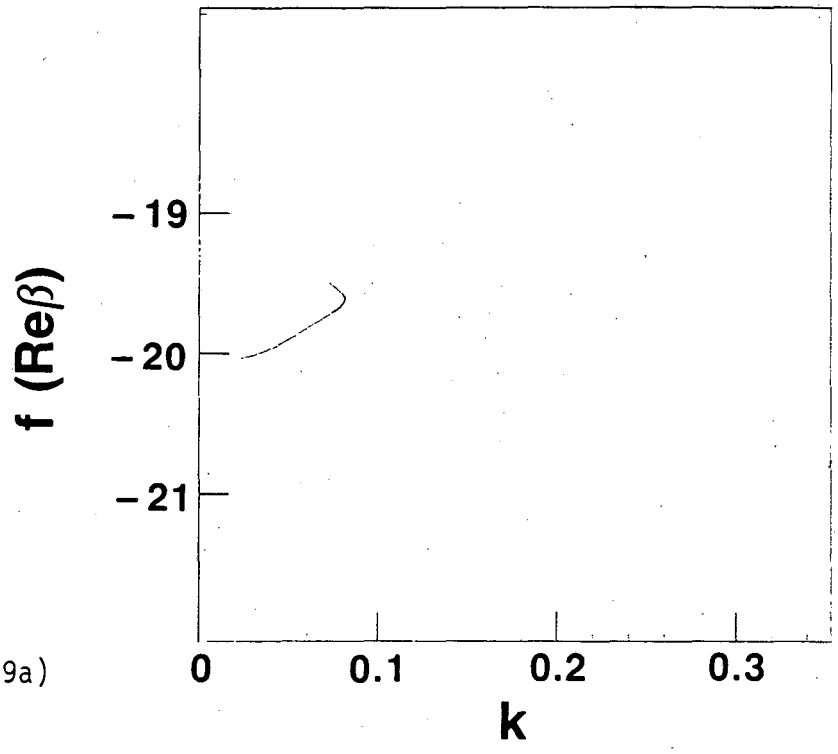

Figure (3.9a)

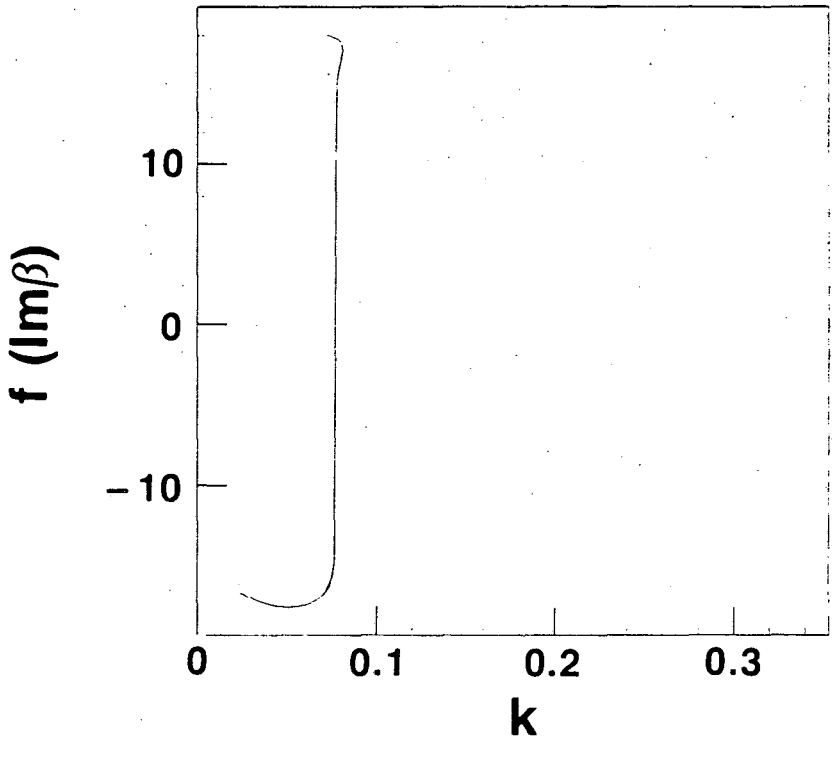

XBL 838-3003

Figure (3.9b)

Figure (3.10) (a) Initial velocity distribution at point A ($\delta = 5.0$, $n_b = 0.05$, $k = 0.05$, and $u \sim 16.0$) in Fig. (3.8a) as seen in the wave frame. (b) The lowest order correction to the spatially homogeneous component of the distribution function. Shown for point A in Fig. (3.8a) in the wave frame.

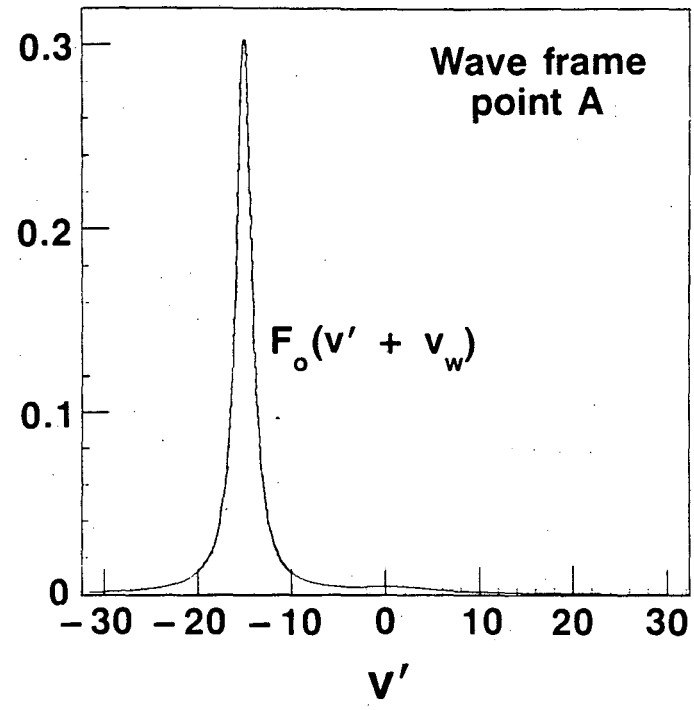

Figure (3.10a)

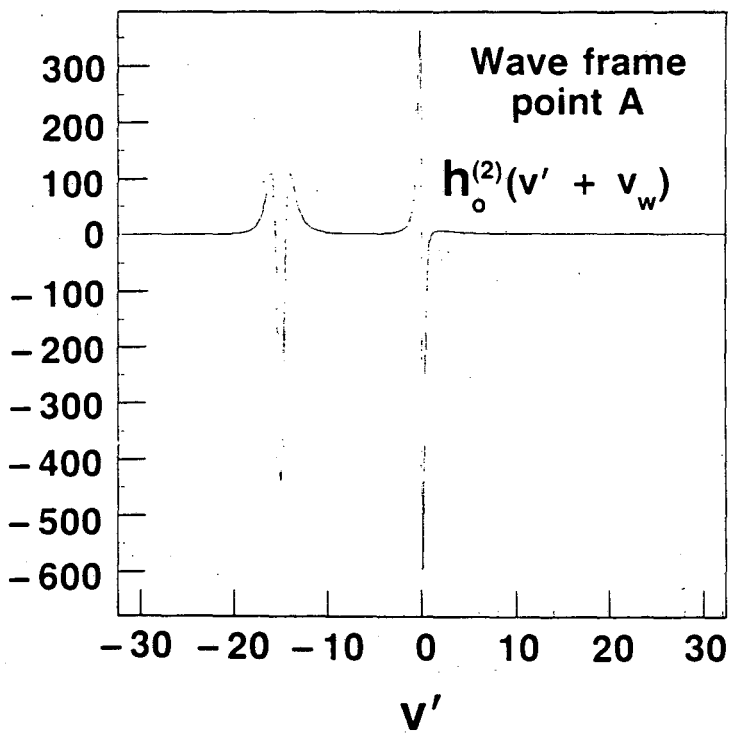

Figure (3.10b)

XBL 838-2973

Figure (3.11) The homogeneous component of the saturated distribution function showing the (negligible) effect of the lowest order correction. γ is as in Fig. (3.6). Shown for point A in Fig. (3.8a) in the wave frame.

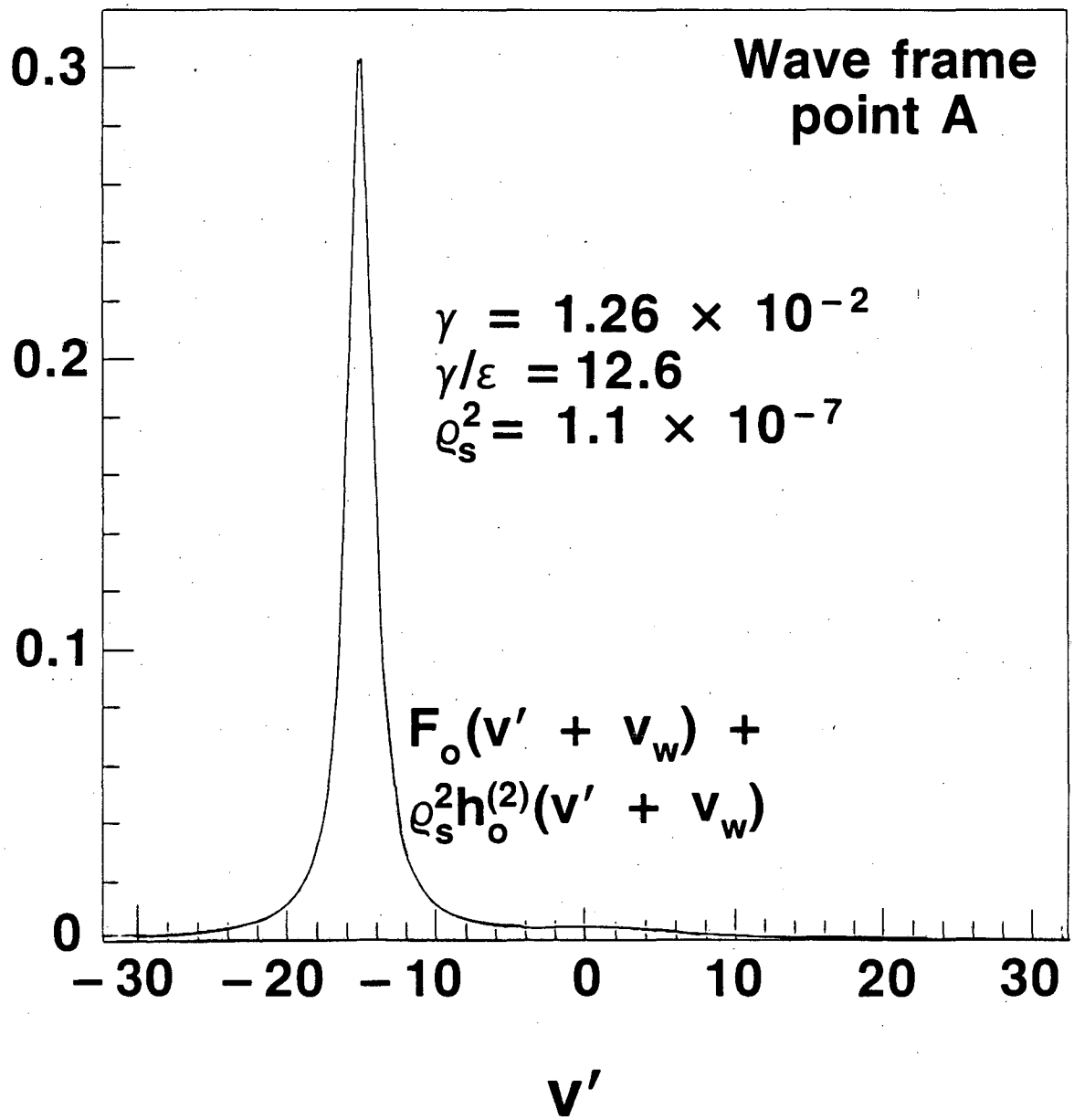

XBL 838-2976

Figure (3.11)

Figure (3.12) (a) The initial velocity distribution at point B ($\delta = 5.0$, $n_b = 0.05$, $k = 0.05$, and $u \sim 23.0$) in Fig. (3.8a) as seen in the wave frame. (b) The lowest order correction to the spatially homogeneous component of the distribution function. Shown for point B in Fig. (3.8a) in the wave frame.

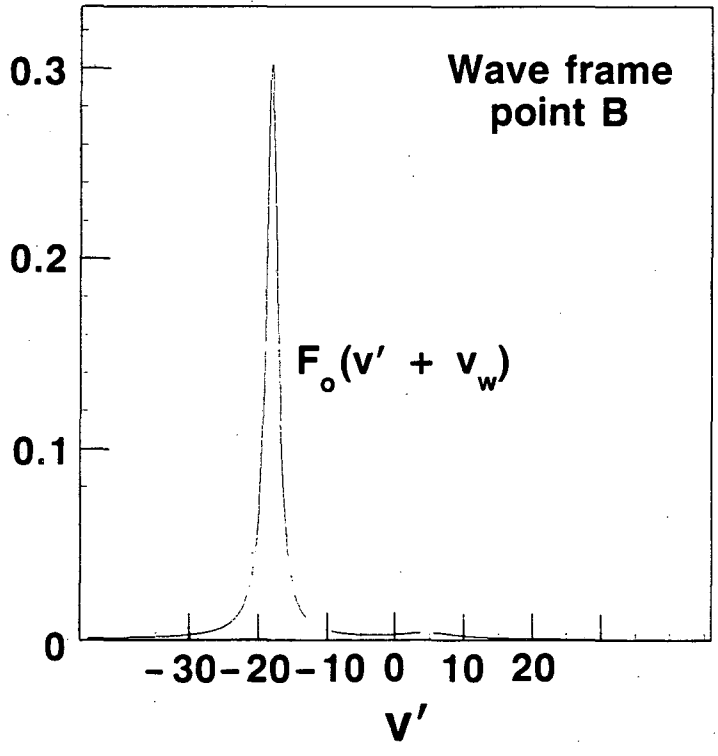

Figure (3.12a)

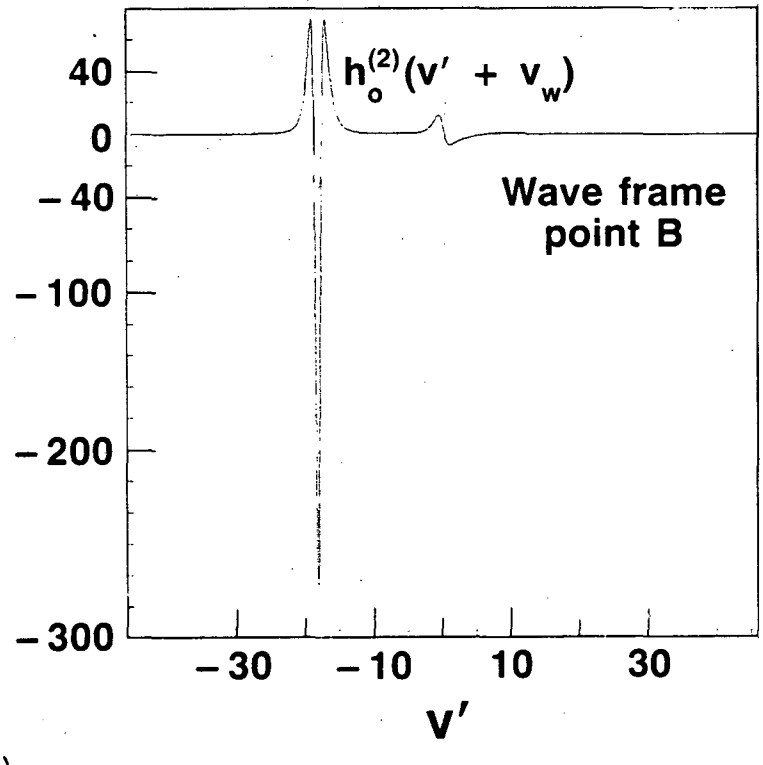

Figure (3.12b)

XBL 838-2999

Figure (3.13) The homogeneous component of the saturated distribution function showing the effect of the lowest order correction. γ is as in Fig. (3.6). Shown for point B in Fig. (3.8a) in the wave frame.

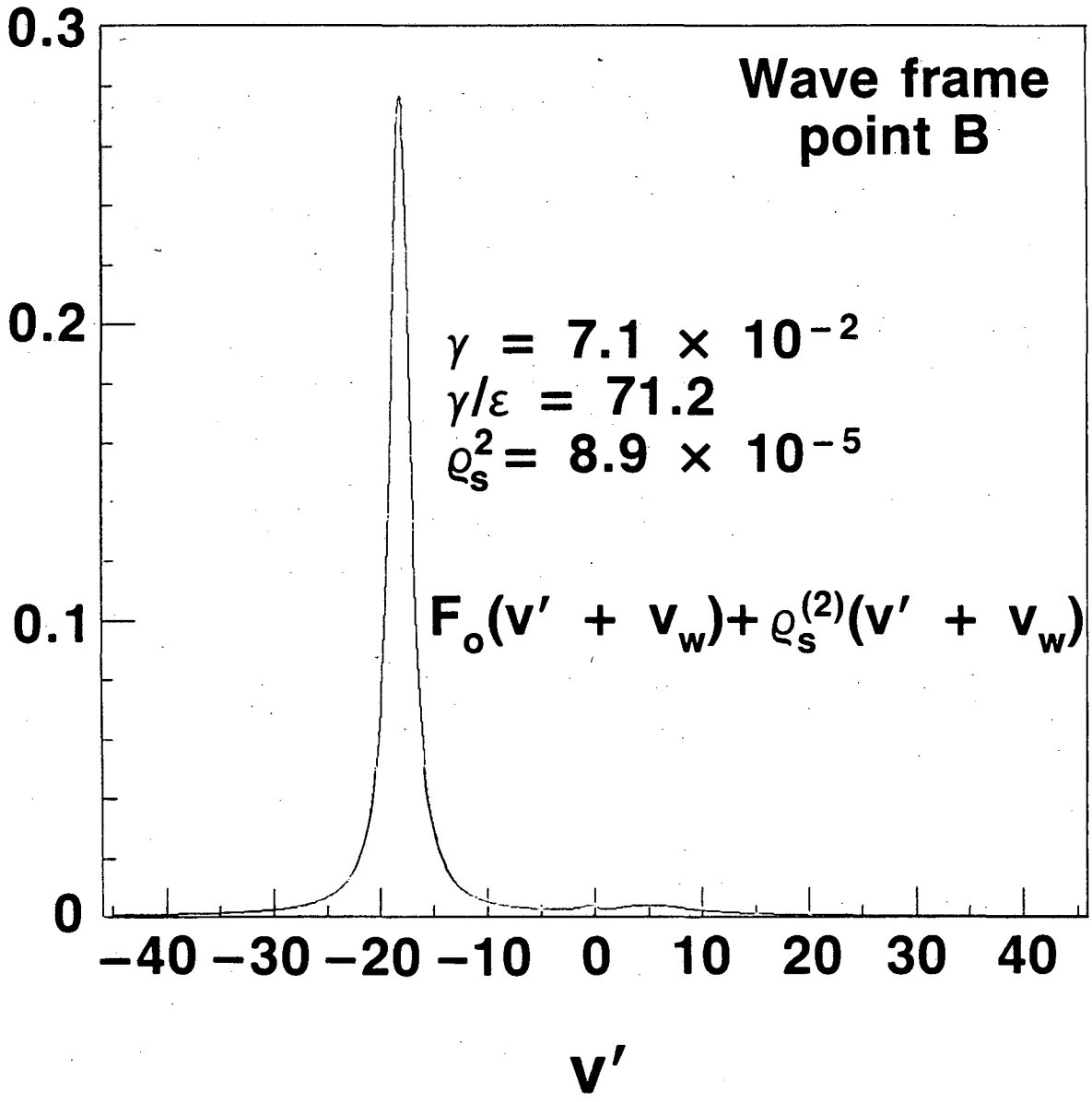

XBL 838-2978

Figure (3.13)

Figure (3.14) (a) Bifurcation surface for a cool, equal density beam (solid line). Also shown is the bifurcation surface for $2k$ (dotted line), the intersection is a double Hopf bifurcation. Points $\bar{A}$ and B for $k = 0.26$ are the selected points of low and high growth rate. (b) The four solutions to the dispersion relation in (3.65) for $k = 0.26$. The real part of the frequency $\omega = \text{Re}\, kz$ is plotted against the drift frequency in units where $\omega_e = 1$. On the branch indicated, the imaginary part of z satisfies condition (3.67) for a linear instability. The remaining three roots correspond to stable solutions.

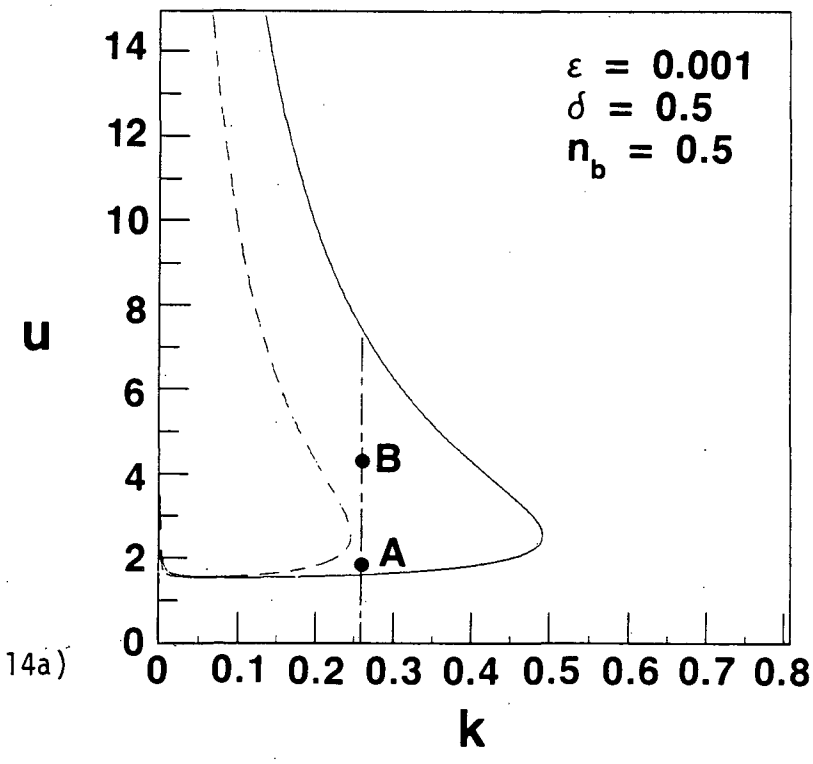

Figure (3.14a)

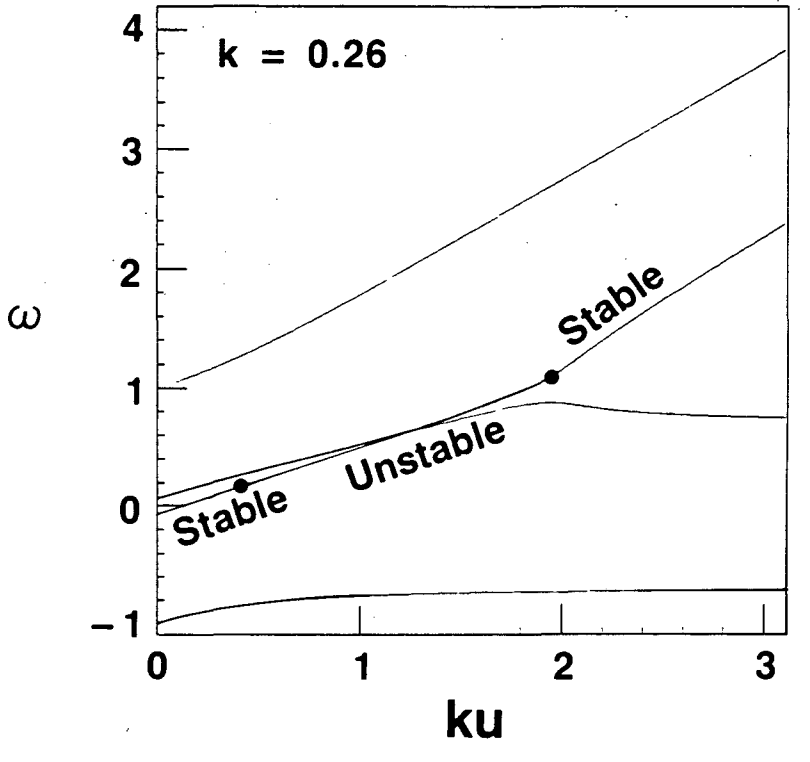

Figure (3.14b)

XBL 838-2970

Figure (3.15) Logarithmic plots of β along the bifurcation surface shown in Fig. (3.14a). The curves presented here should be correlated with Fig. (3.14a) by matching their endpoints at $k \sim 0$ and $k \sim 0.1$ to the corresponding endpoints on the bifurcation surface. As in Fig. (2.2a), $f(\beta) \equiv \mathrm{sgn}(\beta)\log(1.0 + \beta)$.

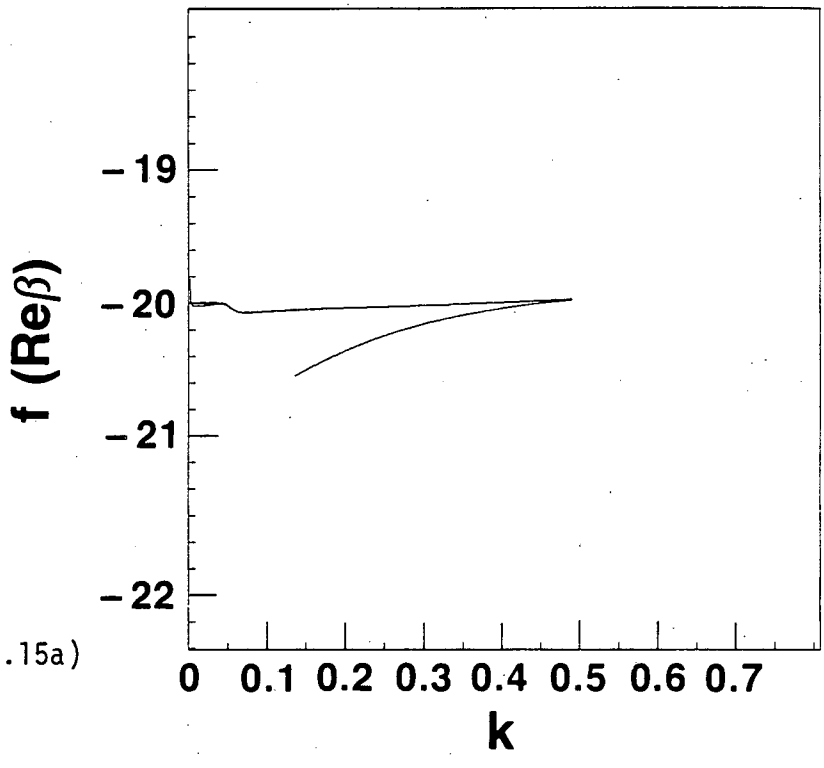

Figure (3.15a)

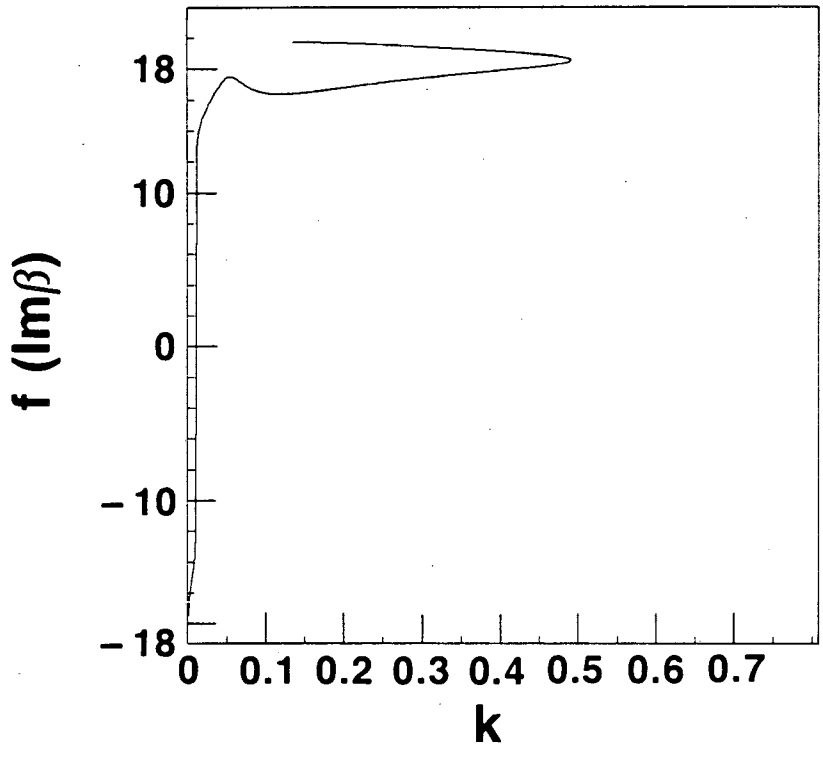

Figure (3.15b)

XBL 838-3004

Figure (3.16) (a) Initial velocity distribution at point A ($\delta = 0.5$, $n_b = 0.5$, $k = 0.26$, and $u \sim 1.5$) in Fig. (3.14a) as seen in the wave frame. (b) The lowest order correction to the spatially homogeneous component of the distribution function. Shown for point A in Fig. (3.14a) as seen in the wave frame.

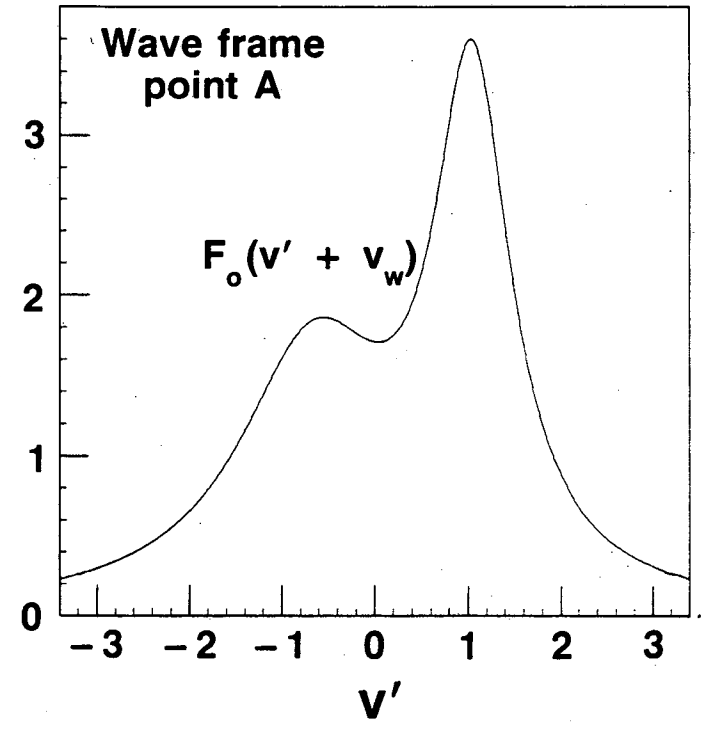

Figure (3.16a)

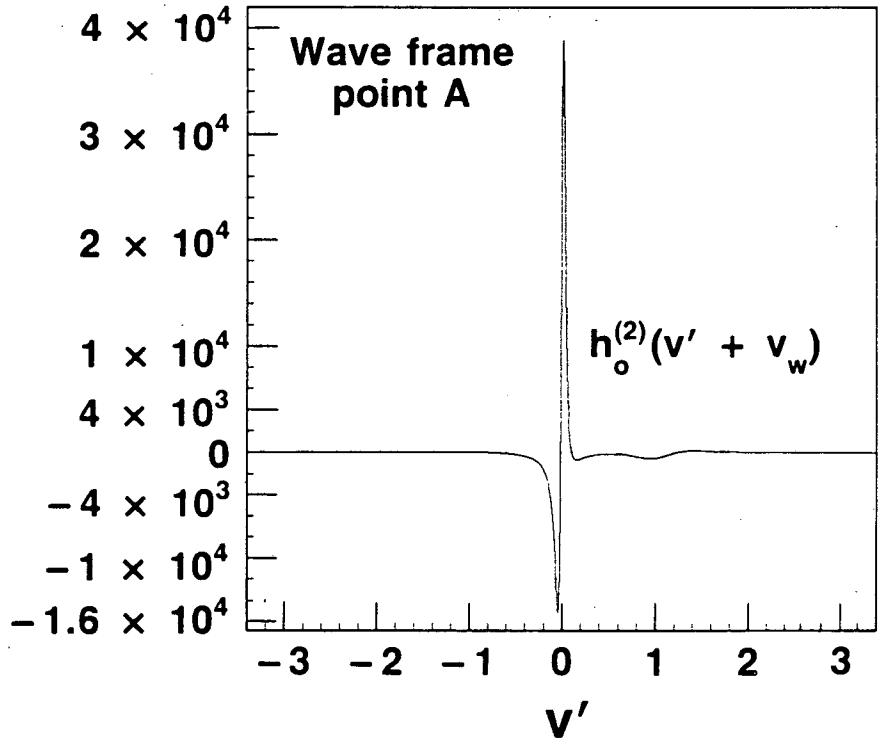

Figure (3.16b)

XBL 838-2971

Figure (3.17) The homogeneous component of the saturated distribution function showing the effect of the lowest order correction (visible only at the resonance $v' = 0$). γ is as in Fig. (3.6). Shown for point A in Fig. (3.14a) in the wave frame.

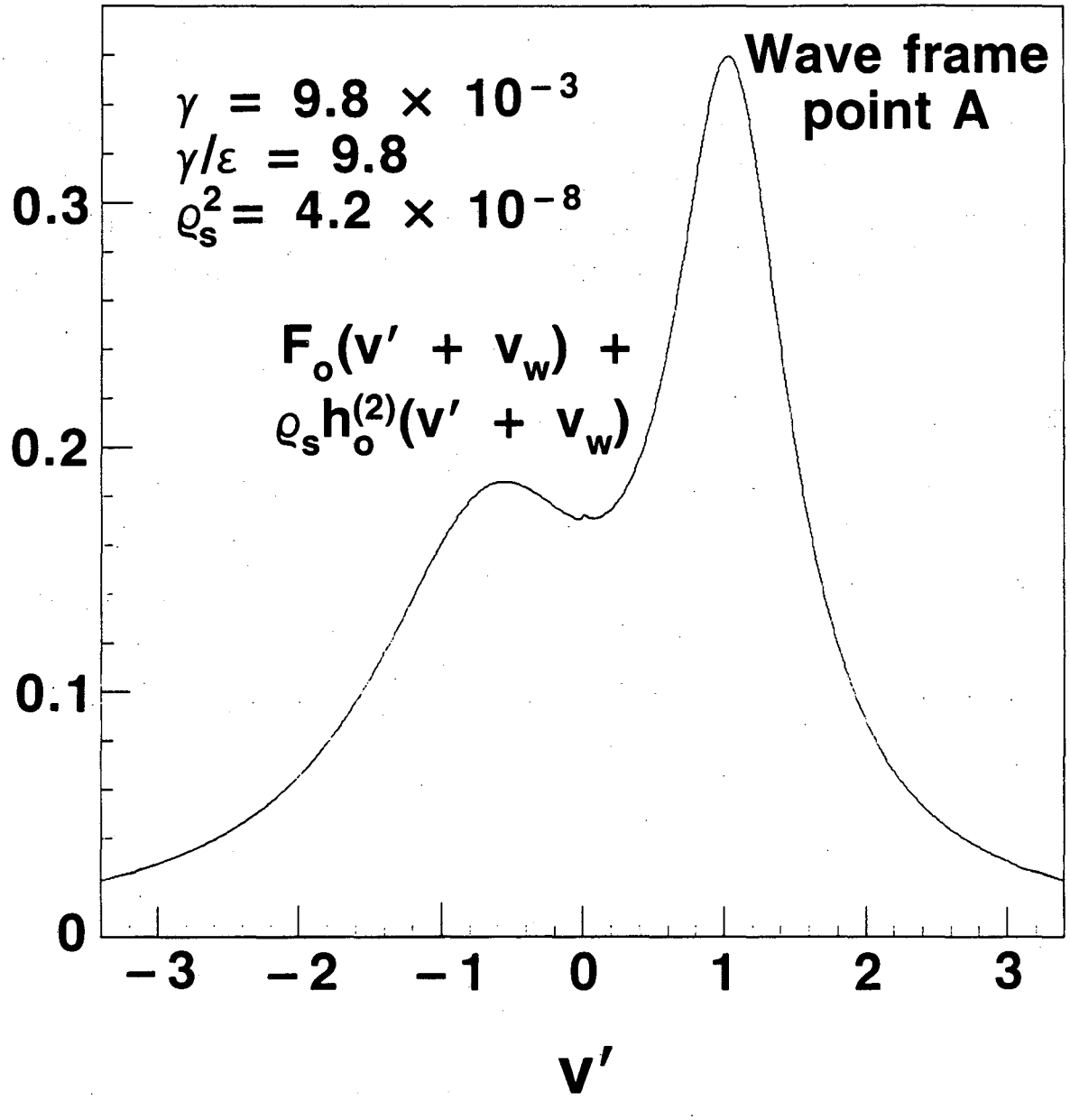

XBL 838-2972

Figure (3.17)

Figure (3.18) (a) The lowest order correction to the spatially homogeneous component of the distribution function. Shown for point B ($\delta = 0.5$, $n_b = 0.5$, $k = 0.26$, and $u \sim 4.5$) in Fig. (3.14a) in the wave frame. (b) The initial velocity distribution (dotted line) and the homogeneous component of the saturated distribution function (solid line) showing the effect of the lowest order correction. γ is as in Fig. (3.6). Shown for point B in Fig. (3.14a) in the wave frame.

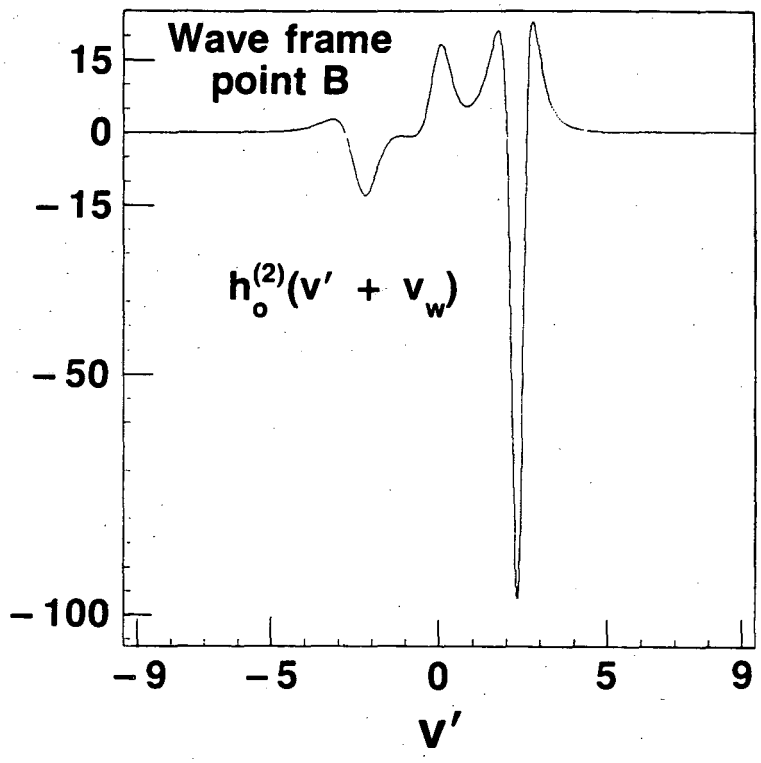

Figure (3.18a)

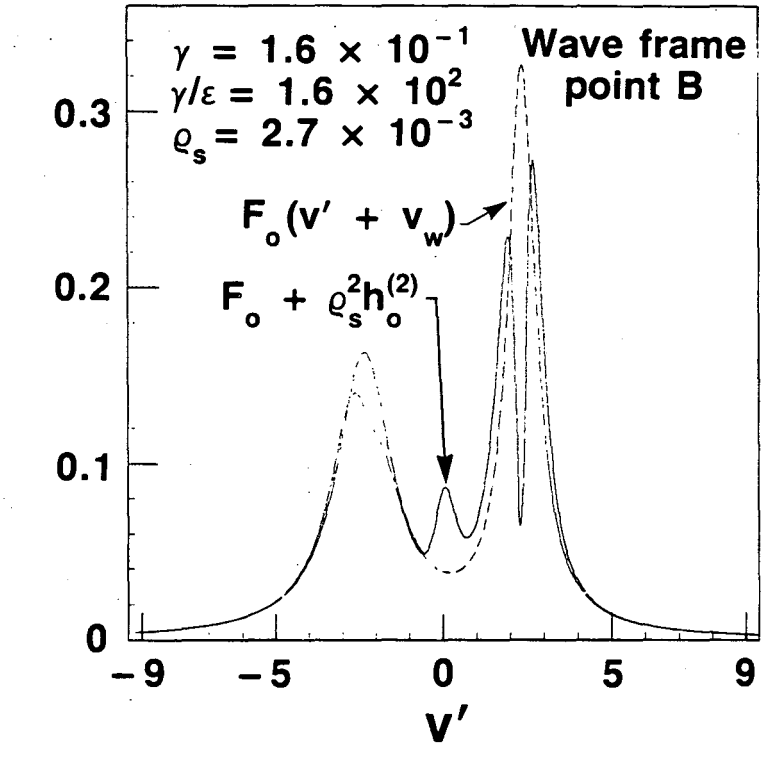

Figure (3.18b)

XBL 838-3009

Figure (3.19) (a) Bifurcation surface for an equal temperature, equal density beam (solid line). Also shown is the bifurcation surface for $2k$ (dotted line), the intersection is a double Hopf bifurcation. Points A and B for $k = 0.18$ are the selected points of low and high growth rate. (b) The four solutions to the dispersion relation in (3.65) for $k = 0.18$. The real part of the frequency $\omega = \text{Re}\, kz$ is plotted against the drift frequency in units where $\omega_e = 1$. On the branch indicated, the imaginary part of z satisfies condition (3.67) for a linear instability. The remaining three roots correspond to stable solutions.

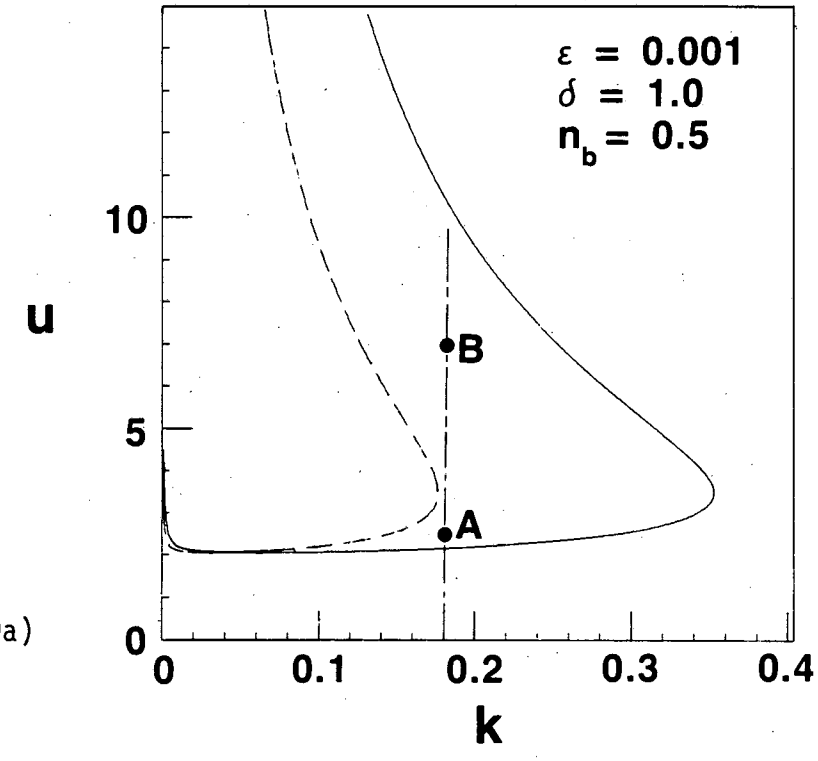

Figure (3.19a)

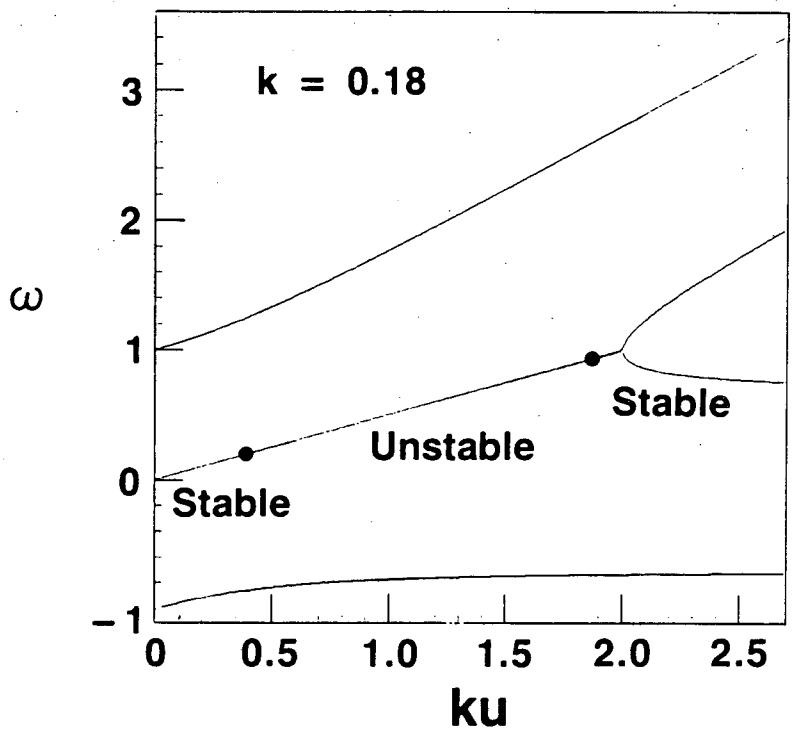

Figure (3.19b)

XBL 838-2997

Figure (3.20) Logarithmic plots of β along the bifurcation surface shown in Fig. (3.19a). The curves presented here may be correlated with Fig. (3.19a) by matching their endpoints at $k \sim 0$ and $k \sim 0.13$ to the corresponding endpoints on the bifurcation surface. As in Fig. (2.2a), $\mathrm{f}(\beta) \equiv \mathrm{sgn}(\beta)\log(1.0+\beta)$.

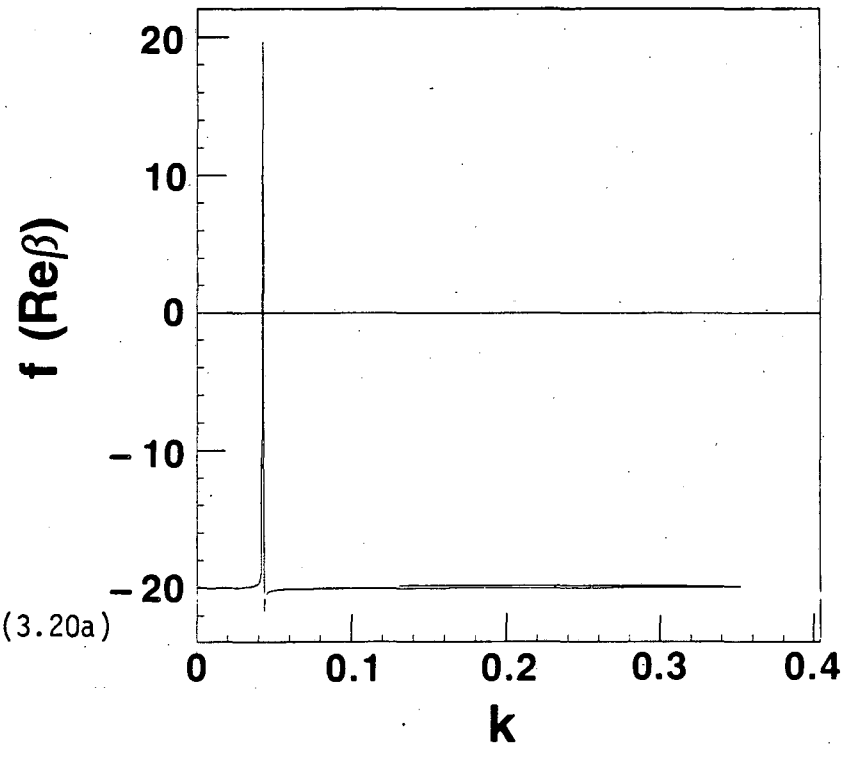

Figure (3.20a)

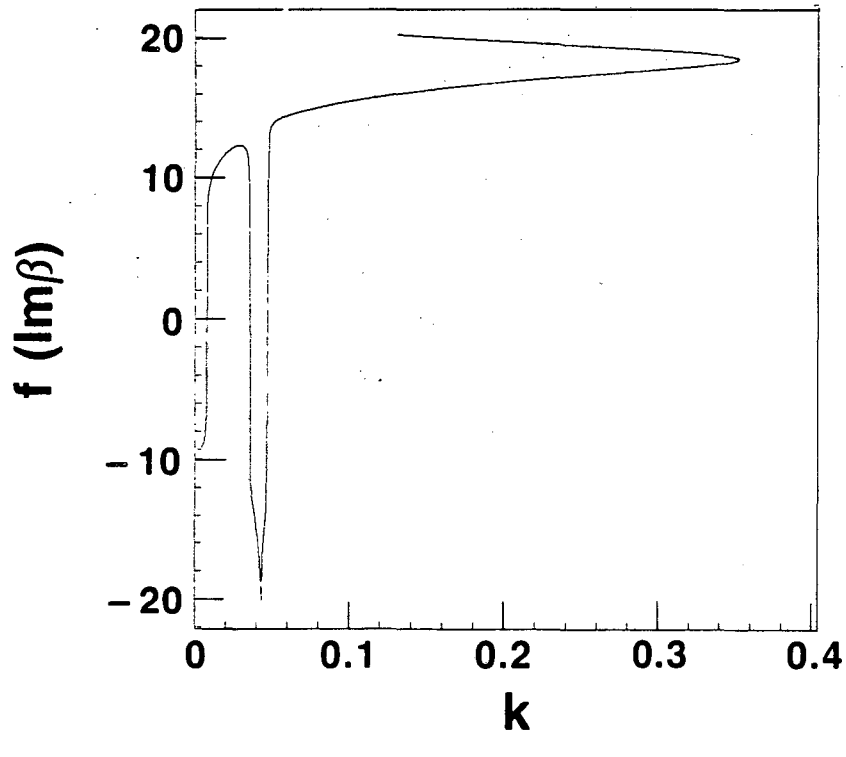

Figure (3.20b)

XBL 838-2996

Figure (3.21) (a) Initial velocity distribution at point A ($\delta = 1.0$, $n_b = 0.5$, $k = 0.18$, and $u \sim 2.1$) in Fig. (3.19a) as seen in the wave frame. (b) The lowest order correction to the spatially homogeneous component of the distribution function. Shown for point A in Fig. (3.19a) in the wave frame.

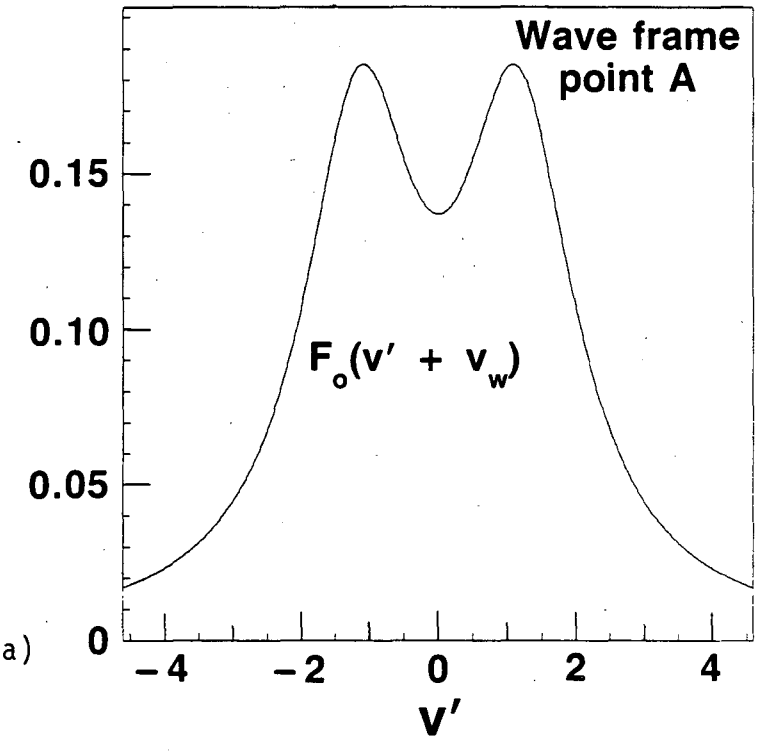

Figure (3.21a)

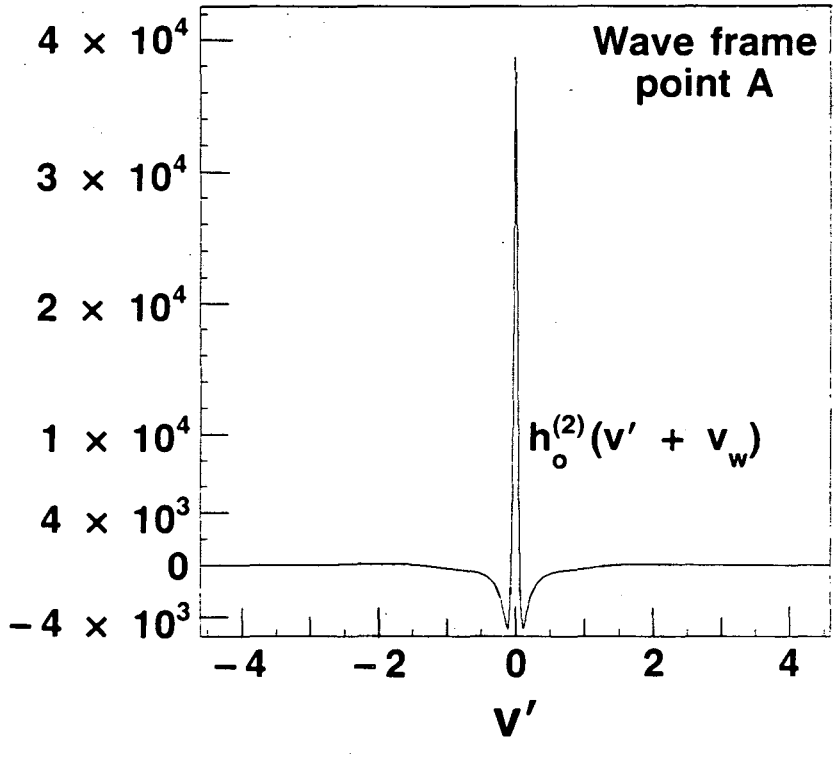

Figure (3.21b)

XBL 838-2995

Figure (3.22) The homogeneous component of the saturated distribution function showing the effect of the lowest order correction. γ is as in Fig. (3.6). Shown for point A in Fig. (3.19a) in the wave frame.

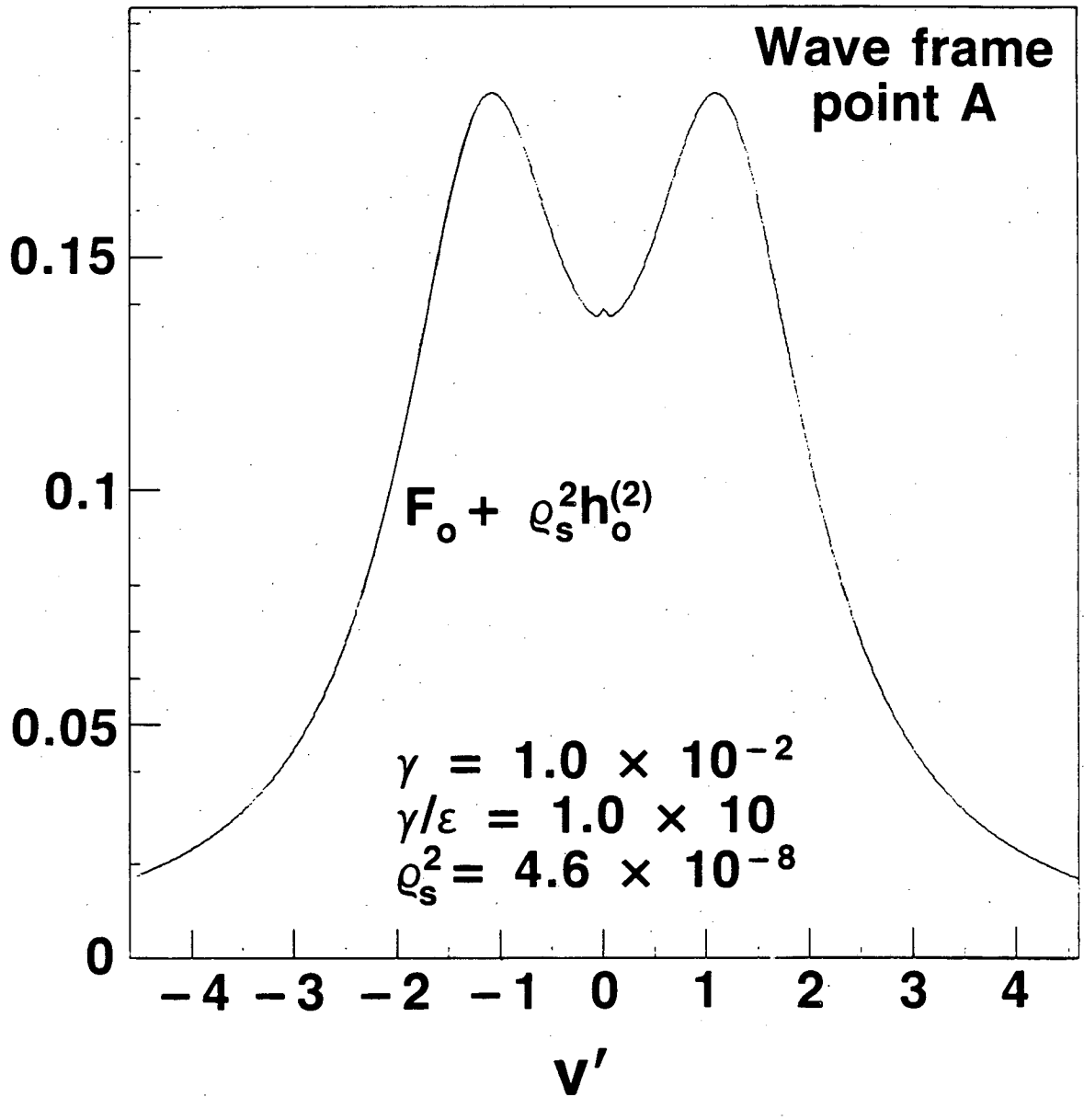

XBL 838-2994

Figure (3.22)

Figure (3.23) (a) The lowest order correction to the spatially homogeneous component of the distribution function. Shown for point B ($\delta = 1.0$, $n_b = 0.5$, $k = 0.18$, and $u \sim 6.5$) in Fig. (3.19a) in the wave frame. (b) The initial velocity distribution (dotted line) and the homogeneous component of the saturated distribution function (solid line) showing the effect of the lowest order correction. γ is as in Fig. (3.6). Shown for point B in the wave frame.

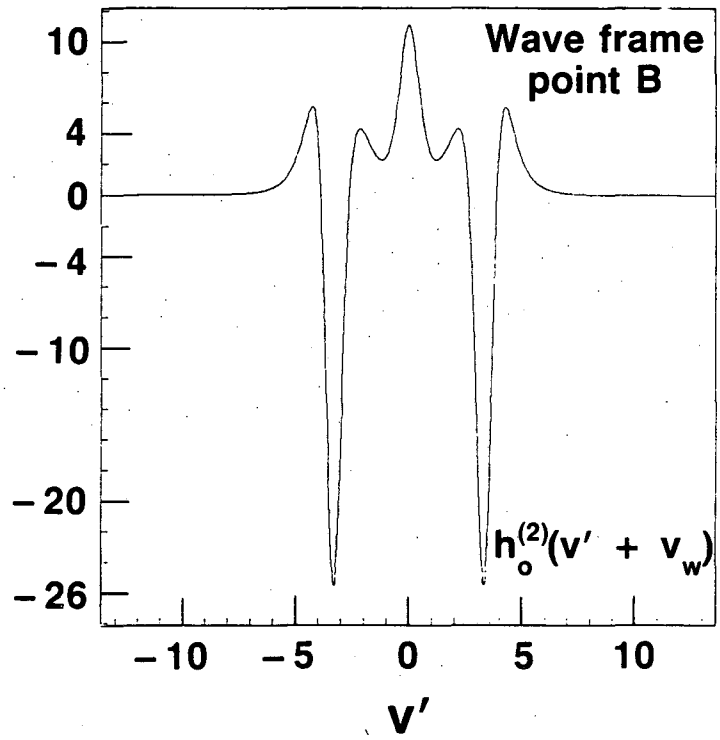

Figure (3.23a)

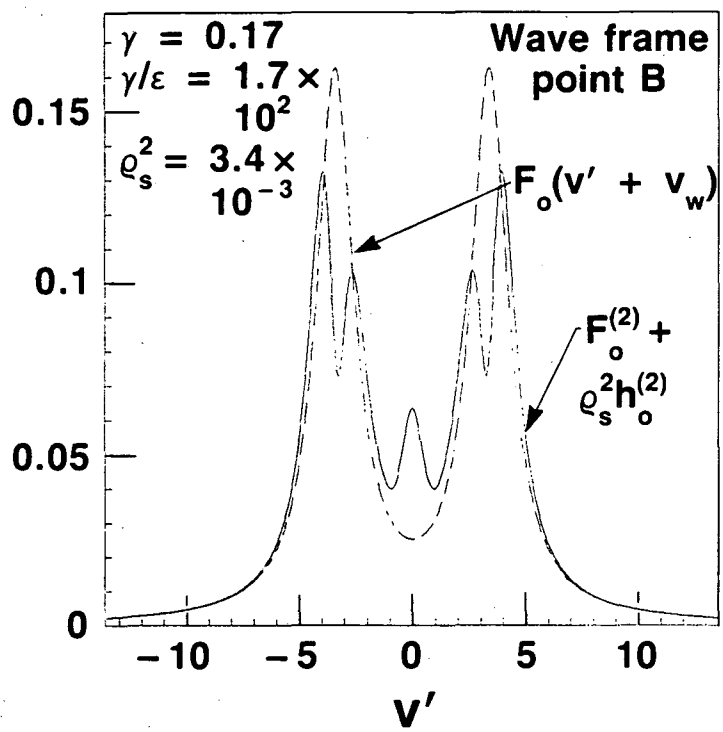

Figure (3.23b)

XBL 838-2980

Figure (3.24) (a) Bifurcation surface for a warm, equal density beam (solid line). Also shown is the bifurcation surface for $2k$ (dotted line), the intersection is a double Hopf bifurcation. Points A and B for $k = 0.14$ are the selected points of low and high growth rate. (b) The four solutions to the dispersion relation in (3.65) for $k = 0.14$. The real part of the frequency $\omega = \mathrm{Re}\, kz$ is plotted against the drift frequency in units where $\omega_e = 1$. On the branch indicated the imaginary part of z satisfies condition (3.67) for a linear instability. The remaining three roots ccorrespond to stable solutions.

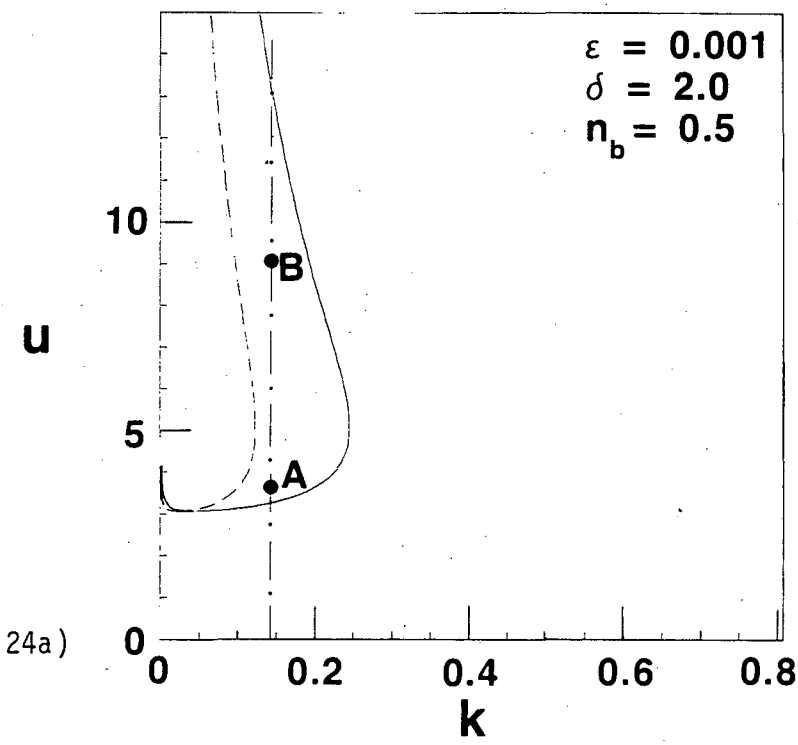

Figure (3.24a)

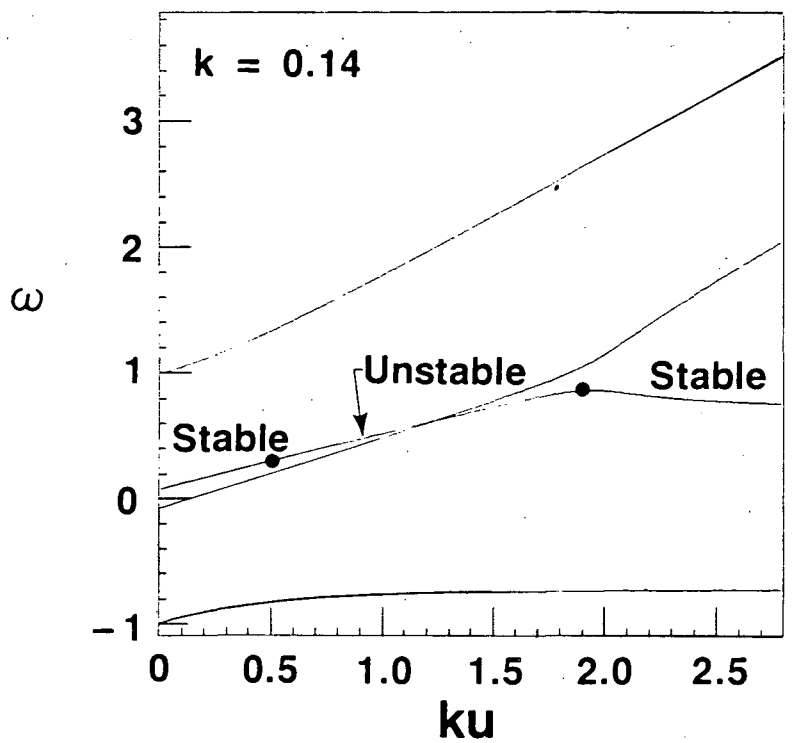

Figure (3.24b)

XBL 838-2981

Figure (3.25) (a) Logarithmic plots of β along the bifurcation surface shown in Fig. (3.24a). The curves presented here may be correlated with Fig. (3.24a) by matching their endpoints at $k \sim 0$ and $k \sim 0.1$ to the corresponding endpoints on the bifurcation surface. As in Fig. (2.2a), $f(\beta) \equiv \mathrm{sgn}(\beta)\log(1.0 + \beta)$.

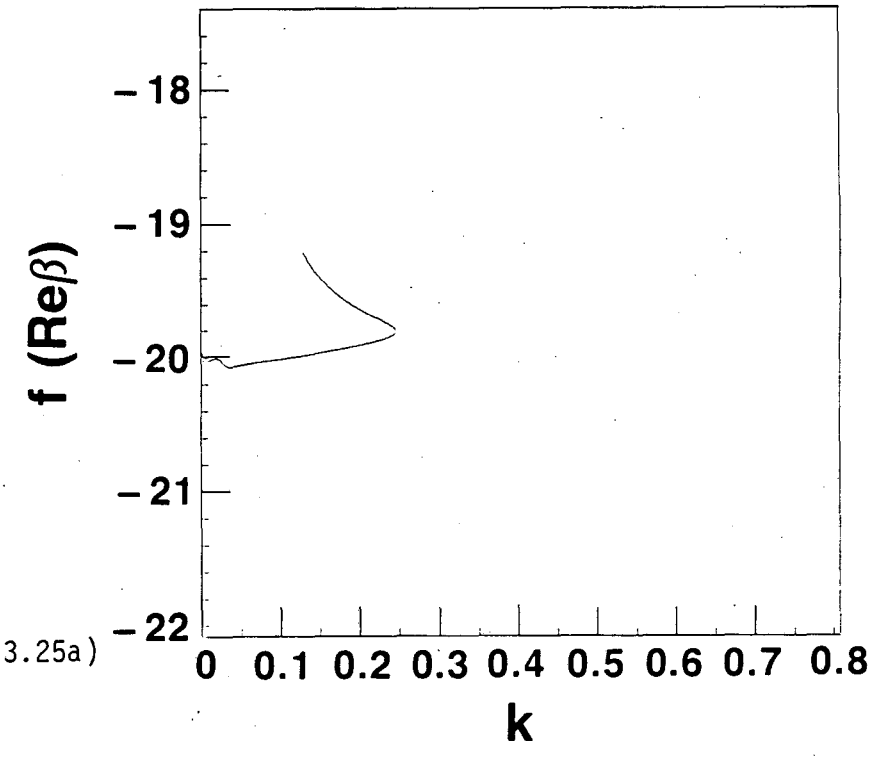

Figure (3.25a)

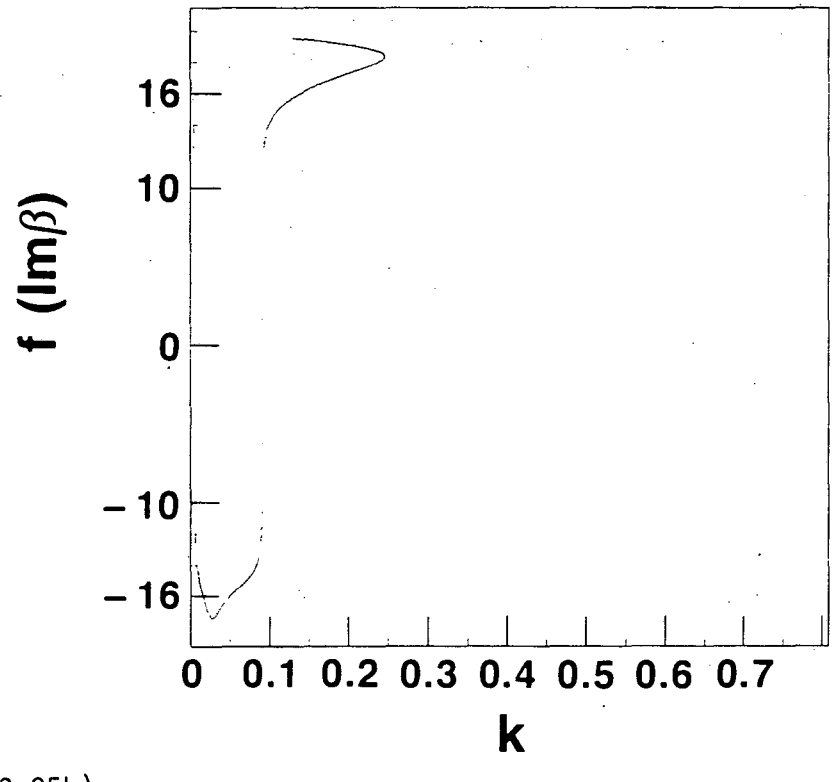

Figure (3.25b)

XBL 838-2984

Figure (3.26) (a) Initial velocity distribution at point A ($\delta = 2.0$, $n_b = 0.5$, $k = 0.14$, and $u \sim 3.5$) in Fig. (3.24a) as seen in the wave frame. (b) The lowest order correction to the spatially homogeneous component of the distribution function. Shown for point A in Fig. (3.24a) in the wave frame.

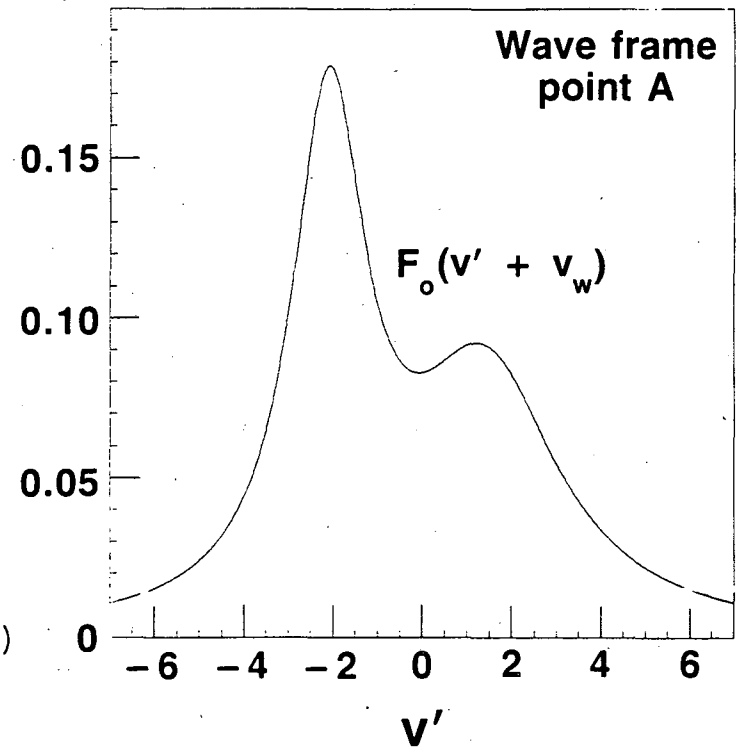

Figure (3.26a)

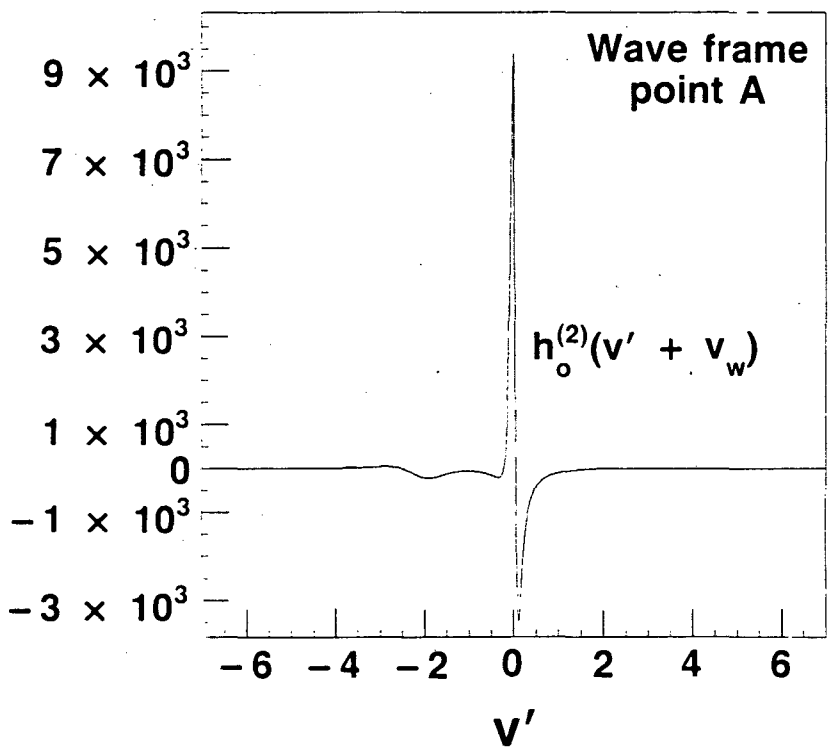

Figure (3.26b)

XBL 838-2985

Figure (3.27) The homogeneous component of the saturated distribution function showing the effect of the lowest order correction. γ is as in Fig. (3.6). Shown for point A in Fig. (3.24a) in the wave frame.

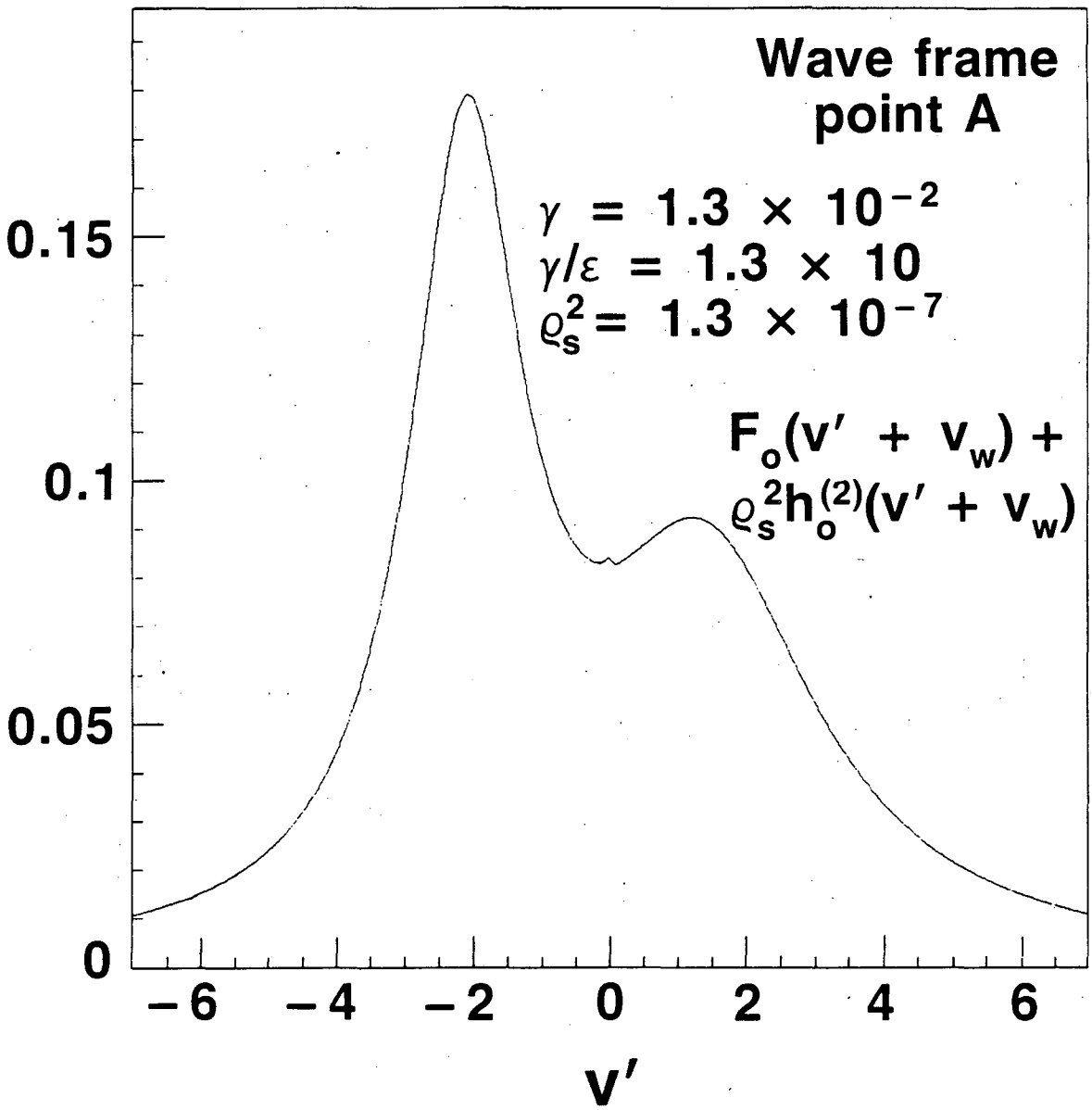

XBL 838-2979

Figure (3.27)

Figure (3.28) (a) The lowest order correction to the spatially homogeneous component of the distribution function. Shown for point B ($\delta = 2.0$, $n_b = 0.5$, $k = 0.14$, and $u \sim 8.7$) in Fig. (3.24a) in the wave frame. (b) The initial velocity distribution (dotted line), and the homogeneous component of the saturated distribution function (solid line) showing the effect of the lowest order correction. γ is as in Fig. (3.6). Shown for point B in the wave frame.

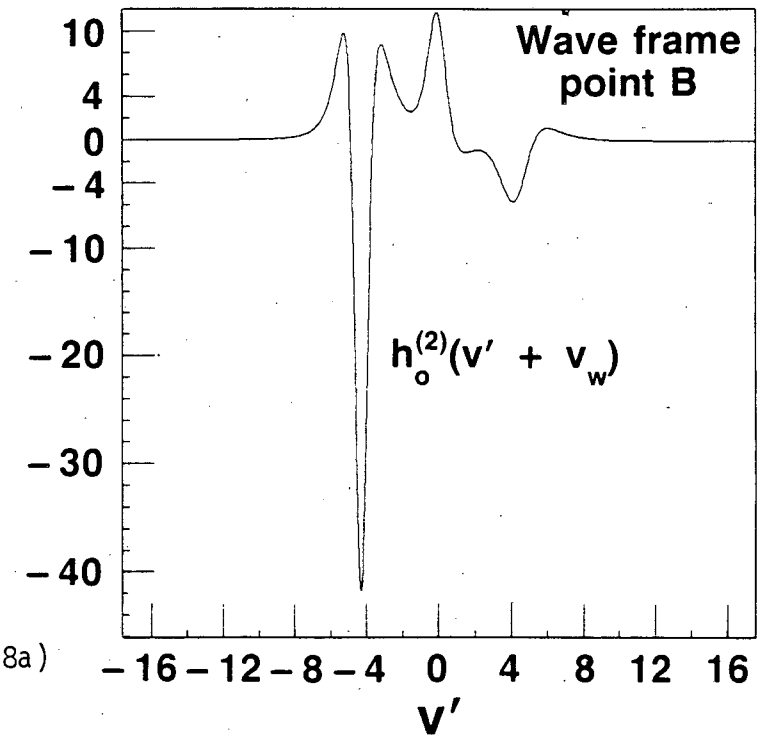

Figure (3.28a)

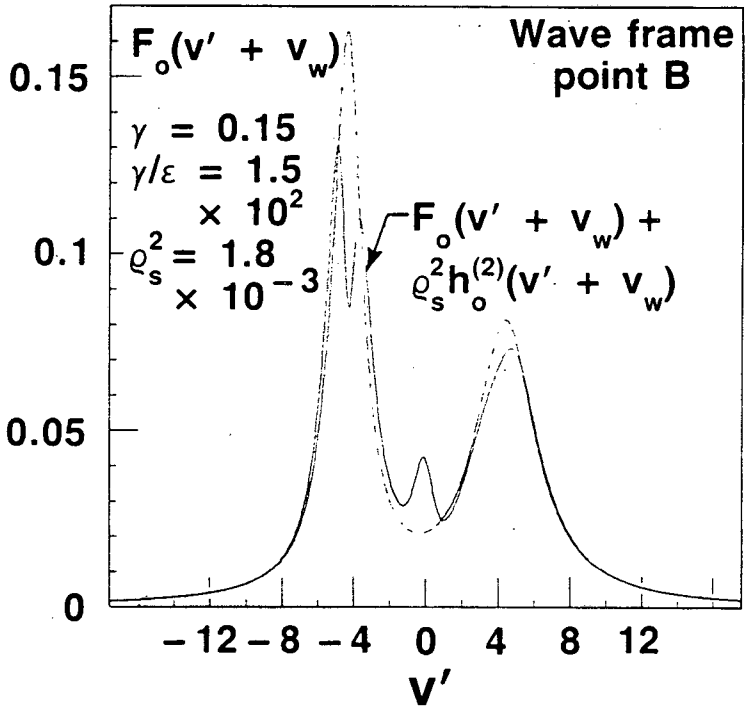

Figure (3.28b)

XBL 838-2983

Appendix

In Chapter 1 the two dimensional vector field,

$$\frac{d\varsigma}{dt} = \mathcal{V}(\varsigma) = \mathcal{V}^{(1)}(\varsigma) + \mathcal{V}^{(2)}(\varsigma) + \cdots \tag{A.1}$$

was transformed by a local nonlinear change of coordinates,

$$\eta = \Phi(\varsigma) \tag{A.2}$$

into the normal form

$$\frac{d\eta}{dt} = \mathcal{V}^{(1)}(\eta) + \sum_{k=3,5,\ldots} \Big[\tilde{\nu}_+^{(k,(k+1)/2)} \, \xi_+^{(k,(k+1)/2)}(\eta) + \tilde{\nu}_-^{(k,(k-1)/2)} \, \xi_-^{(k,(k-1)/2)}(\eta) \Big]. \tag{A.3}$$

In polar variables, this normal form vector field was

$$\begin{aligned} \frac{dr}{dt} &= \mu r + a_1 r^3 + a_2 r^5 + O(r^7) \\ \frac{d\theta}{dt} &= -\Lambda + b_1 r^2 + b_2 r^4 + O(r^6) \end{aligned} \tag{A.4}$$

where

$$a_1 = \text{Re}\ \tilde{\nu}_+^{(3,2)}$$
$$a_2 = \text{Re}\ \tilde{\nu}_+^{(5,3)}$$
$$b_1 = \text{Im}\ \tilde{\nu}_+^{(3,2)}$$
$$b_2 = \text{Im}\ \tilde{\nu}_+^{(5,3)}.$$

In this appendix, I derive the explicit relations between $\tilde{\nu}_+^{(3,2)}$, $\tilde{\nu}_+^{(5,3)}$ and the components of the original vector field $\mathcal{V}(\varsigma)$. This determines the normal form coefficients through fifth degree as functions of the parameters in the original problem. These results slightly generalize the calculation of Hassard and Wan (1978) in that the coefficients a_2 and b_2 are obtained for arbitrary μ. Other differences between the normal form coefficients derived here and those computed by Hassard and Wan (1978) are explained at the end of the appendix.

To begin, recall from Chapter 1 that in the Taylor expansion of $\mathcal{V}(\varsigma)$ the terms of degree k, denoted $\mathcal{V}^{(k)}(\varsigma)$, could be expanded in terms of the basis for $\mathcal{H}^{(k)}(\Re^2)$ formed by the eigenvectors of $L^{(k)}$.

$$\mathcal{V}^{(k)}(\varsigma) = \sum_{l=0}^{k} \left[\nu_+^{(k,l)} \xi_+^{(k,l)}(\varsigma) + \nu_-^{(k,l)} \xi_-^{(k,l)}(\varsigma) \right] \tag{A.5}$$

where

$$L^{(k)} \xi_\pm^{(k,l)} = \lambda_\pm^{(k,l)} \xi_\pm^{(k,l)}.$$

The relations between the components $\nu_\pm^{(k,l)}$ in this eigenbasis and the components of $\mathcal{V}^{(k)}(\varsigma)$ in a real basis will be given later; for the moment the eigen-

basis components $\mathcal{V}_{\pm}^{(k,l)}$ are to be regarded as known complex-valued functions of the parameters in the problem.

To remove inessential nonlinear terms, through terms of fifth degree, requires a coordinate change of the form

$$\eta = \Phi(\varsigma) = \varsigma + \phi^{(2)}(\varsigma) + \phi^{(3)}(\varsigma) + \phi^{(4)}(\varsigma) + \phi^{(5)}(\varsigma) \tag{A.6}$$

where $\phi^{(k)}(\varsigma)$ is homogeneous of degree k in ς. Now $\phi^{(4)}(\varsigma)$ removes terms of degree four and generates higher order terms, but only of degree greater than five. Similarly $\phi^{(5)}(\varsigma)$ eliminates the inessential fifth degree terms, but these terms can be identified without explicitly evaluating $\phi^{(5)}(\varsigma)$. Thus, in practice, to compute the normal form through fifth degree requires only that $\Phi(\varsigma)$ be implemented through terms of third degree, i.e. up to $\phi^{(3)}(\varsigma)$.

Calculation of the Transformed Vector Field

With this in mind the calculation of the transformed vector field (through fifth degree) is straightforward. From (A.1) and (A.6) $d\eta/dt$ is given by

$$\frac{d\eta}{dt} = D\Phi(\Phi^{-1}(\eta)) \cdot \mathcal{V}(\Phi^{-1}(\eta)). \tag{A.7}$$

To evaluate this, first determine $\Phi^{-1}(\eta)$. Let

$$\Phi^{-1}(\eta) = \eta + \psi^{(2)}(\eta) + \psi^{(3)}(\eta) + \psi^{(4)}(\eta) + \psi^{(5)}(\eta) + \cdots$$

and determine the $\psi^{(k)}(\eta)$ by solving

$$\varsigma = \Phi^{-1}(\eta). \tag{A.8}$$

Inserting η from (A.6) into each $\psi^{(k)}(\eta)$ and expanding through fifth order gives

$$\begin{aligned}
\psi^{(2)}(\varsigma + \phi^{(2)}(\varsigma) + \phi^{(3)}(\varsigma)) &= \psi^{(2)}(\varsigma) + D\psi^{(2)}(\varsigma)\cdot[\phi^{(2)}(\varsigma) + \phi^{(3)}(\varsigma)] \\
&\quad + \frac{1}{2}D^2\psi^{(2)}(\varsigma):[\phi^{(2)}(\varsigma) + \phi^{(3)}(\varsigma)][\phi^{(2)}(\varsigma) + \phi^{(3)}(\varsigma)] \\
&= \psi^{(2)}(\varsigma) + D\psi^{(2)}(\varsigma)\cdot\phi^{(2)}(\varsigma) + D\psi^{(2)}(\varsigma)\cdot\phi^{(3)}(\varsigma) \\
&\quad + \frac{1}{2}D^2\psi^{(2)}(\varsigma):\phi^{(2)}(\varsigma)\phi^{(2)}(\varsigma) + D^2\psi^{(2)}(\varsigma):\phi^{(2)}(\varsigma)\phi^{(3)}(\varsigma) \\
&\quad + \cdots \\
\psi^{(3)}(\varsigma + \phi^{(2)}(\varsigma) + \phi^{(3)}(\varsigma)) &= \psi^{(3)}(\varsigma) + D\psi^{(3)}(\varsigma)\cdot[\phi^{(2)}(\varsigma) + \phi^{(3)}(\varsigma)] \\
&\quad + \frac{1}{2}D^2\psi^{(3)}(\varsigma):\phi^{(2)}(\varsigma)\phi^{(2)}(\varsigma) + \cdots \\
&= \psi^{(3)}(\varsigma) + D\psi^{(3)}(\varsigma)\cdot\phi^{(2)}(\varsigma) + D\psi^{(3)}(\varsigma)\cdot\phi^{(3)}(\varsigma) \\
&\quad + \frac{1}{2}D^2\psi^{(3)}(\varsigma):\phi^{(2)}(\varsigma)\phi^{(2)}(\varsigma) + \cdots \\
\psi^{(4)}(\varsigma + \phi^{(2)}(\varsigma) + \phi^{(3)}(\varsigma)) &= \psi^{(4)}(\varsigma) + D\psi^{(4)}(\varsigma)\cdot\phi^{(2)}(\varsigma) + \cdots \\
\psi^{(5)}(\varsigma + \phi^{(2)}(\varsigma) + \phi^{(3)}(\varsigma)) &= \psi^{(5)}(\varsigma) + \cdots.
\end{aligned}$$

Here a notation such as $D^2\psi^{(2)}(\varsigma):\phi^{(2)}(\varsigma)\phi^{(3)}(\varsigma)$ represents a vector field whose i^{th} component is

$$\left(D^2\psi^{(2)}(\varsigma):\phi^{(2)}(\varsigma)\phi^{(3)}(\varsigma)\right)^i = \frac{\partial^2(\psi^{(2)})^i}{\partial\varsigma^j\partial\varsigma^k}(\phi^{(2)}(\varsigma))^j(\phi^{(3)}(\varsigma))^k$$

with repeated indices summed. Collecting terms of the same degree, (A.8) becomes

$$\begin{aligned}\varsigma = \varsigma &+ \left[\phi^{(2)}(\varsigma) + \psi^{(2)}(\varsigma)\right] + \left[\phi^{(3)}(\varsigma) + D\psi^{(2)}(\varsigma)\cdot\phi^{(2)}(\varsigma) + \psi^{(3)}(\varsigma)\right] \\ &+ \left[D\psi^{(2)}(\varsigma)\cdot\phi^{(3)}(\varsigma) + \frac{1}{2}D^2\psi^{(2)}(\varsigma):\phi^{(2)}(\varsigma)\phi^{(2)}(\varsigma) + D\psi^{(3)}(\varsigma)\cdot\phi^{(2)}(\varsigma)\right. \\ &\qquad \left. + \psi^{(4)}(\varsigma)\right] \\ &+ \left[D^2\psi^{(2)}(\varsigma):\phi^{(2)}(\varsigma)\phi^{(3)}(\varsigma) + D\psi^{(3)}(\varsigma)\cdot\phi^{(3)}(\varsigma)\right. \\ &\qquad \left. + \frac{1}{2}D^2\psi^{(3)}(\varsigma):\phi^{(2)}(\varsigma)\phi^{(2)}(\varsigma) + D\psi^{(4)}(\varsigma)\cdot\phi^{(2)}(\varsigma) + \psi^{(5)}(\varsigma)\right] \\ &+ \cdots.\end{aligned}$$

The $\psi^{(k)}(\varsigma)$ are determined recursively. At second order (A.8) requires

$$\psi^{(2)}(\varsigma) = -\phi^{(2)}(\varsigma) \tag{A.9}$$

as was noted previously in (1.16). Using (A.9) and (A.8) at third order gives

$$\psi^{(3)}(\varsigma) = -\phi^{(3)}(\varsigma) + D\phi^{(2)}(\varsigma)\cdot\phi^{(2)}(\varsigma). \tag{A.10}$$

With (A.9) and (A.10), $\psi^{(4)}(\varsigma)$ is

$$\psi^{(4)}(\varsigma) = D\phi^{(2)}(\varsigma)\cdot\phi^{(3)}(\varsigma) - \frac{1}{2}D^2\phi^{(2)}(\varsigma):\phi^{(2)}(\varsigma)\phi^{(2)}(\varsigma) - (D\phi^{(2)}(\varsigma))^2\cdot\phi^{(2)}(\varsigma) + D\phi^{(3)}(\varsigma)\cdot\phi^{(2)}(\varsigma). \tag{A.11}$$

Finally, after eliminating $\psi^{(2)}(\varsigma)$, $\psi^{(3)}(\varsigma)$, and $\psi^{(4)}(\varsigma)$, the result for $\psi^{(5)}(\varsigma)$ is

$$\begin{aligned}\psi^{(5)}(\varsigma) = {} & D^2\phi^{(2)}(\varsigma):[D\phi^{(2)}(\varsigma)\cdot\phi^{(2)}(\varsigma)]\phi^{(2)}(\varsigma) + \frac{1}{2}D\phi^{(2)}(\varsigma)\cdot[D^2\phi^{(2)}(\varsigma):\phi^{(2)}(\varsigma)\phi^{(2)}(\varsigma)] \\ & + (D\phi^{(2)}(\varsigma))^2\cdot[D\phi^{(2)}(\varsigma)\cdot\phi^{(2)}(\varsigma)] - \frac{1}{2}D^2\phi^{(3)}(\varsigma):\phi^{(2)}(\varsigma)\phi^{(2)}(\varsigma) \\ & - D\phi^{(3)}(\varsigma)\cdot[D\phi^{(2)}(\varsigma)\cdot\phi^{(2)}(\varsigma)] - D\phi^{(2)}(\varsigma)\cdot[D\phi^{(3)}(\varsigma)\cdot\phi^{(2)}(\varsigma)] \\ & - D^2\phi^{(2)}(\varsigma):\phi^{(2)}(\varsigma)\phi^{(3)}(\varsigma) - (D\phi^{(2)}(\varsigma))^2\cdot\phi^{(3)}(\varsigma) \\ & + D\phi^{(3)}(\varsigma)\cdot\phi^{(3)}(\varsigma).\end{aligned} \tag{A.12}$$

Equations (A.9) through (A.12) determine $\Phi^{-1}(\eta)$ through fifth degree. Returning to (A.7) for the transformed vector field, now expand $\mathcal{V}(\Phi^{-1}(\eta))$.

$$\mathcal{V}(\Phi^{-1}(\eta)) = \mathcal{V}^{(1)}(\Phi^{-1}(\eta)) + \mathcal{V}^{(2)}(\Phi^{-1}(\eta)) + \cdots + \mathcal{V}^{(5)}(\Phi^{-1}(\eta)) + \cdots \tag{A.13}$$

where

$$\mathcal{V}^{(1)}(\Phi^{-1}(\eta)) = \mathcal{V}^{(1)}(\eta) + D\mathcal{V}^{(1)}(\eta)\cdot[\psi^{(2)}(\eta) + \psi^{(3)}(\eta) + \psi^{(4)}(\eta) + \psi^{(5)}(\eta)] + \cdots$$

$$\begin{aligned}\mathcal{V}^{(2)}(\Phi^{-1}(\eta)) = {} & \mathcal{V}^{(2)}(\eta) + D\mathcal{V}^{(2)}(\eta)\cdot[\psi^{(2)}(\eta) + \psi^{(3)}(\eta) + \psi^{(4)}(\eta)] \\ & + \frac{1}{2}D^2\mathcal{V}^{(2)}(\eta):\psi^{(2)}(\eta)\psi^{(2)}(\eta) + D^2\mathcal{V}^{(2)}(\eta):\psi^{(2)}(\eta)\psi^{(3)}(\eta) + \cdots\end{aligned}$$

$$\nu^{(3)}(\Phi^{-1}(\eta)) = \nu^{(3)}(\eta) + D\nu^{(3)}(\eta)\cdot[\psi^{(2)}(\eta) + \psi^{(3)}(\eta)] + \frac{1}{2}D^2\nu^{(3)}(\eta):\psi^{(2)}(\eta)\psi^{(2)}(\eta) + \cdots$$

$$\nu^{(4)}(\Phi^{-1}(\eta)) = \nu^{(4)}(\eta) + D\nu^{(4)}(\eta)\cdot\psi^{(2)}(\eta) + \cdots$$

and

$$\nu^{(5)}(\Phi^{-1}(\eta)) = \nu^{(5)}(\eta) + \cdots.$$

Collecting terms of the same degree, (A.13) becomes

$$\begin{aligned}\nu(\Phi^{-1}(\eta)) = \nu^{(1)}(\eta) &+ \left[\nu^{(2)}(\eta) + D\nu^{(1)}(\eta)\cdot\psi^{(2)}(\eta)\right] \\ &+ \left[\nu^{(3)}(\eta) + D\nu^{(2)}(\eta)\cdot\psi^{(2)}(\eta) + D\nu^{(1)}(\eta)\cdot\psi^{(3)}(\eta)\right] \\ &+ \Big[\nu^{(4)}(\eta) + D\nu^{(3)}(\eta)\cdot\psi^{(2)}(\eta) + D\nu^{(2)}(\eta)\cdot\psi^{(3)}(\eta) \\ &\quad + \frac{1}{2}D^2\nu^{(2)}(\eta):\psi^{(2)}(\eta)\psi^{(2)}(\eta) + D\nu^{(1)}(\eta)\cdot\psi^{(4)}(\eta)\Big] \qquad \text{(A.14)} \\ &+ \Big[\nu^{(5)}(\eta) + D\nu^{(4)}(\eta)\cdot\psi^{(2)}(\eta) + D\nu^{(3)}(\eta)\cdot\psi^{(3)}(\eta) \\ &\quad + \frac{1}{2}D^2\nu^{(3)}(\eta):\psi^{(2)}(\eta)\psi^{(2)}(\eta) + D\nu^{(2)}(\eta)\cdot\psi^{(4)}(\eta) \\ &\quad + D^2\nu^{(2)}(\eta):\psi^{(2)}(\eta)\psi^{(3)}(\eta) + D\nu^{(1)}(\eta)\cdot\psi^{(5)}(\eta)\Big] + \cdots.\end{aligned}$$

Since all terms in (A.14) are at least first degree, to expand (A.7) through fifth degree requires $D\Phi(\Phi^{-1}(\eta))$ through fourth degree. From (A.6), and the form of $\Phi^{-1}(\eta)$, this expansion is

$$\begin{aligned} D\Phi(\Phi^{-1}(\eta)) &= I + D\phi^{(2)}(\Phi^{-1}(\eta)) + D\phi^{(3)}(\Phi^{-1}(\eta)) + \cdots \\ &= I + D\phi^{(2)}(\eta) + D^2\phi^{(2)}(\eta)\cdot[\psi^{(2)}(\eta) + \psi^{(3)}(\eta) + \psi^{(4)}(\eta)] \\ &\quad + D\phi^{(3)}(\eta) + D^2\phi^{(3)}(\eta)\cdot[\psi^{(2)}(\eta) + \psi^{(3)}(\eta)] \\ &\quad + \frac{1}{2}D^3\phi^{(3)}(\eta):\psi^{(2)}(\eta)\psi^{(2)}(\eta) + \cdots \end{aligned}$$

where I is the $2x2$ identity matrix. Collecting terms of the same degree yields

$$\begin{aligned} D\Phi(\Phi^{-1}(\eta)) = I &+ D\phi^{(2)}(\eta) + \left[D^2\phi^{(2)}(\eta)\cdot\psi^{(2)}(\eta) + D\phi^{(3)}(\eta)\right] \\ &+ \left[D^2\phi^{(2)}(\eta)\cdot\psi^{(3)}(\eta) + D^2\phi^{(3)}(\eta)\cdot\psi^{(2)}(\eta)\right] \\ &+ \left[D^2\phi^{(2)}(\eta)\cdot\psi^{(4)}(\eta) + D^2\phi^{(3)}(\eta)\cdot\psi^{(3)}(\eta)\right. \\ &\quad \left. + \frac{1}{2}D^3\phi^{(3)}(\eta):\psi^{(2)}(\eta)\psi^{(2)}(\eta)\right] + \cdots. \end{aligned} \tag{A.15}$$

Now left multiplying (A.14) by (A.15) and keeping only terms up to fifth degree yields the desired expansion of (A.7). After terms of the same degree have been collected this multiplication yields,

$$\begin{aligned}
\frac{d\eta}{dt} &= \nu^{(1)}(\eta) + \Big\{\nu^{(2)}(\eta) + D\nu^{(1)}(\eta)\cdot\psi^{(2)}(\eta) + D\phi^{(2)}(\eta)\cdot\nu^{(1)}(\eta)\Big\} \\
&\quad + \Big\{\nu^{(3)}(\eta) + D\nu^{(2)}(\eta)\cdot\psi^{(2)}(\eta) + D\nu^{(1)}(\eta)\cdot\psi^{(3)}(\eta) \\
&\qquad + D\phi^{(2)}(\eta)\cdot[\nu^{(2)}(\eta) + D\nu^{(1)}(\eta)\cdot\psi^{(2)}(\eta)] + D^2\phi^{(2)}(\eta):\psi^{(2)}(\eta)\nu^{(1)}(\eta) \\
&\qquad + D\phi^{(3)}(\eta)\cdot\nu^{(1)}(\eta)\Big\} \\
&\quad + \Big\{\nu^{(4)}(\eta) + D\nu^{(3)}(\eta)\cdot\psi^{(2)}(\eta) + D\nu^{(2)}(\eta)\cdot\psi^{(3)}(\eta) \\
&\qquad + \frac{1}{2}D^2\nu^{(2)}(\eta):\psi^{(2)}(\eta)\psi^{(2)}(\eta) + D\nu^{(1)}(\eta)\cdot\psi^{(4)}(\eta) \\
&\qquad + D\phi^{(2)}(\eta)\cdot[\nu^{(3)}(\eta) + D\nu^{(2)}(\eta)\cdot\psi^{(2)}(\eta) + D\nu^{(1)}(\eta)\cdot\psi^{(3)}(\eta)] \\
&\qquad + [D^2\phi^{(2)}(\eta)\cdot\psi^{(2)}(\eta) + D\phi^{(3)}(\eta)]\cdot[\nu^{(2)}(\eta) + D\nu^{(1)}(\eta)\cdot\psi^{(2)}(\eta)] \\
&\qquad + D^2\phi^{(2)}(\eta):\psi^{(3)}(\eta)\nu^{(1)}(\eta) + D^2\phi^{(3)}(\eta):\psi^{(2)}(\eta)\nu^{(1)}(\eta)\Big\} \\
&\quad + \Big\{\nu^{(5)}(\eta) + D\nu^{(4)}(\eta)\cdot\psi^{(2)}(\eta) + D\nu^{(3)}(\eta)\cdot\psi^{(3)}(\eta) \\
&\qquad + \frac{1}{2}D^2\nu^{(3)}(\eta):\psi^{(2)}(\eta)\psi^{(2)}(\eta) + D\nu^{(2)}(\eta)\cdot\psi^{(4)}(\eta) \\
&\qquad + D^2\nu^{(2)}(\eta):\psi^{(2)}(\eta)\psi^{(3)}(\eta) + D\nu^{(1)}(\eta)\cdot\psi^{(5)}(\eta) \\
&\qquad + D\phi^{(2)}(\eta)\cdot[\nu^{(4)}(\eta) + D\nu^{(3)}(\eta)\cdot\psi^{(2)}(\eta) \\
&\qquad\qquad + D\nu^{(2)}(\eta)\cdot\psi^{(3)}(\eta) + \frac{1}{2}D^2\nu^{(2)}(\eta):\psi^{(2)}(\eta)\psi^{(2)}(\eta) + D\nu^{(1)}(\eta)\cdot\psi^{(4)}(\eta)] \\
&\qquad + [D^2\phi^{(2)}(\eta)\cdot\psi^{(2)}(\eta) + D\phi^{(3)}(\eta)]\cdot[\nu^{(3)}(\eta) + D\nu^{(2)}(\eta)\cdot\psi^{(2)}(\eta) \\
&\qquad\qquad + D\nu^{(1)}(\eta)\cdot\psi^{(3)}(\eta)] \\
&\qquad + [D^2\phi^{(2)}(\eta)\cdot\psi^{(3)}(\eta) + D^2\phi^{(3)}(\eta)\cdot\psi^{(2)}(\eta)]\cdot[\nu^{(2)}(\eta) + D\nu^{(1)}(\eta)\cdot\psi^{(2)}(\eta)] \\
&\qquad + D^2\phi^{(2)}(\eta):\psi^{(4)}(\eta)\nu^{(1)}(\eta) + D^2\phi^{(3)}(\eta):\psi^{(3)}(\eta)\nu^{(1)}(\eta) \\
&\qquad + \frac{1}{2}D^3\phi^{(3)}(\eta):\psi^{(2)}(\eta)\psi^{(2)}(\eta)\nu^{(1)}(\eta)\Big\} \\
&\qquad + \cdots.
\end{aligned} \tag{A.16}$$

By fixing $\phi^{(2)}(\eta)$ and $\phi^{(3)}(\eta)$ this expression will be greatly simplified.

Determining $\phi^{(2)}(\eta)$ and $\phi^{(3)}(\eta)$

First, as described in Chapter 1, by introducing the operator $L^{(k)}$

$$L^{(k)}: \mathcal{Y}^{(k)} \to \mathcal{Y}^{(k)}$$

$$L^{(k)}(Y) \equiv DY \cdot \mathcal{V}^{(1)} - D\mathcal{V}^{(1)} \cdot Y$$

the terms of second degree in (A.16) become

$$\mathcal{V}^{(2)}(\eta) + D\mathcal{V}^{(1)}(\eta) \cdot \psi^{(2)}(\eta) + D\phi^{(2)}(\eta) \cdot \mathcal{V}^{(1)}(\eta) = \mathcal{V}^{(2)}(\eta) + L^{(2)}(\phi^{(2)}(\eta)) \quad \text{(A.17)}$$

where (A.9) for $\psi^{(2)}(\eta)$ has been used. $\phi^{(2)}(\eta)$ is uniquely determined by

$$L^{(2)}(\phi^{(2)}(\eta)) = -\mathcal{V}^{(2)}(\eta). \quad \text{(A.18)}$$

Expanding $\phi^{(2)}(\eta)$ in the eigenbasis,

$$\phi^{(2)}(\eta) = \sum_{l=0}^{2} \left[\phi_+^{(2,l)} \xi_+^{(2,l)}(\eta) + \phi_-^{(2,l)} \xi_-^{(2,l)}(\eta) \right]$$

and plugging into (A.18) using (A.5) yields

$$\phi_\pm^{(2,l)} = \frac{-\mathcal{V}_\pm^{(2,l)}}{\lambda_\pm^{(2,l)}} \quad \text{(A.19)}$$

which is a special case of (1.23). This choice for $\phi^{(2)}(\eta)$ eliminates the quadratic terms in (A.16); moreover it implies from (A.17) three identities:

$$\mathcal{V}^{(2)}(\eta) + D\mathcal{V}^{(1)}(\eta) \cdot \psi^{(2)}(\eta) + D\phi^{(2)}(\eta) \cdot \mathcal{V}^{(1)}(\eta) = 0, \quad \text{(A.20a)}$$

$$\begin{aligned} D\mathcal{V}^{(2)}(\eta) + D\mathcal{V}^{(1)}(\eta) \cdot D\psi^{(2)}(\eta) \\ + D^2\phi^{(2)}(\eta) \cdot \mathcal{V}^{(1)}(\eta) + D\phi^{(2)}(\eta) \cdot D\mathcal{V}^{(1)}(\eta) = 0, \end{aligned} \quad \text{(A.20b)}$$

and

$$D^2\mathcal{V}^{(2)}(\eta) + D\mathcal{V}^{(1)}(\eta)\cdot D^2\psi^{(2)}(\eta) + D^2\phi^{(2)}(\eta)\cdot D\mathcal{V}^{(1)}(\eta) + D^2\phi^{(2)}(\eta)\cdot D\mathcal{V}^{(1)}(\eta) = 0 \tag{A.20c}$$

where (A.20b,c) are derivatives of (A.20a). Contracting (A.20b) with $\psi^{(2)}(\eta)$ gives

$$D\mathcal{V}^{(2)}(\eta)\cdot\psi^{(2)}(\eta) + D\phi^{(2)}(\eta)\cdot D\mathcal{V}^{(1)}(\eta)\cdot\psi^{(2)}(\eta) + D^2\phi^{(2)}(\eta):\psi^{(2)}(\eta)\mathcal{V}^{(1)}(\eta) = -D\mathcal{V}^{(1)}(\eta)\cdot D\psi^{(2)}(\eta)\cdot\psi^{(2)}(\eta). \tag{A.21}$$

This identity greatly simplifies the terms of third degree in (A.16); applying (A.21) and (A.10) to these terms leads to the compact expression,

$$\{\text{Third degree terms in (A.16)}\} = \mathcal{V}^{(3)}(\eta) + D\phi^{(2)}(\eta)\cdot\mathcal{V}^{(2)}(\eta) + L^{(3)}(\phi^{(3)}(\eta)). \tag{A.22}$$

Now $\phi^{(3)}(\eta)$ is chosen to remove the inessential components of $\mathcal{V}^{(3)}(\eta) + D\phi^{(2)}(\eta)\cdot\mathcal{V}^{(2)}(\eta)$. With the expansions

$$\mathcal{V}^{(3)}(\eta) + D\phi^{(2)}(\eta)\cdot\mathcal{V}^{(2)}(\eta) = \sum_{l=0}^{3}\left[\tilde{\mathcal{V}}_+^{(3,l)}\xi_+^{(3,l)}(\eta) + \tilde{\mathcal{V}}_-^{(3,l)}\xi_-^{(3,l)}(\eta)\right]$$
$$\phi^{(3)}(\eta) = \sum_{l=0}^{3}\left[\phi_+^{(3,l)}\xi_+^{(3,l)}(\eta) + \phi_-^{(3,l)}\xi_-^{(3,l)}(\eta)\right] \tag{A.23}$$

the components of $\phi^{(3)}(\eta)$ are

$$\phi_+^{(3,l)} = \frac{-\tilde{\mathcal{V}}_+^{(3,l)}}{\lambda_+^{(3,l)}} \qquad l = 0,1,3$$
$$\phi_-^{(3,l)} = \frac{-\tilde{\mathcal{V}}_-^{(3,l)}}{\lambda_-^{(3,l)}} \qquad l = 0,2,3 \tag{A.24}$$

and $\phi_+^{(3,2)} = \phi_-^{(3,1)} = 0$. (As noted in Chapter 1, this choice for $\phi_+^{(3,2)}$, $\phi_-^{(3,1)}$ is not unique.)

With the following definition of $K^{(3)}(\eta)$

$$K^{(3)}(\eta) \equiv \tilde{\nu}_+^{(3,2)} \xi_+^{(3,2)}(\eta) + \tilde{\nu}_-^{(3,1)} \xi_-^{(3,1)}(\eta) \tag{A.25}$$

the equation satisfied by $\phi^{(3)}(\eta)$ is

$$K^{(3)}(\eta) = \mathcal{V}^{(3)}(\eta) + D\phi^{(2)}(\eta) \cdot \mathcal{V}^{(2)}(\eta) + L^{(3)}(\phi^{(3)}(\eta)). \tag{A.26}$$

Differentiating (A.26) yields identities which simplify the remaining terms of higher degree in (A.16). For X, Y arbitrary vectors these identities are

$$\begin{aligned} DK^{(3)}(\eta) \cdot X = {} & D\mathcal{V}^{(3)}(\eta) \cdot X + D^2\phi^{(2)}(\eta) : \mathcal{V}^{(2)}(\eta) X \\ & + D\phi^{(2)}(\eta) \cdot D\mathcal{V}^{(2)}(\eta) \cdot X + D^2\phi^{(3)}(\eta) : \mathcal{V}^{(1)}(\eta) X \\ & + D\phi^{(3)}(\eta) \cdot D\mathcal{V}^{(1)}(\eta) \cdot X - D\mathcal{V}^{(1)}(\eta) \cdot D\phi^{(3)}(\eta) \cdot X \end{aligned} \tag{A.27a}$$

and

$$\begin{aligned} D^2K^{(3)}(\eta) : XY = {} & D^2\mathcal{V}^{(3)}(\eta) : XY + D^2\phi^{(2)}(\eta) : [D\mathcal{V}^{(2)}(\eta) \cdot Y] X \\ & + D^2\phi^{(2)}(\eta) : [D\mathcal{V}^{(2)}(\eta) \cdot X] Y + D\phi^{(2)}(\eta) \cdot [D^2\mathcal{V}^{(2)}(\eta) : XY] \\ & + D^3\phi^{(3)}(\eta) : \mathcal{V}^{(1)}(\eta) XY + D^2\phi^{(2)}(\eta) : [D\mathcal{V}^{(1)}(\eta) \cdot Y] X \\ & + D^2\phi^{(3)}(\eta) : [D\mathcal{V}^{(1)}(\eta) \cdot X] Y \\ & - D\mathcal{V}^{(1)}(\eta) \cdot [D^2\phi^{(3)}(\eta) : XY]. \end{aligned} \tag{A.27b}$$

Here X, Y are simply placeholders to distinguish terms such as $D^2\phi^{(2)}(\eta)\!:\![D\mathcal{V}^{(2)}(\eta)Y]X$ and $D^2\phi^{(2)}(\eta)\!:\![D\mathcal{V}^{(2)}(\eta)\cdot X]Y$.

As noted previously, the terms of fourth degree are (in principle) removed by $\phi^{(4)}(\eta)$ which does not perturb the fifth degree terms. Thus the fourth order terms in (A.16) may be simply dropped, and then only the simplification of the fifth degree terms remains. First, using (A.20b) and (A.20c), derive the identities,

$$\begin{aligned} -D\mathcal{V}^{(1)}(\eta)\cdot D\psi^{(2)}(\eta)\cdot\psi^{(4)}(\eta) \;&= D\mathcal{V}^{(2)}(\eta)\cdot\psi^{(4)}(\eta) + D^2\phi^{(2)}(\eta)\!:\!\mathcal{V}^{(1)}(\eta)\psi^{(4)}(\eta) \\ &\quad + D\phi^{(2)}(\eta)\cdot D\mathcal{V}^{(1)}(\eta)\cdot\psi^{(4)}(\eta) \end{aligned} \tag{A.28a}$$

and

$$\begin{aligned} -D\mathcal{V}^{(1)}(\eta)\cdot D^2\psi^{(2)}(\eta)\!:\!\psi^{(2)}(\eta)\psi^{(3)}(\eta) \;&= D^2\mathcal{V}^{(2)}(\eta)\!:\!\psi^{(2)}(\eta)\psi^{(3)}(\eta) \\ &\quad + D^2\phi^{(2)}(\eta)\!:\![D\mathcal{V}^{(1)}(\eta)\cdot\psi^{(2)}(\eta)]\psi^{(3)}(\eta) \\ &\quad + D^2\phi^{(2)}(\eta)\!:\![D\mathcal{V}^{(1)}(\eta)\cdot\psi^{(3)}(\eta)]\psi^{(2)}(\eta). \end{aligned} \tag{A.28b}$$

The terms appearing on the right in (A.28) may be located among the fifth degree terms of (A.16); after substituting from (A.28) these fifth degree terms become

$$\begin{aligned}\{\text{Fifth degree terms of (A.16)}\} = &-D\mathcal{V}^{(1)}(\eta)\cdot D\psi^{(2)}(\eta)\cdot\psi^{(4)}(\eta)\\ &- D\mathcal{V}^{(1)}(\eta)\cdot D^2\psi^{(2)}(\eta):\psi^{(2)}(\eta)\psi^{(3)}(\eta) + \mathcal{V}^{(5)}(\eta)\\ &+ D\mathcal{V}^{(4)}(\eta)\cdot\psi^{(2)}(\eta) + D\mathcal{V}^{(3)}(\eta)\cdot\psi^{(3)}(\eta)\\ &+ \frac{1}{2}D^2\mathcal{V}^{(3)}(\eta):\psi^{(2)}(\eta)\psi^{(2)}(\eta) + D\mathcal{V}^{(1)}(\eta)\cdot\psi^{(5)}(\eta)\\ &+ D\phi^{(2)}(\eta)\cdot[\mathcal{V}^{(4)}(\eta) + D\mathcal{V}^{(3)}(\eta)\cdot\psi^{(2)}(\eta)\\ &\qquad + D\mathcal{V}^{(2)}(\eta)\cdot\psi^{(3)}(\eta)\\ &\qquad + \frac{1}{2}D^2\mathcal{V}^{(2)}(\eta):\psi^{(2)}(\eta)\psi^{(2)}(\eta)]\\ &+ D^2\phi^{(2)}(\eta):\psi^{(2)}(\eta)[\mathcal{V}^{(3)}(\eta) + D\mathcal{V}^{(2)}(\eta)\cdot\psi^{(2)}(\eta)]\\ &+ D\phi^{(3)}(\eta)\cdot[\mathcal{V}^{(3)}(\eta) + D\mathcal{V}^{(2)}(\eta)\cdot\psi^{(2)}(\eta)\\ &\qquad + D\mathcal{V}^{(1)}(\eta)\cdot\psi^{(3)}(\eta)]\\ &+ D^2\phi^{(2)}(\eta):\psi^{(3)}(\eta)\mathcal{V}^{(2)}(\eta)\\ &+ D^2\phi^{(3)}(\eta):\psi^{(2)}(\eta)[\mathcal{V}^{(2)}(\eta) + D\mathcal{V}^{(1)}(\eta)\cdot\psi^{(2)}(\eta)]\\ &+ D^2\phi^{(3)}(\eta):\psi^{(3)}(\eta)\mathcal{V}^{(1)}(\eta)\\ &+ \frac{1}{2}D^3\phi^{(3)}(\eta):\psi^{(2)}(\eta)\psi^{(2)}(\eta)\mathcal{V}^{(1)}(\eta).\end{aligned} \tag{A.29}$$

Now choosing $X = \psi^{(3)}(\eta)$ in (A.27a) and $X = Y = \psi^{(2)}(\eta)$ in (A.27b) produces the identities,

$$\begin{aligned}D\mathcal{V}^{(1)}(\eta)\cdot D\phi^{(3)}(\eta)\cdot\psi^{(3)}(\eta) + D\mathcal{K}^{(3)}(\eta)\cdot\psi^{(3)}(\eta) &= D\mathcal{V}^{(3)}(\eta)\cdot\psi^{(3)}(\eta)\\ &+ D^2\phi^{(2)}(\eta):\mathcal{V}^{(2)}(\eta)\psi^{(3)}(\eta)\\ &+ D\phi^{(2)}(\eta)\cdot D\mathcal{V}^{(2)}(\eta)\cdot\psi^{(3)}(\eta) + D^2\phi^{(3)}(\eta):\mathcal{V}^{(1)}(\eta)\psi^{(3)}(\eta)\\ &+ D\phi^{(3)}(\eta)\cdot D\mathcal{V}^{(1)}(\eta)\cdot\psi^{(3)}(\eta)\end{aligned} \tag{A.30a}$$

and

$$\frac{1}{2}\Big[D^2K^{(3)}(\eta):\psi^{(2)}(\eta)\psi^{(2)}(\eta) + D\mathcal{V}^{(1)}(\eta)\cdot[D^2\phi^{(3)}(\eta):\psi^{(2)}(\eta)\psi^{(2)}(\eta)]\Big] =$$

$$\begin{aligned}
&\frac{1}{2}D^2\mathcal{V}^{(3)}(\eta):\psi^{(2)}(\eta)\psi^{(2)}(\eta)\\
&+D^2\phi^{(2)}(\eta):[D\mathcal{V}^{(2)}(\eta)\cdot\psi^{(2)}(\eta)]\psi^{(2)}(\eta)\\
&+\frac{1}{2}D\phi^{(2)}(\eta)\cdot[D^2\mathcal{V}^{(2)}(\eta):\psi^{(2)}(\eta)\psi^{(2)}(\eta)]\\
&+\frac{1}{2}D^3\phi^{(3)}(\eta):\mathcal{V}^{(1)}(\eta)\psi^{(2)}(\eta)\psi^{(2)}(\eta)\\
&+D^2\phi^{(3)}(\eta):[D\mathcal{V}^{(1)}(\eta)\cdot\psi^{(2)}(\eta)]\psi^{(2)}(\eta).
\end{aligned} \tag{A.30b}$$

Again the terms on the right in (A.30a,b) appear in (A.29); after they are eliminated (A.29) reads,

$$\begin{aligned}
\{\text{Fifth degree terms of (A.16)}\} = D\mathcal{V}^{(1)}(\eta)\cdot[&-D\psi^{(2)}(\eta)\cdot\psi^{(4)}(\eta)\\
&-D^2\psi^{(2)}(\eta):\psi^{(2)}(\eta)\psi^{(3)}(\eta)\\
&+\psi^{(5)}(\eta)+D\phi^{(3)}(\eta)\cdot\psi^{(3)}(\eta)\\
&+\frac{1}{2}D^2\phi^{(3)}(\eta):\psi^{(2)}(\eta)\psi^{(2)}(\eta)]\\
+DK^{(3)}(\eta)\cdot\psi^{(3)}(\eta)&+\frac{1}{2}D^2K^{(3)}(\eta):\psi^{(2)}(\eta)\psi^{(2)}(\eta)\\
+\mathcal{V}^{(5)}(\eta)&+D\mathcal{V}^{(4)}(\eta)\cdot\psi^{(2)}(\eta)\\
+D\phi^{(2)}(\eta)\cdot[\mathcal{V}^{(4)}(\eta)&+D\mathcal{V}^{(3)}(\eta)\cdot\psi^{(2)}(\eta)]\\
+D\phi^{(3)}(\eta)\cdot[\mathcal{V}^{(3)}(\eta)&+D\mathcal{V}^{(2)}(\eta)\cdot\psi^{(2)}(\eta)]\\
+D^2\phi^{(2)}(\eta):\psi^{(2)}(\eta)&\mathcal{V}^{(3)}(\eta)\\
+D^2\phi^{(3)}(\eta):\psi^{(2)}(\eta)&\mathcal{V}^{(2)}(\eta)
\end{aligned} \tag{A.31}$$

where all the terms left multiplied by $D\mathcal{V}^{(1)}(\eta)$ have been grouped together;

these terms cancel identically. This can be verified by direct calculation from (A.10), (A.11), and (A.12). Thus the fifth degree terms come down to,

$$\begin{aligned}\{\text{Fifth degree terms of (A.16)}\} = {} & \mathcal{V}^{(5)}(\eta) + DK^{(3)}(\eta)\cdot\psi^{(3)}(\eta) \\ & + \frac{1}{2}D^2K^{(3)}(\eta):\psi^{(2)}(\eta)\psi^{(2)}(\eta) + D\mathcal{V}^{(4)}(\eta)\cdot\psi^{(2)}(\eta) \\ & + D\phi^{(2)}(\eta)\cdot[\mathcal{V}^{(4)}(\eta) + D\mathcal{V}^{(3)}(\eta)\cdot\psi^{(2)}(\eta)] \\ & + D^2\phi^{(2)}(\eta):\psi^{(2)}(\eta)\mathcal{V}^{(3)}(\eta) \\ & + D\phi^{(3)}(\eta)\cdot[\mathcal{V}^{(3)}(\eta) + D\mathcal{V}^{(2)}(\eta)\cdot\psi^{(2)}(\eta)] \\ & + D^2\phi^{(3)}(\eta):\psi^{(2)}(\eta)\mathcal{V}^{(2)}(\eta)\end{aligned} \tag{A.32}$$

which can be rewritten as

$$\begin{aligned}\{\text{Fifth degree terms of (A.16)}\} = {} & \mathcal{V}^{(5)}(\eta) + \frac{1}{2}D^2K^{(3)}(\eta):\phi^{(2)}(\eta)\phi^{(2)}(\eta) \\ & + DK^{(3)}(\eta)\cdot[-\phi^{(3)}(\eta) + D\phi^{(2)}(\eta)\cdot\phi^{(2)}(\eta)] \\ & - D\mathcal{V}^{(4)}(\eta)\cdot\psi^{(2)}(\eta) + D\phi^{(2)}(\eta)\cdot\mathcal{V}^{(4)}(\eta) \\ & + D\phi^{(3)}(\eta)\cdot\mathcal{V}^{(3)}(\eta) \\ & - D[D\phi^{(3)}(\eta)\cdot\mathcal{V}^{(2)}(\eta) \\ & \qquad + D\phi^{(2)}(\eta)\cdot\mathcal{V}^{(3)}(\eta)]\cdot\phi^{(2)}(\eta)\end{aligned} \tag{A.33a}$$

using (A.9) and (A.10). Now, as for the cubic terms in (A.23), the right hand side of (A.33a) is expanded in the eigenbasis

$$
\begin{aligned}
&\mathcal{V}^{(5)}(\eta) + DK^{(3)}(\eta)\cdot[-\phi^{(3)}(\eta) + D\phi^{(2)}(\eta)\cdot\phi^{(2)}(\eta)] \\
&\quad + \frac{1}{2}D^2K^{(3)}(\eta):\phi^{(2)}(\eta)\phi^{(2)}(\eta) - D\mathcal{V}^{(4)}(\eta)\cdot\psi^{(2)}(\eta) \\
&\quad + D\phi^{(2)}(\eta)\cdot\mathcal{V}^{(4)}(\eta) + D\phi^{(3)}(\eta)\cdot\mathcal{V}^{(3)}(\eta) \\
&\quad - D[D\phi^{(3)}(\eta)\cdot\mathcal{V}^{(2)}(\eta) + D\phi^{(2)}(\eta)\cdot\mathcal{V}^{(3)}(\eta)]\cdot\phi^{(2)}(\eta) \\
&\qquad\qquad = \sum_{l=0}^{5}\left[\tilde{\mathcal{V}}_+^{(5,l)}\xi_+^{(5,l)}(\eta) + \tilde{\mathcal{V}}_-^{(5,l)}\xi_-^{(5,l)}(\eta)\right]
\end{aligned}
\tag{A.33b}
$$

and all components except

$$
K^{(5)}(\eta) \equiv \tilde{\mathcal{V}}_+^{(5,3)}\xi_+^{(5,3)}(\eta) + \tilde{\mathcal{V}}_-^{(5,3)}\xi_-^{(5,3)}(\eta) \tag{A.34}
$$

will be removed by $\phi^{(5)}(\eta)$. This of course does not have to be done explicitly; the final form for (A.16) is then

$$
\frac{d\eta}{dt} = \mathcal{V}^{(1)}(\eta) + K^{(3)}(\eta) + K^{(5)}(\eta) + \cdots. \tag{A.35}
$$

Calculation of $\tilde{\mathcal{V}}_+^{(3,2)}$ and $\tilde{\mathcal{V}}_+^{(5,3)}$

The desired normal form coefficients, $\tilde{\mathcal{V}}_+^{(3,2)}$ and $\tilde{\mathcal{V}}_+^{(5,3)}$, can now be evaluated in terms of the components of $\mathcal{V}(\eta)$. To extract $\tilde{\mathcal{V}}_+^{(3,2)}$ from (A.23) requires the $\xi_+^{(3,2)}$ component of $D\phi^{(2)}(\eta)\cdot\mathcal{V}^{(2)}(\eta)$. To expand $D\phi^{(2)}(\eta)\cdot\mathcal{V}^{(2)}(\eta)$ in the eigenbasis involves the expansion of products such as $D\xi_\pm^{(k,l)}\cdot\xi_\pm^{(k',l')}$.

The calculation of $D\xi_+^{(k,l)} \cdot \xi_+^{(k',l')}$ is representative. From the definitions in Chapter 1, see (1.22),

$$\begin{aligned} D\xi_+^{(k,l)} \cdot \xi_+^{(k',l')} &= \begin{pmatrix} lz^{l-1}(\bar{z})^{k-l} & (k-l)z^l(\bar{z})^{k-l-1} \\ 0 & 0 \end{pmatrix} \begin{pmatrix} z^{l'}(\bar{z})^{k'-l'} \\ 0 \end{pmatrix} \\ &= \begin{pmatrix} lz^{l+l'-1}(\bar{z})^{k+k'-(l+l')} \\ 0 \end{pmatrix} \\ &= l\xi_+^{(k+k'-1,l+l'-1)} \end{aligned}$$

Similar calculations yield the useful relations

$$\begin{aligned} D\xi_\pm^{(k,l)} \cdot \xi_+^{(k',l')} &= l\xi_\pm^{(k+k'-1,l+l'-1)} \\ D\xi_\pm^{(k,l)} \cdot \xi_-^{(k',l')} &= (k-l)\xi_\pm^{(k+k'-1,l+l')} \end{aligned} \tag{A.36}$$

and

$$\begin{aligned} D^2\xi_\pm^{(k,l)} : \xi_+^{(k',l')}\xi_+^{(k'',l'')} &= l(l-1)\xi_\pm^{(K-2,L-2)} \\ D^2\xi_\pm^{(k,l)} : \xi_+^{(k',l')}\xi_-^{(k'',l'')} &= l(k-l)\xi_\pm^{(K-2,L-1)} \\ D^2\xi_\pm^{(k,l)} : \xi_-^{(k',l')}\xi_-^{(k'',l'')} &= (k-l)(k-l-1)\xi_\pm^{(K-2,L)} \end{aligned} \tag{A.37}$$

where $L = l + l' + l''$ and $K = k + k' + k''$.

Applying (A.36) to (A.23), gives explicit results for $\tilde{\nu}_+^{(3,l)}$ (note that $\tilde{\nu}_-^{(3,l)}$ may be obtained from $\tilde{\nu}_+^{(3,l)} = \overline{\tilde{\nu}_-^{(3,3-l)}}$),

$$\begin{aligned}
\nu^{(3)}(\eta) + D\phi^{(2)}(\eta)\cdot\nu^{(2)}(\eta) &= \sum_{j=0}^{3}\nu_+^{(3,j)}\xi_+^{(3,j)}(\eta) \\
&\quad + \left(\sum_{l=0}^{2}\phi_+^{(2,l)}D\xi_+^{(2,l)}(\eta)\right)\cdot\left(\sum_{l'=0}^{2}\left[\nu_+^{(2,l')}\xi_+^{(2,l')}(\eta)\right.\right. \\
&\qquad \left.\left. + \nu_-^{(2,l')}\xi_-^{(2,l')}(\eta)\right]\right) \\
&= \sum_{j=0}^{3}\nu_+^{(3,j)}\xi_+^{(3,j)}(\eta) \\
&\quad + \sum_{l,l'=0}^{2}\left[l\phi_+^{(2,l)}\nu_+^{(2,l')}\xi_+^{(3,l+l'-1)}(\eta)\right. \\
&\qquad \left. + (2-l)\phi_+^{(2,l)}\nu_-^{(2,l')}\xi_+^{(3,l+l')}(\eta)\right] \\
&\quad + \cdots.
\end{aligned}$$

Hence from (A.23),

$$\begin{aligned}
\tilde{\nu}_+^{(3,0)} &= \nu_+^{(3,0)} + \phi_+^{(2,1)}\nu_+^{(2,0)} + 2\phi_+^{(2,0)}\nu_-^{(2,0)} \\
\tilde{\nu}_+^{(3,1)} &= \nu_+^{(3,1)} + \phi_+^{(2,1)}(\nu_+^{(2,1)} + \nu_-^{(2,0)}) \\
&\quad + 2(\phi_+^{(2,2)}\nu_+^{(2,0)} + \phi_+^{(2,0)}\nu_-^{(2,1)}) \\
\tilde{\nu}_+^{(3,2)} &= \nu_+^{(3,2)} + \phi_+^{(2,1)}(\nu_+^{(2,2)} + \nu_-^{(2,1)}) \\
&\quad + 2(\phi_+^{(2,2)}\nu_+^{(2,1)} + \phi_+^{(2,0)}\nu_-^{(2,2)}) \\
\tilde{\nu}_+^{(3,3)} &= \nu_+^{(3,3)} + \phi_+^{(2,1)}\nu_-^{(2,2)} + 2\phi_+^{(2,2)}\nu_+^{(2,2)}.
\end{aligned} \tag{A.38}$$

This result for $\tilde{\mathcal{V}}_+^{(3,2)}$ quite generally expresses the normal form coefficients a_1 and b_1 (see (A.4)) in terms of the quadratic and cubic terms of $\mathcal{V}(\eta)$. The other components in (A.38) determine $\phi^{(3)}(\eta)$ through (A.24).

A similar evaluation of $\tilde{\mathcal{V}}_+^{(5,3)}$ from (A.33b) is more painful; listed below are the contributions of each term on the left hand side of (A.33b).

$$\mathcal{V}^{(5)}(\eta) = \mathcal{V}_+^{(5,3)} \xi_+^{(5,3)}(\eta) + \cdots \tag{A.39a}$$

$$DK^{(3)}(\eta) \cdot \phi^{(3)}(\eta) = \tilde{\mathcal{V}}_+^{(3,2)} (2\phi_+^{(3,0)} + \phi_-^{(3,1)}) \xi_+^{(5,3)}(\eta) + \cdots \tag{A.39b}$$

$$\begin{aligned} DK^{(3)}(\eta) \cdot D\phi^{(2)}(\eta) \cdot \phi^{(2)}(\eta) = 3\tilde{\mathcal{V}}_+^{(3,2)} \Big[& 2(\phi_+^{(2,2)} \phi_+^{(2,1)} + \phi_-^{(2,2)} \phi_+^{(2,0)}) \\ & + \phi_-^{(2,1)} \phi_+^{(2,1)} + \phi_-^{(2,1)} \phi_-^{(2,0)} \Big] \xi_+^{(5,3)}(\eta) \\ & + \cdots \end{aligned} \tag{A.39c}$$

$$\frac{1}{2}D^2K^{(3)}(\eta):\phi^{(2)}(\eta)\phi^{(2)}(\eta) = 2\tilde{\nu}_+^{(3,2)}\Big[\phi_+^{(2,2)}\phi_+^{(2,1)} + \phi_+^{(2,2)}\phi_-^{(2,0)} + \phi_+^{(2,1)}\phi_-^{(2,1)} + \phi_+^{(2,0)}\phi_-^{(2,2)}\Big]\xi_+^{(5,3)}(\eta) + \cdots \tag{A.39d}$$

$$D\nu^{(4)}(\eta)\cdot\phi^{(2)}(\eta) = \Big[4\nu_+^{(4,4)}\phi_+^{(2,0)} + \nu_+^{(4,3)}(3\phi_+^{(2,1)} + \phi_-^{(2,0)}) + 2\nu_+^{(4,2)}(\phi_+^{(2,2)} + \phi_-^{(2,1)}) + 3\nu_+^{(4,1)}\phi_-^{(2,2)}\Big]\xi_+^{(5,3)}(\eta) + \cdots \tag{A.39e}$$

$$D\phi^{(2)}(\eta)\cdot\nu^{(4)}(\eta) = \Big[2(\phi_+^{(2,2)}\nu_+^{(4,2)} + \phi_+^{(2,0)}\nu_-^{(4,3)}) + \phi_+^{(2,1)}(\nu_+^{(4,3)} + \nu_-^{(4,2)})\Big]\xi_+^{(5,3)}(\eta) + \cdots \tag{A.39f}$$

$$D\phi^{(3)}(\eta)\cdot\nu^{(3)}(\eta) = \Big[3(\phi_+^{(3,3)}\nu_+^{(3,1)} + \phi_+^{(3,0)}\nu_-^{(3,3)}) + \phi_+^{(3,2)}(2\nu_+^{(3,2)} + \nu_-^{(3,1)}) + \phi_+^{(3,1)}(\nu_+^{(3,3)} + 2\nu_-^{(3,2)})\Big]\xi_+^{(5,3)}(\eta) + \cdots \tag{A.39g}$$

and finally,

$$
\begin{aligned}
&D(D\phi^{(3)}(\eta)\cdot\nu^{(2)}(\eta)+D\phi^{(2)}(\eta)\cdot\nu^{(3)}(\eta))\cdot\phi^{(2)}(\eta)\\
&\quad=\Big\{3\phi_+^{(3,0)}\Big[2(\nu_-^{(2,2)}\phi_+^{(2,2)}+\nu_-^{(2,2)}\phi_-^{(2,1)})+3\nu_-^{(2,1)}\phi_-^{(2,2)}\Big]\\
&\qquad+\phi_+^{(3,1)}\Big[2(\nu_+^{(2,2)}\phi_+^{(2,2)}+\nu_+^{(2,2)}\phi_-^{(2,1)}+\nu_-^{(2,2)}\phi_-^{(2,0)})+3\nu_+^{(2,1)}\phi_-^{(2,2)}\\
&\qquad\quad+4(\nu_-^{(2,1)}\phi_+^{(2,2)}+\nu_-^{(2,1)}\phi_-^{(2,1)})+6(\nu_-^{(2,2)}\phi_+^{(2,1)}+\nu_-^{(2,0)}\phi_-^{(2,2)})\Big]\\
&\qquad+\phi_+^{(3,2)}\Big[\nu_-^{(2,1)}\phi_-^{(2,0)}+2(\nu_-^{(2,0)}\phi_-^{(2,1)}+\nu_-^{(2,0)}\phi_+^{(2,0)}+\nu_+^{(2,2)}\phi_-^{(2,0)})\\
&\qquad\quad+3\nu_-^{(2,1)}\phi_+^{(2,1)}+4(\nu_-^{(2,2)}\phi_+^{(2,0)}+\nu_+^{(2,1)}\phi_-^{(2,1)}+\nu_+^{(2,1)}\phi_+^{(2,2)})\\
&\qquad\quad+6(\nu_+^{(2,0)}\phi_-^{(2,2)}+\nu_+^{(2,2)}\phi_+^{(2,1)})\Big]\\
&\qquad+3\phi_+^{(3,3)}\Big[\nu_+^{(2,1)}\phi_-^{(2,0)}+2(\nu_+^{(2,0)}\phi_-^{(2,1)}+\nu_+^{(2,0)}\phi_+^{(2,2)})\\
&\qquad\quad+3\nu_+^{(2,1)}\phi_+^{(2,1)}+4\nu_+^{(2,2)}\phi_+^{(2,0)}\Big]\\
&\qquad+2\phi_+^{(2,0)}\Big[\nu_-^{(3,3)}\phi_-^{(2,0)}+2(\nu_-^{(3,2)}\phi_-^{(2,1)}+\nu_-^{(3,2)}\phi_+^{(2,2)})\\
&\qquad\quad+3(\nu_-^{(3,1)}\phi_-^{(2,0)}+\nu_-^{(3,3)}\phi_+^{(2,1)})\Big]\\
&\qquad+\phi_+^{(2,1)}\Big[\nu_-^{(3,2)}\phi_-^{(2,0)}+\nu_+^{(3,3)}\phi_-^{(2,0)}+2(\nu_-^{(3,1)}\phi_-^{(2,1)}+\nu_-^{(3,1)}\phi_+^{(2,2)}\\
&\qquad\quad+\nu_+^{(3,2)}\phi_-^{(2,1)}+\nu_+^{(3,2)}\phi_+^{(2,2)})+3(\nu_-^{(3,0)}\phi_-^{(2,2)}+\nu_-^{(3,2)}\phi_+^{(2,1)}\\
&\qquad\quad+\nu_+^{(3,1)}\phi_-^{(2,2)}+\nu_+^{(3,3)}\phi_+^{(2,1)})+4\nu_-^{(3,3)}\phi_+^{(2,0)}\Big]\\
&\qquad+2\phi_+^{(2,2)}\Big[\nu_+^{(3,2)}\phi_-^{(2,0)}+2(\nu_+^{(3,1)}\phi_-^{(2,1)}+\nu_+^{(3,1)}\phi_+^{(2,2)})\\
&\qquad\quad+3(\nu_+^{(3,0)}\phi_-^{(2,2)}+\nu_+^{(3,2)}\phi_+^{(2,1)})+4\nu_+^{(3,3)}\phi_-^{(2,0)}\Big]\Big\}\xi_+^{(5,3)}(\eta)\\
&\qquad+\cdots.
\end{aligned}
\tag{A.39h}
$$

By reexpressing $\phi_{\pm}^{(k,l)}$ in terms of $\mathcal{V}_{\pm}^{(k,l)}$ these formulas can be compressed somewhat, but basically they are lengthy because of their generality. In applications they are most easily left in approximately this form, and evaluated numerically. This completes the calculation of $\tilde{\mathcal{V}}_{+}^{(3,2)}$ and $\tilde{\mathcal{V}}_{+}^{(5,3)}$ in terms of the components of the original vector field, $\mathcal{V}_{\pm}^{(k,l)}$.

These components however are relative to the eigenbasis, and the center manifold vector field is frequently obtained in a real basis. A final (though practical) chore is to relate the components of the two bases.

Change of Basis Formulas

At second order $\mathcal{V}^{(2)}(\zeta)$ in (A.1) has the form

$$\mathcal{V}^{(2)}(\zeta) = \begin{pmatrix} M_{11}x^2 + M_{12}xy + M_{13}y^2 \\ M_{21}x^2 + M_{22}xy + M_{23}y^2 \end{pmatrix}$$

in the real basis for $\mathcal{H}^{(2)}(\mathfrak{R}^2)$:

$$\begin{pmatrix} x^2 \\ 0 \end{pmatrix}, \begin{pmatrix} y^2 \\ 0 \end{pmatrix}, \begin{pmatrix} xy \\ 0 \end{pmatrix}, \begin{pmatrix} 0 \\ x^2 \end{pmatrix}, \begin{pmatrix} 0 \\ y^2 \end{pmatrix}, \begin{pmatrix} 0 \\ xy \end{pmatrix}.$$

It is a straightforward calculation to express these basis vectors in terms of the eigenbasis $\{\xi_{\pm}^{(2,l)}\}_{l=0}^{2}$, then re-expand $\mathcal{V}^{(2)}(\zeta)$ to determine the $\mathcal{V}_{\pm}^{(2,l)}$ in terms of the M_{ij}.

$$\begin{aligned} \mathcal{V}_{+}^{(2,0)} &= m_1 + im_2 = \overline{\mathcal{V}_{-}^{(2,2)}} \\ \mathcal{V}_{+}^{(2,1)} &= m_3 + im_4 = \overline{\mathcal{V}_{-}^{(2,1)}} \\ \mathcal{V}_{+}^{(2,2)} &= m_5 + im_6 = \overline{\mathcal{V}_{-}^{(2,0)}} \end{aligned} \tag{A.40a}$$

where

$$m_1 = \frac{1}{4}(M_{11} - M_{13} - M_{22})$$
$$m_2 = \frac{1}{4}(M_{12} + M_{21} - M_{23})$$
$$m_3 = \frac{1}{2}(M_{11} + M_{13})$$
$$m_4 = \frac{1}{2}(M_{21} + M_{23})$$
$$m_5 = \frac{1}{4}(M_{11} - M_{13} + M_{22})$$
$$m_6 = \frac{1}{4}(M_{21} - M_{12} - M_{23}).$$

At third order for

$$\nu^{(3)}(\zeta) = \begin{pmatrix} M_{11}x^3 + M_{12}x^2y + M_{13}xy^2 + M_{14}y^3 \\ M_{21}x^3 + M_{22}x^2y + M_{23}xy^2 + M_{24}y^3 \end{pmatrix}$$

the eigenbasis components are

$$\nu_+^{(3,0)} = m_1 + im_2 = \overline{\nu_-^{(3,3)}}$$
$$\nu_+^{(3,1)} = m_3 + im_4 = \overline{\nu_-^{(3,2)}}$$
$$\nu_+^{(3,2)} = m_5 + im_6 = \overline{\nu_-^{(3,1)}}$$
$$\nu_+^{(3,3)} = m_7 + im_8 = \overline{\nu_-^{(3,0)}}$$

where

$$
\begin{aligned}
m_1 &= \frac{1}{8}(M_{11} + M_{24} - M_{13} - M_{22}) \\
m_2 &= \frac{1}{8}(M_{21} - M_{14} - M_{23} + M_{12}) \\
m_3 &= \frac{1}{8}(3(M_{11} - M_{24}) + M_{13} - M_{22}) \\
m_4 &= \frac{1}{8}(3(M_{21} + M_{14}) + M_{23} + M_{12}) \\
m_5 &= \frac{1}{8}(3(M_{11} + M_{24}) + M_{13} + M_{22}) \\
m_6 &= \frac{1}{8}(3(M_{21} - M_{14}) + M_{23} - M_{12}) \\
m_7 &= \frac{1}{8}(M_{11} - M_{24} - M_{13} + M_{22}) \\
m_8 &= \frac{1}{8}(M_{21} + M_{14} - M_{23} - M_{12}).
\end{aligned}
$$

At fourth order for

$$
\nu^{(4)}(\varsigma) = \begin{pmatrix} M_{11}x^4 + M_{12}x^3y + M_{13}x^2y^2 + M_{14}xy^3 + M_{15}y^4 \\ M_{21}x^4 + M_{22}x^3y + M_{23}x^2y^2 + M_{24}xy^3 + M_{25}y^4 \end{pmatrix}
$$

$$
\begin{aligned}
\nu_+^{(4,4)} &= m_1 + im_2 = \overline{\nu_-^{(4,0)}} \\
\nu_+^{(4,3)} &= m_3 + im_4 = \overline{\nu_-^{(4,1)}} \\
\nu_+^{(4,2)} &= m_5 + im_6 = \overline{\nu_-^{(4,2)}} \\
\nu_+^{(4,1)} &= m_7 + im_8 = \overline{\nu_-^{(4,3)}} \\
\nu_+^{(4,0)} &= m_9 + im_{10} = \overline{\nu_-^{(4,4)}}
\end{aligned}
\qquad \text{(A.40c)}
$$

where

$$
\begin{aligned}
m_1 &= \frac{1}{16}(M_{11} - M_{13} + M_{15} + M_{22} - M_{24}) \\
m_2 &= \frac{1}{16}(-M_{12} + M_{14} + M_{21} - M_{23} + M_{25}) \\
m_3 &= \frac{1}{16}(4(M_{11} - M_{15}) + 2(M_{22} + M_{24})) \\
m_4 &= \frac{1}{16}(-2(M_{12} + M_{14}) + 4(M_{21} - M_{25})) \\
m_5 &= \frac{1}{16}(6(M_{11} + M_{15}) + 2M_{13}) \\
m_6 &= \frac{1}{16}(6(M_{21} + M_{25}) + 2M_{23}) \\
m_7 &= \frac{1}{16}(4(M_{11} - M_{15}) - 2(M_{22} + M_{24})) \\
m_8 &= \frac{1}{16}(2(M_{12} + M_{14}) + 4(M_{21} - M_{25})) \\
m_9 &= \frac{1}{16}(M_{11} - M_{13} + M_{15} - M_{22} + M_{24}) \\
m_{10} &= \frac{1}{16}(M_{12} - M_{14} + M_{21} - M_{23} + M_{25}),
\end{aligned}
$$

and at fifth order

$$
\nu^{(5)}(\varsigma) = \begin{pmatrix} M_{11}x^5 + M_{12}x^4y + M_{13}x^3y^2 + M_{14}x^2y^3 + M_{15}xy^4 + M_{16}y^5 \\ M_{21}x^5 + M_{22}x^4y + M_{23}x^3y^2 + M_{24}x^2y^3 + M_{25}xy^4 + M_{26}y^5 \end{pmatrix}
$$

$$
\begin{aligned}
\nu_+^{(5,5)} &= m_1 + im_2 = \overline{\nu_-^{(5,0)}} \\
\nu_+^{(5,4)} &= m_3 + im_4 = \overline{\nu_-^{(5,1)}} \\
\nu_+^{(5,3)} &= m_5 + im_6 = \overline{\nu_-^{(5,2)}} \\
\nu_+^{(5,2)} &= m_7 + im_8 = \overline{\nu_-^{(5,3)}} \\
\nu_+^{(5,1)} &= m_9 + im_{10} = \overline{\nu_-^{(5,4)}} \\
\nu_+^{(5,0)} &= m_{11} + im_{12} = \overline{\nu_-^{(5,5)}}
\end{aligned}
\qquad \text{(A.40d)}
$$

where

$$m_1 = \frac{1}{32}(M_{11} - M_{13} + M_{15} + M_{22} - M_{24} + M_{26})$$

$$m_2 = \frac{1}{32}(-M_{12} + M_{14} - M_{16} + M_{21} - M_{23} + M_{25})$$

$$m_3 = \frac{1}{32}(5M_{11} - 3M_{15} - M_{13} - 5M_{26} + 3M_{22} + M_{24})$$

$$m_4 = \frac{1}{32}(5M_{16} - 3M_{12} - M_{14} + 5M_{21} - 3M_{25} - M_{23})$$

$$m_5 = \frac{1}{32}(10M_{11} + 2(M_{13} + M_{15}) + 10M_{26} + 2(M_{22} + M_{24}))$$

$$m_6 = \frac{1}{32}(-10M_{16} - 2(M_{12} + M_{14}) + 10M_{21} + 2(M_{23} + M_{25}))$$

$$m_7 = \frac{1}{32}(10M_{11} + 2(M_{13} + M_{15}) - 10M_{26} - 2(M_{22} + M_{24}))$$

$$m_8 = \frac{1}{32}(10M_{16} + 2(M_{12} + M_{14}) + 10M_{21} + 2(M_{23} + M_{25}))$$

$$m_9 = \frac{1}{32}(5M_{11} - 3M_{15} - M_{13} + 5M_{26} - 3M_{22} - M_{24})$$

$$m_{10} = \frac{1}{32}(-5M_{16} + 3M_{12} + M_{14} + 5M_{21} - 3M_{25} - M_{23})$$

$$m_{11} = \frac{1}{32}(M_{11} - M_{13} + M_{15} - M_{22} - M_{26} + M_{24})$$

$$m_{12} = \frac{1}{32}(M_{12} - M_{14} + M_{16} + M_{21} - M_{23} + M_{25}).$$

Now from (A.40a-d) the complex components of $\mathcal{V}(\varsigma)$ through fifth degree are computable, and from the complex components, using (A.38) and (A.39), the normal form coefficients through fifth degree are computable.

Final Remarks

If the result for $\tilde{\mathcal{V}}_+^{(3,2)}$ in (A.38) is compared to the equivalent result in Hassard, Kazarinoff, and Wan (1981) (see pages 86-90 of Hassard, Kazarinoff, and Wan) there is disagreement for $\mu \neq 0$; away from criticality the lowest order normal form coefficients differ. This can be traced to differing choices for the components $\phi_+^{(3,2)}$ and $\phi_-^{(3,1)}$ of the coordinate change. In (A.24) of my calculation these components were set to zero; however Hassard et al. (1981) adopt a different choice, namely,

$$\phi_+^{(3,2)} = 3\phi_+^{(2,2)}\phi_+^{(2,1)} + 2\phi_+^{(2,0)}\phi_-^{(2,2)} + \phi_+^{(2,1)}\phi_-^{(2,1)} = \overline{\phi_-^{(3,1)}}$$

which alters the form of $\tilde{\mathcal{V}}_+^{(3,2)}$ for $\mu \neq 0$.

The practical consequence of this is simply to remind us that the normal form results tend to mix different orders of the parameter $\sqrt{\mu}$. For example in the expression for the Hopf frequency $d\theta/dt = -\Lambda + b_1 r_0^2 + b_2 r_0^4 + \cdots$, since $r_0^2 \sim O(\mu)$, both $b_1 r_0^2$ and $b_2 r_0^4$ contain contributions of $O(\mu^2)$. In effect, different choices for the component $\phi_+^{(3,2)}$ will alter the way the $O(\mu^2)$ contribution is divided between these two terms. A similar remark holds for higher order normal form terms and higher order corrections in μ^2 as well.

References

Abraham, R. and J. Marsden. 1978. *Foundations of Mechanics*. 2nd ed. Addison-Wesley, Reading, Mass.

Armstrong, T.P. and D. Montgomery. 1969. Numerical Study of Weakly Unstable Electron Plasma Oscillations, Phys. Fluids, **12**, 2094.

Arnol'd, V.I. 1972. Lectures on bifurcations in versal families, Russ. Math Surveys, **27**, 54.

Arnol'd, V.I. 1973. *Ordinary Differential Equations*. MIT Press, Cambridge, Mass.

Arthur, M.D., W. Greenberg, and P.F. Zweifel. 1977. Vlasov theory of plasma oscillations: Linear approximation, Phys. Fluids, **20**, 1296.

Broer, H. 1981. Formal normal form theorems for vector fields and some consequences for bifurcations in the volume preserving case, Springer Lec. Notes in Math., **898**, 54.

Bussac, M.N. 1982. Asymptotic Solutions of the Nonlinear Three-Wave System, Phys. Rev. Lett., **49**, 1939.

Carr, J. 1981. *Applications of Centre Manifold Theory*, Applied Mathematical Sciences, Vol. **35**, Springer, Berlin.

Cary, J. 1981. Lie Transform Perturbation Theory for Hamiltonian Systems,

Physics Reports, **79**, 129.

Cary, J. and A. Kaufman. 1981. Ponderomotive effects in collisionless plasma: A Lie transform approach, Phys. Fluids, **24**, 1238.

Case, K.M. 1959. Plasma Oscillations, Ann. Phys., **7**, 349.

Case, K.M. 1978. Plasma Oscillations, Phys. Fluids, **21**, 249.

Chen, F.F. 1974. ***Introduction to Plasma Physics.*** Plenum Press, New York.

Chow, S.N. and J. Mallet-Paret. 1977. Integral averaging and bifurcation, J. Diff. Eqns., **26**, 112.

Chow, S.N. and J.K. Hale. 1982. ***Methods of Bifurcation Theory.*** Springer-Verlag, New York.

Davidson, R.C. 1972. ***Methods in Nonlinear Plasma Theory.*** Academic Press, New York.

Feigenbaum, M. 1980. Universal Behavior in Nonlinear Systems, Los Alamos Science, Summer, 4.

Fenichel, N. 1979. Geometric Singular Perturbation Theory for Ordinary Differential Equations, J. Diff. Eqns., **31**, 53.

Galeev, A.A. and R.Z. Sagdeev. 1978. Nonlinear Plasma Theory, ***Reviews of Plasma Physics***, Vol. **7**, Plenum, New York.

Golubitsky, M. and W.F. Langford. 1981. Classification and Unfoldings of

Degenerate Hopf Bifurcations, J. Diff. Eqns., **41**, 375.

Guckenheimer, J. 1981. On a codimension two bifurcation, Springer Lec. Notes in Math., **898**, 99.

Guckenheimer, J. 1984. Multiple Bifurcation Problems of Codimension Two, Siam J. Math. Analysis, in press.

Guckenheimer, J. and P. Holmes. 1983. ***Nonlinear Oscillations, Dynamical Systems and Bifurcations of Vector Fields***, Springer Applied Math. Sciences, Vol. **43**.

Hassard, B.D. and Y-H. Wan. 1978. Bifurcation formulae derived from center manifold theory, J. Math. Anal. Appl., **63**, 297.

Hassard, B.D., N.D. Kazarinoff, and Y-H. Wan. 1981. ***Theory and Applications of Hopf Bifurcation***, London Math. Soc. Lec. Notes, Vol. **41**.

Hohenberg, P. and B. Halperin. 1977. Theory of dynamic critical phenomena, Rev. Mod. Phys., **49**, 435.

Holmes, P.J. 1981. Center Manifolds, Normal Forms, and Bifurcations of Vector Fields with Applications to Coupling Between Periodic and Steady Motions, Physica, **2D**, 449.

Holmes, P.J. and J. Marsden. 1978. Bifurcation to divergence and flutter in flow-induced oscillations: an infinite dimensional analysis, Automatica, **14**, 367.

Iooss, G. and D.D. Joseph. 1980. *Elementary Stability and Bifurcation Theory.* Springer-Verlag, Berlin.

Jordan, D. and P. Smith. 1977. *Nonlinear Ordinary Differential Equations.* Oxford University Press, Oxford.

Kelley, A. 1967. The stable, center stable, center, center unstable, and unstable manifolds, J. Diff. Eqns., **3**, 546.

Knobloch, E. and M.R.E. Proctor. 1981. Nonlinear Periodic Convection in Double Diffusive Systems, J. Fluid Mech., **108**, 291.

Krall, N. and A.W. Trivelpiece. 1973. *Principles of Plasma Physics.* McGraw-Hill, New York.

Langford, W.F. 1979. Periodic and Steady-State Mode Interactions Lead to Tori, Siam J. Appl. Math., **37**, 22.

Littlejohn, R. 1979. A guiding center Hamiltonian: A new approach, J. Math. Phys., **20**, 2445.

Marsden, J. and M. McCracken. 1976. *The Hopf Bifurcation and its Applications*, Springer Applied Math. Sciences, Vol. **19**.

Marsden J. and A. Weinstein. 1982. The Hamiltonian structure of the Maxwell-Vlasov equations, Physica, **4D**, 394.

McLaughlin, J.B. 1981. Period-Doubling Bifurcations and Chaotic Motion for a Parametrically Forced Pendulum, J. Stat. Phys., **24**, 375.

Meunier, C., M.N. Bussac, and G. Laval. 1982. Intermittency at the Onset of Stochasticity in Nonlinear Resonant Coupling Processes, Physica, **4D**, 236.

Meyer K.R. and D.S. Schmidt. 1971. Periodic Orbits near L_4 for Mass Ratios near the Critical Mass Ratio of Routh, Celest. Mech., **4**, 99.

Morrison, P. 1980. The Maxwell-Vlasov equations as a continuous Hamiltonian System, Phys. Lett., **80A**, 383.

Newell, A.C. 1979. Bifurcation and Nonlinear Focusing, Proceedings of the International Symposium on Synergetics, Schloss Elmau, 244.

Newell, A.C. and J.A. Whitehead. 1969. Finite bandwidth, finite amplitude convection,J. Fluid Mech., **38**, 279.

O'Neil, T. and J. Malmberg. 1968. Transition of the Dispersion Roots from Beam-Type to Landau-Type Solutions, Phys. Fluids, **11**, 1754.

Palis, J. and W. de Melo. 1982. *Geometric Theory of Dynamical Systems: An Introduction.* Springer-Verlag, New York.

Rand, D. 1982. Dynamics and Symmetry: Predictions for Modulated Waves in Rotating Fluids, Arch. Rational Mech. Anal., **79**, 1.

Roos, B. 1969. *Analytic Functions and Distributions in Physics and Engineering,* J. Wiley and Sons, Inc., New York.

Ruelle, D. and F. Takens. 1971. On the Nature of Turbulence, Comm. Math. Phys., **20**, 167.

Scheurle, J. and J. Marsden. 1982. Bifurcation to Quasi-Periodic Tori in the Interaction of Steady State and Hopf Bifurcations, Center for Pure and Applied Mathematics, Univ. of Calif., Berkeley, PAM-113, preprint.

Siewart, C. 1977. On an Exceptional Case concerning Plasma Oscillations, J. Math. Phys., **18**, 2509.

Simon, A. and M. Rosenbluth. 1976. Single-mode saturation of the bump-on-tail instability: Immobile ions, Phys. Fluids, **19**, 1567.

Spiegel, E. 1983. private communication.

Takens, F. 1974. Singularities of Vector Fields, Publ. IHES, **43**, 47.

van Kampen, N.G. 1955. On the Theory of Stationary Waves in Plasmas, Physica, **XXI**, 949.

Wan, Y.H. 1977. On the uniqueness of invariant manifolds, J. Diff. Eqns., **24**, 268.

Wersinger, J.-M., J.M. Finn, and Edward Ott. 1980. Bifurcation and "strange" behavior in instability saturation by nonlinear three-wave mode coupling, Phys. Fluids, **23**, 1142.

TECHNICAL INFORMATION DEPARTMENT
LAWRENCE BERKELEY LABORATORY
UNIVERSITY OF CALIFORNIA
BERKELEY, CALIFORNIA 94720